MARÍA GARRIDO BARROS

PRECISION IMMUNOTHERAPY IN METASTATIC NON-SMALL CELL LUNG CANCER PATIENTS TREATED WITH IMMUNE CHECKPOINT BLOCKADE THERAPY

DOCTORAL THESIS

Supervised by

Dra. Isabel Barragán Mallofret and Dra. Elisabeth Pérez Ruiz

Academic Tutor

Dr. Antonio Rueda Domínguez

PhD Program in Biomedicine, Translational Research and New Health Technologies,
Faculty of Medicine

MÁLAGA, 2023

AUTORA: María Garrido Barros

https://orcid.org/0000-0002-0256-5027

EDITA: Publicaciones y Divulgación Científica. Universidad de Málaga

RESUMEN

El uso clínico de terapias basadas en Inhibidores de puntos de Control Inmunitario (ICI) en el Cáncer de Pulmón No Microcítico (CPNM) metastásico, ha mejorado drásticamente la supervivencia en este grupo de pacientes. En el contexto de malignidad, las células tumorales pueden adoptar múltiples mecanismos utilizando las vías propias de inhibición inmunológica. En situaciones de estimulación inmunológica crónica, el sistema inmunológico utiliza estos puntos de bloqueo para mantener la auto-tolerancia, evitando la muerte de células inmunológicas y reduciendo así el daño y la inflamación en los tejidos sanos. Actualmente, la inmunoterapia, que inhibe estos puntos de control inmunitarios, ha sido la primera en restaurar con éxito las respuestas inmunológicas anticancerígenas clásicamente identificadas en ensayos clínicos. La eficacia de las terapias basadas en ICI surge del restablecimiento de la respuesta antitumoral de las células T en el microambiente tumoral, y conlleva un conjunto de reacciones asociadas que promueven dicha respuesta. De esta manera, el bloqueo de las moléculas de puntos de control inmunitario, (como la proteína de muerte celular programada 1 (PD-1), el ligando de muerte celular programada 1 (PD-L1) y la proteína asociada a linfocitos T citotóxicos 4 (CTLA-4)), permite que el sistema inmunológico adaptativo ataque a las células tumorales. Los pacientes tratados con inmunoterapia presentan efectos adversos menos agresivos que los descritos por terapias clásicas como la quimioterapia o la radioterapia. Sin embargo, las tasas de respuesta varían ampliamente entre diferentes tipos de cáncer y pacientes, y solo algunos de ellos experimentan una respuesta clínica duradera.

Esto en gran medida se debe a la heterogeneidad interindividual, el potencial metastásico de los tumores y la susceptibilidad a la resistencia al tratamiento. A pesar de los grandes avances en nuestra comprensión de la biología molecular del tumor, el problema de la heterogeneidad interindividual para un tipo de tumor dado, tanto en lesiones primarias como metastásicas, afecta al éxito del tratamiento, especialmente en etapas avanzadas. El desarrollo y la aparición de metástasis en áreas distantes de los tumores primarios son la principal causa de mortalidad en la mayoría de los pacientes con tumores avanzados. Esta complejidad se debe en parte a la dificultad para identificar perfiles de expresión génica diferencial de las células que inician la metástasis. Además, estas células son escasas en la circulación y presentan una notable plasticidad. Por otro lado, la resistencia a la intervención terapéutica constituye otro problema importante que debe caracterizarse y revertirse o prevenirse. La resistencia adquirida, producida en el caso de tumores sólidos por diversos mecanismos entre los que se encuentran cambios en el patrón de uniones intercelulares dentro del tumor primario que afectan la permeabilidad de fármacos o anticuerpos, es otro problema importante en los tratamientos contra el cáncer. En el caso de los nuevos tratamientos basados en la inmunoterapia, también se da la resistencia innata debida al estado inmunológico de los pacientes. Poder identificar patrones moleculares o celulares específicos que definan cada uno de estos problemas antes del inicio del tratamiento es fundamental para mejorar la posterior decisión clínica. Por lo tanto, la identificación de biomarcadores predictivos y pronósticos que puedan evaluarse mediante procedimientos mínimamente invasivos sin necesidad de biopsia tumoral podría facilitar la detección temprana de

pacientes no respondedores y por consiguiente la elección óptima del tratamiento.

Sin duda, la identificación de biomarcadores relacionados con tratamientos basados en ICI se vuelve aún más necesaria en pacientes metastásicos con cáncer de pulmón, que es el tipo de cáncer que presenta mayor mortalidad, representando el 18% de la mortalidad total asociada a procesos neoplásicos. El Cáncer de Pulmón No Microcítico (CPNM) comprende el 85% de los casos de cáncer de pulmón e incluye como principales subtipos el adenocarcinoma de pulmón y el carcinoma de células escamosas de pulmón. Un tercer subtipo menos común es el carcinoma de células grandes el cual se considera un diagnóstico de exclusión debido a su pobre diferenciación y a la ausencia de buenos clasificadores inmunohistoquímicos o de microscopía electrónica. Los subtipos de CPNM presentan diferencias significativas, principalmente debidas al diferente origen celular dentro de los tejidos pulmonares, teniendo cada tipo celular patrones moleculares y biológicos distintos, lo que conlleva usar estrategias de tratamiento diferentes. Precisamente, las directrices actuales de la Asociación Internacional para el Estudio del Cáncer de Pulmón y la Asociación Internacional de Patología Molecular, sugieren la evaluación del perfil molecular de los pacientes con CPNM, que incluye la búsqueda de mutaciones en determinados genes como *EGFR, KRAS ALK, ROS-1, RET, BRAF, MET, NTRK* o *HER-2*, que son objetivos terapéuticos recientemente aprobados. Las plataformas de secuenciación genómica Oncomine y Foundation One CDx® son opciones que incorporan la evaluación de estos perfiles genéticos recomendados. Sin embargo, pese a los

grandes esfuerzos en la estratificación de pacientes con CPNM y en el diagnóstico precoz, todavía la mayoría de los pacientes con CPNM suele recibir un diagnóstico tardío y en etapas muy avanzadas, por lo que las estrategias de tratamiento en la enfermedad metastásica son de gran relevancia. Las opciones terapéuticas en estos casos se utilizan principalmente para intentar mejorar la supervivencia y la calidad de vida. Cuando los pacientes no tienen mutaciones específicas con posibilidad de terapias dirigidas, son elegibles para terapias basadas en ICI, que se pueden administrar solas o en combinación con otros fármacos, principalmente quimioterapéuticos.

En esta Tesis se han explorado diferentes componentes de sangre periférica de pacientes con CPNM para caracterizar la resistencia a terapias basadas en ICI y generar nuevos biomarcadores predictivos y pronósticos no invasivos. La principal fortaleza y objetivo de este estudio radica en el análisis prospectivo y longitudinal de indicadores moleculares y celulares procedentes de 97 pacientes con CPNM metastásico (CPNMm), además de la realización de un perfil multiómico, en diferentes tiempos de administración del tratamiento a lo largo de 12 meses, junto con una caracterización clínica y un seguimiento de dichos pacientes hasta la progresión o el fallecimiento en ese intervalo. Dentro de los objetivos específicos relacionados con esos componentes moleculares y celulares hemos evaluado la concentración de ADN libre circulante (ADNlc) y hemos perfilado en el mismo marcadores epigenéticos asociados a resistencia a inmunoterapia. También se han evaluado como marcadores pronósticos y predictivos moléculas de ARN de tamaño pequeño que forman parte del cargo de vesículas extracelulares (VE) derivadas del plasma,

así como la distribución y dinámica durante el tiempo de tratamiento de poblaciones inmunes circulantes relevantes para la respuesta a inmunoterapia.

Finalmente se ha llevado a cabo un análisis multivariante para la integración. Dichos biomarcadores moleculares y de los parámetros clínicos en modelos de predicción. Uno de los principales resultados de este trabajo de Tesis es la asignación de un valor pronóstico y predictivo a la concentración de ADNlc en el contexto de la inmunoterapia basada en ICI. La necrosis, la secreción por apoptosis o la NETosis, son algunos de los mecanismos mediante los cuales el ADN celular puede ser liberado a la circulación. Al estudiar las fuentes celulares de producción de ADNlc se ha demostrado recientemente que corresponden a diversos tipos celulares, siendo las células leucocitarias la mayoritaria. Además, en pacientes con cáncer, el ADNlc puede incluir ADN tumoral circulante (ADNtc) derivado de células tumorales. Algunos estudios indican que los pacientes con cáncer tienen concentraciones más altas de ADNlc en comparación con sujetos sanos. Sin embargo, el uso global del ADNtc sin la necesidad de su perfilación mutacional y por tanto del conocimiento de las alteraciones que presenta cada paciente está menos explotado debido en parte a las concentraciones tan bajas en las que se encuentra en plasma. Hasta ahora los resultados basados en investigaciones sobre el ADNtc han sido muy variables por lo que aún no se ha utilizado como biomarcador en ensayos clínicos para pacientes que reciben tratamiento basado en ICI. La cuantificación fluorométrica del ADNlc que se realizó como parte del presente trabajo de doctorado, mostró que los pacientes con CPNMm no respondedores tratados con fármacos basados en ICI tenían una mayor concentración basal de ADNlc que los pacientes respondedores. Y esto

ocurría no sólo en la predicción de la respuesta temprana sino a diferentes tiempos de evaluación de la respuesta tumoral. Además, fue muy importante definir un umbral cuantitativo, de manera que el análisis de supervivencia demostró que una concentración basal de ADNlc más alta de 0.55 ng/µl predice una peor supervivencia global en pacientes con CPNMm que van a ser tratados con ICI.

El siguiente objetivo de este proyecto de Tesis fue la determinación del perfil epigenético en ADNlc asociado a la respuesta y el pronóstico de pacientes tratados con terapias basadas en ICI. La mayoría de las investigaciones se han venido centrando en las alteraciones genómicas del ADNlc previamente caracterizadas en los tejidos tumorales, bien de manera informada o bien utilizando paneles con las mutaciones más frecuentes. Sin embargo, los cambios epigenéticos tienen el valor añadido de informar sobre programas de transcripción y estados celulares en diversas condiciones y tejidos, aportando información sobre el origen del ADNlc. La metilación (5-metilcitosina, 5mC) y la hidroximetilación (5-hidroximetilcitosina, 5hmC) en el carbono 5 de la citosina del ADN, han sido las principales modificaciones epigenéticas para la comprensión del silenciamiento génico y las posteriores consecuencias transcripcionales. Sin embargo, la modificación 5hmC está menos explorada. Algunos estudios iniciales la relacionan con la tumorigénesis y la reprogramación transcriptómica, sobre la cual tiene impacto positivo en lugar de silenciamiento. De hecho, está enriquecida principalmente en loci genómicos activos. Las enzimas dioxigenasas de metilcitosina "*ten-eleven-translocation*" 1, 2 y 3 (TET1, TET2 y TET3) convierten la 5mC en 5hmC como

parte del proceso de desmetilación activa del ADN. 5hmC constituye el intermediario más estable de este proceso. Por la información sobre el estado transcripcional y de tejido que aportan estas marcas, la evaluación epigenética del ADNlc en la dinámica del tratamiento con inmunoterápicos puede proporcionar tanto el perfil tumoral como las respuestas inmunológicas que estén marcando conjuntamente la respuesta a la terapia y el pronóstico. Aunque las firmas epigenéticas tumorales tienen utilidad diagnóstica y pronóstica en múltiples tipos de cáncer, los perfiles epigenéticos longitudinales del ADNlc en CPNMm en el contexto de la terapia con ICI aún no han sido completamente caracterizados. Durante esta Tesis, ambas marcas epigenéticas, 5mC y 5hmC, fueron analizadas conjuntamente y por separado, en un panel de secuenciación masiva de genes candidatos diseñado por nuestro equipo, con regiones génicas relacionadas con el cáncer y con marcadores predictivos y pronósticos de inmunoterapia identificados en trabajos previos. Los protocolos de detección de las marcas conjuntas (5mC+5hmC) así como de sus contribuciones individuales se optimizaron en el transcurso de esta Tesis para muestras de ADN en condiciones subóptimas, como son las propias del ADNlc (fragmentado y en concentraciones bajas). De hecho, se redujo la cantidad de ADNlc inicial necesaria a 10-20 ng en lugar de los 200 ng recomendados por el protocolo original. Los resultados aquí expuestos mostraron que después de 3-4 semanas de la administración del tratamiento basado en ICI, el número de sitios CpG y de regiones genómicas diferencialmente metiladas (DM) en los pacientes en respuesta, aumentó en comparación con las diferencias basales. Además, estos sitios CpG DM en ese momento del segundo ciclo de ICI estratificaron mejor a los pacientes según respuesta. Aunque la mayoría de los sitios y regiones DM

estaban asociados con p valores no ajustados probablemente por el tamaño muestral, los genes asociados resultaron ser muy relevantes para caracterizar los mecanismos de resistencia que podrían estabilizarse o desencadenarse como consecuencia de la administración de la terapia. Cuando se analizaron las regiones genómicas DM después de 3-4 semanas de tratamiento, la mayoría de los genes relacionados estaban directamente involucrados en el cáncer o actuaban como supresores tumorales. Uno de los mecanismos más interesantes es el sugerido por la identificación del gen *POU2AF1*, involucrado en la señalización y maduración de los linfocitos B, hipermetilado en los pacientes respondedores de nuestro estudio. Este coactivador transcripcional es clave para establecer la respuesta de las células B frente a antígenos y la formación de centros germinales, y se ha observado sobreexpresado en pacientes con melanoma que responden a terapias basadas en ICI en estudios previos publicados por nuestro equipo. Para poder entender el mecanismo asociado, se debe tener en cuenta que en esta sección se evaluaron ambas marcas conjuntas de 5mC+5hmC, y la hipermetilación podría ser tanto hiper5mC como hiper5hmC. Como se sugiere a partir de estos resultados, perfilar individualmente 5mC y 5hmC es relevante para aquellos genes que son susceptibles a variantes de 5hmC. Por ello, en esta Tesis se ha llevado a cabo una prueba piloto donde se ha caracterizado la abundancia de 5hmC en los genes de este panel. De acuerdo con esto, el protocolo optimizado en esta Tesis reveló variaciones interindividuales en respondedores que no se detectaron con el perfil conjunto de 5mC+5hmC. Sumado al hecho de que las diferencias según la respuesta fueron más prominentes después del inicio del tratamiento que antes del mismo, se podría hipotetizar que marcas 5hmC específicas también

determinan la reprogramación inducida después de la exposición a terapias basadas en ICI y que es necesario un estudio diferencial de ambas marcas para identificar firmas que estratifiquen de forma óptima a los pacientes en el contexto de la respuesta a mediano y largo plazo.

Otro de los biomarcadores objeto de estudio de esta investigación fueron los micro ARN (miARN) derivados de vesículas extracelulares (VE) procedentes del plasma. Estas moléculas representan un grupo de biomarcadores con muchas posibilidades en el CPNMm. La hipótesis de trabajo en esta sección se basó en que los miARN derivados de VE plasmáticas pueden proporcionar información sobre propiedades basales relevantes para la respuesta a la terapia con ICI y sobre las alteraciones tempranas en el tumor inducidas por la propia terapia. Las VE forman parte de sistemas de comunicación celular postulándose como herramientas potenciales para el diagnóstico molecular no invasivo, el pronóstico y el seguimiento del tratamiento en pacientes con cáncer. Estas VE, al mediar la comunicación intracelular, representan el tercer tipo más importante de señalización célula a célula. Además, una serie de estudios de alta relevancia han establecido una fuerte correlación entre los miARN derivados de VE y el microambiente tumoral inmunosupresor, lo que afecta la inmunogenicidad del tumor en varios tipos de cáncer. Desde la perspectiva de la biopsia líquida, el estudio de los miARN derivados de VE en plasma solo requiere una muestra de sangre del paciente y ofrece ventajas en entornos clínicos, debido a la protección del contenido que ejerce la bicapa lipídica. En los análisis propuestos en esta Tesis el estudio de los miARN derivados de VE en plasma ha revelado firmas de expresión génica

distintas entre pacientes respondedores y no respondedores. Estas firmas incluyen hasta 8 miARN previamente descritos como supresores de tumores en tejidos pulmonares y en CPNMm, como *hsa-miR-144-5p*, *hsa-miR-1224-5p* o *hsa-miR-451-a*, entre otros. Un análisis más detallado ha identificado miARN específicos que permanecen regulados a la baja en los pacientes respondedores una vez comenzado el tratamiento basado en ICI, como *hsa-miR-375-3p* y *hsa-miR-134-5p*, sugiriendo su posible papel como supresores del crecimiento tumoral mediante la modulación de la apoptosis y la proliferación celular. Cuando se llevaron a cabo análisis de enriquecimiento antes del tratamiento entre los pacientes respondedores y no respondedores se observó una firma de determinados miARN sobreexpresados y miARN infraexpresados relacionados principalmente con las células asesinas naturales CD56+. Esto se correlaciona con estudios previos en los que proporciones más bajas de células asesinas naturales CD56+ CD16- PDL-1+, con capacidades reguladoras, se asociaron con una mayor supervivencia global en pacientes con cáncer de pulmón que recibían inmunoterapia. Por tanto, todos estos resultados sugieren que los miARN contenidos en VE del plasma podrían ser una herramienta razonable para predecir la respuesta a los inhibidores de puntos de control inmunológico en diferentes tumores, como el CPNMm. Además, la adaptación temprana a la terapia, como sugiere la dinámica de expresión de estos ARN pequeños, podría impactar en la supervivencia libre de progresión o en la supervivencia global de los pacientes, como muestran nuestros estudios de supervivencia.

El tercer biomarcador que se ha evaluado en esta Tesis es el macroambiente tumoral, referido a los eventos inmunológicos sistémicos que

se desarrollan a distancia del tumor primario y que reflejan la respuesta local o la resistencia a terapias ICI. Por ello, se realizó una caracterización celular de diferentes poblaciones inmunes que en diferentes estudios en los últimos años se habían propuesto como biomarcadores útiles para predecir la eficacia de la inmunoterapia. En este sentido, el objetivo del estudio fue proporcionar un análisis detallado de diferentes subconjuntos de células inmunitarias circulantes antes y después del tratamiento con terapias basadas en ICI en la cohorte de pacientes con CPNMm. Los resultados mostraron que a nivel basal la única población que presentaba diferencias significativas fue la de células monocíticas, que se encontraban en mayor nivel en pacientes no respondedores. Además, el análisis postratamiento mostró cómo estas diferencias aumentaban cuantitativamente entre ambos grupos de pacientes. Por un lado, las células CD4+ T, conocidas por su capacidad antitumoral, aumentaron durante el tratamiento con terapias ICI en pacientes respondedores, y estas diferencias se mantuvieron a lo largo del tiempo, correlacionándose con la respuesta tumoral en diferentes evaluaciones. También, se observaron oscilaciones de las células T CD8+ y de los neutrófilos asociados al tumor, teniendo además los respondedores una menor expresión de PD-L1 en las células T CD8+. Los no respondedores, por otro lado, mostraron una mayor presencia de neutrófilos circulantes y un índice neutrófilo/linfocito más alto durante el tratamiento con terapias ICI, indicando un posible papel de estos biomarcadores en la resistencia a la terapia. Sorprendentemente, los eosinófilos, células inmunitarias relacionadas con alérgenos e infecciones, aumentaron en los pacientes respondedores a los seis meses del inicio del tratamiento. Es conocido que al expresar moléculas MHC de clase II y moléculas

coestimuladoras (estas células inmunitarias pueden regular la proliferación de las células T. Sin embargo, la actividad antitumoral de los eosinófilos asociados al tumor difiere entre los diferentes tipos de tumores y también entre pacientes con el mismo tipo tumoral.

Con la finalidad de evaluar la capacidad pronóstica de todas estas poblaciones linfocitarias, en este objetivo también se llevaron análisis de supervivencia. Estos análisis revelaron que los niveles de monocitos basales no tenían correlaciones significativas con la supervivencia global. Sin embargo, después de 3-4 semanas de tratamiento, algunas células inmunitarias circulantes se correlacionaron significativamente con la supervivencia. Específicamente, se demostró una supervivencia significativamente mejor en pacientes con niveles elevados de células T CD3+CD4+. Por el contrario, los niveles elevados de neutrófilos después del segundo ciclo de terapias ICI se asociaron con una supervivencia global más corta. Finalmente, la abundancia de eosinófilos mejoró la supervivencia global de manera independiente a otros factores pronósticos estándar.

La integración de todos los biomarcadores predictivos y pronósticos en el contexto del tratamiento con terapias ICI ha permitido en los últimos años alcanzar especificidades mucho mayores que con los marcadores monogénicos previos, así como una mejor estratificación de pacientes con enfoques terapéuticos personalizados más eficientes. Por ello, como objetivo final de esta Tesis, se desarrolló un modelo piloto de pronóstico multivariable integrando las variables clínicas actuales y el umbral no arbitrario de ADNlc de 0,55 ng/uL. Los resultados mostraron que este umbral mejoró los algoritmos de predicción

de supervivencia en comparación con los modelos construidos solo con variables clínicas de mal pronóstico, como edad, escala funcional del Eastern Cooperative Oncology Group (ECOG), valores de lactato deshidrogenasa (LDH) y expresión de PDL1, lo cual es especialmente relevante dada la alta resistencia asociada con terapias basadas en ICI.

Finalmente, es importante resaltar que todos los biomarcadores propuestos en esta Tesis pueden evaluarse mediante métodos no invasivos, lo que es más aceptado clínicamente por los pacientes en comparación con otros métodos invasivos, como la biopsia de tejido tumoral. Además, todos ellos han demostrado permitir la monitorización constante de la progresión de la enfermedad, lo que sugiere un impacto en la optimización del uso de la evaluación por técnicas de imagen, como la tomografía computarizada (TC) o la resonancia magnética (RM), que son útiles, pero implican costes económicos elevados y costes laborales altamente especializados que limitan su uso clínico de rutina.

A todos y cada uno de los pacientes de Immunomark, por su lucha constante y su generosidad.

Y, a todos los que me habéis acompañado durante esta etapa, gracias por vuestra infinita paciencia.

AGRADECIMIENTOS

En 2016, tras un evento muy desafortunado, decidí que solo haría una tesis doctoral que verdaderamente me apasionara. En 2018, y de forma repentina, me ofrecieron la oportunidad de poder cumplir ese sueño. Lo que nunca imaginé cuando hice las maletas y dejé Madrid, fue todo el aprendizaje personal y profesional que me tocaría afrontar. Yo, por aquel entonces, pensaba que la vida se podía planear y plasmar en un protocolo, con todos los pasos bien detallados, con las medidas exactas para un resultado digno de *Nature*. Y, sin embargo, años después, una tesis sin poder finalizar, un grupo nuevo y la cuenta atrás para terminar la que aquí presento, me han demostrado que los protocolos es mejor diseñarlos sabiendo que pueden fallar, y que se han de cambiar y adaptar. Por suerte, aquí estoy, dedicándome a un tema, que, si cabe, me apasiona aún más. No ha sido un camino de rosas, y todas aquellas personas que han estado a mi lado durante esta cuenta atrás lo han sufrido conmigo; años en los que he sido mi peor, pero también mi mejor versión. Lo importante, es que hoy por hoy, *pertenezco a esa clase de guerrero en el cual se han unido lo viejo y lo nuevo*.

Como ya os he regalado bastante drama, llantos y días malos durante estos años, me gustaría poder agradeceros en esta sección, aunque no sea suficiente, a todos los que habéis formado parte de esto.

En primer lugar, quiero expresar mi profundo agradecimiento a todos los pacientes que han participado en este estudio. Gracias a vosotros podemos hacer ciencia. No puedo decir más que sois un ejemplo de superación. Quiero agradecer a mis directoras de tesis, Isabel y Elisabeth y a mi tutor Antonio, por

darme la posibilidad de poder continuar con la ciencia a su lado, por su orientación, apoyo y paciencia a lo largo de todo el proceso de investigación. Agradezco también al departamento de Oncología, IBIMA y a la Universidad de Málaga, por proporcionarme los recursos necesarios para llevar a cabo esta investigación.

Mencionar a mi "*IMK team*", quienes me han brindado su apoyo incondicional en los momentos de dificultad, pero, sobre todo, la ayuda me han diaria necesaria para poder llevar a cabo todos los experimentos. Sois el mejor equipo y compañía, sin la que no podría haber seguido adelante. Bea, has sido mi *partner in crime*, has estado al pie del cañón para que no me faltara ni una sola muestra de cfDNA, para escucharme y apoyarme en todo momento. Me alegra pensar, que, aunque no vayamos a vernos diariamente, siempre tendré una pequeña parte de ti en mi muñeca. Juanlu, esta tesis es también tuya, porque sin tu magia no habría sido posible. Gracias por tu paciencia, por tu capacidad para mantener la calma durante el caos, y por ser la persona que eres. No tengo duda de que conseguirás lo que te propongas.

Me gustaría añadir, que esta tesis, no hubiera sido posible sin una persona, que me ha acompañado durante los últimos tres años de esta carrera a contrarreloj, sin soltarme de la mano. Gracias Javi, por ser amigo, compañero y confidente. Pero, sobre todo, gracias por ser el mejor maestro de ciencia y de vida que se pueda tener. Han sido muchas horas de trabajo y de conversaciones en las que no he podido más que disfrutar y aprender. Hiciste que recuperara la fuerza y la pasión con la que empecé el doctorado y que se fueron diluyendo durante el camino. Compartir tiempo contigo es un verdadero lujo. Espero que seas una de las variables fijas en mi vida.

Como dije al principio, en la vida hay variables que no se pueden controlar, por más que queramos. He aprendido que los que te rodean, vienen y van, pero que siempre aprendes de todos aquellos que han formado parte de tu vida. Por eso, me gustaría agradecer a los que se alejaron de mi camino por haber formado parte de él, y por haberme dado tanto durante ese tiempo. Sois parte de mí.

También agradecer a los que habéis aparecido por casualidad, porque el camino con vosotros es más bonito. A aquellos que siempre habéis estado y seguís estando, gracias. Mis amistades de siempre, que después de casi dos décadas son más fuertes y valiosas que nunca. Y amistades que aparecen de casualidad, sin buscarlas, y que de repente parece que han estado toda la vida. Habéis estado presentes aun cuando yo estaba ausente, y aquí seguís. Solo espero poder daros algún día toda la ayuda y amor que he recibido.

Escribiendo estas páginas, me doy cuenta de que soy feliz. Sentada, en mi escritorio de siempre, en la casa donde he crecido. Hacía más de siete años que no pasaba tiempo aquí, mi refugio, donde todo tiene solución, donde encuentro paz y consuelo incondicional. Y todo gracias a ellos, mi familia, que son el motor de mi vida. Son el ATP que me permite avanzar y no rendirme nunca. Cuando me miro en el espejo, me siento orgullosa de ser quien soy. Y soy quien soy por ellos. Habéis combatido conmigo cada una de las consecuencias de mis decisiones, sin reproches, con la valentía y fuerza que a veces a mí me faltaba, y siempre, haciéndome consciente de que la vida se enfrenta y se disfruta a partes iguales. Tengo la inmensa suerte de tener unos padres que me han educado en los tesoros más valiosos que una persona puede tener: honestidad y humildad. Cuando creáis que os habéis equivocado,

criándonos en ser buenas personas, honestas y ante todo conscientes de nuestros actos, pensad en toda la gente que nos quiere y en que nuestro propósito es, de alguna manera, hacer de este mundo algo mejor. Sentíos orgullosos, porque le habéis dado a dos personas los valores más difíciles de inculcar. Pablo, podría escribir una trilogía más larga que el señor de los anillos narrando la admiración que siento hacia ti. Sin duda, eres la persona a la que más admiro y admiraré siempre. Porque tu bondad, humildad, honestidad y capacidad de trabajo no tienen límites, y te han llevado a ser quién eres hoy, un gran científico y una gran persona. Todo lo que has conseguido y vas a conseguir, sin pedir nada a cambio, es más que merecido. Trajiste a nuestra familia a una persona que para mí es como la hermana que nunca tuve, la que jamás me ha juzgado y me ha querido tal como soy. Tenéis suerte de teneros y quereros de la manera que lo hacéis. Y ahora, gracias a vosotros, estoy queriendo de una manera nueva, un sentimiento que nunca había sentido por nadie. Oliver, cuando puedas leer esto, que será pronto con lo inteligente que eres con tan solo año y medio, me gustaría que supieras que voy a ser la tía más guay del mundo, tu confidente y la persona a la que podrás acudir siempre. Tendrás que soportar a cambio, todos los regalos científicos y frikadas que te iré dando intencionadamente.

Ojalá nos demos cuenta de lo importante que es educar en la ciencia. Enseñar que la ciencia mueve el mundo, mejora nuestra sociedad, cambia la vida de aquellos que aún no quieren irse.

ABSTRACT

The introduction of immune checkpoint blockade (ICB) therapy in metastatic Non-Small Cell Lung Cancer (mNSCLC) has dramatically improved survival in this group of patients. However, only some experience durable clinical response and many will develop immune-related adverse events (irAEs). The identification of predictive and prognostic biomarkers which can be assessed without a tumor biopsy, may facilitate early detection of non-responders and optimal targeting of treatment. In this Thesis, the biomarking capacity of multiple components of peripheral blood has been exploited to characterize ICB resistance and to generate novel non-invasive predictive and prognostic biomarkers. The main strength of this study lies in the analysis of prospective longitudinal samples and on the clinical characterization and follow up of the patients for a median of 34 months. There is emerging evidence to show that the concentration of circulating-cell free DNA (cfDNA) has prognostic and predictive value in the context of ICB, but this has yet to be fully characterized. cfDNA is derived predominantly from leukocytes, but in patients with cancer it can include circulating tumor DNA. Epigenetic assessment of cfDNA may provide tumor profiling and reflect immune responses that can jointly mark the ICB response and/or prognosis in these patients. Although epigenetic tumor signatures have diagnostic and prognostic utility across multiple cancer types, epigenetic cfDNA profiles in mNSCLC and following ICB are not yet fully characterized. In addition, plasma derived extracellular vesicles (EV)-miRNA present another promising avenue for biomarkers in mNSCLC. Here, it was hypothesized that plasma-derived EV-miRNA can inform of basal properties relevant for ICB response and of eary disturbances in the tumor induced by the therapy. In addition, the third concept

that this Thesis work characterizes is cancer “macroenvironment”: systemic immune events developing at a distance from the tumor that reflect local response or resistance to immunotherapy. A comprehensive analysis of peripheral blood immune cell subsets was performed to identify those events predictive or prognostic in the context of ICB. With this approach, this thesis aims to contribute to the introduction of clinically relevant tools for guiding treatment decisions in immunotherapy-eligible NSCLC patients.

CONTENTS

LIST OF FIGURES

LIST OF TABLES

Table 17: Multivariant prognosis model.

Supplementary Table 1.A: Correlation between cfDNA concentrations before ICB and categorical clinical characteristics.

Supplementary Table 1.B: Correlation between cfDNA concentrations before ICB and numerical clinical characteristics.

Supplementary Table 2. Correlation between cfDNA concentrations at different ICB treatment cycles and response criteria.

Supplementary Table 3: Correlation between clustered responder patients based on basal DE miRNA and clinical characteristics.

GLOSSARY OF TERMS AND ABBREVIATIONS

5caC:5-carboxylcytosine

5fC: 5-formylcytosine

5hmC: 5-hydroxymethylcytosine

5mC: 5-methylcytosine

ADCC: Antibody-dependent cell-mediated cytotoxicity

ALDH1A2: Aldehyde Dehydrogenase 1 Family Member A2

ALK: Anaplastic lymphoma kinase

APC: Antigen presenting cells

APOBEC: Apolipoprotein B mRNA editing enzyme

ASPN: Asporin

AUC: Area Under the Curve

BCCs: Biomarker Characterization Centers

BRC: B-cell receptor

BDLs: Biomarker Developmental Laboratories

BER: Base excision repair

BEST: Biomarkers, EndpointS, and other Tools

bTMB: Blood-based TMB

BRLs: Biomarker Reference Laboratories

CAMA: Cancer Associations with Molecular Aging

CD2AP-DT: CD2AP Divergent Transcript

CENPP: Centromere Protein P

cfDNA: Circulating-cell free DNA

cIBC: combination ICB

CLR:Type C lectin receptor

TUMOURS: Copy number aberration

CORO1B: Coronin 1B

CR: Complete response

CRP: C-reactive protein

CTCs: Circulating tumor cells

ctDNA: Circulating tumor DNA

CTLA-4: Cytotoxic T lymphocyte associated protein 4

CVCs: Clinical Validation Centers

DAMPs: Damage-associated molecular patterns

DAI: Differential agretopicity index

DCB: Durable clinical benefit

DCS: Dendritic cells

DDR: DNA damage response

DH: Differentially hydroxymethylated

DM: Differentially methylated

DMCCs: Data Management and Coordinating Centers

dMMR: MMR deficiency

dNLR: Peripheral blood derived neutrophil-to-lymphocyte ratio

DR: Direct repair

EBV: Epstein-Barr virus

ECM: Extracellular matrix

ECOG: Eastern Cooperative Oncology Group

EDRN: Early Detection Research Network

EFGR: Epidermal growth factor receptor

EM-seq: Enzymatic methyl-seq

EMT: Epithelial-to-mesenchymal transition

ENR: Extreme non responders

EPCAM: Epithelial cell adhesion molecule

ER: Extreme responder

EV: Extracellular vesicles

FcγR: Fc receptor

FBS: Fetal Bovine Serum

FDA: Food and Drug Administration

GWAS: Genome-wide association studies

HCC: Hepatocellular carcinoma

HIV: Human immunodeficiency virus

HRR: Homologous recombination repair

HPV: Human papillomavirus

ICB: Immune checkpoint blockade

ICOS: Inducible T cell co-stimulator

IDO: Indoleamine-2,3-dioxygenase

IFITM1: Interferon Induced Transmembrane Protein 1 gene

IFN-γ: Interferon-γ

IgG1: immunoglobulin G1

IHC: Immunohistochemistry

Indel: Insertions and deletions

irAES: Immune-related adverse events

IR-index: Immune repertoire index

ITH: Intra-tumor heterogeneity

KRT126P: Pseudogene keratin 126

LAG-3: Lymphocyte activation gene 3

LCC: Large cell carcinoma

LDH: Lactate dehydrogenase

LDH-ST: Low-dose helical computed tomography

LOF: Loss of function

LOH: Loss of heterogeneity

LTR: Long-term responders

LTNR: Long-term non-responders

LUAD: Lung adenocarcinoma

MAMPs: Microbe- or pathogen-associated molecular patterns

MDM2: Murine doble minute 2

MDSCs: Myeloid-derived suppressor cells

MHCI/MHCII: Major histocompatibility complex

miRNA: Micro-RNA

MMR: Mismatch repair

mNSCLC: Metastatic Non-Small Cell Lung Cancer

MRGPRF: MAS Related GPR Family Member F

MSI: Microsatellite instability

nDCB: Non-durable clinical benefit

NELSON: Nederlands–Leuvens Longkanker Screenings Onderzoek

NER: Nucleotide excision repair

NGS: Next Generation Sequencing

NHEJ: Nonhomologous end-joining

NK: Natural killers

NLR: Neutrophile-to-lymphocyte ratio

NLRs: NOD-like receptors

NLST: National Lung Screening Trial

NNK: nitrosamine ketone derived from nicotine

nonTLs: Non-target lesions

NSCLC: Non- small cell lung cancer

NSV: Non-virally related tumors

ORFs: Open reading frames

ORR: Overall response ratio

OS: Overall survival

PD-1: Programmed cell death 1

PD: Progressive disease

pDCs: Plasmacytoid dendritic cell

PD-L1: Programmed cell death 1 ligand 1

PF4: Platelet factor 4

PFS: Progression free survival

POLE/POLD1: Polymerase gene epsilon/delta 1

POU2AF1: POU Class 2 Homeobox Associating Factor 1

PPRs: Pattern-recognition receptors

PR: Partial response

RATS: Robot-assisted thoracoscopic surgery

RBPMS: RNA Binding Protein, MRNA Processing Factor

RINe: RNA integrity number equivalent

RLRs: RIG-I-like receptor

ROC: Receiver operating characteristic

SCC: Squamous cell carcinoma

SCLC: Small cell lung cancer

scRNA-SEQ: single-cell mRNA sequencing

sICB: single ICB

SNVs: Single-nucleotide variation

STARD3: StAR Related Lipid Transfer Domain Containing

T4-BGT: T4 Phage ß-glucosyltransferase

TCGA: The cancer genome atlas

TCR: T cell receptor

TET2: Ten eleven translocation 2

TILs: Tumor infiltrating lymphocytes

TIM-3: T-cell immunoglobulin and mucin domain-3

TLR: Toll-like-receptors

TLs: target lesions

TMB: Tumor mutation burden

TME: Tumor microenvironment

TNM: tumor, node, metastasis

tNGS: Targeted Next Generation Sequencing

TNF-α: Tumor necrosis factor-α

TSNAs: Tobacco-specific nitrosamines

USPSTF: U.S. Preventive Services Task Force

VATS: Video-assisted thoracoscopic surgery

WES: Whole exome sequencing

WHO: World Health Organization

CHAPTER I: INTRODUCTION

1.1. Biomarkers

Biomarker-based precision medicine may be used in the clinic to assess cancer risk, cancer diagnosis, treatment selection and/or treatment response assessment. Thus, they offer a promising avenue for early detection, treatment, monitoring, and cancer research. However, all these areas need to be further exploited to advance in the fight against tumors because cancer is still one of the leading causes of death worldwide. In 2022, 19.3 million new cancer cases and almost 10.0 million cancer deaths were calculated by the International Agency of Cancer Research. When evaluated by tumor type, approximately 1.8 million deaths (18%) were attributed to lung cancer, still leading mortality among tumor types (Sung et al., 2021a). On top of that, the pandemic situation triggered by SARs-CoV-2 infection had a negative impact on the diagnosis and treatment of cancer. Late diagnosis and thus delayed treatment in cancer patients during pandemic ended up in a slight decrease in the incidence of new cases followed by an increase in the disease progression and mortality (Yabroff et al., 2022). In 2040 the number of cancer cases is expected to increase by 47% from 2020 reported by Globocan (Sung et al., 2021b). However, the 2022 report on cancer statistics elaborated by the American Cancer Society, the variations are cancer type dependent. For example, incidence and mortality experienced an acceleration decline for lung cancer, a decrease for breast cancer, and a stabilization for prostate cancer. This is directly dependent on the advances in treatment and screening, which naturally are not homogeneous for the whole spectrum of cancer (Siegel et al., 2022).

That arises partly from the fact that tumors differ in the interindividual heterogeneity, metastatic potential, and susceptibility for treatment resistance. Despite advances in our understanding of tumor molecular biology, the issue of interindividual heterogeneity for a given tumor type, both in primary and metastatic lesions, impairs the treatment success particularly in advance-stage cases (Wilhelm-Benartzi et al., 2017). The development and occurrence of metastasis in distant areas from the primary tumors are the main cause of mortality in most patients with advanced tumors. This complexity is partly due to the difficulty in identifying differential gene expression profiles of the metastasis-initiating cells. Also, these cells are scarce in circulation and present notable plasticity (Samatov et al., 2013). Finally, resistance to therapeutic intervention constitutes another major issue that needs to be characterized and reverted or prevented. Acquired resistance in solid tumors is induced by intercellular junctions within the primary tumor affecting the permeability of drugs or antibodies. Furthermore, new treatments based on immunotherapy have revealed immunologic innate resistance (Tredan et al., 2007). Being able to identify specific molecular or cellular patterns that define each of these issues before the start of the treatment is fundamental to improve the management of cancer.

1.1.1. Definition and classification

The term “biomarker” was coined in the 1980s, but the underlying concept had been in use for centuries. The first known malignancy marker dates back

approximately 2000 years when it was used to distinguish malignancy (breast cancer) from benign condition (mastitis). In 1847, Bence Jones identified the first "tumors biomarker" which was a urine precipitate from patients suffering multiple myeloma. This was the first milestone in understanding cancer-related proteins and their potential diagnostic significance (S. Sharma, 2009).

Currently, the U.S. Food and Drug Administration (FDA) defines a biomarker as a *"characteristic that is objectively measured and evaluated as an indicator of normal biological processes, pathogenic processes, or pharmacologic response to a therapeutic intervention"* (Margaret Sullivan Pepe, Ruth Etzioni, Ziding Feng, John D. Potter, Mary Lou Thompson, Mark Thornquist, Marcy Winget, Yutaka Yasui, 2001). In the context of medical research and drug development, biomarkers can be used to evaluate the safety and efficacy of treatments, predict disease risk, and monitor disease progression or response to therapy. They provide valuable information for making clinical decisions and advancing medical science. Features of a good biomarker include: tumor type specificity, high sensitivity and concentration, informativity on disease stage and response to therapy (Henry & Hayes, 2012) (Califf, 2018).

In the spring of 2015, the FDA-NIH Joint Leadership Council identified the harmonization of terms used in translational science and medical product development as a priority need, with a focus on terms related to study endpoints and biomarkers. Both agencies developed the BEST (Biomarkers, EndpointS, and other Tools) Resource, which comprises a glossary that clarifies important definitions and describes some of the hierarchical relationships, connections, and

dependencies among the terms it contains. BEST glossary includes a broad classification of biomarkers. Of them, disease-specific biomarkers refer to those biomarkers involved in **i)** disease detection, **ii)** disease, stage evaluation **iii)** disease progression or recurrence, **iv)** treatment response and **v)** treatment efficacy and monitoring. All these categories are summarized into three main types (FDA-NIH Biomarker Working Group, 2016):

- Diagnostic biomarkers to determine the specific health disorder of the patient.
- Prognostic biomarkers to chart the likely course of the disease.
- Predictive biomarkers to indicate the probable response to a particular drug.

Sometimes, the same biomarker might represent a good prognostic and predictive factor, which makes the classification more difficult and sometimes can be practically confusing. Both types of biomarkers cannot generally be distinguished when only patients who have received a particular therapy are studied (FDA-NIH Biomarker Working Group, 2016). Both must be specific to the cancer type and sensitive, with their concentration reflecting disease stage or treatment response. To categorize them for specific cancer types, different molecular profiling mainly of DNA and RNA variants is employed including genetic variation, DNA methylation changes, and gene expression alterations in coding and regulatory RNAs. This molecular profiling intends to identify the interindividual variability that can help to predict prognosis and/or response and is the base of

precision medicine aiding in the clinical management of cancer (Nalejska et al., 2014).

1.1.2. Biomarker development process

Advances in diverse omics that inform of tumor processes important for the tumor detection and eradication have transformed the cancer biomarker field. Given that early detection is key for effective treatment, massive efforts have been focused on the development of early diagnosis. However, the irruption of new therapies that increase the survival probabilities in advanced tumors have promoted the investment in prognosis and response biomarkers for the treatment selection and the optimal use of commonly the unique window of opportunity for these patients. Initiatives such as the Early Detection Research Network (EDRN) organized by The National Cancer Institute established aim to promote efficient and rigorous research collaboration in biomarker development. EDRN's goal is to coordinate biomarker research, validation laboratories, clinical repositories, and population-screening programs to boost the efficiency and rigor in the field. Following EDRN guidelines, a five-phase biomarker development framework was proposed, in increasing evidence levels (Srivastava & Kramer, 2000) (Sullivan et al., 2001) summarize these developing phases, for a diagnostic biomarker **(Figure 1)**. The biomarker discovery process begins with phase I or preclinical studies, comparing tumor and non-tumor tissues to identify unique features for potential cancer detection tests. The primary aim in this phase is to identify leads for potentially useful biomarkers and prioritize those identified leads. Identification may be done by traditional methods like immunohistochemistry and western blots

and newer technologies like gene-expression microarrays, mass spectrometry-based protein profiles or assessing antibodies against cancer.

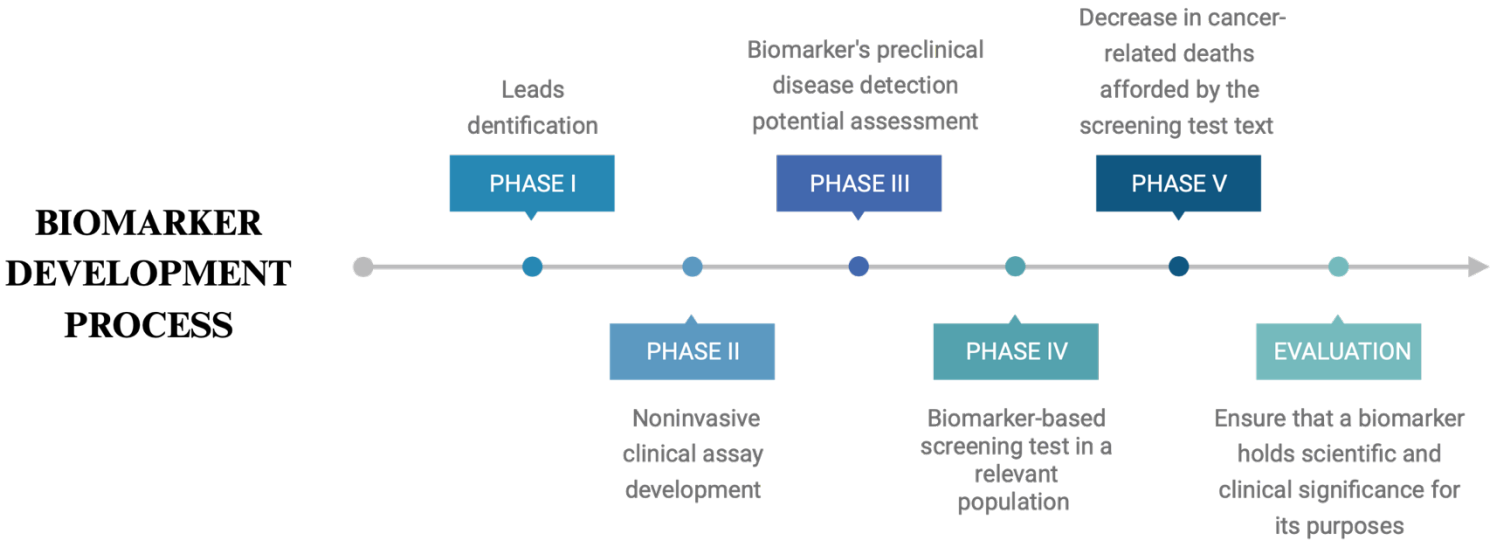

Figure 1. Biomarker development process and evaluation following EDRN guidelines and summarized by Sullivan et al. 2001. Five different phases and a final evaluation phase comprise the process that is designed to develop biomarkers with scientific and clinical significance. (This figure was created with BioRender.com).

Solid biopsies, however, cannot usually be used for clinical screening purposes because its procurement is too invasive. Thus, the development of a clinical assay based on bodily fluids levels of proteins expressed by the identified genes for example, or on antibodies levels to those proteins would be the goal of the Phase II, which focuses on developing a noninvasive clinical assay. This clinical assay should effectively distinguish individuals with cancer from those without it, but it doesn't assess early detection capabilities since the subjects have already an established disease. Estimation of true and false positive rates (TPR or FP

respectively) and the Receiver Operating Characteristic (ROC) curve are the primary forms of the biomarker assessment.

Phase III involved the retrospective longitudinal evaluation of the proposed biomarkers in pre-diagnosis clinical specimens from cancer cases. The comparison with controls reveals the biomarker's preclinical disease detection potential. If case levels deviate from controls only near diagnosis, screening potential is limited. On the other hand, divergent levels between cases and controls months or years before symptoms indicate early detection promise. With this, the criteria for positive screening results and preclinical detection potential are established and ready for Phase IV.

The phase IV goal is to assess the performance of the biomarker-based screening test in a relevant population by establishing both the detection rate and the false referral rate. In this phase, prospective assessment with real-time screening, diagnostics, and case identification will be performed. Critical in this phase is therefore the consideration of the ethical issues and the prevalence of the tumor type, sometimes implying the collection of large number of patients. Finally, phase V examines whether screening decreases the cancer burden in the population. Even if the biomarker can early detect the disease, it might not provide a clear benefit. This can be attributed to the lack of effective treatments for detected tumors, low program compliances, economic and health costs, and a possible overdiagnosis. Justifying population-wide screening requires high confidence in its benefit. Regrettably, for some tests like prostate cancer screening, we lack substantial evidence of their benefits. Thus, the primary

objective of phase V is to assess the decrease in cancer-related deaths afforded by the screening test (Sullivan et al., 2001).

After this development process, the next stage in the assessment and adoption of a given biomarker is the evaluation, which includes the analytical validation and the utilization assessment. The analytical validation encompasses the analytical performance of the assay, together with a qualification of available evidence that demonstrates the impact in the clinical outcomes. Finally, the utilization assessment is a contextual analysis to identify the relevance of the proposed specific usage. This involves determining whether the conducted validation and qualification offer adequate backing for the proposed usage.

As mentioned, EDRN provides with a working consortium where more than 300 researchers at academic institutions and in the private sector are working together to bring the biomarkers to clinical use (**Figure 2)** (Srivastava & Wagner, 2020):

- Biomarker Characterization Centers (BCCs)
    - Biomarker Developmental Laboratories (BDLs): these laboratories discover and develop new biomarkers and refine existing ones. They perform the initial assays to detect candidate biomarkers and the pre-validation studies.
    - Biomarker Reference Laboratories (BRLs): the assays for EDRN validation trials are conducted blindly, minimizing analysis bias, and ensuring the independent verification of the assay performance. These centers are also responsible for the analytical validation of the evaluation process.

- Clinical Validation Centers (CVCs) and Data Management and Coordinating Centers (DMCCs) work together to conduct biomarker validation trials. They provide high-quality, well-annotated biospecimens to the BDLs and assist with protocol design, monitoring the trial, and maintenance of the data and biospecimen tracking system.

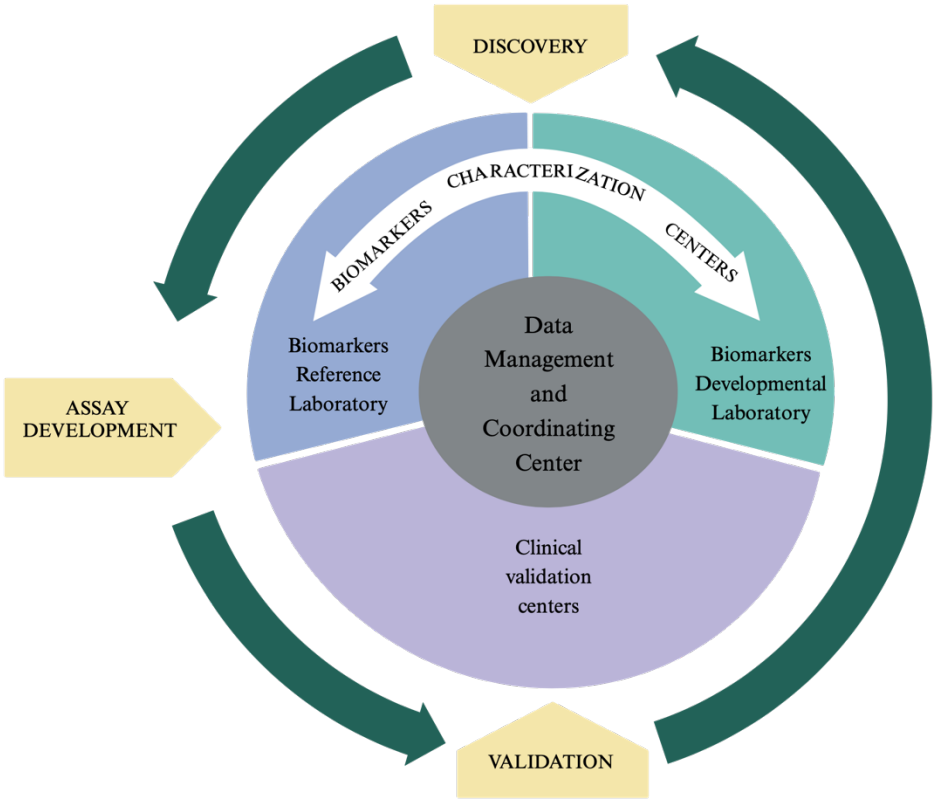

Figure 2. EDRN components involved in biomarker development and evaluation process. BDLs and BRLs are part of the Biomarker Characterization Centers (BCCs) responsible for biomarker discovery, trial, and analytical validation and evaluation process. CVCs and DMCCs give support regarding all clinical trial validation systems. EDRN, Early Detection Research Network BDLs; BDLs, Biomarker Developmental Laboratories; BRLs, Biomarker Reference Laboratories; CVCs, Clinical Validation Centers; DMCCs, Data Management and Coordinating Centers. According to the NIH statistics on current biomarkers development, there are thousands of organ-specific biomarkers being tested in phase I. When filtered by organs, breast and lung cancer are the organs with most biomarkers in development. (This figure was created with BioRender.com).

1.1.3. Omics-derived biomarkers in oncology

High-throughput omics technologies enable the collection of significant volumes of information about a particular class of molecules in a single experiment. Numerous omics technologies have emerged, collectively referred to as "omics," which involve the comprehensive study of various types of molecules within an organism's cells. These encompass fields like genomics, transcriptomics, proteomics, metabolomics, epigenomics, lipidomics, metagenomics, glycomics, connectomics, cellomics and even foodomics (Yadav, 2007).

This recent omics revolution represents a significant qualitative leap in the identification of biological mechanisms associated with treatment response and tumor evolution. The use of these high-throughput omics technologies has led to the rapid discovery of many candidate biomarkers. However, few biomarkers have made their way to the oncology clinic so far, with an existing gap between the number of omics-based biomarkers found in basic research literature and those introduced to the clinic. Tumor heterogeneity, both intertumoral and intratumoral, non-optimal study design, and poor methodological robustness and reproducibility are the primary reasons behind the considerable divide between the abundance of omics-based biomarkers in research literature and their practical use in clinical settings. For this reason, currently, there are no independent or absolute predictive response and prognostic biomarkers (Quezada et al., 2017).

Neoplasia is influenced by both genetic and environmental factors, and understanding these factors can aid in prevention and early detection. Genetic

risk factors are typically identified through genome-wide association studies (GWAS), but the declining cost of next-generation sequencing (NGS) may shift the preference towards NGS for identifying genetic risk factors. Additionally, rare genetic variants and non-additive genetic effects may play a more significant role than previously thought. In the context of cancer, NGS has become a valuable tool for studying mutation profiles in tumors, shedding light on the biological underpinnings of the disease. However, distinguishing driver mutations, which contribute to tumor phenotype, from passenger mutations, which result from genomic instability but do not impact the tumor, remains a challenge. Furthermore, the number of biomarkers far exceeds the drugs targeting the disrupted genes and proteins, highlighting the need for continued research to identify relevant biomarkers. Clinical trials incorporating omics-based biomarkers are on the rise, reflecting the active pursuit of precision medicine in oncology (Olivier et al., 2019).

The single-parameter analysis of biomarkers, with studies conducted on both paraffin-embedded biopsies and peripheral blood samples, has limited the predictive capacity for treatment response when evaluating various markers individually. Despite the description of several response biomarkers, none of them has been prospectively validated, preventing their application in routine clinical practice. Hence, it is probable that distinct omics approaches evaluate several facets of the intricate pathophysiology associated with the development and progression of cancer (Yugi et al., 2016).

However, there are some challenges in omics data analysis. Firstly, data handling of large datasets involves data filtering, cleaning, imputation, transformation, normalization, and scaling. Moreover, there is no universal gold standard for omics data analysis, and documenting analysis pipelines is crucial. Annotation of biomolecules in omics datasets may also be problematic, especially for non-standard model organisms. Another crucial aspect is the study design and analytic assumptions for robust and reproducible results. Balancing the number of samples and quantified molecules is indeed an ongoing challenge in omics data analysis. Regarding multiplexing capabilities in the data generation, genomics and transcriptomics often offer extensive ones, while metabolomics lacks multiplexing workflows. Also, data standards are needed for re-analysis and data integration is not possible in some omics fields due to the lack of standardized nomenclature, data formatting, and public access to datasets (Misra et al., 2019).

One of the most appealing approaches to improve the biomarkers quality and informativity is the integration of diverse omics. Although omics integration is far from been optimized for clinical value algorithms, diverse statistical and machine learning tools are being currently applied for dimension reduction, clustering, association with clinical data, and disease prediction. Interestingly, some web-based tools that do not require computational training have become available. Paint omics, 3Omics, and Galaxy are user-friendly and accessible to non-experts. Advanced users may opt for more versatile options like IntegrOmics, SteinerNet, Omics Integrator, and MixOmics. These tools provide greater control over data analysis through parameter customization (Cai et al., 2022).

1.2. Immunotherapy and cancer

Immunotherapy has been considered a potential and key strategy to limit the advancement of numerous malignant tumors during the last decade because of the immune system's critical involvement in cancer control. However, cancer cells may be involved in dynamic and complicated cell networks inside the tumor microenvironment (TME) to limit effective antitumor immunity (Kubli et al., 2021). The emergence of immunotherapy, especially immune-checkpoint blockade (ICB), chimeric antigen receptor (CAR) T cells and bispecific antibodies, have significantly changed the therapeutic landscape, which for years has been led by conventional oncological treatments such as surgery, chemotherapy, or radiotherapy. In particular, ICB therapy has accelerated the clinical application of a wide range of single drugs and combination immunotherapies in different malignancies, with durable responses and significant survival ratios in a proportion of the patients (Postow et al., 2015) (Lei et al., 2021).

In the setting of malignancy, tumor cells may assume multiple mechanisms based on immunological inhibitory pathways that the immune system uses to maintain self-tolerance, preventing cell death in T cells and decreasing damage and inflammation in healthy tissues. Nowadays, immunotherapy that inhibits these immunological inhibitory checkpoint targets has been the first to successfully restore classically identified anticancer immune responses in clinical trials (Qin et al., 2019). The efficacy of ICB results from unleashing the antitumor response from T cells in TME. Thus, the blockade of the immune checkpoint molecules (such as programmed cell death 1 (PD-1), programmed cell death ligand 1 (PD-L1), and cytotoxic T lymphocyte associated protein 4 (CTLA-4) allows the adaptive immune

system to attack tumor cells. Nevertheless, ICB has a number of drawbacks, including a high extent of resistance, a distinct spectrum of toxicities and immune-related side events, and the fact that the clinical advantages have been limited to specific subsets of cancer patients (Barrueto et al., 2020).

1.2.1. The inflamed tumor and cancer immunity cycle

Tumor inflammation is one of the hallmarks of cancer and one of the elements of cancer immunity that govern the anticancer response. Therefore, it is important to take it into consideration for the correct assignment of the biomarkers of response to ICB. The Cancer-Immunity Cycle is a sequence of self-mediated sequential events in tumors that must be initiated and allowed to proceed and expand to effectively kill cancer cells. Negative feedback mechanisms developed by tumor cells may interfere with all the steps of this cycle of cancer immunity and may be an obstacle to effective clinical responses development. As a result, ICB functions by reactivating all the phases in the cycle, which may have synergistic effects in the preservation of the cancer immunity cycle (Chen & Mellman, 2013) (Pio et al., 2019). The cycle includes seven steps, which are described in (Chen & Mellman, 2013) (Figure 3): i) Dendritic cells (DCs) capture and process neoantigens created by tumor cells. This is accompanied by immunogenic signals such as proinflammatory cytokines or factors from dying tumor cells, ii) Cancer antigens are presented to T cells on MHC-I and MHC-II (major histocompatibility complex) molecules iii) and T cells are activated against the cancer-specific antigens. At this point, a ratio between T effector cells and T regulatory cells is a key step to the final response and outcome, iv) Activated and

effector T cells migrate from activation sites towards tumor microenvironment **v)** to infiltrate it **vi)** and recognize tumoral neoantigens bound to MHC-I molecules in tumoral cells through T cell receptor (TCR). **Vii)** Once recognition is accomplished, T cells try to kill tumor cells. As a consequence of this cytotoxic process, tumor cells release additional tumor-associated antigens (step i) to increase the response in subsequent cycles. In order to coordinate the cycle, each step requires stimulatory or immunogenic and inhibitory or tolerogenic signals which promote immunity and reduce immune activity, respectively. Some of the immune inhibitory signals (immune checkpoints) are discussed in the next sections.

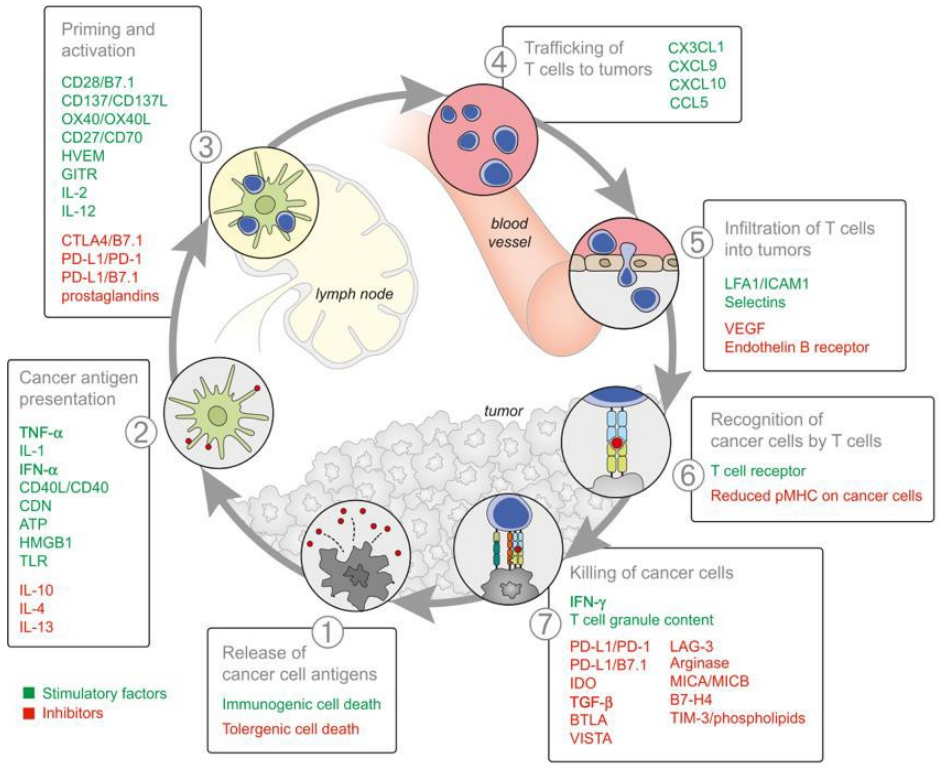

Figure 3. Immuno-oncology cycle described by (Chen & Mellman, 2013). Seven processes are proposed to take place in the immune-oncology cycle.

During all the cycle, damage-associated molecular patterns (DAMPs) are responsible for regulating the generation of immunogenic or tolerogenic signals. DAMPs are molecules secreted by dying cells, like tumoral cells, which are recognized by pattern-recognition receptors (PRRs) which sense danger by detecting these altered molecular patterns. PRRs consist of five families (TLRs, CLRs, RLRs, NLRs, and CD) which are mainly expressed in antigen presenting cells such as dendritic cells and macrophages and other immune cells performing a dual regulatory role in cancer immunity. PRRs may not only initiate an innate and subsequent acquired immune response to kill tumor cells, but they may also induce the generation of inhibitory immune cell subsets, anti-inflammatory cytokines, and inhibitory signals, which can lead to tumor development, invasion, and metastasis (Pio et al., 2019) (L. Bai et al., 2020).

As previously mentioned, in order to reduce the efficacy of the T cell-mediated action in the cycle, tumor cells, in most cancer patients, interfere in every step of the cycle employing several mechanisms such as impairing neoantigens recognition by DC, masking foreign antigens or increasing T regulatory cell response. All these mechanisms may eventually affect the action of ICB (Motz & Coukos, 2013).

1.2.2. Immune checkpoint blockade therapy

One of the hallmarks of cancer, proposed many years ago, is the ability of tumors to develop immune evasion mechanisms. The accumulation of genetic alterations in tumor cells results in the release of neoantigens that can be part of cancer-specific MHC-I complexes and recognized by CD8+ T cell specific receptors

(Boon et al., 1994). However, this mechanism has rarely been found to be successful in cancer patients to fully eradicate the tumor. Recent studies have demonstrated that this can be explained by the presence of certain factors in the TME that are able to inhibit antitumor T cell immune responses after binding to membrane proteins in the surface of these immune cells, known as immune checkpoints (Mullard, 2013).

1.2.2.1. Immune checkpoints

To avoid a continuous presence of activated cytotoxic cells that would damage healthy tissue, the immune system has developed immunological control pathways for self-tolerance, including the surface expression of checkpoint ligands that, upon engagement, can prevent the triggering of the proliferation and cytotoxic response of T cells. The fine-tuned balance between stimulatory and inhibitory tumor will determine the response of the immune system.

The immune checkpoint proteins that have most actively been studied in the context of clinical cancer immunotherapy are the programmed cell death protein 1 (PD-1 or CD279) and the cytotoxic T-lymphocyte-associated antigen 4 (CTLA-4; also known as CD152). PD-1 has two known ligands: programmed death ligand 1 (PD-L1 or CD274) and PD-L2. PD-1 engagement inhibits T-cell proliferation and expression of interferon-γ (IFN-γ), tumor necrosis factor-α (TNF-α), and IL-2, while it reduces T-cell survival. Taking advantage of this checkpoint mechanism, tumor expressing PDL1 can engage PD-1 in the surface of immune cells, preventingthe expansion and function of effector T cells; this eventually results in T-cell exhaustion, leading to tumor immune evasion (Pardoll, 2012).

Antigen presenting cells (APC) may express surface CD80 and CD86 proteins, which are able to bind CD28 molecules in the surface of T cells, leading to the proliferation and activation of the latter. CTLA-4 is a CD28 homolog, but with a higher affinity for its ligands, and unlike its counterpart, it does not trigger activation of T cells; moreover, some studies suggest that it may have instead inhibitory effects (Fallarino et al., 1998). Although both CTLA-4 and PD-1 binding have similar negative effects on T-cell activity, they show different downregulation timing, tumor mechanisms, and anatomic locations. CTLA-4 is specific of T cells and binds to exclusively APC-expressed molecules, while PD-1 is more broadly expressed, including activated T, B and myeloid cells, and its ligands are also expressed among different cell types in peripheral tissues (Buchbinder & Desai, 2016).

As said above, CTLA4 and PD1 are the two immune checkpoints with the most clinical information available now. However, there are many other regulators of the activity of the immune cells, and therefore candidates for newly developed therapies. For example, there has been a recent interest in better understanding other immune checkpoints such as LAG-3, TIM-3, CD27/CD70, Siglec-15, VISTA (PD-1L)/VSIG3, CD47/SIRPA, APOE/LILRB4, among many others. An interesting review on the tumor mechanisms of these and other immune checkpoints can be found in (He & Xu, 2020).

Lymphocyte activation gene 3 (LAG-3) tumor has been shown to have an inhibitory function in the activation and function of Th1 cells and is expressed ona variety of immune cells including activated CD4+ and CD8+ T cells, Tregs, NK cells (natural killers), B cells and plasmacytoid dendritic cells (pDCs).

Its tumor pathway involves the binding of FGL-1[4]. T-cell immunoglobulin and mucin domain-3 (TIM-3) was first identified as a protein selectively expressed on CD4+ Th1 and CD8+ T cytotoxic 1 (Tc1) cell, but B cells, Tregs, NK cells, DCs, monocytes, and macrophages are found among the immune cells that also contain this protein. In solid tumor, increased TIM-3 expression was linked to a poor prognosis, and preclinical models have confirmed the therapeutic effect of TIM-3 blockade in limiting tumor growth, especially when combined with PD-1 blockade (Qin et al., 2019).

1.2.2.2. Immune Checkpoints Blockade mechanism of action

Traditionally, cancer treatment was limited to surgery, chemotherapy, and radiotherapy. The surge of immunotherapy, particularly ICB therapy, has led to a revolution in the treatment of several cancer pathologies (Topalian et al., 2020) and is currently one of the most promising approaches for activating therapeutic antitumor immunity. Immune checkpoint modulating drugs aim to remove the inhibitory mechanisms developed by tumor cells, and to boost the adaptive immune response against cancer cells. Generally, these therapies are based on antibodies designed against the receptor or ligand, aiming to intercept the binding. CTLA-4 and PD-1, together with PD-L1, have been successfully targeted and antibodies affecting these molecules have been approved by the US Food and Drug Administration (FDA) for therapy against several cancer types (Davis & Patel, 2019).

The development of numerous immunotherapies targeting the PD-L1 pathway have demonstrated rapid antitumor activity, and this has been exhaustively revised in (Chen & Mellman, 2013), including monotherapy with anti-PDL1 atezolizumab or MPDL3280A, an engineered immunoglobulin G1 (IgG1) modified to eliminate antibody-dependent cell-mediated cytotoxicity (ADCC) by altering FcγR (Fcγ receptor) binding (Herbst et al., 2014), or anti-PD-1 IgG4 nivolumab and lambrolizumab (Isaacs et al., 2003). Nivolumab and atezolizumab have demonstrated clinically significant efficacy for various malignancies including NSCLC (non-small cell lung cancer) (Blumenthal & Pazdur, 2017). Other drugs, such as pembrolizumab, demonstrated a response rate of about 45% in a population with high positivity for PDL1 by IHC (immunohistochemistry) in NSCLC (Garon et al., 2015). Pembrolizumab, together with the anti–CTLA-4 antibody Ipilimumab, have received FDA approval and shown highly promising clinical results, long-term disease control, and even enhanced survival for the treatment of melanoma and NSCLC. One of the hypotheses for the rapid restoration of T cell activity upon ICB is that T cells have not been damaged in their cytotoxic activity, while the unleashing failure might be a sign of irreversible damage (P. Sharma & Allison, 2015).

1.2.2.3. Immune checkpoint blockade in the clinic

The survival rate in certain cancers is increasing significantly with the advent of immunotherapy based on ICB (Hirsch et al., 2017). However, despite the significant impact of ICBs, objective response rates in patients with advanced tumors with monotherapy continue to be found between 20% and 30%, with

complete responses being rare (Brueckl et al., 2020). Largely due to the complexity of the immune system, immunotherapy's success or failure depends on numerous factors and variables, including patient habits, gut microbiome, underlying infections, etc. Therefore, a better understanding of the physiology of immune cells in their response against tumor can contribute to therapy tailoring. Immunotherapy has demonstrated to offer a fast, long-lasting, and adaptive response. It has the potential to be self-propagating, and therefore reinforce the immune response against the tumor. Unfortunately, there has been an increasing number of immune-related adverse events (irAEs) reports after the introduction of ICB treatments. These adverse events are usually treatable and reversible, but they tend to have a delayed onset and prolonged duration, can affect any organ or system, and in some cases lead to the treatment discontinuation (Ramos-Casals et al., 2020).

Hence, the identification of predictive biomarkers emerges as a crucial area of research. Not only for enhancing patient selection and treatment effectiveness but also for developing alternative strategies in managing patients with unfavorable biomarker profiles. Such initiatives aim to prevent inadvertent harm and curtail healthcare expenses (Assi et al., 2018).

1.2.2.4. Main mechanisms of resistance to ICB

Here, it has already elaborated about how ICB has revolutionized cancer therapies. However, a significant number of patients are unresponsive, or will develop resistance to ICB over time. In addition, 9% of patients receiving anti-PD-1/PD-L1 monotherapy showed hyperprogression with poor overall survival

(Champiat et al., 2017). The origin of resistance is often found in intra-tumor molecular heterogeneity, which is due to the lack of genetic repair mechanisms. In this situation, a fraction of the cells develops the ability to escape to the antitumor effects, and undergo uncontrolled proliferation in an immunodeficient microenvironment, driving tumor progression therefore. This tumor heterogeneity has been shown to alter important ICB response modulators such as PD-L1. Moreover, there have been reports in NSCLC patients treated with anti- CTLA4 and anti-PD-1, where tumor clonality works as a predictor of enhanced response to immunotherapy (Xiao et al., 2020).

The "immunoediting" hypothesis states how tumor cells evolve towards expansion to escape immune surveillance, by changing the gene expression to minimize immune recognition (Xiao et al., 2020). For instance, a low neoepitope load has been found associated with the immune pressure happening after response to therapy, and it seems to contribute to ICB resistance. This effect is particularly interesting in patients who were initially responsive but later developed acquired resistance, as the impaired immunogenicity in the microenvironment could have led to tumor progression (Anagnostou et al., 2017).

There are a number of specific genetic and transcriptomic aberrations that have been proposed as candidates for ICB response biomarkers, including amplifications in the *MDM2* gene family (murine doble minute 2), *EFGR* (epidermal growth factor receptor) alterations involved in aggressive progression in diseases with anti-CTLA-4 or PD-1/PD-L1 immunotherapy, besides alterations that trigger the activation of the canonical Wnt/ß-catenin tumor pathway (Xiao et al., 2020).

Several immune-related mechanisms can also be involved, including the decrease of PD-L1 levels and IFN-γ pathway impairment caused by desensitization of T cells. The IFN-γ gene expression score can be used as a predictor marker of the response to pembrolizumab, while the lack of IFN-γ expression is associated with a bad response to ICB treatment in melanoma, NSCLC, and gut cancers. These transcriptomic signatures are efficient prognostic and predictive markers of the response to anti-PD-1 therapies (X. Li et al., 2019) (Galon et al., 2013).

1.2.2.5. ICB Predictive and prognostic biomarkers

Although ICB immunotherapy can provide significant therapeutic benefits to individuals with various malignancies, it has already discussed that only a small percentage of them may benefit from it and that they can be associated with moderate to severe immunological side effects. Also, the significant cost of ICB therapy per patient has been estimated as 1000,000-250,000 USD. Considering all this, a significant medical need to identify strategies for accurately selecting those patients who are most likely to respond favorably arises. It has also commented that important technological advances have aided in the proliferation of many candidates' predictive biomarkers. Importantly, the consideration of tumor-host immunity interaction mechanisms has also unmasked relevant determinants of response that are specific to this type of treatment. As a result, clinical decision-making for personalized anti-tumor immunotherapy has experienced a significant advance, together with the ability to monitor efficacy and disease progression. In this section, we will describe in depth the predictive ICB biomarker reported so far, categorizing them as those related to the tumors, to the tumor environment,

and to the host, and considering the advances in non- invasive biomarkers **(Figure 4)** (R. Bai et al., 2020).

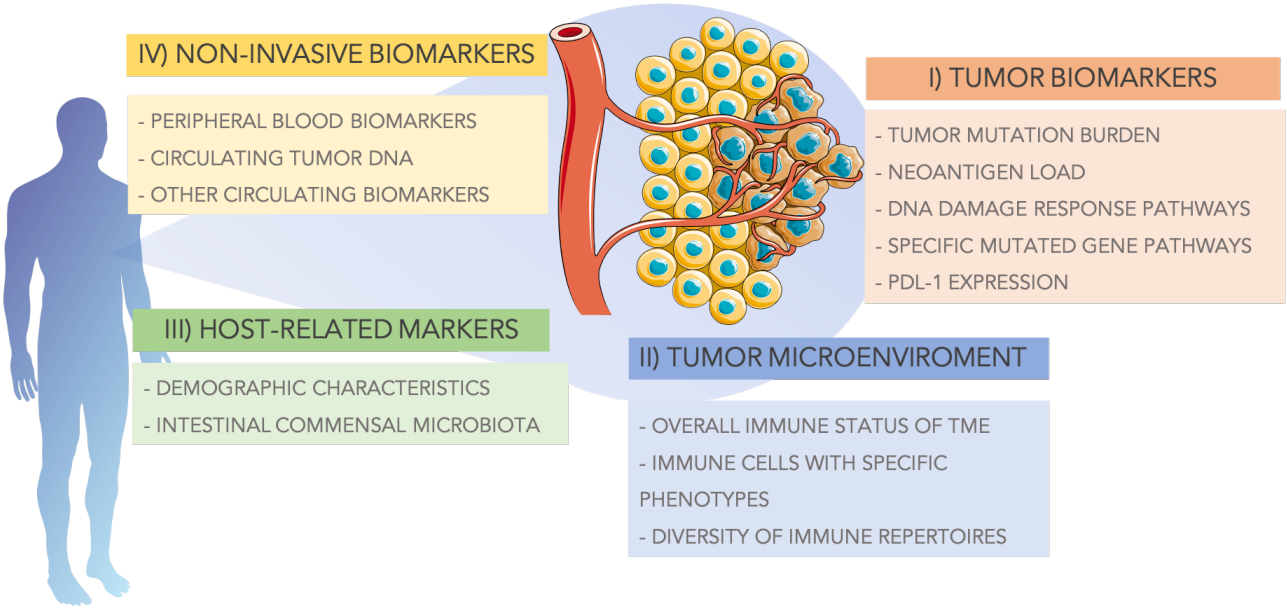

Figure 4. Source of predictive biomarkers to IBC efficacy. Biomarkers analyzed from tumor cells, the tumor microenvironment or those host related. In addition, there has been an increasing advance in non-invasive liquid biopsy biomarkers from peripheral blood. (This figure was created with BioRender.com).

1.2.2.5.1. Tumor biomarkers

i) Tumor mutation burden

Cancer disease has been described as a result of the accumulation of both germline derived and somatic mutations. Accumulated mutations may result in the development of neoantigens that are expressed on the surface of tumor cells and have elevated immunogenicity leading to the activation of T cells during the cancer immunity cycle. Tumors with high numbers of neoantigens may develop immune checkpoint mechanisms refractory to the triggering of neoantigen-

specific T cell activation and thus may be susceptible to ICB therapy (Yi, Jiao, et al., 2018). Tumor Mutational Burden (TMB) is defined as the number of somatic mutations (non-synonymous single nucleotide variants) per megabase and it is postulated as one of the current response biomarkers to ICB. TMB can be examined using a variety of methods that investigate the total number of sequence variants or mutations per tumor genomic region. It is strongly variable among different cancer types and even among tumors of the same histotype, and more prominent in tumor originating from carcinogen exposure (Fumet et al., 2020). TMB became a clinically relevant biomarker because it was demonstrated that high levels are associated with response to ICB and with clinical benefit in some types of tumors. The putative mechanism is an abundance in neoantigens and a consequent increase in immunogenicity (Walk et al., 2020) (Bindea et al., 2014).

However, other retrospective studies show response rates to ICB of less than 15% in cancer patients with high TMB, such as urothelial cancer (Rosenberg et al., 2016), melanoma (Snyder et al., 2014) or NSCLC (Hellmann et al., 2018). (Wolf et al., 2019) in an attempt to explain this variability in the correlations of TMB with response to ICB, demonstrated that intra-tumor heterogeneity impacts immune response because the anti-tumor immunity triggering PD-L1 expression is diluted along with the tumor growth. Thus, patients with low intra-tumor heterogeneity (ITH) and high TMB may show PD-L1 expression and benefit from PD-1 blockade, resulting in longer progression-free survival (PFS) (McGranahan et al., 2016). Indeed, patients who have low TMB or immunogenicity of their underlying disease, lack pre-existing anti-tumor T-cell responses and do not benefit from ICB (Galuppini et al., 2019).

Due to the complex dynamics that underlie the host immune response in the context of tumor cells and their microenvironment, TMB may not be sufficiently robust as an exclusive response biomarker to ICB to differentiate responders from non-responders and, alone, may not represent a direct evidence of tumor immunogenicity (Lei et al., 2021). Furthermore, technical, and clinical aspects need to be considered when it comes to TMB clinical implementation. TMB evaluation is not exempt to financial and technical issues, thus it is crucial to first create a list of tumors that are more likely to be extensively mutated and hence, to prioritize candidates for this analysis. In principle, TMB is expected to be high in malignancies caused by germline mutations in genes encoding proteins involved in DNA repair and replication, as well as in cancers induced by exposure to potent carcinogenic and mutagenic agents (e.g. tobacco smoke and UV-A) (Galuppini et al., 2019).

Once those patients with high TMB and low ITH are selected, whole exome sequencing (WES) can be used to evaluate TMB, but it is relatively expensive and has extremely long turnaround times, making it unsuitable for large-scale and routine clinical applications (Steuer & Ramalingam, 2018). To address this issue, determining TMB using targeted Next Generation Sequencing (tNGS) to assess the mutational status of a specific gene panel seems a more powerful technique for translating TMB assessment into clinical practice. This method correlated well with WES evaluation in many clinical studies (Devarakonda et al., 2018), (Rizvi et al., 2018). tNGS may provide several advantages comparing with WES: **i)** tNGS is available in many academic and clinical oncology centers: **ii)** WES is significantly more expensive than tNGS; **iii)** in tNGS, the turnaround time for analytical assays is shorter than 10 days, which is the suggested period for clinical decision making,

based on molecular characterization of neoplasms, and finally **iv)** other crucial prognostic and predictive parameters may also be revealed by tNGS ("Lung Cancer with a High Tumor Mutational Burden," 2018).

Despite tNGS techniques providing a more accessible TMB assessment, TMB testing in the clinic is still challenging due to additional limiting factors. **I)** The need for specialized equipment and highly trained workers ("High TMB Predicts Immunotherapy Benefit," 2018). **Ii)** The lack of a standardized cutoff score which will make TMB amenable for clinical validation. In this respect, it has been hypothesized that different tumor types may have distinct TMB cutoffs to accurately predict response (Rizvi et al., 2018). **Iii)** It has been shown that tNGS gene panels of less than 1 Mb have increased variance coefficients (Chalmers et al., 2017). **Iv)** Sufficient quantity, quality of the tumor samples and sufficient resulting DNA yields are required. It is important to note that, while TMB testing should be performed early during the clinical decision process, biopsy collection may be difficult due to poor performance status or metastatic disease of the patients (Rizvi et al., 2018). This is why less invasive sampling procedures are an imperative need in this field (Fassan, 2018). Indeed, *Gandara et al (2018),* showed in a retrospective study of two randomized studies (the OAK and POPLAR trials, ClinicalTrials.gov Identifiers: NCT02008227 and NCT01903993 respectively) that blood based TMB (bTMB) could be a potential alternative predictive biomarker (Gandara et al., 2018).

ii) Neoantigen load

As previously stated, only a small percentage of neoantigens produced from mutations are presented by MHC receptors and then recognized by activated T cells. Thus, the quantity of peptides in a tumor's neoantigen load could play a key role in tumor-specific T cell-mediated antitumor immunotherapy. The Cancer-Immunity cycle theory, mentioned before in section 1.2.1, was established in 2013 to describe the anti-tumor immune response triggered by the mutation-derived neoantigens. Because all steps of the cancer-immunity cycle are interdependent, the efficacy of ICB therapies is influenced from neoantigen presentation to the effector T cell killing of tumor cells. As a result, neoantigen load is proposed as a new predictive biomarker for ICB, as well as a potential therapy target for ICB affecting various steps of the Cancer-Immunity cycle (Chen & Mellman, 2013) (Yi, Qin, et al., 2018).

Nonsynonymous genetic modifications, such as single-nucleotide variations (SNVs), insertions and deletions (indel), gene fusions, frameshift mutations, and structural variants, could cause neoantigens both in non-virally related tumor (NSVs) and in virally associated tumor (Schumacher & Schreiber, 2015). Thus, in human papillomavirus (HPV)–related cervical or oropharyngeal cancer, Merkel cell polyomavirus or Epstein-Barr virus (EBV)–related head and neck cancers, antigens derived from open reading frames (ORFs) of the viral genome contributing to the potential source of neoantigens (Feng et al., 2008). This patent variability in the source and abundance of neoantigens may constitute a useful tool for predicting the effectiveness of immunotherapy. Beyond that, it could allow us to use those epitopes as target treatment offering the promise of a potentially superior tumor

control in the form of therapeutic vaccines or adoptive T cell transfer (Schumacher et al., 2019).

There are several methods to neoantigen assessment. For neoantigen prediction, NGS, a common clinical technology, has greatly contributed to the identification of tumor-specific genetic alterations affecting protein coding genes. Machine learning methods could be used to anticipate possible neoepitope targets by modelling components of the MHC-I processing and presentation route using patient tumor exome data (Pritchard et al., 2015). A specifical algorithm called differential agretopicity index (DAI), was built to predict the neoantigen peptide-binding capacity with respect to the wild-type counterpart (Duan et al., 2014). This analysis has been used in several clinical studies where different cohorts (NSCLC, melanoma, and advanced melanoma) were treated with more than one ICBs. Neopeptides and their clonal state were determined using genomic data from The Cancer Genome Atlas, and the mean DAI was found to be strongly linked with overall survival in three out of five cohorts, indicating superiority over nonsynonymous mutational and neoantigen load. This correlation between mean DAI, survival and immune activity suggests that DAI would outperform TMB in predicting survival and that further clinical studies on neoantigen based immunotherapies are relevant to get further insight on the therapeutic potential on neopeptide-based vaccines (Ghorani et al., 2018).

Coherently with the association of high TMB and low ITH with ICB efficacy, the need to consider both neoantigen load and heterogeneity is also clear. In (Wolf et al., 2019) the authors report a median of 326 neoantigens predicted per tumors. The distribution among intratumorally regions is not homogeneous, with 44%

neoantigen heterogeneity. Moreover, the combination of high load and low intratumoral heterogeneity (less than 1%) using the TCGA (The Cancer Genome Atlas) lung adenocarcinoma database, than 1%) was substantially associated with overall survival (OS) and with long-lasting clinical benefit under ICB treatment, an association that was more significant that considering either variable alone. Finally, promoter DNA hypermethylation of neoantigen genes has also been proposed as an essential immunoediting strategy to resist immune response. In this respect, DNA methylation stands as a mark of downregulation of neoantigens that in turn can promote immunoediting and the subsequent immune evasion, as described in **Figure 5** (Yi et al., 2019):

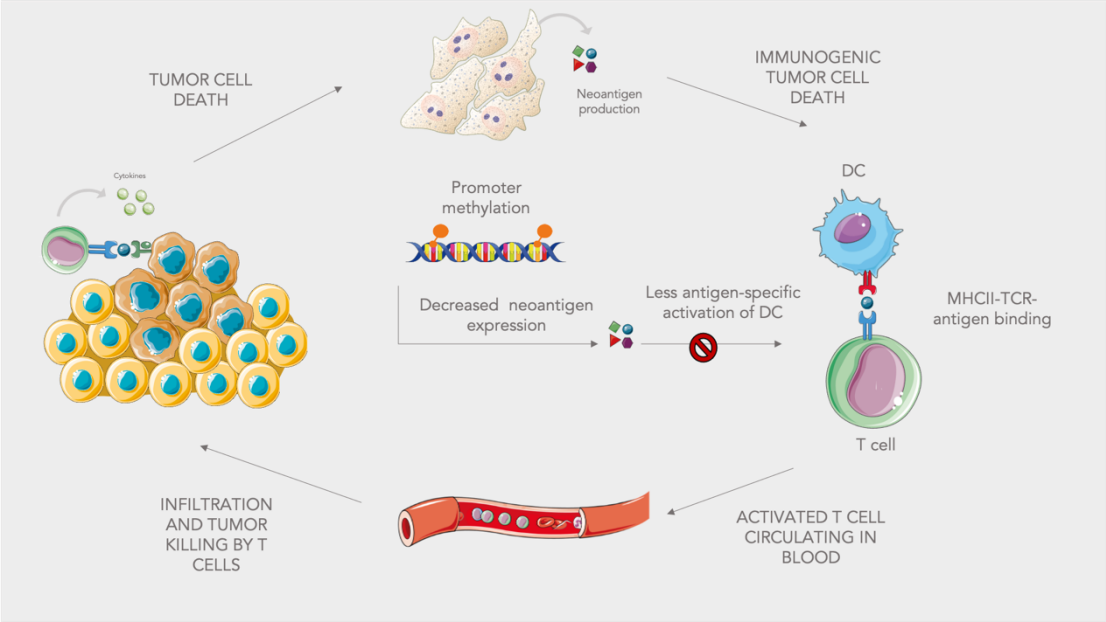

Figure 5. Methylation of promotors in tumor cells. The evasion of the cancer immune response may be caused by promoter methylation, which leads to a decreasing antigen production. The generation of many neoantigens induces anti-cancer immune response by the mediated activation of APC-T cells. T cells are activated in peripheral lymphoid organs and travel into tumor sites to infiltrate it. Once here, T cells recognize cancer cells and kill them generating more neoantigens. Thus, the anti-cancer immune response is propagated by additional neoantigens. (This figure was created with BioRender.com).

iii) DNA damage response pathways (MMR and MSI)

Several alterations of DNA damage response (DDR) pathways, which lead to genomic instability and promote malignant transformation, have been detected in many cancer types. The DDR machinery protects cells from some acquired genomic changes caused by external or endogenous damage. Direct repair (DR), base excision repair (BER), mismatch repair (MMR), nucleotide excision repair (NER), homologous recombination repair (HRR), and nonhomologous end-joining (NHEJ) are some of the routes of the DDR system, depending on the type of damage (Jiang et al., 2021).

The MMR system detects mismatches (insertion or deletion loops) and induces a single strand incision, followed by DNA repair through polymerase, nuclease, and ligase enzymes. Any genetic variation associated to dMMR (MMR deficiency) may lead to microsatellite instability (MSI) (high predisposition to mutation) which is typically found in tumoral cells with high TMB, increased numbers of CD8+ tumor infiltrating lymphocytes (TILs), PD-1+TILs, and *IDO*+ expression. There are some clinical trials, which have demonstrated the effectiveness of ICB in patients with MMR/MSI. Two of them are the global, multicenter phase 2 studies KEYNOTE KN164 and KN158, which have achieved durable responses to ICB PD-1 blockade (pembrolizumab) including multiple tumor types in patients with dMMR/MSI (ClinicalTrials.gov Identifiers: NCT02335411 and NCT04221945 respectively). As a result, the US Food and Drug Administration approved pembrolizumab for the treatment of any advanced solid tumor with MMR/MSI-H (Marabelle et al., 2020). dMMR may be related as well with other previously mentioned response biomarkers. dMMR may generate DNA polymerase

gene epsilon/delta 1 (POLE/POLD1) mutations, increasing neoantigen load and higher TMB, which could correlate with OS. It is worth noting that co-mutations of distinct DDR tumor pathways have a more extensive implication in high TMB or neoantigen burden; also, co-mutant patients have a better overall response ratio (ORR) and a longer PFS/OS (F. Wang et al., 2019).

iv) Specific mutated gene pathways in tumor cells

The responsiveness to ICB may be influenced by changes in other biological tumor pathways in tumor cells. In different clinical trials the whole exome from tumor and normal tissue has been sequenced to identify genetic variation which correlates with clinical benefit to ICB. Among all the identified mutations and considering only those highly deleterious variants that are known hotspot or putative truncating (frameshift insertion or deletion, nonsense mutation, or splice-site) mutations, those in interferon IFN-γ pathway genes such as IFNGR1/2, JAK1/2 and IRF1, are associated with resistance to ICB. The underlying mechanism of resistance implies the immunotherapy induced downregulation or alteration of the IFN-γ tumor pathway (and thus the genes implied in the JAK/STAT tumor) to avoid IFN-γ action (Possick, 2017). Another important gene is PBRM1, which is enriched in loss of function (LOF) mutations in tumor from patients that achieved complete response (CR) or partial response (PR) vs patients that experienced progressive disease (PD) under ICB. In addition, co-mutation of PBRM1/LOF and B2M (ß2 microglobulin), which codes for a protein involved in antigen

presentation, has been shown in some patients with PD, providing a possible reason for the lack of clinical benefit from ICB despite having PBRM1/LOF (Miao et al., 2018). Also, LOH in PBAF gene, which is a chromatin-remodeling complex, may also lead to more efficient ICB response by recruiting a higher number of T cells into tumor due to the increased production of CXCL9/CXCL10 chemokines.

The NOTCH tumor pathway is essential for cell communication, as it contains gene regulation mechanisms that control many cell differentiation processes during embryonic and adult life. It is also related to tumor development and prognosis, particularly associated with cancer stem cells. Analysis of multiple-dimensional genomic, transcriptomic, and clinical data from NSCLC patients treated with ICB, showed that deletion of NOTCH may be used as a potential favorable predictor of ICB treatment in some tumors (Zhang et al., 2020).

Other important alterations in the tumor genome that can be associated with response occur in genes of tumor cell proliferation and infiltration such as EGFR, anaplastic lymphoma kinase (ALK), MDM2/MDM4 and ARID1A. Similarly, co-mutated KRAS and TP53 or certain BRAF, MET or STK11/LKB1 alterations can also affect ICB efficacy (Ross et al., 2017).

All these genomic studies of various cellular pathway alterations underscore the necessity of genomic profiling in immunotherapy for cancer patients who require tailored treatment. Interestingly, a novel biomarker strategy recently approved by the FDA consists of combining several pan-cancer biomarkers. Pan-cancer analysis consists of assessing the occurrence of similar genomic alterations in different tumor types. One example of this comprehensive genomic analysis assay is the FoundationOne CDx, developed by Foundation Medicine as a

companion diagnostic, which provides potential genomic information about solid tumor (Takeda et al., 2021).

v) PD-L1 expression

By interacting with the PD-1 receptor, programmed cell death protein 1 (PD-1) suppresses immunological responses and establishes self-tolerance regulating T-cell activity, inducing apoptosis of antigen-specific T cells, and blocking apoptosis of regulatory T cells **(Figure 6)**. Thus, inhibitors of programmed death 1 protein 1 (PD-1) and its ligand PD-L1 (pembrolizumab (Keytruda, Merck), nivolumab (Opdivo, Bristol-Myers Squibb), and atezolizumab (Tecentriq, Genentech)) are effective therapies for some types of cancers (Han et al., 2020). The association of PD-L1 expression and response to ICB, even in first-line combined therapy, have been demonstrated in a variety of malignancies, and PD-L1 immunohistochemistry (IHC) has been used as a companion diagnosis for anti-PD-1 therapy in some patients. However, several studies have not found a correlation between PD-L1 expression and ICB response, and PD-L1 negative patients can still benefit clinically from ICB treatment or a combination of it.

In addition, PD-L1 cannot currently be used as an independent biomarker in clinical practice to measure efficacy because there is not a standardized assay for PD-L or a positive score or cut-off value and because PD-L1 expression is temporally and spatially heterogeneous, not only being expressed on tumoral cells, but also on immune cells such as lymphocytes and macrophages and stromal cells. In fact, high levels of PD-L1 expression on the surface of TILs before ICB

treatment, but not on tumor cells, correlates with clinical response (Herbst et al., 2014), (K. Wu et al., 2019).

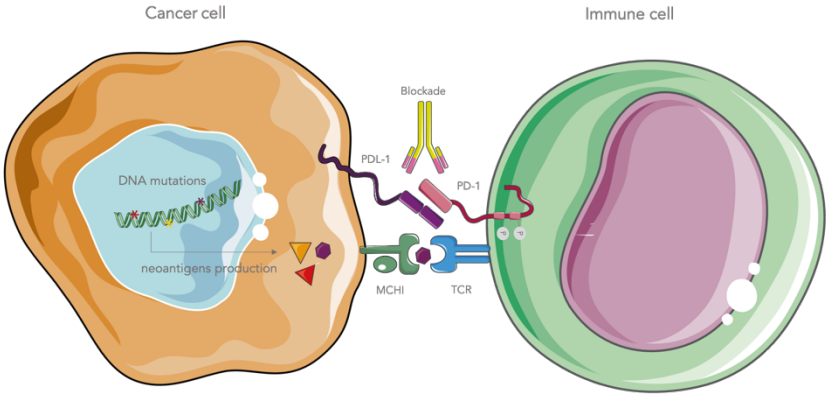

Figure 6. PD-L1 and PD-1 recognition. TCR and MHC-I binding activates the adaptive immune response. The binding of PD1 and PD-L1 can reduce the immune response by preventing T cells from tumors, while anti-PD-1/PD-L1 blockade can restore the inhibition (This figure was created with BioRender.com).

1.2.2.5.2. Tumor microenvironment biomarkers

i) Overall immune status of the TME

Tumors are highly heterogeneous tissues in which malignant cells are surrounded by and interact with a complex TME, which includes a diverse range of immune cells. Examining histological sections of tumor biopsies in clinical studies has provided the definition of three different tumor phenotypes that correlate with a patient response to some ICB therapy, based on (Chen & Mellman, 2017) (**Figure 7). 1)** Immune-inflamed phenotype: Enriched in CD4 and CD8 expressing T cells, myeloid and monocytic cells close to tumor cells and many

proinflammatory cytokines. In addition, those immune cells and tumor cells may express PD-L1. **2)** Immune-excluded phenotype: Many immune cells may be present in these tumor sections, but they remain in the stroma of the tumor and do not enter the parenchyma. The rate-limiting stage in the cancer–immunity cycle for this trait is T-cell migration from the stoma to the tumor. **3)** Finally, Immune-desert phenotype, which lacks tumor stromal and parenchymal T cells, inducing ICB resistance. The probable rate-limiting step in this phenotype is the generation of tumor -specific T cells.

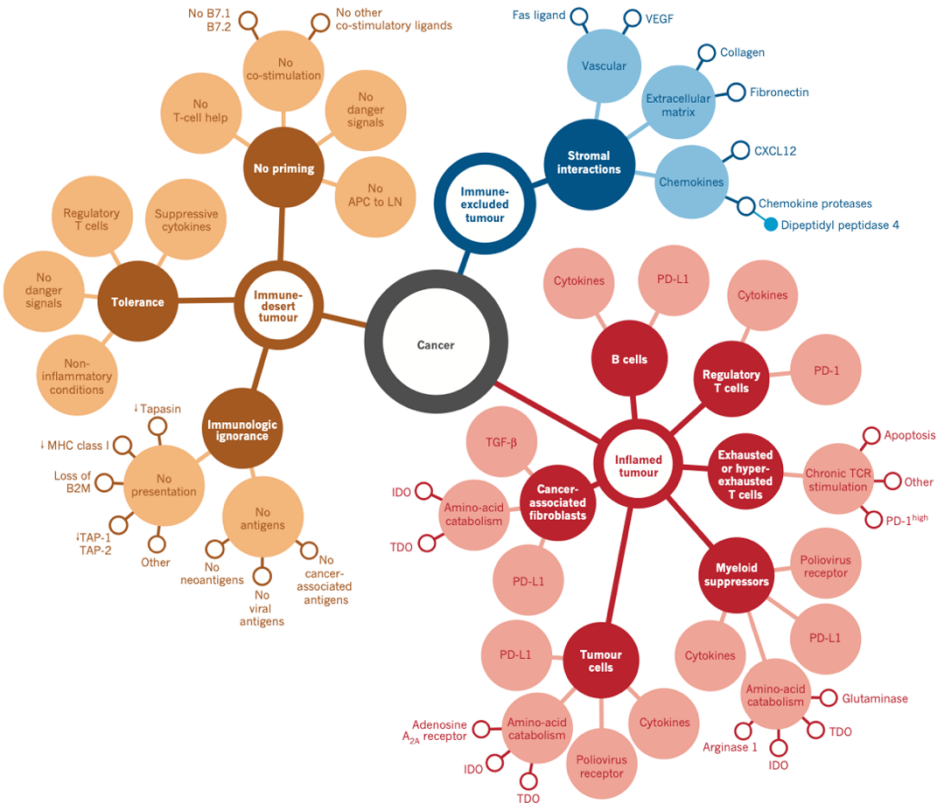

Figure 7. Tumor phenotypes proposed by (Chen & Mellman, 2017). Three phenotypes described with specific underlying biological mechanisms. In red dots, it is represented the inflamed tumor phenotype loaded with several immune cells. In blue dots, immune-excluded phenotype, where immune cells are presented just in the stroma area. Finally, in yellow dots Immune-desert phenotype, which lacks immune T cells in the stoma and parenchymal areas.

The significant associations of the degree of immune cell infiltration in tumor as categorized with this strategy with the clinical outcome of patients were the foundation of immunoscore, a reliable indicator of the immunological state of the TME, which classify tumor regarding the density of CD3+, CD8+ lymphocyte populations and CD45RO+ memory T cells in the stroma and parenchyma of the tumor. The immunoscore of several tumor types such as colorectal tumor was calculated, confirming an association with survival and OS. Immunoscore is now validated in other histologies such as melanoma and NSCLC (Bindea et al., 2014) (Mlecnik et al., 2011).

Finally, another evaluation of the overall immune status of TME has recently been suggested. It includes the wider assessment of immune gene expression profiling by total transcriptome analysis. At least a 2.5-fold rise in the expression of 22 immune-related genes has been discovered in some studies such as CD8, *perforin 1, granzyme B,* Th1 cytokines, *MHC-II, NKG7, ICO1, IGK, GBP1, STAT1, IGLL5, OCLN* and IFN-γ-induced immune gene signature which may be used all of them as prognostic biomarkers (Ascierto et al., 2012).

ii) Immune cells with specific phenotypes in TME

As it has been mentioned above, CD4 and CD8- expressing T cells are found in some phenotype tumor, and the phenotype of tumor infiltrated lymphocytes influences ICB therapy. Using specific techniques such as single-cell mRNA sequencing (scRNA-seq), several specific T cells phenotypes can be identified and characterized. The ratio between CD8+TCF7+ memory-like T cells and CD8+TCF7-T cells has been correlated with better response and survival in some tumor treated with ICB. In addition, a small proportion of CD39+CD8+ TILs are responsible for the recognition of tumor

mutation-associated antigens, being CD39 molecules a promising predictive biomarker. CD4+ and CD8+ T cells, FOXP3+ T cells, CD20+ B cells, CD134+ and CD137+ cells, and NKp46+ cells in TME were also positively associated with OS after ICB treatment. In addition, tumor associated macrophages which expressed PD-1, can capture anti PD-1 drugs from the surface of T cells resulting in ICB resistance and poor prognosis. However, high numbers of natural killer cells and CD8 with low number of TAMs and myeloid cells are associated with better response to ICB (R. Bai et al., 2020) (Sade-Feldman et al., 2018).

iii) Diversity of immune repertoires in TME

Because effective T cell responses require the activation and development of specific antigen-reactive T cell clones, the richness and clonality of immunological repertoire in intratumoral or peripheral tissues can be evaluated and utilized to predict ICB responses. How TIL clonality correlates with response under ICB remains unclear. Responding patients used the TCR (T cell receptor) beta chain in a more restricted way (i.e., had a more clonal, less diverse population) than patients with PD, and those clones increased 10-fold after treatment, implying a tumor-specific response to treatment in these patients. In addition, TIL density may not be correlated with baseline TCR clonality. To address this issue, the frequency of common TCR clones in TILs and peripheral PD-1+CD8+ T cells was measured by the recently proposed immune repertoire (IR)-Index. Neoantigen-stimulated TCR correlated with the IR-Index, and those patients with a high IR-index had superior immune activation and higher gene expression profiles scores, confirming the prognostic utility of the IR-index to assess ICB efficacy. Interestingly, these non-invasive predictors based on TCR repertoire variety and clonality of peripheral PD-1+CD8 +T cells constitute an alternative to the challenging process of collecting PD-

1 T cells from tumor tissue. In this context, adoptive T cell therapy stands as an option to counteract resistance by harnessing the T cells with engineered TCRs against specific tumor antigens (Manfredi et al., 2020) (Tumeh et al., 2014).

1.2.2.5.3. Host-related markers

i) Demographic characteristics

ICB have anticancer activity that is dependent on the immune response, which is influenced by the patient's demographic and clinical features. The role of sex and how it may correlate with ICB efficacy is not completely understood although it has been assessed in many clinical trials that evaluated ICB versus other therapies in different groups of male and female patients. Sex involvement in response to ICB is based on the fact that biological factors (genetic polymorphisms in some genes such as hormonal genes or other genetic alterations) and sociological factors (gender difference) have been shown to affect immune responses. Patients' overall survival was more influenced by sex when treated with CTLA-4 inhibitors compared to PD-1 ones, according to data examined from various ICB studies, albeit the difference was not significant when comparing patients treated with ICB overall against controls. Moreover, the influence of the sex in the effectiveness of PD-1 and CTLA-4 inhibitors is heterogenous, so a deeper insight into these correlations p0is still needed(Y. Wu et al., 2018).

Age is associated with accumulation of specific molecular alterations such as DNA mutations and methylation changes that may weaken the immune system activity and drive carcinogenesis. Among age-related immune changes are the loss of TCR diversity, the decrease in cytotoxic cell capacity, increased inflammation,

TMB increase and augmented expression of immune checkpoint genes in some cancer types. Despite this general age-related immune deterioration, a comprehensive analysis of age-related variations in the genomic, transcriptomic, and immune tumor environment published by (Erbe et al., 2021) suggests an upregulation of immune response pathways in aged immune tumor microenvironment samples. According to these findings, patients' survival outcomes are worsened as a result of the increased systemic frailty rather than due to a decreasing therapeutic efficacy. In view of this, large-scale cohort studies of aged populations with frailty measurements and genomic analyses are required to fully understand the effects of age on the immune response to cancer.

Other host-related determinants of response to ICB comprise alterations induced by specific habits such as tobacco smoking or high-fat diet. Tobacco smoking's mutagenic effects have long been known to raise the risk of malignancies of the lung, head and neck, and other anatomic sites. Smoking patients with NSCLC showed higher TMB and PD-L1 with longer PFD and duration of response to ICB. Physical differences in fat distribution and obesity are responsible for bad prognosis and tumor progression. This obesity-related mechanism finds its fundament in the alteration of STAT3 tumor and the subsequent PD-1 expression in T cells, responsible for the T cell exhaustion. Although the relevance of these general features in ICB efficacy is completely elucidated, they could be used as stratification factors in future clinical trials (Gainor et al., 2018), (Z. Wang, Aguilar, et al., 2019).

ii) Intestinal commensal microbiota

The commensal microbiota and the human host show a symbiotic relationship for fitness. The bacterial component of the microbiota has been the subject of a very prolific recent research. Changes in the normal microbiota have been related to the development of a variety of illnesses. Some bacteria have been implicated in the carcinogenesis process both in the setting of cancer, and in modifying the efficacy and toxicity of ICB therapy. Moreover, the formation and regulation of the local and systemic immune systems are intricately linked to the gut microbiome. For example, commensal bacteria are locally required for normalizing LP CD4+ T cell numbers and for proper programming of the local Treg/Th17 balance. Also, systemically circulating bacteria-derived molecules (microbe- or pathogen-associated molecular patterns, MAMPs and PAMPs, respectively) stimulate the proper development of distant lymphoid tissues (Fessler et al., 2019).

In addition, multiple studies suggest that gut microorganisms have an important role in ICB immunotherapy, such as activating T cells or enhancing tumor infiltration of particular TILs. Bifidobacteria enhanced anti-PD-1 antibody response by increasing the DC function, which correlates with PFS and OS improvement. In addition, relative abundance of Akkermansia muciniphilia, also correlates with clinical response and the efficacy of PD-1 antibodies in an IL-12-dependent manner. Furthermore, immune-related toxicity of ICB has also been linked to the composition of the gut microbiome (Sivan et al., 2015) (Dubin et al., 2016).

1.2.2.5.4. Non-invasive biomarkers

Until now, all the biomarkers reviewed were tumoral tissue or host-based which have shown variable predictive value depending on cancer type and host feature. Non-invasive methods are increasingly being used to test a patient's blood

as a powerful tool for capturing tumor progression in real time and providing information about the tumor's genomic and cellular composition. Several are the studies about the clinical value and utility of liquid biopsies. However, preanalytical factors must be standardized, and cross-platform comparative studies must be conducted. Initiatives in Europe and the United States (Cancer-ID and Blood Profiling Atlas respectively) have been implemented to standardize preanalytical variables and compare the performance of different liquid biopsy assays in the same patient samples. There are different response biomarkers which may be assessed from blood patients and the simultaneous analysis of all of them may also be required to fully understand the clinical role of liquid biopsy (Rossi & Ignatiadis, 2019).

i) Peripheral blood biomarkers

Different immune cell subsets have been associated with response in ICB clinical trials. In this context, less than ≤25% of CD45RO+/CD8+ memory T cells has been found in approximately 80% of non-responders and more than ≥ 30% in all responders in melanoma patients. Also, in melanoma patients treated with ICB, low amounts of CD69+MIP1B+ NK cells and CD14+CD16-HLA-Drhi cells after treatment are associated with low response to ICB. In these patients, high basal levels of T regs were found. Interestingly, a decrease after 12 weeks of anti CTLA-4 treatment was associated with better OS. In addition, anti CTL4 treatments seemed to induce the activation of inducible T cell co-stimulator (ICOS) pathway, a costimulatory molecule expressed in activated T cells and Tregs. ICOS is responsible of rising IFN-γ production and inducing tumor neoantigens recognition by CD4+ICOS+ T cells (Tietze et al., 2017) (Liakou et al., 2008).

As is described in the study by (Delyon et al., 2013) a monocentric prospective observational study in metastatic melanoma patients who received ipilimumab, there was an increased count of eosinophils and lymphocytes between the first and second infusions of treatment and that correlated with an improved OS. Furthermore, in melanoma and NSCLC patients, the neutrophil-to-lymphocyte ratio (NLR) has been demonstrated to be a substantial predictor of poor prognosis in patients treated with ICB, with lower ORR and shorter PFS. In line with this, low baseline lactate dehydrogenase (LDH) levels seem to be associated with prolonged OS in ICB treatment, and the significance of baseline-determined NLR and LDH levels as predictive indicators has recently been proposed. If further validated, the LDH level, which may be a measurement of tumor burden, and the dNLR which may be a measurement of the immune system, could be considered an inexpensive and practical prognostic marker for potential stratification in prospective ICB trials, according to an exploratory analysis of 11 randomized clinical multinational trials evaluating ICB among patients with metastatic non- small cell lung cancer (mNSCLC) (Kazandjian et al., 2019). Finally, circulating tumor cells (CTCs) can also be detected in blood samples. They are defined as tumor single cells or tumor cell

clusters sourced mainly from the metastatic precursor cells from the primary tumor site responsible for the development of metastasis. CTCs may contribute to the understanding of potential therapeutic targets and medication resistance mechanisms. However, they have a limited half-life in the bloodstream, between 1–2.4 hours. It is still up for debate whether the CTC release into the bloodstream is a random process or is predetermined by a specific biologic program, but they will almost certainly go through a rigorous screening process to ensure they can withstand difficult conditions in the circulation. They are cleared by extravasation of surviving CTCs into secondary organs. Because tumor cell dispersion requires a

perilous journey via the circulatory system, it is aided by tight interaction with activated platelets and macrophages forming hetero-aggregates that aid in endothelial adhesion and, as a result, lead to metastasis (Alix-Panabières & Pantel, 2016). CTCs are frequently detected using epithelial markers such as EPCAM and cytokeratins, which are not expressed on the surrounding mesenchymal blood cells. Epithelial tumor cells, on the other side, can undergo an EMT, which results. in a low expression of epithelial markers, increased plasticity and migration and invasion capacity, and resistance to anoikis, all of which are crucial for CTC continued existence and dissemination (Alix-Panabières & Pantel, 2014). It has previously been suggested that this transition affects tumor cells with stem cell-like properties. Consequently, it is likely that the parent cells of overt metastases (also referred as “metastatic stem cells”) in CTCs have relatively low levels of epithelial markers. However, it is now believed that tumor cells that have experienced partial EMT, also known as the "intermediate phenotype," could better adapt to the conditions found at secondary sites. Underlying epigenetic regulatory alterations permit this adaptability. The reversibility of the EMT process necessitates broad gene expression reprogramming, implying that epigenetic regulators play a key role in this process (Tam & Weinberg, 2013). Several recent studies have suggested that detecting and quantifying circulating tumor cells (CTCs) could be a potential circulating biomarker candidate in ICB. In addition, PD-L1 was shown to be strongly expressed in CTCs from advanced head and neck cancer patients, suggesting that PD-L1+CTCs could be used as an ICB response biomarker (Xiao et al., 2020).

ii) Biomarkers of circulating tumor DNA

Since the discovery of the presence of circulating free DNA (cfDNA) in the

blood of healthy individuals and subsequently in cancer patients, the study of cfDNA as a potential biomarker has been on the rise. In 1977, it was demonstrated that higher levels of cfDNA were found in cancer patients and those with metastatic disease compared to healthy individuals and non-metastatic cases,64 respectively. Years later, in 1994, the identification of somatic point mutations in cfDNA began (Vasioukhin et al., 1994). Part of the cfDNA originates from normal cells in the body, while a very small proportion comes from primary tumour metastatic sites, or circulating tumor cells (CTCs), and is known as circulating tumor DNA (ctDNA). A recent study published by (Mattox et al., 2023), showed that 47% of cancer patients had higher cfDNA concentrations compared with those generally observed in healthy subjects. Methylation profiles of cfDNA exhibited that the major contributor of cfDNA in all samples was leukocytes, accounting for ~76% of cfDNA, with neutrophils predominating. This fact demonstrated that tumor cells are not the main source of cfDNA, suggesting that cancers may have a systemic effect on cell turnover or DNA clearance. As for the mechanism of cfDNA release, it has been shown that some cfDNA fragments are similar in size to apoptotic DNA, suggesting that apoptosis is one of the possible sources of cfDNA production. Necrosis or active secretion, with DNA included in exosomes or DNA-lipoprotein complexes, are other possible mechanisms of cfDNA production. Cancer-specific somatic mutations can be found in circulating tumor DNA (ctDNA) in peripheral blood plasma without intrusive testing. ctDNA is produced from apoptotic or necrotic tumor cells and then released into the bloodstream, where it provides therapeutic guidance for several cancer treatment approaches **(Figure 8).**

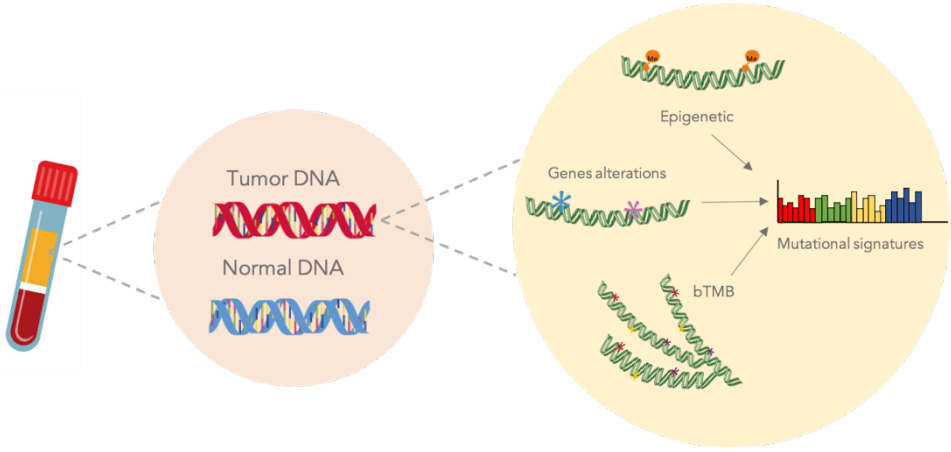

Figure 8. Approaches investigated from cfDNA. cfDNA is released from apoptotic or necrotic tumor cells to the bloodstream and may be used to study Tumor Mutational Burden, specific genes alterations or epigenetic marks. (This figure was created with BioRender.com).

ctDNA levels in some tumors under ICB treatments may predict tumour burden and are predictive of response before clinical manifestation. For example, in multiple studies, melanoma patients with consistently high ctDNA after PD-1 antibody therapy had a worse response and a shorter PFS and OS, according to (Lee et al., 2017). Furthermore, cancer-specific alterations such as single nucleotide mutations or copy number aberrations (TUMOURS), detected in ctDNA, predict disease progression in patients with a variety of malignancies treated with immunotherapy. Also, TMB can be evaluated using circulating tumor DNA, which has been related to PFS in patients treated with anti-PD-1/L1 treatment. Proving its potential as a predictive biomarker, bTMB can be exploited as a biomarker of clinical benefit in some patients treated with ICBs (Gandara et al., 2018).

Despite a considerable number of studies and its potential, the results are very diverse and ctDNA has yet to be used in clinical trials for patients receiving ICB treatment (Z. Wang, Duan, et al., 2019). Interestingly, with the development of next generation sequencing, a recent proof-of-concept study showed that tumor-

specific methylation patterns of ctDNA (5mC and 5hmC mutations) may constitute biomarkers for cancer diagnosis and prognosis of different tumors. In line with this, RASSF1A promoter methylation has been found to be the most frequently discovered epigenetic alteration in hepatocellular carcinoma (HCC) in several studies. The validity of these findings has been hampered by small cohort sizes, different treatment regimens, and different ctDNA detection methodologies (Xiao et al., 2020) (Weiss et al., 2017).

iii) Other circulating biomarkers

Plasma-derived extracellular vesicles (EV) are one of these circulating and non-invasive biomarkers. They are small particles (30-200 nm) with the main biological function of cell-to-cell communication resealed by most cell types, into body fluids (Mathivanan et al., 2010). Microvesicles (MVs), exosomes, and. apoptotic bodies are the three main subtypes of EV, which are differentiated based upon their biogenesis, release pathways, size, content, and function. They have different protein profiles; however, substantial overlap of some other protein profiles is often observed, due in part to the lack of standardized isolation and analysis methods of EV (Doyle & Wang, 2019).The lipid layer of these EV protects their cargo from degradation and they play a relevant role in maintaining67 tissue homeostasis, regulating immune response and are implicated in cellular processes in both health and disease (Kalluri & LeBleu, 2020). Exosomes are a subtype of EV formed by an intracellular endosomal route and are typically 30–150 nm in diameter. Regarding exosome formation, it appears that may be stimulated by growth factors and the cell adjusts its exosome production according to its needs (Kalluri, 2016) . MV are EV that form by direct outward budding of the cell's plasma membrane which

involves the shedding of small vesicles into the extracellular space. They typically have a size range of 100 nanometers to 1 micrometer in diameter. This places them in the intermediate range between smaller exosomes and larger apoptotic bodies (Bebelman et al.,2018) . The applications of and uses of MVs in the clinical setting are like those of exosomes. Finally apoptotic bodies, which are reported to have a range in size from 50 nm up to 500 nm and they are released by dying cells into the extracellular space (Kalluri, 2016). Regarding onco-biological processes, tumor derived extracellular vesicles(TDEV) may function as mediators of metastasis and may be responsible for engraftment and survival of metastatic cells. Remarkably, several studies have concluded that EV may have an impact on immune system regulation, drug resistance and tumor cell growth in NSCLC. It has been previously described the correlation between exo-PD-L1 and disease progression in NSCLC patients with advanced TNM tumor stage and distant metastasis (Y. Li et al., 2022). Also, regarding extracellular vesicles RNA, it has been analyzed EVP small-RNA and their role in NSCLC progression and treatment resistance (Grimolizzi et al., 2017). Importantly, cancer cell release EV at a rate noticeably higher than normal cells, indeed, due to their different protein and small-RNAs composition of EVP produced by tumor may be exploited as tumor biomarkers (J. Wu et al., 2021). In this context, with an average size of 22 nucleotides, they may regulate targeted mRNA translation or stability. They are implicated in a wide variety of biological processes including regulation of immune cell maturation, differentiation, proliferation, and activation. Several miRNA families were found to be enriched in exosomes from different cancer types. Therefore, many studies have recently focused on the significance of plasma-derived exo-miRNA in tumor diagnosis, prognosis, and therapy (Peng & Croce, 2016). EV miRNA additionally displayedvariable levels of expression in cancer patients compared to healthy controls. This fact has been

demonstrated in several studies in lung cancer, where cancer patients have higher amounts of both circulating exosomes and exosomal miRNA when compared to the corresponding levels in controls (Hu et al., 2020) (Silva et al., 2011). Thus, plasma vesicle-derived miRNA obtained by noninvasive methods could serve as circulating tumor biomarkers of discriminating and prognostic value.

Furthermore, high amounts of cytokines such as CXCL4, CXCL7, CXCL11 and CXCL9, CXCL10, drive tumor cells through the vasculature and they are often required for metastatic cell migration in circulation. Other soluble proteins (e.g., sCD163, sNKG2DL) and inflammatory factors (e.g. tumor necrosis factor alpha (TNF-alpha) interleukin 6 (IL-6), IL-8 or C-reactive protein (CRP), have been investigated as potential predictive biomarkers for ICB efficacy. CRP and IL-6 baseline levels in melanoma patients' serum were found to be strongly linked with poor response and shorter survival after treatment with nivolumab, with comparable results reported with ipilimumab and combination therapy (Nakamura, 2019) (Manz et al., 2019).

1.3. Non-small cell lung cancer and Immune Checkpoint Blockade

Lung cancer is the leading cause of most cancer-related deaths, with an approximate estimate of 1.8 million fatalities, representing 18% of the total mortality associated with neoplastic processes, as described in the Globocan 2020 report. Despite technological advancements in the field of medicine, the survival rate still does not exceed 5 years in Europe, the United States, and most developing countries.

An essential part of the diagnosis is early screening in patients with high

risk of developing lung cancer. Several clinical studies have demonstrated how early diagnosis works in preventing lives. The clinical screening trial National Lung Screening Trial (NLST), funded by the National Cancer Institute of the United States (clinical trial registration number: NCT 00047385), showed the importance of early lung cancer detection. The primary endpoint of this multicenter, randomized, and controlled trial was lung cancer mortality in high-risk participants using low-dose helical computed tomography (LDH-CT) technique and chest radiography. The study, completed in 2011, included 53,454 participants evenly distributed between both arms, who underwent an initial assessment and two annual evaluations with a median follow-up of six and a half years. The results were promising, as there was a 20% reduction in mortality among patients assessed using LDH-CT (The National Lung Screening Trial Research Team, 2011).

In the NELSON trial (Nederlands–Leuvens Longkanker Screenings Onderzoek) (clinical trial registration number NL580), there was also a decrease in lung cancer mortality rates. There was a decrease of 24% in men and 33% in women among high-risk patients who had been also assessed with LDH-CT. These clinical trials aimed to promote the implementation of new early lung cancer diagnostic measures into clinical practice. In fact, the U.S. Preventive Services Task Force (USPSTF) proposed an annual screening initiative for patients aged 55 to 80 with a history of smoking 30 or more pack-years, either current smokers or those who quit within the past 15 years. Unfortunately, in 2017, the survey results conducted in American centers regarding the USPSTF guidelines for annual LDH-CT in current and former heavy smokers were published. The results indicated that the clinical use of LDH-CT for diagnosis remained very low after this USPSTF recommendation, despite its significant potential for early lung cancer detection (Jemal & Fedewa, 2017).

Despite early diagnosis is highly beneficial, it is minor, with most lung cancer cases diagnosed in patients at advanced stages with common symptoms such as breathing difficulties, cough, chest pain, fatigue, or hemoptysis. The latter one has the highest positive predictive value (between 2.4% and 7.5%), although it is only present in one-fifth of lung cancer cases (Duma et al., 2019).

Metastatic lung diagnosis differs from other types of cancer when it comes to metastasis process. There are organ-specific differences regarding the metastases prognosis, notwithstanding that all of them have a bad prognosis. For instance, brain, bone or liver prone to lung cancer metastasis and frequently, lung cancer often metastasizes to multiple body areas (Li et al., 2019). Survival in metastatic patients varies due to biological differences and treatment approaches. Thus, better knowledge about distant metastasis patterns is crucial for tailored treatments and follow-up plans.

1.3.1. Molecular pathogenesis and diagnosis

The World Health Organization (WHO) has established that a valid diagnosis should primarily rely on morphology, supported by immunohistochemical, molecular, and imaging techniques (Nicholson et al., 2022). To achieve this, obtaining a tissue biopsy with sufficient and appropriate material is essential for identifying the subtype through histopathological and molecular analysis techniques. Among the procedures employed for obtaining lung biopsies, bronchoscopy with biopsy or fine needle aspiration, mediastinoscopy, endobronchial ultrasound, image-guided needle aspiration through the chest wall, pleural fluid analysis (thoracentesis), thoracoscopy are the available surgical approaches. However, these procedures are costly and carry potential complications for the patient (Shim et al., 2013).

Through histological evaluation, lung cancer can be categorized into two main categories. Small cell lung cancer (SCLC), that accounts for 15% of lung cancer cases, exhibits neuroendocrine characteristics and high mortality rates. On the other hand, non-small cell lung cancer (NSCLC) makes up the remaining 85% of cases. Within NSCLC, lung adenocarcinoma (LUAD) and lung squamous cell carcinoma (LUSC) are the most common subtypes. (Molina et al., 2008). Another NSCLC subtype is large cell carcinoma (LCC), which is considered a diagnosis of exclusion due to its poor differentiation and inability to be classified through immunohistochemistry or electron microscopy. All these subtypes present significant differences. Mainly, they originate from different lung tissue cells with highly distinct molecular and biological patterns, leading to differing treatment strategies for each lung cancer type (Seidel et al., 2013). This tumor heterogeneity knowledge and the presence of cellular subpopulations with distinct molecular characteristics have represented a significant advancement in the treatment of (NSCLC). These therapies evolve from cytotoxic therapies to personalized medicine or immunotherapy, owing to the presence of specific genetic alterations or PD-L1 status (Herbst et al., 2018). Thanks to the advent of more advanced diagnostic approaches, such as immunohistochemistry techniques or tumors genetic profiling, it has enabled better pathological categorization of NSCLC. Also, more detailed characterization of molecular driver alterations for the development of targeted therapies in patients with a defined mutational profile. Currently, oncogenic driver mutations can be found across all histological types of lung cancer, in all age groups, and etiological profiles (Chevallier et al., 2021). In the **Figure 9,** proposed by (Thai et al., 2021) there are NSCLC classification based on more frequently oncogenic driver mutations.

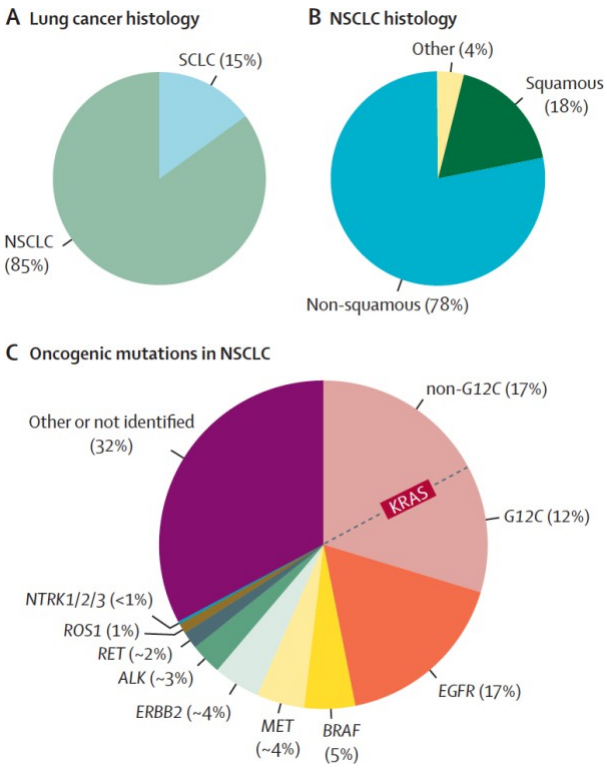

Figure 9. Histological classification of Lung Cancer. A) Lung Cancers are categorized as SCLC or NSCLC, **B)** with further subdivisions into squamous and non-squamous histology. **C)** The prevalence of common oncogenic driver mutations in NSCLC, based on a cohort of 4,064 patients with metastatic NSCLC.

Currently, the molecular profiling recommended by guidelines established by the International Association for the Study of Lung Cancer and the International Association of Molecular Pathology includes the assessment of *EGFR* mutations through immunohistochemistry and assays with a sensitivity of 5% for the *EGFR T790M* mutation in patients exhibiting secondary resistance to *EGFR* inhibitors. These guidelines encompass the evaluation of *ALK*, *ROS-1*, and *RET* rearrangements using immunohistochemistry as an alternative to fluorescence in situ hybridization, the detection of the *BRAF Val600E* mutation, and the identification of *MET* exon 14 skipping mutations (Lindeman et al., 2018).

In addition to the study of these latter mutations, other mutations can be evaluated despite being found in a minor percentage of patients. This is because they serve as targetable alterations for recently approved targeted therapies by regulatory agencies. Two of those mutations are *NTRK* gene fusions or overexpression of the *HER-2* gene, which is currently in the clinical approval process (Paz-Ares et al., 2019) (Yu et al., 2023).

Oncomine platform, specifically OCA-Plus version, encompasses 501 genes, including those recommended by the International Association for the Study of Lung Cancer and the International Association of Molecular Pathology. Another NGS platform that incorporates these recommendations is Foundation One CDx®, covering a total of 324 genes (Vestergaard et al., 2021).

Regarding KRAS mutation, specifically the glycine-to-cysteine substitution at codon 12 (G12C), is one of the most frequent mutations in most tumors including non-small cell lung cancer (NSCLC). However, KRAS mutations have been considered difficult to address with therapies until now, due to their complexity or the lack of effective pharmacological options. (Ricciuti et al., 2022). Nevertheless, numerous clinical trials are attempting to tackle this challenge by developing targeted therapies for KRAS mutations.

An example is the phase two clinical trial of the compound called sotorasib, a KRAS G12C inhibitor, in patients with NSCLC (Clinical trial registration number NCT03600883). The results reveal that up to 40% of the patients showed clinical benefit reason why the Food and Drug Administration (FDA) granted the

accelerated approval for the use of this inhibitor (Skoulidis et al., 2021). With adagrasib, another KRAS G12C inhibitor, up to 43% NSCLC non-small cell lung patients have achieved clinical benefit. This trial, which started in phase two with 116 patients, is currently in a phase two expansion with ongoing recruitment (Clinical trial registration number NCT03785249) (Jänne et al., 2022).

It is important to highlight the immunomodulatory effect of KRAS mutations in various solid tumors, such as NSCLC. Among these effects, there is an increase in the expression of PD-L1 or induction of apoptosis in CD3+ T cells. Also, a decrease in MHC-I molecules has been observed, leading to a reduced capacity of CD8+ cytotoxic T cells to recognize tumor antigens and the polarization of CD4+ cells into regulatory T cells immunomodulatory mechanisms suggest that PD-L1 blockade through immunotherapy could restore the antitumor immunity of T cells in NSCLC with KRAS mutations (Chen et al., 2017), (Zdanov et al., 2016).

With regard to imaging techniques, they are crucial to assess the tumor stage at the time of diagnosing lung cancer and to select the most appropriate therapy for patients. Imaging techniques such as fluorodeoxyglucose positron emission tomography (FDG-PET) scans and magnetic resonance imaging (MRI) are employed for determining the tumor stage. Along with CT scans, FDG- PET provides information about the presence of tumor clones in mediastinal lymph nodes or distant metastases from the primary tumor. Potentially it may even avoid 3thoracic interventions and the associated risks. It's important to note that staging diagnosis with FDG-PET does not reliably detect lesions smaller than 1 cm due to its low sensitivity for such lesions (Farsad, 2020).

1.3.2. Etiology

There are many risk factors associated with the development of NSCLC. They may be classified into two risk factors categories: modifiable and non-modifiable risk factors. Tobacco consumption, diet, asbestos exposure, and exposure to ionizing radiation are some of modifiable risk factors, meaning that they may be reduced through specific measures. On the other hand, non-modifiable risk factors are those that cannot be altered, such as age, sex, ethnicity, family history, or genetic predisposition (Clark & Alsubait, 2023).

Tobacco remains one of the primary risk factors for most types of lung cancer. There has not been a single predominant causal factor that may fully explain lung cancer in individuals who have never smoked. However, important risk factors for non-smokers include second-hand smoke, exposure to radon, environmental exposures such as indoor air pollution, asbestos, arsenic and additionally history of lung diseases, and genetic factors. It is the most avoidable risk factor, thanks to public health initiatives that have led to a reduction in its consumption. Nevertheless, despite continuous efforts to decrease tobacco sale and consumption, it continuously has serious adverse effects not only limited to the risk of lung cancer development (Steuer et al., 2021). According to reports published by the Smoking and Health Office, belonging to the Center for Disease Control and Prevention in the United States, there is an average increase of 50% in mortality in patients who are smokers at the time of diagnosis, with a lower percentage in those who were former smokers at the time of diagnosis.

Furthermore, the health status is significantly diminished at 12 and even 6 months in patients who continue smoking after diagnosis. During the 1980s, tobaccoconsumption reached its peak in women, two decades later than in men. This growing consumption led to an increasing incidence of NSCLC in women. However, currently, tobacco consumption in women has decreased, following by a declining in the incidence and mortality rate. Thus, now the incidence in men is 1.5 million of new cases compared to 800,000 new cases in women (National Center for Chronic Disease Prevention and Health Promotion (US) Office on Smoking and Health, 2014).

The primary issue in lung cancer is that several tobacco compounds are carcinogenic, with the ability to bind to DNA molecules. Some of these particularly concerned agents are tobacco-specific nitrosamines (TSNAs) formed through the nicotine nitrosation process during tobacco processing and smoking. They may directly access the lungs through inhalation. The nitrosamine ketone derived from nicotine (NNK) is the most potent TSNA carcinogen which covalently binds to the DNA of lung cells, forming adducts. _This type of DNA damage to DNA may be repaired by cell DNA repair mechanisms or apoptosis in case this damage cannot be repaired. However, continued exposure to these compounds and issues in the DNA adduct repair processes lead to the permanent occurrence of mutations, ultimately triggering the activation of oncogenes and thus initiating the tumorigenic process (Zheng & Takano, 2011).

All histological lung cancer types are associated with tobacco consumption, being the association stronger in LUSC. Conversely, LUAD is the NSCLC subtype that has been more prevalent in non-smokers, accounting for 62% in non-

smokercompared to 19% in smokers. Although the LUAD incidence is increasing in smokers in the last years (Gabrielson, 2006).

Other factors that may influence NSCLC appearance include alcohol use, environmental exposure to secondhand smoke, asbestos, radon, arsenic, chromium, nickel, as well as exposure to ionizing radiation, and polycyclic aromatic hydrocarbon (Zhou, 2019). Remarkably, other pathological conditions like pulmonary fibrosis or human immunodeficiency virus (HIV) are also important when it comes to NSCLC etiology. Patients with pulmonary fibrosis have been found to have an approximately sevenfold increase in the risk of developing lung cancer, and this has been shown to be independent of tobacco use (Hubbard et al., 2000). In addition, the incidence of lung cancer in patients with HIV has also been found to be increased compared to the uninfected population, and this has been shown to be independent of smoking status or antiretroviral therapy use in the HIV population (Kirk et al., 2007).

1.3.3. Treatment

There are almost 590 therapies which are being developed for the treatment of NSCLC. Almost 50% of those therapies are based in immunotherapy whereas the other 50% are based in the non-region-oncology space. This trend of a larger number of therapies in the late phases of clinical trials, leads NSCLC space with the highest number of treatment options in oncology clinical trials. The treatment strategy should consider histology, molecular pathology, disease stage age, performance status, comorbidities, and patient's preferences (Reck et al., 2014).

Surgery has proven to be the most effective therapy when early-stage t tumors are diagnosed in stages I, II, and in some cases, stage IIIA. However, a high percentage of lung patients are diagnosed at advanced stages of the disease. Thus, platinum-based cytotoxic therapies in combination or not with other chemotherapies have been the standard therapy for many years. It was not until the end of the last century, that EGFR inhibitors use began to be employed as targeted therapy with drugs such as gefitinib and erlotinib. However, currently, with genetic and immunological profile analysis at diagnosis, there has been a significant increase in the development of other targeted therapies. The use of target therapy, immunotherapy alone or combined with chemotherapy depends on the mutational profile and the expression of PD-L1 in the tumor (Hirsch et al., 2017).

The standard treatment for patients with early stages I, II, and some IIIA stages is surgery. In these cases, the disease is considered as resectable. Different types of surgery may be used. Minimally invasive techniques included video-assisted thoracoscopic surgery (VATS) and robot-assisted thoracoscopic surgery (RATS). VATS is a safe technique with low morbidity rates and less postoperative complications. Despite current skepticism regarding long-term oncological benefits, different stage I retrospective studies in lung cancer patients have shown no difference in terms of lymph node staging improvement and 5-year survival in patients undergoing VATS compared to thoracoscopic resections (Yang et al., 2019). In addition, surgery may be followed (adjuvant) by chemotherapy, radiotherapy, immunotherapy or EGFR targeted therapy in some stages I, stage II and III (Pulla et al., 2022). Recently, in patients with resectable stage IIIA or IIIB

NSCLC, perioperative treatment with nivolumab plus chemotherapy resulted in a higher percentage of patients with longer survival than chemotherapy alone (Provencio et al., 2023). NSCLC locally advanced (LA) stages typically correlates with limited treatment options and a 5-year survival rate ranging from 4% to 25%. Most of LA-NSCLC patients in stage III have inoperable disease. Thus, stages IIIB and IIIC of LA-NSCLC are treated with chemotherapy that may be in combination with radiation therapy given as separate treatments or at the same period (Felip et al., 2023). Also, chemotherapy and radiation may be followed by immunotherapy with ICB such as anti PD-L1 durvalumab (Antonia et al., 2017). When stage IV NSCLC is newly diagnosed or progressive and is relapsed to previous early-stage treatments, there are other treatments options but here, the prognosis is bad, and the treatment used only increased the OS **(Figure 10).**

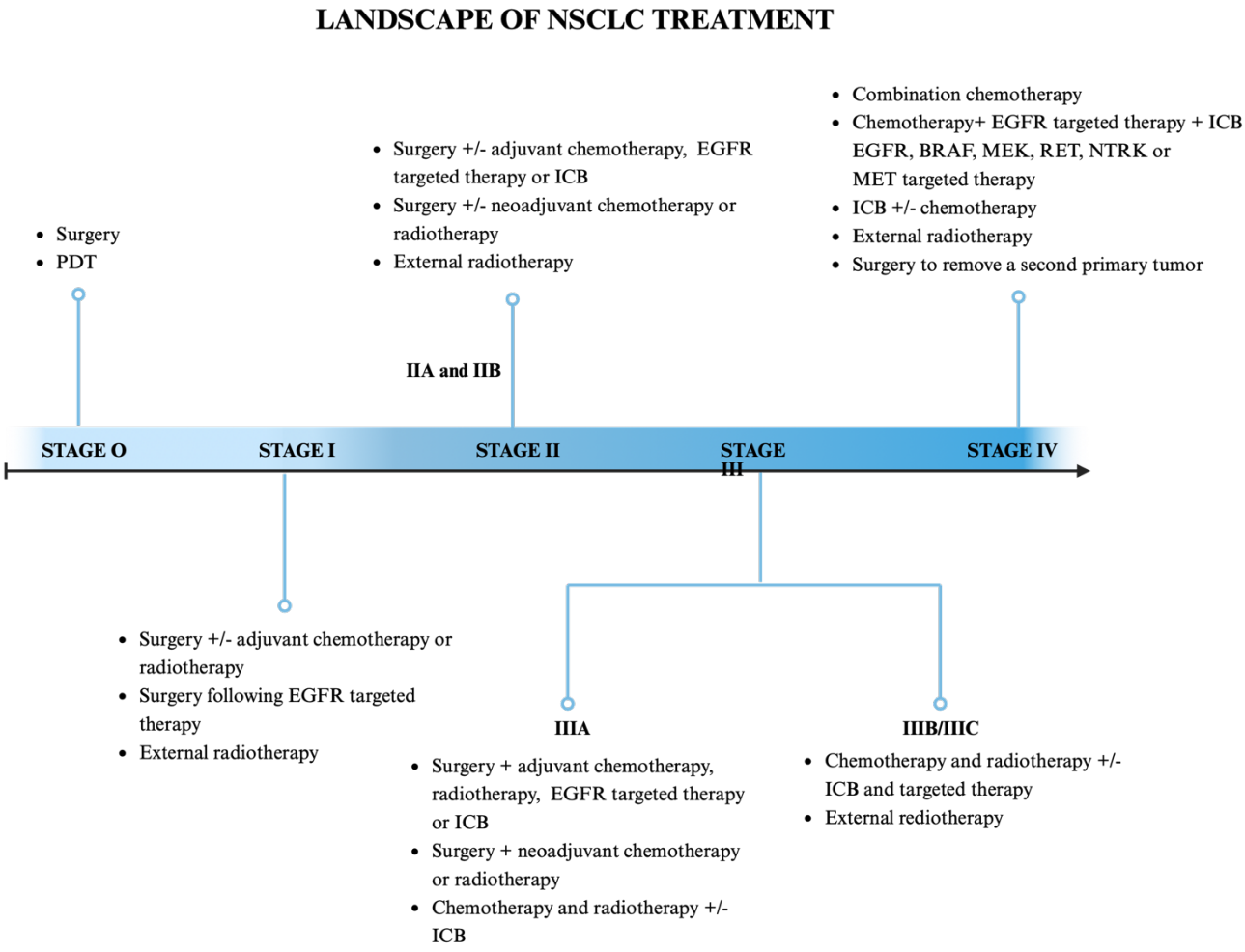

Figure 10. Landscape of NSCLC treatment. (This figure was created with BioRender.com)

Following European Society for Medical Oncology (ESMO) guidelines, in metastatic lung cancer, therapy is used mainly to improve survival and quality of life with the aim to reduce symptoms. Currently, research efforts in metastatic lung cancer have been primarily focused on identifying potential drug targets that are essential for tumor cell survival or their evasion of the immune system. Once a target is identified, therapeutic interventions are tailored to the specific characteristics of each patient's tumor. As it shown in **Figure 11**, molecular testing using broad sequencing panels is performed to evaluate multiple genetic

alterations that are therapeutic targets. Together with molecular testing, PD-L1 assessment is also carried out to evaluate the possibility of ICB treatment. In both cases, combination with chemotherapy may be the treatment choice depend on patient clinical situation. Thus chemotherapy, combinatorial platinum-based chemotherapy regimens, such as carboplatin combined with paclitaxel or carboplatin combined with pemetrexed, have demonstrated enhanced survival rates compared to single-agent chemotherapy. Cytotoxic chemotherapy also provides benefits to patients with a limited performance status of 2. In some cases, patients experience only mild to moderate toxicities, allowing them to maintain their regular activities, However, there are other many cases with several adverse effects such as alopecia, nausea, myelosuppression, and fatigue (Hendriks et al., 2023).

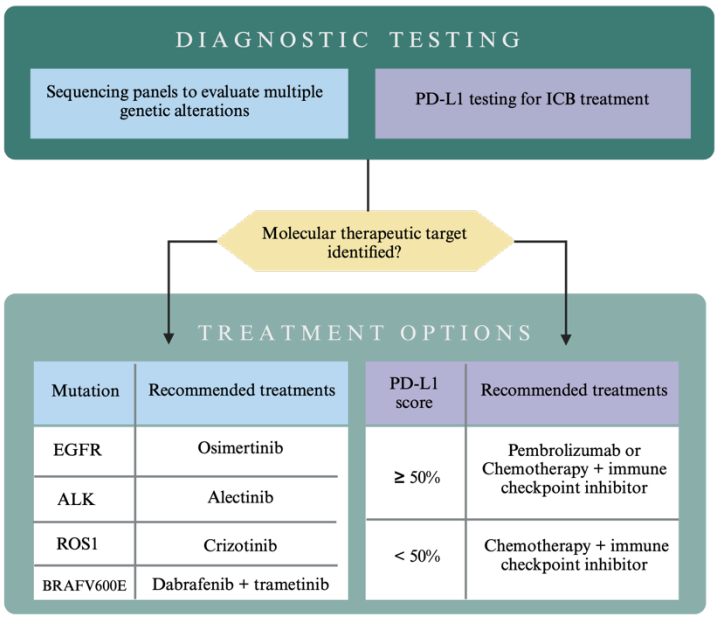

Figure 11. Therapy options for patients with metastatic NSCLC. (This figure was created with BioRender.com)

If molecular targeted mutations are found, there are a vast of targeted therapies recommended depend on that mutation. Some targeted therapies are EGFR tyrosine kinase inhibitor for *EGFR mutation* (osimertininb, gefitinib, erlotinib etc), AKL inhibitor against *ALK rearrangements* (alectinib, lorlatinib, crizotinib, etc) BRAF-V600E or *MEK* inhibitors (dabrafenib plus trametinib) and *RET, NTRK or MET* inhibitors for these gen alterations (selpercatinib, Larotrectinib or tepotinib respectively) (Tsuboi et al., 2023) (Arbour & Riely, 2019).

When PD-L1 expression is greater than 50%, patients may be candidates to receive ICB treatment as single agent. Several pembrolizumab clinical trials have shown that among patients with a PD-L1 tumor proportion score of 50% or greater, pembrolizumab has been found to be superior vs chemotherapy as an initial treatment. (Reck et al., 2016). Regarding other ICB treatments like nivolumab (another PD-1 inhibitor) and durvalumab (an antibody to PD-L1) first-line trials have demonstrated non superiority vs platinum-based chemotherapy among patients with advanced NSCLC (Carbone et al., 2017) (Rizvi et al., 2018). However, among patients with lower PD-L1 tumor proportion scores, the treatment role of single-agent pembrolizumab remains less certain. In these cases, ICB combined with chemotherapy is the treatment choice. Regarding chemotherapy, evidence has suggested that the antitumor effect of chemotherapy is mediated through both a cytotoxic effect and immunological effects (Galluzzi et al., 2015). Phase 2 cohort of open-label KEYNOTEE-021 study (ClinicalTrials.gov, number NCT02039674) demonstrated that the group with the combination of carboplatin, pemetrexed, and pembrolizumab in patients with metastatic NSCLC achieved more objective responses compared with patients in the chemotherapy group (Langer et al., 2016).

Lately, several phase 3 randomized trials confirmed that the combination of chemotherapy and pembrolizumab showed an improved response rate, progression-free survival, and overall survival rates (Gandhi et al., 2018) (Paz-Ares et al., 2018). These studies have resulted in incorporation of immunotherapy into the first line setting for all patients except those with molecular alterations that respond to drug therapy. Surgery together with radiation is currently being investigated for patients with limited metastatic disease often referred to as oligometastatic disease. This condition is defined by having a restricted number of disease sites, typically ranging from 3 to 5 locations.

The knowledge of genetic alterations that drives the tumor growing or how can be used the immune system against tumor have improved the prognosis of lung cancer but in metastatic disease, the curative treatment doesn´t exist and a lot of patients do not response to the treatment and suffer side effects secondary to the drugs used. In this sense, it is very important to search biomarkers that can help us to choose the best treatment.

1.4. Hypothesis and Objectives

1.4.1. Hypothesis

The development of immunotherapies based on immune checkpoint blockade is heading the beginning of a new era in cancer treatment, with a 20-40% tumor response rate in non-small cell lung cancer. However, the clinical use of these agents is limited due to the lack of prognosis and predictive response biomarkers. The recent revolution in the so-called “omics” represents a qualitative leap in the identification of biological mechanisms associated with

treatment response, as not only genetic but also epigenetic variation can affect the transcriptome and modulate the response phenotype. This can occur in both tumors and immune cells. Thus, the purpose of this thesis is to identify prognosis and predictive biomarkers of response to immune checkpoint blockade treatments used in patients with metastatic non-small cell lung carcinoma. These biomarkers should be valid for translational use in patients, specifically for the development of decision-making algorithms in treatment guidelines and for the identification of new targets to address resistance to these immunotherapeutic treatments.

1.4.2. Objectives

Identification of non-invasive prognosis and predictive biomarkers of ICB therapy in patients with metastatic non-small cell lung carcinoma. This is a prospective observational longitudinal study where multiomics profiling is performed at different time points in several blood components collected over 12 months from patients that were clinically characterized with a follow up until death.

1.4.2.1. Specific objectives:

A) Generation and evaluation of molecular and cellular readouts as prognosis or predictive biomarkers in the context of ICB.
    - cfDNA concentration and cfDNA tumor and immune epigenetic marks
    - Small-RNAs from plasma-derived extracellular vesicles (EV)
    - Circulating immune cells and other circulating molecules

B) Multivariate analysis for the integration of molecular and clinical biomarkers in prediction models

CHAPTER II: MATERIALS AND METHODS

2.1. Patient cohort

2.1.1. Immunomark research project

This doctoral Thesis is part of a prospective cohort study called Immunomark with a cohort of 259 patients with metastatic NSCLC or melanoma tumors treated with ICB **(Figure 12)**, and clinically followed up for a median of twelve months.

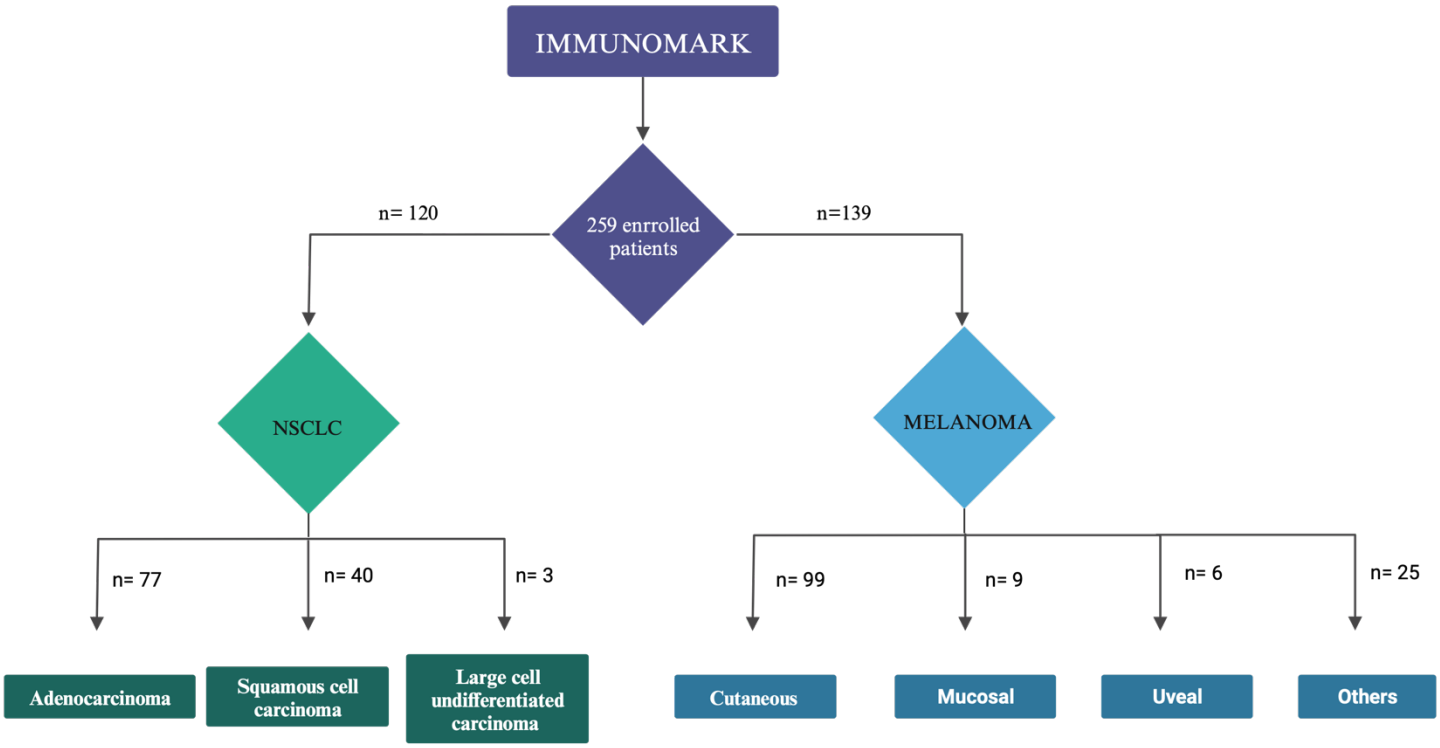

Figure 12. Number of total enrolled patients in Immunomark. Metastatic NSCLC and melanoma enrolled patients until September 2023, treated with different ICB therapies. (This figure was created with BioRender.com).

Patients were treated with different ICB therapies, in combination (cICB) and with single agent (sICB). Single agent like anti PD-1 (pembrolizumab or nivolumab) or anti PD-L1 (atezolizumab) and in combination (with chemotherapy or other investigational drugs as inhibitors or new immunotherapy). The biomarkers were searched for in serial blood samples from patients starting these treatments collected just before treatment (T1), at the second cycle (three to four weeks after the start of therapy) (T2), and six and twelve months after the start of the treatment (T3 and T4). Also, blood samples at the time of progression were taken when possible. Clinical and imaging evaluations were performed at months three, sex and twelve after the start of the treatment **(Figure 13).**

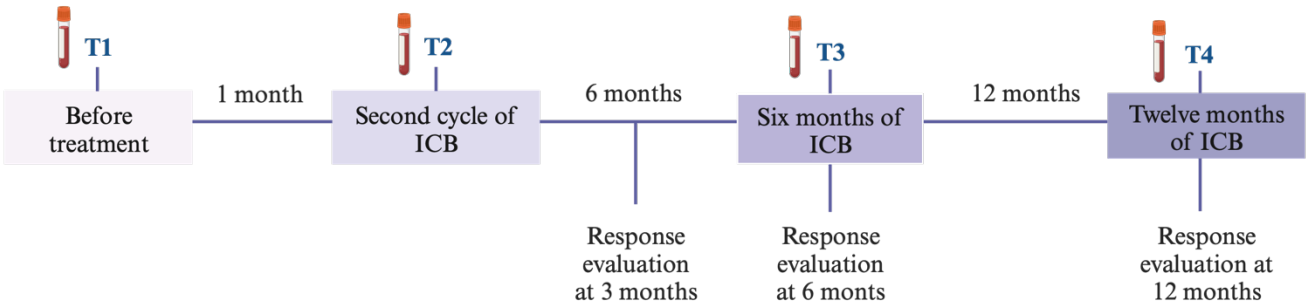

Figure 13. Sample collection and evaluation flowchart. Blood samples from patients with NSCLC and melanoma were collected before treatment (T1), after the second cycle of treatment (T2), after six and twelve months of treatment (T3, T4) and at time of progression. Imaging evaluation was performed at three, six and twelve months following RECIST v1.1 guide. (This figure was created with BioRender.com)

This Thesis project in associated to Immunomark research line. It was initially financed by the European Commission in 2018 and found continuation with several programs including Health Strategic Projects and Technology Transfer Projects from Carlos III Health Institute. The study protocol strictly complied with

the principles of the WMA Declaration of Helsinki and the Department of Health and Human Services Belmont Report Good Clinical Practice guidelines. Also, Immunomark was submitted and approved by Ethics Committee of Provincial Research of Málaga (Málaga, Spain), approval reference 26/10/2017. The approval date was 26 October 2017, and the title of the research project was "Omics integration for precision cancer immunotherapy" (799818, H2020-MSCA- IF-2017).

The main objective is the study of immunotherapy biomarkers in patients diagnosed with solid tumors and undergoing first-line or subsequent-line immunotherapy treatment. Following a careful and detailed exposition of the study, its objectives, and procedures, written informed consent was obtained from all patients. All diagnoses were confirmed by pathologists from the patients' respective original hospitals through appropriate histological and immunohistochemical studies. The study was conducted following the REMARK guidelines (McShane et al., 2005) and the requirements proposed (Simon et al., 2009)

2.1.1.1. Inclusion and exclusion criteria:

Patients were included in the study is they complied with the following criteria **(Table 1)**: histological confirmation of metastatic Non-Small Cell Lung Cancer, being of age, having a functional status of Eastern Cooperative Oncology Group (ECOG) less than 2, and presenting normal hepatic, renal, cardiac, and bone marrow organ function. Availability of a pre-treatment biopsy with sufficient tumor material for histological and molecular studies was considered relevant for patient selection. Patients were enrolled regardless of the stage, orpersonal/family history of cancer at time of cancer diagnosis.

Regarding exclusion criteria, refusal to participate in the study after informed consent, contraindications to receive immunotherapy and chemotherapy, having other uncontrolled infectious diseases, the coexistence of a different neoplastic diseases, or autoimmune diseases implied exclusion.

Table 1. Immunomark inclusion and exclusion criteria.

INCLUSION CRITERIA	EXCLUSION CRITERIA
Histological Diagnosis of NSCLC	Contraindications to immunotherapy or chemotherapy
Patients over 18 years old with the capacity to understand the study's characteristics and signing of informed consent	Refusal to participate in the study after informed consent
Functional status (ECOG) < 2	Presence of uncontrolled infectious diseases or coexistence of a different neoplastic disease
Tumoral stage of IIIB-IV	Presence of autoimmune diseases
Adequate renal, hepatic, cardiac, and bone marrow organ function	Prior antineoplastic therapy of any kind

2.1.1.2. Clinical data:

Clinical data across the cohort was obtained at baseline and different blood sample extraction and evaluations mentioned before in **Figure 13**. All patient data were obtained, treated, and stored following applicable legislation (Organic Law 03/2018) on Protection for Personal Data). Data from blood samples were used to analyze different biomarkers with potential prognostic and predictive value as

previously described in section 1.4.2. In addition, anatomopathological, clinical, and epidemiological characteristics of the patients were collected and subsequently correlated with the results. All clinical characteristics were collected due to their importance as prognostic and predictive factors for immunotherapy treatment: sex, age, diagnosis, smoking status, performance status at the time of treatment (ECOG), TNM (tumor, node, metastasis) stage at the time of diagnosis, presence and location of metastases, tumor burden defined as the number of metastatic lesions, previous treatments, ICB used, treatment response, progression, and levels of PDL1 in the tumor stroma. In **Table 2** all clinical and molecular variables are described.

Table 2: Clinical and molecular variables of Immunomark studio. Classification was made n based on variable name, type of variable and measure unit.

VARIABLE	TYPE OF VARIABLE	MEASURE UNIT
Clinical variables		
Age	Quantitative dichotomous	(Less than 60, more than 60)
Sex	Qualitative dichotomous	(male, female)
Smoking status	Qualitative polychotomous	(never, exsmoker, active)
Diagnosis subtype	Qualitative polychotomous	(LUAD, SCC, others)
Stage at diagnosis	Qualitative polychotomous	(I, II, III, IV)
ICB treatment	Qualitative dichotomous	(ICB, ICB+others)
Previous treatment lines	Quantitative polychotomous	(1,2,3, more)
Number of metastases	Quantitative polychotomous	(1,2,3, more)
Site of metastases	Qualitative polychotomous	(lung, brain, nodes, liver, bones)
ECOG	Quantitative polychotomous	(0,1,2,3)
Toxicity to ICB (all grades)	Qualitative dichotomous	(yes, no)
Maximum toxicity grade	Quantitative polychotomous	(0,1,2,3,4)
Progression	Qualitative dichotomous	(Yes, No)
State last evaluation	Qualitative polychotomous	MCE, VSE, VCE
PDL1	Quantitative variable	% of positivity
LDH	Quantitative variable	% of amount
Molecular variables		
cfDNA	Quantitative variable	Concentration
Transcriptomic variables	Quantitative variable	Log2fold change
Epigenetic variables	Quantitative variable	% 5mC/5hmC
Circulating immune cells	Quantitative variable	Cell number/%

Radiological responses were evaluated from computed tomography (CT) scans according to "Response Evaluation Criteria in Solid Tumors" (RECIST v1.1 guide) measuring the sum of the largest diameter of lesions. Complete response (CR) was defined as the disappearance of all target lesions (TLs) and absence of new non-target lesions (nonTLs). Partial response (PR) was defined as decrease of

the sum of TLs ≥ 30%. Stable disease (SD) was defined if the criteria of CR or PR were not met and objective evidence for tumor progression was absent. Progressive disease (PD) was defined as an increase of the sum of TLs ≥ 20% or the appearance of new nonTLs (Schwartz et al., 2016).

Parameters such as time-to-progression, overall survival (OS), progression free survival (PFS) and death status were assessed. Overall Survival was defined as the time between the start date of ICB treatment to death from any cause. Progression-free Survival was defined as time between the start date of ICB treatment to the date of disease progression according to either death or disease progression on imaging on those evaluation assessments. If a patient died without a confirmed radiological progression, the date of his/her death was considered as his/her progression date. Per iRECIST criteria, any radiological progression required confirmation in a second radiological valuation if available, to exclude pseudoprogression phenomena (Seymour et al., 2017). Several patients' groupings according to response have been evaluated in this Thesis project. One classification used was based on extreme phenotypes. Extreme responders (ER) were those patients that did not present PD for at least one year in treatment. Extreme non responders (ENR) were those patients with PD in less than 3 months from the start of ICB. Patients could also be classified as early and non-early responders if the progression status was defined at 3 months of ICB. An intermediate classification used the status after 6 months of treatment and finally the long-term responders (LTR) and non-responders (LTNR) corresponded to the 12 months clinical evaluation. The development of immune-related adverse

events ('irAEs') was noted as per the National Cancer Institute Common Terminology Criteria for Adverse Events (CTCAE) (National Cancer Institute, 2021).

2.2. Sample processing

2.2.1. Blood processing:

Blood samples were collected in a total of eight collection tubes and were processed differently depending on the liquid biopsy component to be studied **(Figure 14).** For cfDNA isolation, blood was collected in three CellSave preservative tubes (Menarini Silicon Biosystem Inc) of 10 ml each. The other five tubes are X100 K2-EDTA tubes of 10 ml (2 tubes, one for exosome isolation and one for flow cytometry) and 3 ml (3 tubes for the separation of the PBMCs fraction, which includes any existing CTCs). Three CellSave tubes and the 10 ml X100 K2-EDTA tube were centrifuged at 1600 rpm 10 min. The remaining plasma is centrifuged again at 4750 rpm 10 min. The cleaned plasma is then stored at -80°C in 3 mL cryovials. For PBMCs isolation, blood from three X100 K2-EDTA tubes of 3 ml each were slowly poured over Ficoll (Cytiva) for differential centrifugation at 400g for 30 minutes at room temperature and off brakes. The buffy coat fraction was then cleaned up and centrifuged at 16,000g for 10 min at 4°C. The final pellet was diluted in Fetal Bovine Serum (FBS) (Sigma-Aldric) and then stored in liquid nitrogen in 3 mL cryovials. The remaining X100 K2-EDTA 10 ml tube was used to determinate the immune profile phenotype of circulating immune cells by flow cytometry.

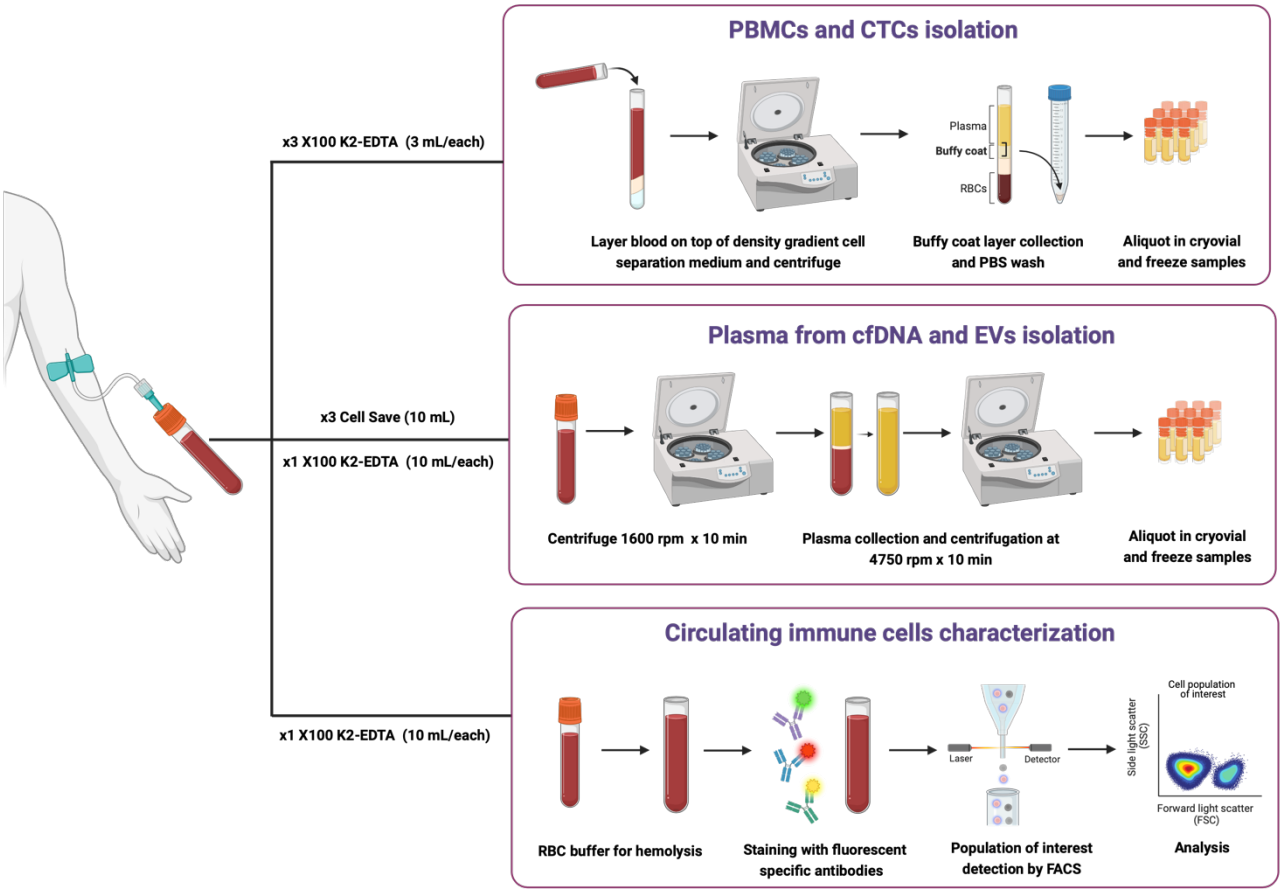

Figure 14: Schematic workflow of blood sample processing. Three different blood processing protocols were performed (This figure was created with BioRender.com)

2.2.2. Tissue biopsy collection and storage:

Tumor blocks from patients preserved in paraffin were requested to Biobank by official form for each patient. Each patient's petition was sent password-protected, by email or directly to the biobank personnel. Following this, the biobank provided us with the material with the Pathology Report containing the sample diagnosis, the available paraffin block, a staining section with hematoxylin and eosin staining also evaluated by the pathologist. This later evaluation involves a remarkable section of the tumor area specifying the percentage of tumor within this area. Blocks were then stored until the extraction date. Then, biopsies, with

enough size, were selected to continue with further analysis. Firstly, those selected blocked were registered in Immunomark database and then they were cut following the Cutting Formalin-Fixed, Paraffin-Embedded using the microtome HM340E (ThermoFisher).

2.3. Biomarkers identification

2.3.1. Quantification of cfDNA in blood samples from mNSCLC

2.3.1.1. cfDNA isolation and quantification:

All samples were collected in CellSave preservative tubes (Menarini Silicon Biosystem Inc) and processed following 2.2.1 **(Figure 14).** 3 ml of frozen plasma were used to extract cfDNA with QIAamp Circulating Nucleic Acid kit (Qiagen, 55114) according to the manufacturer's procedure. The concentration of cfDNA was measured by 1X Qubit High Sensitivity and NanoDrop (Thermo Fisher Scientific). Also, fragment size and concentration in the typical cfDNA size range were evaluated additionally using Bioanalyzer 2100 (Agilent Technologies).

2.3.1.2. Statistical methods:

All statistical analyses were performed using the R software version 4.0.2. To determine the association between cfDNA concentration, clinical variables and response criteria, different statistical tests were used. Wilcoxon and Kruskal-Wallis Test were used to compare cfDNA concentration with categorical variables. Fisher's exact or Chi-squared tests analyzed categorical variables, and Pearson

correlation tests were used for continuous variables. Time-to-event outcomes, PFS and OS were described via the Kaplan–Meier method from the start of therapy to the date of first reported PD for PFS and death for OS. PFS and OS survival curves were stratified by high and low cfDNA concentration at basal and post-therapy and compared using the Log-rank test. Cut-off estimation was performed using Maxstat package for cfDNA baseline and cfDNA concentration after second cycle of ICB. Thus, cfDNA concentration in both cases was dichotomized using a cut-off of 0.55 ng/µL. Univariate and multivariate Cox regression models were used to assess different variables associated with survival and to estimate hazard ratios (HR) such us age, ECOG, LDH or PDL-1 and cfDNA. Area Under the Curve (AUC) was used to evaluate the performance of these different Cox regression models.

2.3.2. Identification of epigenetic marks in cfDNA

2.3.2.1. Epigenetic cfDNA libraries preparation and targeted sequencing

3 mL of frozen plasma from all sample collection times were used for the isolation of cfDNA as described in **Figure 14**. Departing from cfDNA, custom epigenetic libraries were prepared adapting the enzymatic methyl-seq (EM-seq) protocol with NEBNext Enzymatic Methyl-seq kit (New England Biolabs). This method detects 5mC and 5hmC using three enzymatic reactions as shown in **Figure 15**. The rationale of specific 5mC and 5hmC profiling in cfDNA is to use naturally existing enzymes that act on these modifications with minimal impact of DNA integrity. This procedure uses two enzymes present in the de-methylation processes in mammals: ten eleven translocation 2 (TET2) and apolipoprotein B mRNA editing enzyme, catalytic polypeptide-like (APOBEC3A). TET2 produces 5-

carboxylcytosine from 5-methylcytosine/5-hydroxymethylcytosine with 5-formilcytosine as an intermediate product. APOBEC3A deaminates native and modified cytosine towards different products depending on the cytosine state: if native, into Uracil (Thymine after PCR); if 5mC, into Thymine; if 5hmC, into 5hmUracile (Thymine after PCR). It does not deaminate 5caC. The third enzyme is T4 Phage ß-glucosyltransferase (T4-BGT), which transfers the glucose moiety of uridine diphosphoglucose (UDP-glucose) to the 5-hydroxymethylcytosine residues in double-stranded DNA generating ß-glucosyl-5 hydroxymethylcytosine. This infers protection from TET2 and APOBEC3A enzymatic action. The discrimination of 5mC from 5hmC is achieved through the treatment of the cfDNA with T4-BGT+APOBEC3A±TET2. The combination of T4-BGT+APOBEC3A yields the specific 5hmC signal, since native and 5-methylated Cytosines are deaminated and seen as Thymines after sequencing. On the other hand, the full combination T4-BGT+APOBEC3A+TET2 detects the composite signal of 5mC and 5hmC, conceptually equivalent to the bisulfite approaches, because 5mC is oxidized to 5caC and therefore also avoids deamination by APOBEC3A. 5hmC and 5mC will be finally detected as Cytosines and only native Cytosines will still be deaminated and detected as Thymines. The percentage of composite (5mC+5hmC) methylationwill be calculated on the basis of the sequenced Cytosines at the CpG sites, and the 5mC component in the subtraction of the 5hmC signal from the composite one.

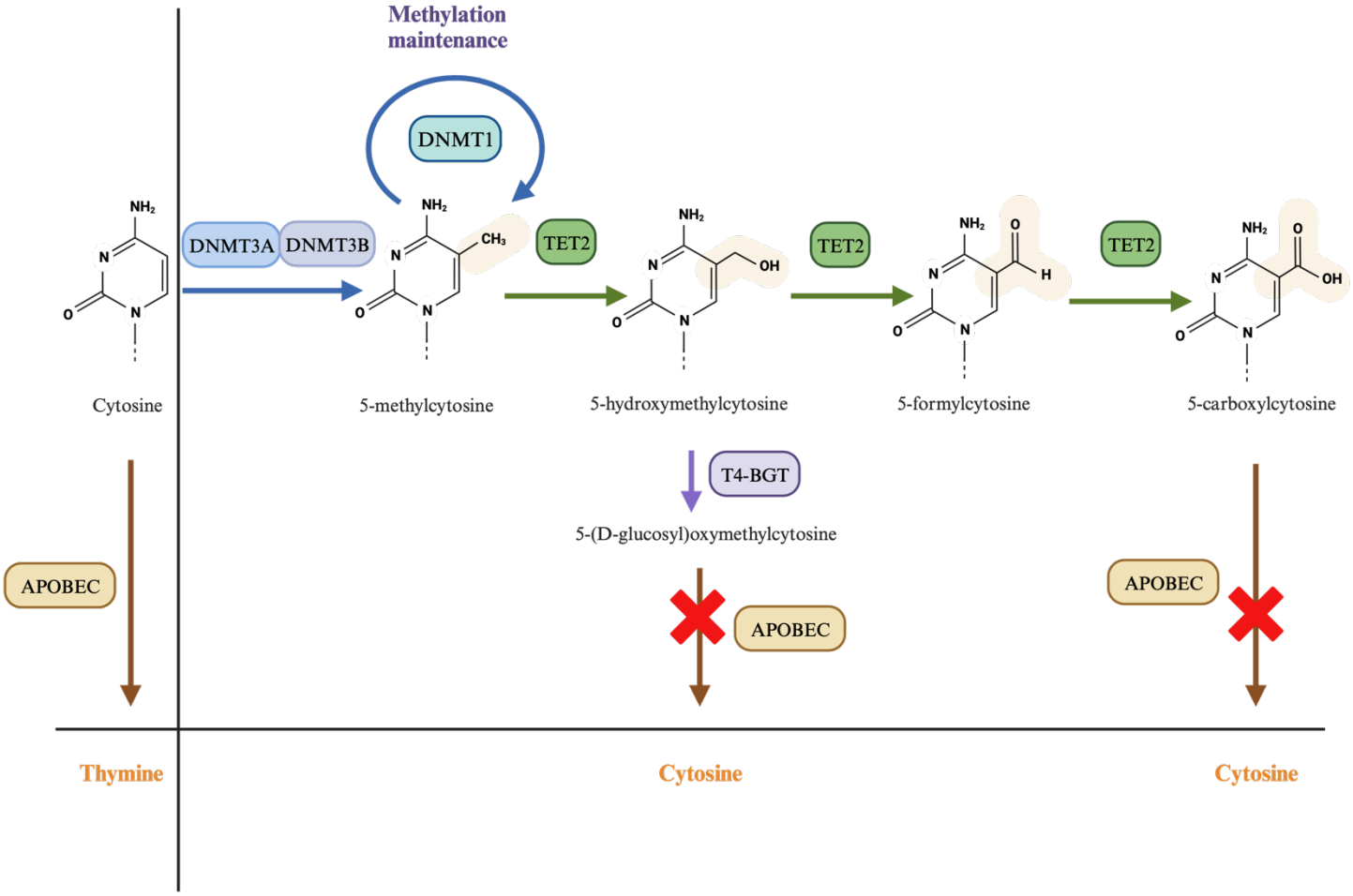

Figure 15. Enzymatic methyl-seq (EM-seq) concept. In nature, cytosine may be methylated by DNA (5-cytosine)-methyltransferases 3A and 3B (DNMT3A/DNMT3B). Depending on cellular situation, this methyl group may also be continuously maintained by DNA (5-cytosine)-methyltransferase 1 (DNMT1). Modified 5C might endure other modifications in its process of elimination. The 5-methyl group may be hydroxylated and 5-methylcytosine (5mC) is converted into 5-hydroxymethylcytosine (5hmC), a reaction catalyzed by TET2 enzyme. 5hmC may undergo different processes. TET2 may continue catalyzing 5hmC, generating other intermediates products such as 5-formylcytosine (5fmC) and 5-carboxycytosine (5caC). (This figure was created with BioRender.com)

Figure 16 depicts the library preparation workflow The According to the manufacturers of the NEBNext Enzymatic Methyl-seq (New England Biolabs), 200 ng of good quality genomic DNA are recommended. However, the protocol has been modified to adapt the cfDNA as starting material due to typical low concentrations and quality of this compound compared with genomic DNA.

Another technical modification was the omission of the shearing step based on the natural fragmentation of cfDNA and to decrease the risk of degradation. Starting cfDNA amounts were optimized to 10-20 ng for 5mC and >20 ng for 5hmC because extended enzymatic incubations were also established to secure full C and 5mC deamination. T4-BGT incubation time for this 5hmC track was also doubled and we optimized the T4-BGT versions according to performance.

In the library amplification step, PCR cycles were finally settled 12 as a balance number to increase the final amount of cfDNA libraries with the minimal effect on duplicates. Fragment size and concentration of the 5hmC and 5mC+5hmC libraries were evaluated using the Bioanalyzer 2100 system (Agilent Technologies) to determine the amount required for the subsequent probe capture process via hybridization of specific cfDNA regions of our customized gene panel.

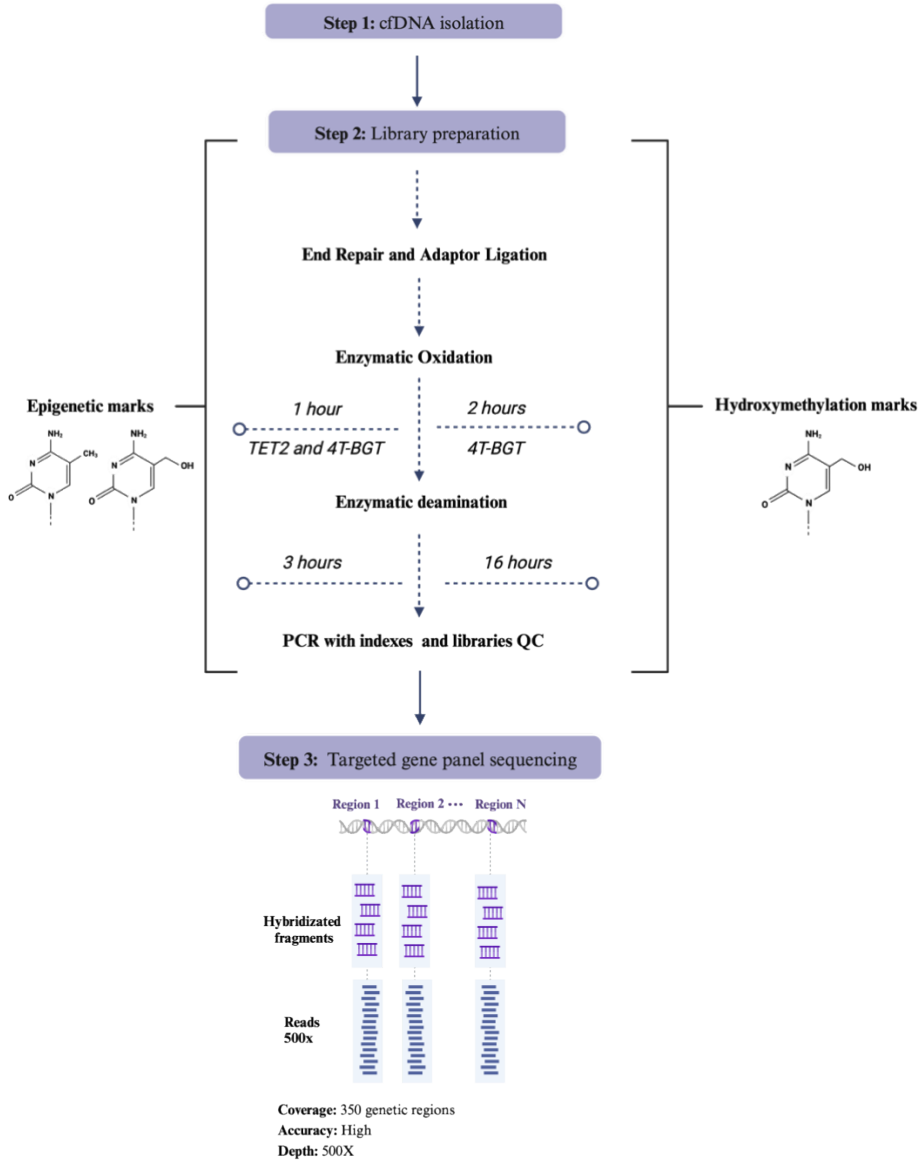

Figure 16. cfDNA epigenetic libraries workflow. After cfDNA isolation from plasma samples **(Step 1),** cfDNA quantification and initial amount optimization led to the library preparation step **(Step 2).** Here, T4-BGT+APOBEC3A±TET2were used in duplicate cfDNA samples to profile both epigenetic marks. End repair and universal adaptor ligation was followed by incubation in T4-BGT for 5hmC (2h) and TET2 and T4-BGT for 5mC+5hmC (1h). The next step was APOBEC3A deamination for 16 hours to detect 5hmC and 3 hours to detect just 5mC+5hmC. Finally, amplification with specific indexes was performed for both workflows. 5hmC and 5mC+5hmC libraries from the same patient were then hybridized with the panel probes and sequenced with a vertical coverage of 500X **(Step 3).** (This figure was created with BioRender.com).

The genetic panel encompassing 344 genes (2276 promoter regions) and 841 enhancers, describe all the features that you have of the panel in numbers was previously designed by the team based on transcriptomic data in tumor tissue and particular tumor related genes in NSCLC. These regions included enhancers and promoters; genomic regulatory elements involved in gene expression regulation. Probes against these regions were designed by Twist Bioscience and those with more than 70% of theoretical target coverage were selected to ensure sufficient coverage and probe depth for each target. Also, our Twist Custom Methylation Panel was optimized for methylation detection and includes probes to capture all 4 potential sequences at a given site: methylated, unmethylated, sense and antisense.

Twist Biosciences specific methylated and unmethylated probes were used to hybridize previous cfDNA libraries using the Twist Fast Hybridization Target Enrichment kit. The initial amount for each library is 187.5 ng, and there was also an optimization about different pool hybridization alternatives based on this quantity to avoid sample data loss during sequencing. Those libraries with a final output of 1-4 ng/uL were pooled in a three samples pool, libraries between 5-8 ng/uL were pooled in a six samples pool, and libraries with more than 8 ng/uL were pooled in an eight samples pool. Finally, paired-end sequencing of 150 base pairs is performed using the Illumina NovaSeq sequencer with the S4 200 bp kit (Illumina Inc., San Diego, CA, USA), including 10% PhiX and with a depth sequencing of 500X. The Q-score of the individual reads is calculated using RTA3 software. The results obtained from the NextSeq Control Software (NCS) are

demultiplexed and converted into FastQ format files using the Illumina Bcl2fastq software (v1.9.0).

2.3.2.2. Processing and mapping of methylation and hydroxymethylation data

Raw sequencing data (fastq files) was subjected to initial processing for quality control and adapter removal using Trim Galore. (Babraham Bioinformatics Institute). This step aimed to ensure the removal of low-quality reads and adapter sequences. Processed reads were aligned to the reference genome hg38 using Bismark. Bismark performs alignment specifically tailored for bisulfite-treated sequences, allowing distinction between methylated and unmethylated cytosines. Alignment outputs were further processed within the Bismark pipeline to remove duplicate reads and ensure accurate representation of the methylation and hydroxymethylation profiles (Krueger & Andrews, 2011). Methylation and hydroxymethylation levels were called and quantified from the aligned reads using Bismark's suite of tools: bismark_methylation_extractor. Also, the tool CollectHsMetrics from Picard software was used with previous aligned bam files and our designed panel to compute a set of hybrid selection specific metrics (Broad Institute) **(Figure 17).**

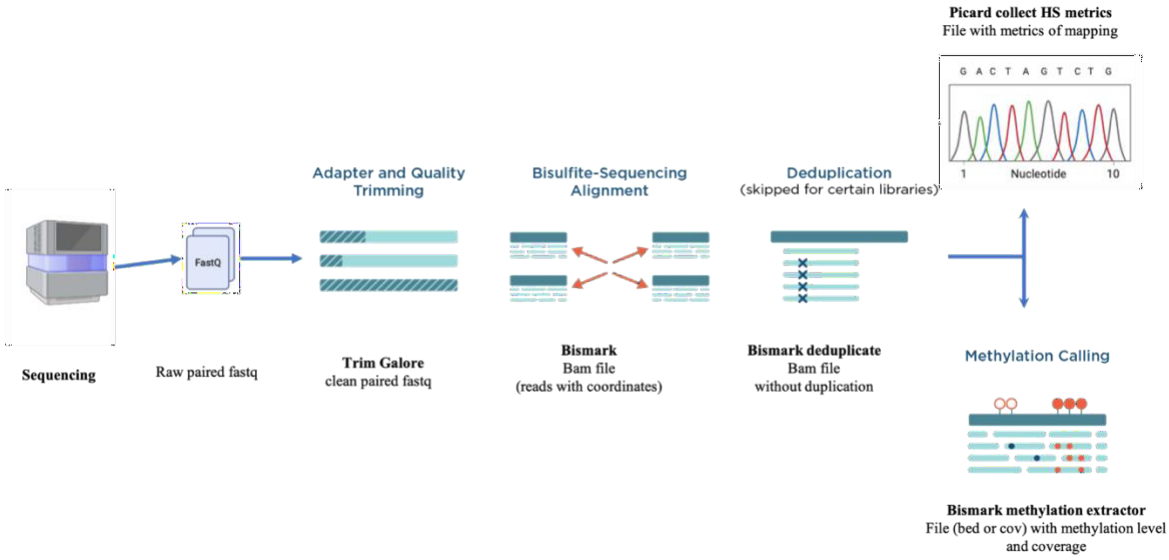

Figure 17: Bioinformatics pipeline for epigenetic data All steps from the fastq file obtained after sequencing. Adapter removal is performed using Trim Galore, aiming to eliminate low-quality reads and adapter sequences. The processed reads are then aligned to the reference genome using Bismark, a tool tailored for bisulfite-treated sequences to distinguish methylated and unmethylated cytosines. Alignment outputs underwent further processing within the Bismark pipeline to remove duplicate reads and ensure accurate representation of methylation and hydroxymethylation profiles. Methylation and hydroxymethylation levels were then determined and quantified using Bismark's suite of tools, particularly bismark_methylation_extractor. Additionally, the tool CollectHsMetrics from Picard software was utilized to compute a set of hybrid selection specific metrics from the aligned bam files and a designed panel. (This figure was created with BioRender.com).

2.3.2.3. Differential enrichment analysis

The analyses below were performed using both 5mC and 5hmC datasets. Differential methylation analysis was used to identify differentially methylated/hidroxymethylated regions (DMR and DHR) with respect to its genomic position at CpG sites, CpG core islands, enhancers, shelves, shores, and transcription factors (TF) between responder and non-responder patients

following response criteria previously described in section 2.1.1.2. For this thesis, R package Methylkit was used with specific analysis parameters such as coverage criteria min vertical-coverage of 10 and min horizontal-coverage of 50% over 10X) (Akalin et al., 2012). Then, principal component analysis was used to check and remove batch effect. Unite tool allowed to assemble the coverage and C's matrix. Also, a table was created with DMR/DHR and their ß-value.

2.3.2.4. General statistical analysis

All statistical analysis described in this thesis were performed within the R package (v4.0.4). The genomic regions and their locations on the genome were downloaded from the Ensembl website and loaded into R studio. Ggplot2 was used to create plots of each condition comparison for the Methylkit results annotated to genes. Heatmaps were created for DM CpG sites in all analysis. However, Only, statistically significant DM CpG sites, CpG core islands, enhancers, shelves, shores and transcription factors (TF) regions with adjusted p-value were made into a bar graph which displayed the number of marks associated with the gene and the direction of the differential methylation/hydroxymethylation (from 0 to 1).

2.3.3. miRNA analysis from plasma- derived extracellular vesicles

Differential expression of miRNA from plasma-derived extracellular vesicles (EV) between responder and non-responder patients to ICB workflow was performed as indicated in **Figure 18:**

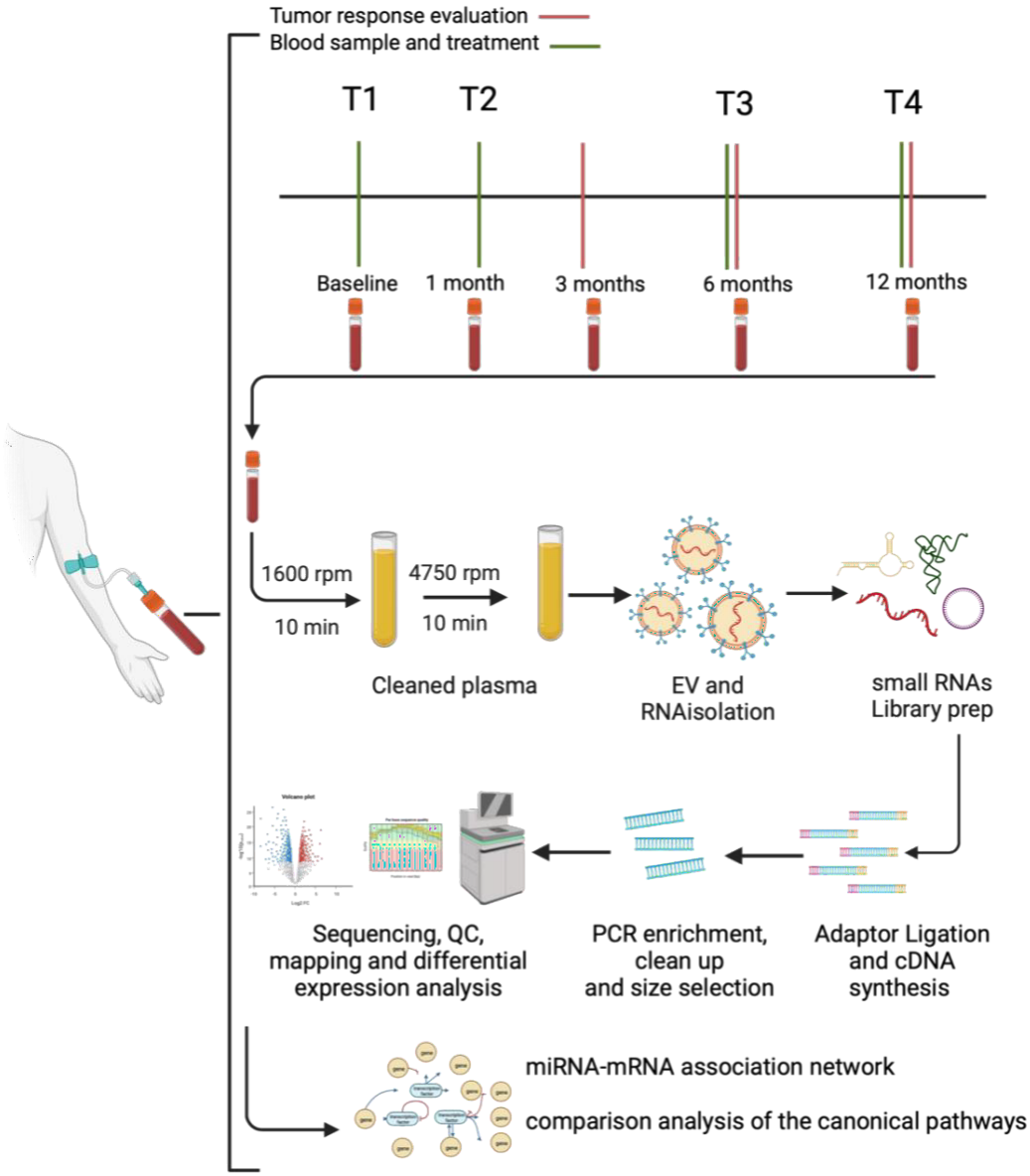

Figure 18: Total RNA isolation from derived-plasma extracellular vesicles and differential expression miRNA analysis flowchart. Plasma samples from patients with mNSCLC were collected at different times. Total RNA from all samples was isolated directly from plasma-derived extracellular vesicles. Small- RNA libraries were performed and sequenced by NGS. Descriptive and differential expression analysis was carried out among responders and non-responders before and after ICB treatment. (This figure was created with BioRender.com).

2.3.3.1. Extracellular vesicles (EV) characterization

Plasma-derived extracellular vesicles from patient's samples were isolated using 1 mL of cryopreserved plasma at -80°C ExoEasy Midi kit (Qiagen) according to the manufacturer's protocol. Then, EV were characterized and visualized by nanoparticle tracking analysis (NTA) using NanoSight NS300 to analyze the total number, concentration, and size diversity. The protocol was performed at Centro de Investigación Príncipe Felipe (Valencia). Samples were diluted 1:1000 in PBS and adjusted until the EV concentrations were in the correct range, between 50-200 particles per frame. After calibrating the equipment with polystyrene beads and cleaning impurities with PBS, the sample was subsequently injected into the machine. A laser was directed into the flow cell and a camera detected the subsequent scatter of light which resulted from contact between the laser and particles in solution Also, same isolated particles were visualized with evaluated transmission electronic microscopy (TEM) also at Centro de Investigación Príncipe Felipe (Valencia) to confirm the presence of particles with the size and structure characteristic of EV.

2.3.3.2. Small RNA libraries and sequencing

As described in 2.2.1. section (Figure 14), total RNA from plasma-derived extracellular vesicles from all patients' samples, was isolated using 1 mL of cryopreserved plasma at -80°C using ExoRNeasy Midi kit (Qiagen) according to the manufacturer's protocol. The quantity and quality of total RNA was then evaluated by Bioanalyzer 2100 (Agilent Technologies). Total RNA from EV was sent to Novogene Co to perform small-RNA libraries using NEBNext Multiplex Small RNA

Library Prep Kit (New England Biolabs) following the manufacturer's instructions. Total RNA fragments are ligated with 3' and 5' adaptors in two different steps. Between both adaptor ligation steps, hybridization of reverse transcription primer prevents adaptor dimer formation. This primer also hybridizes to the excess of 3' adaptor that remains free after thee 3' ligation reaction, generating a molecule that is not a substrate for ligation mediated by T4 RNA ligase 1 and therefore do not ligate to the 5' adaptor. When 5' adaptor is ligated, fragments were reverse transcribed. Final PCR amplifications were performed by adding different indexes to each sample. Libraries were then quantified by TapeStation system from Agilent using DNA 1000 Chips. Then, an average of 50 nt PCR products from small RNAs were sequenced via the Illumina Novaseq platform using single end reads yielding about ten million reads per sample.

2.3.3.3. Data processing

Fastq quality control and smallRNAs profile distribution was performed with two independent software. sRNAtoolbox is composed of seven independent but interrelated tools and one workflow addressing several analysis modalities. sRNAbench was the tool used for expression profiling of smallRNA and later prediction of miRNA with genome mapping and read length statistics. The second sRNAbench tool used was sRNAde to detect differentially expressed smallRNAs and compare them with our independent analysis (Gómez-Martín et al., 2022). Another independent software used was miRMaster to compare results with sRNAtoolbox (Fehlmann et al., 2021). As mentioned before, analysis was made by our team. Thus, reads were trimmed using Fastp (S. Chen et al., 2018) and rRNA sequences

were depleted using Hisat-3N (Zhang et al., 2021). Trimmed fastq files were mapped against the reference (genome build GRCh38) using Bowtie (Langmead et al., 2009) and reference miRNA read quantification was performed with featureCount (Liao et al., 2013). Percentages of uniquely mapped reads and millions of mapped reads were computed with Qualimap 2 (Okonechnikov et al., 2015).

2.3.3.4. Differential enrichment analysis and statistical analysis

To perform the normalization and test for differentially expressed (DE) miRNA Bioconductor package DESeq2 was used (Love et al., 2014). A miRNA was considered DE if the baseMean count was >3 in at least five samples, the absolute log2FC was >1.5 and the adjusted p-value was <0.05. Different analyses of DE miRNA were performed based on response criteria mentioned in 2.1.1.2. section. Statistical analyses were performed using the R software version 4.0.2 and plots were obtained using ComplexHeatmap and ggplot2. Descriptive statistics were performed between clustered patients based on DE miRNA and clinical characteristics. Thus, Fisher's exact or Chi-squared tests for categorical variables, Wilcoxon test for numerical variables and differences for continuous variables were evaluated by ANOVA. Survival analyses were also performed and time-to-event outcomes, PFS and OS were described via the Kaplan–Meier method from the start of therapy to the date of first reported PD or death for PFS and death for OS. Overall survival curves were stratified by basal signature of DE miRNA risk score and compared using the Log-rank test. Cut-off estimation was performed using Maxstat Rpackage for high and low risk depending on basal miRNA signature.

2.3.3.5. Functional enrichment and analysis of miRNA- mRNA interaction networks

To identify functional miRNA-mRNA interaction networks and their biological pathways, Ingenuity Pathway Analysis (IPA) system (Ingenuity® Systems, Ca., Redwood City, EUA) was used with DE miRNA of the different comparisons as inputs: T1 vs T2, T1 vs T2 separately in responders and non-responders. For all these different conditions, canonical pathways analysis was performed. Finally, enrichment analysis and annotation were done using the miEAA 2.0 platform (Kern et al., 2020).

2.3.4. Circulating immune cell characterization

2.3.4.1 Flow cytometry and biochemistry analysis

Flow cytometry was performed to 10 mL of blood sample from each patient before the treatment started and at different treatment times by the Flow Cytometry and Cell Culture Unit from Hospital Regional and Hospital Costa del Sol (Málaga) following **Figure 14** in section 2.2.1. To avoid red blood cells contamination, Red Blood Cell lysis buffer (Sigma-Aldrich) was added to blood to lysis red blood cells in single cell suspension with no effect on the nucleated cells. Also, to avoid nonspecific antibody binding, all Fc-binding receptor sites present on the cell surface were blocked by incubation with an anti-Fc receptor antibody in the blocking buffer (PBS, 20% fetal calf serum (FCS), Fc blocking reagent, Miltenyi Biotec) for 15 min on ice. Following the blocking step, cells were labeled with antibodies listed in Table 3 organized in 12 staining groups for each panel

and each sample. All the antibodies were used at 1:50 dilution unless indicated otherwise. Fluorescence Minus One (FMO) controls were also performed by staining each sample with all the fluorophores minus one of them. This allows us to set the upper boundary for background signal on the omitted label, and thus to identify and gate positive populations in multicolor experiments. The samples were then analyzed by flow cytometry in a BD FACS Canto II (BD Biosciences). Different PBMC subsets from blood at different times were characterized by flow cytometry. Four different panels were designed in our laboratory to cover the vast range of specific lineage circulating cells. **Table 3** shows each panel's characteristics with staining combinations and fluorochromes.

Panel one was designed to study the ratio of T cells (CD3+) and specific cytotoxic CD8+ T cells (CD3+CD8+), antigen presenting T cells expressing PD1 ligand (PDL1) (CD3+CD8+CD274+CD279-), exhausted T lymphocytes (CD3+CD8+CD279+). In panel two, CD4+ T cells (CD4+), regulatory T cells (CD4+CD25+CD127-) were evaluated. Panel three were designed to assess the ratio of natural killer cells (CD56+CD16-), cytotoxic natural killers (CD56+CD16+/) and myeloid suppressor cells (CD11b+CD14+HLADR+). Finally, with panel four the ratio of activated B cells was measured in plasma (CD20+CD19 +), long-lived plasma cells (CD138+CD27+) and memory B cells (CD19+CD20+CD27+).

Table 3: Staining combinations and fluorochromes used in the flow cytometry assay panels.

	Absortion spectra					
	450-475 nm				620-750 nm	
Emission spectra	FITC	PEE	PCPy5.5	PECy7	APC	APCCy7
Panel 1	CD8	CD274		CD3	CD279	
Panel 2	CD4	CD127				
Panel 3	CD14	CD56	CD11b	CD16		HLADR
Panel 4	CD138	CD20		CD27	CD19	

Other circulating immune cells were also determined at each blood sample treatment time by blood biochemistry test. This test was carried out by each Immunomark associated hospital laboratory when blood from patients were taken. Immune cells such as general leukocytes, lymphocytes, monocytes, eosinophiles, basophiles, neutrophiles or platelets are some of them.

2.3.4.2. Data processing and statistical analysis

Sample data from all times were acquired with DIVA software and downloaded for detailed analyses by flowTOTAL (Onieva et al., 2022). A maximum of eight parameters were obtained for each staining, side-scatter, forward-scatter, and six additional fluorochromes. Univariate statistical tests were used to assess the association between the number of specific cell subsets with clinical variables and response criteria. Wilcoxon and Kruskal-Wallis Test were used to

correlate number of immune cells with categorical variables. Pearson correlation was used to correlate continuous variables. Also, survival analysis was performed. Time-to-event outcomes, PFS and OS were described via the Kaplan–Meier method. PFS and OS survival curves were stratified by baseline and on-therapy number of specific circulating subsets and compared using the Log-rank test.

2.3.5. Multi-omics integration of previously studied biomarkers

Biomarkers previously studied in this project demonstrated prognostic role when survival analysis were performed in mNSCLC. Thus, basal concentration of cfDNA, and clinical variables such age, LDH, ECOG and PDL-1 were included in multivariant model. Univariate and multivariate Cox regression model was performed to estimate the hazard ratios (HRs). Statistical analyses were performed using the R software. Finally, the potential prognosis value of cfDNA concentration was compared with the established model based on the mentioned variables using the AUC estimator proposed by (Uno et al., 2007).

CHAPTER III: RESULTS

3.1. Characteristics of the Study Cohort

A total of 97 mNSCLC patients were selected for this thesis work from the Immunomark project, with 42% of them enrolled in clinical trials. When it comes to number of total samples 273 blood samples were processed and analyzed for all objectives exposed in this thesis. There were 97 samples before treatment (T1), 88 samples at cycle 2 (3 to 4 weeks after the start of therapy) (T2), 54 samples 6 months (T3) and 34 samples 12 months (T4) after treatment started **(Figure 19).**

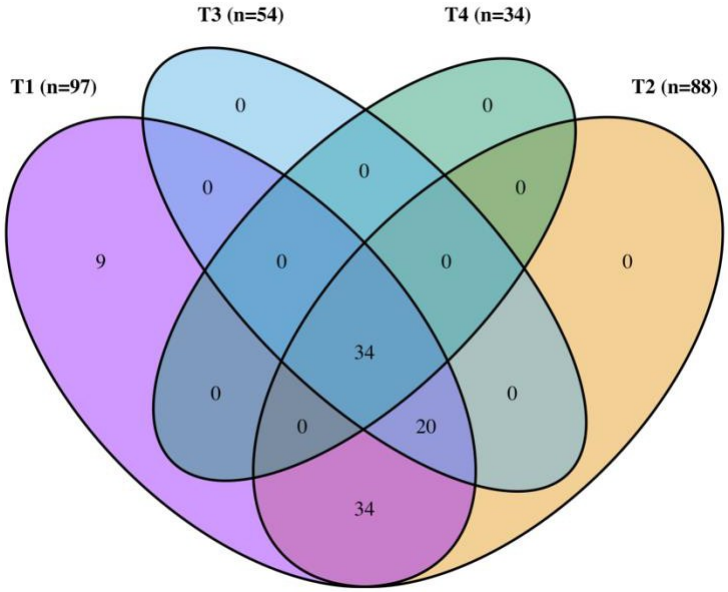

Figure 19. Numbers of the longitudinal cfDNA blood sample collection. Out of 97 patients, only 34 patients could donate the four samples (T1 to T4), and for 9 patients, only the T1 was available.

In **Table 4** are gathered all patient characteristics. Regarding histology, LUAD is the most frequent one (63,9%), while one third of patients are affected by SCC (33%). There is a predominance of male subjects (23,7%). Most patients are smokers (51,54%). Regarding stage at diagnosis, most of the patients were diagnosed with IV stage (73,2%), and no previous treatment before starting this project was indicated in most of the subjects (65%). The treatment schema of 65% of the patients included a combination with other therapies, mainly chemotherapy, while single ICB was administered to around the third part of the patients (34%). The most prevalent number of metastases was 2 (45,4%) and the most frequent type of metastases was lymph node metastasis (56,7%), followed closely by lung metastasis 44,32%). Most patients also presented an acceptable performance status (ECOG score < 2) (92,77%). Predominantly, at diagnosis, PDL1 score was less than 50% (73,19%) and LDHS was mainly normal (not reaching 2fold) (60,82%). Safety assessment was also an important concern in the study. Thus, regarding immune-related toxicity, toxicity grade 1 was the most common toxicity grade (31%)

As mentioned before, iRECIST, were used to classify radiological responses. As expected, radiological progression was related to the subsequent death of the patients. In the first radiological examination, 1 patient met the criteria for CR evaluation, 32 patients were classified as having PR and 35 SD. 23 patients were classified as PD, considering them as early non-responder (ENR) patients. In the second radiological evaluation, 6 months after the start of the treatment, the same patient had CR, 23 patients presented PR and 16 patients SD. The number of patients who progressed increased to 38, and they were considered as patients with non-Durable Clinical Benefit (DCB). After twelve months of treatment, the

third evaluation showed that only 2 patients had CR. 16 patients achieved PR and 11 SD. Again, there was an increase in the number of patients who progressed, with a total of 50 out of 97 patients. Again, there was an increasing number of patients who progressed after one year of ICB treatment, with a total of 50 mNSCLC patients.

Table 4. Clinical variables of the cohort. For each variable, classification and patient distribution are shown. Missing data, termed as "No applicable" (NA) were quantified as well.

PATIENT CHARACTERISTICS	N=97, (%)	NA, (%)
Age		
Less than 60 years	26 (26,8 %)	
More than 60 years	71 (73,2%)	
Sex		
Male	23 (23,7%)	
Female	74 (76,3%)	
Smoking status		6 (6,18%)
Never	5 (5,15)	
Former smoker	36 (37,11)	
Current smoker	50 (51,54%)	
Diagnosis subtype		
LUAD	62 (63,9%)	
SCC	32 (33%)	
Others	3 (3,1%)	
Stage at diagnosis		1(1%)
Stage I	3 (3,1%)	

Stage II	8 (8,25%%)	
Stage III	14 (14,5%)	
Stage IV	71 (73,2%)	
ICI treatment		
ICB	34 (35%)	
ICB + others	63(65%)	
Previous treatment line s		
Yes	32 (33%)	
No	65 (67%)	
Number of metastases		
0	3 (3%)	
1	30 (31%)	
2	44 (45,4%)	
> 3	20 (20,6%)	
Lung metastases		2 (2,06%)
Yes	43 (44,32%)	
No	52 (53,6%)	
Lymph node metastases		2 (2,06%)
Yes	55 (56,7%)	
No	40 (41,23%)	
Skin metastases		1(1,03%)
Yes	32(32,98%)	
No	64 (65,97%)	
Brain metastases		1(1,03%)
Yes	13 (13,4%)	
No	83 (85,56%)	

Bone metastases		2(2,06%)
Yes	29(29,89%)	
No	66 (68,04%)	
Liver metastases		2(2,06%)
Yes	11 (11,34%)	
No	84(86,59%)	
ECOG		3 (3,092%)
0	20 (20,61)	
1	70 (72,16%)	
2	4 (4,123%)	
PDL1		7 (7,21%)
< 50%	74 (73,19%)	
> 50%	19 (19,58%)	
LDH		21 (21,64%)
Normal	59 (60,82%)	
< 2X	10 (10,30%)	
> 2X	7 (7,21%)	
Toxicity to ICB (all grades)		15 (15,46%)
NO	26 (26,8%)	
YES	55 (56,7%)	
Maximum toxicity grade		15 (15,46%)
0	26 (26,8%)	
1	30 (31%)	
2	12 (12,37%)	
>3	13 (13,40%)	
Progression		1 (1%)
No	28 (29%)	
Yes	68 (70%)	

3.2. cfDNA as a predictive and prognostic biomarker in mNSCLC patients treated with ICB.

cfDNA concentration was measured by fluorometry in 273 plasma-derived cfDNA samples from all 97 patients of the cohort There were a total of 97 samples before treatment (T1), 88 samples at second cycle (T2), 54 samples after 6 months (T3) and 34 samples after 12 months (T4) of treatment. **Table 5** summarized analysis characteristics performed to this molecular biomarker.

Table 5: Characteristics of fluorometric quantification of cfDNA. Blood biomarker analyzed in this aim was differences of concentration of plasmatic cell free DNA before treatment started (T1) and after two cycles of ICB (T2) in responder and non- responder patients at three, six and twelve months of tumor evaluation.

Blood biomarker	Treatment time analysis	Response criteria
Plasma-derived cell free DNA concentration	Before treatment starts (T1) At second cycle of ICB (T2)	First tumor evaluation (3 months of ICB) Second tumor evaluation (6 months of ICB) Third tumor evaluation (12 months of ICB) Extreme response

3.2.1. Basal cfDNA concentration is associated with smoking status and bone metastasis.

With the aim of analyzing the predictive and prognostic role of basal cfDNA in mNSCLC patients, different correlation analyses of cfDNA concentration and clinical and molecular characteristics were performed (**Supplementary table 1.A and 1.B.).** It observed no correlations between sample storage time (ranging from 5 to < 1 years in the interval 2019 to 2023) and baseline or post-treatment cfDNA concentrations. Moreover, we did not find significant difference in the median concentrations according to sampling year. Regarding clinical characteristics, there was no statistically significant association between basal cfDNA concentration (T1) and patient's sex, age, diagnosis subtype and stage, ICB treatment, ECOG or PD-L1 status. However, when it comes to smoking status, higher cfDNA concentrations were found to be correlated with those patients who were former smokers (median cfDNA concentration 0.56 $ng{\cdot}uL^{-1}$) before ICB started compared with those who were smokers when ICB started (median cfDNA concentration 0.35 $ng{\cdot}uL^{-1}$) (Wilcoxon Test p-value 0.001) **(Figure 20)**.

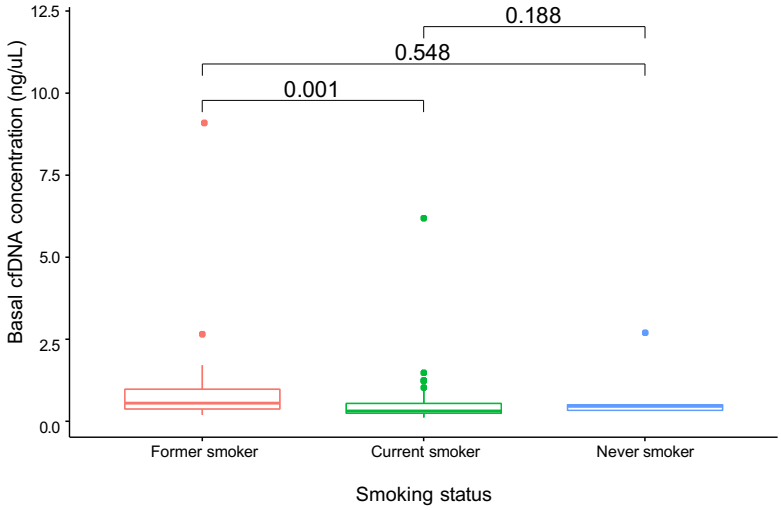

Figure 20: Former smokers present higher basal cfDNA concentrations than current smokers and patients that never smoked patients. Those former smoker patients showed higher basal cfDNA concentration.

Following, we evaluated the association in terms of number of cigarettes packs/year, with 10 packs/year threshold for dichotomization. No differences were identified in cfDNA concentrations **(Figure 21.A)**. Using number of packs/year as numerical variable, we did not find a clear concentration either **(Figure 21.B)**.

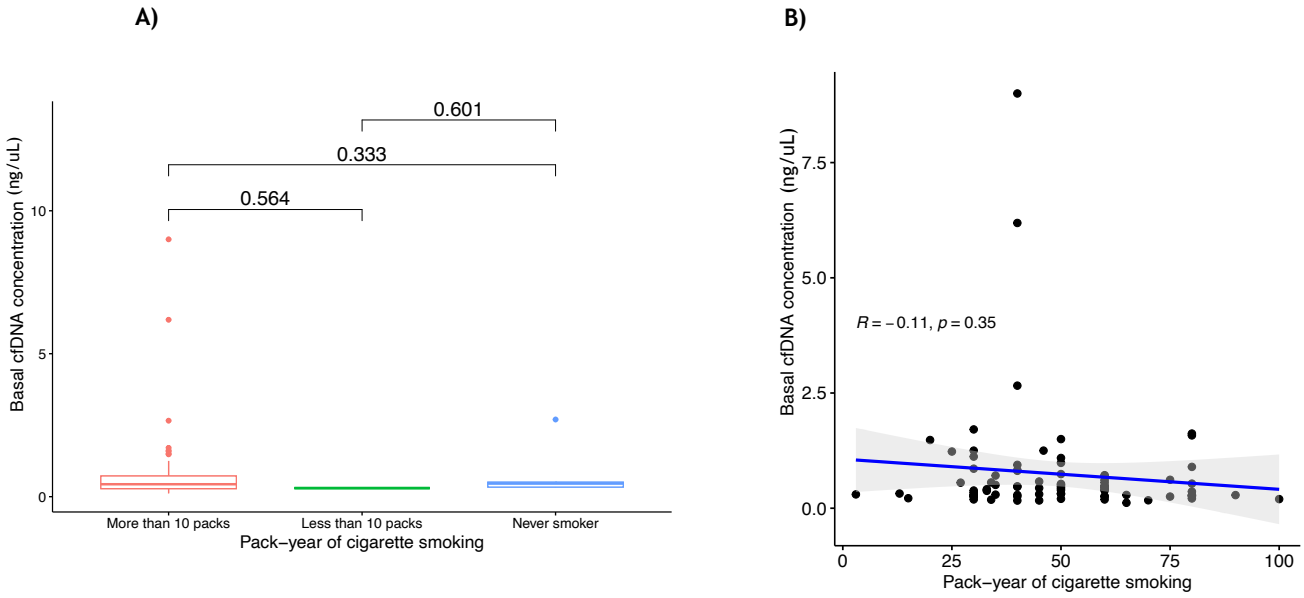

Figure 21. Any correlation found between cfDNA and cigarette packs. A) However, analysis made between cfDNA and pack number categories did not shown any correlation. **B)** In addition, when cigarette pack number was considered as quantitative variable, cfDNA concentration was similar independent of number of cigarette packs.

The second positive correlation identified in the univariant analysis was basal cfDNA concentration (T1) and the presence of bone metastases at diagnosis. The median value was 0.39 ng·uL^{-1} for those patients who had not bone metastases whereas 0.53 ng·uL^{-1} for those with bone metastases (Wilcoxon Test p-value 0.0031) **(Figure 22).** Previous cohort studies of more than 180 mNSCLC patients had demonstrated that most of the patients with bone metastases showed higher cel-free DNA concentrations and worse survival outcomes (Ye et al., 2019).

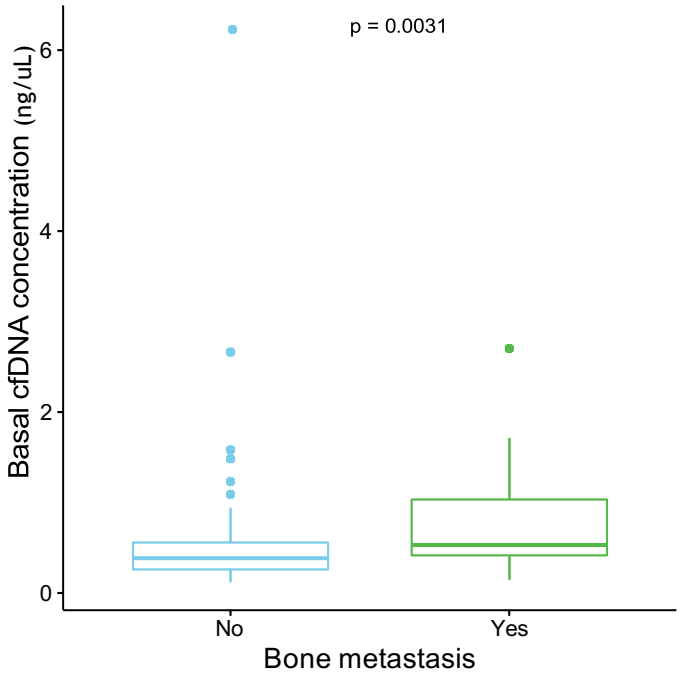

Figure 22. Basal cfDNA concentration is higher in mNSCLC with bone metastases. Those patients with bone metastases showed higher basal cfDNA concentration compared with mNSCLC patients who did not have any bone metastases.

The correlation was also interrogated between basal cfDNA concentration (T1) and post-treatment cfDNA concentration. Interestingly, the basal cfDNA correlated with the T2 one, that was measured only three-four weeks after T1 (Pearson correlation 0.39; p-value 0.00016) (**Figure 23**), but not to cfDNA concentrations after six and twelve months from treatment start (T3, T4) (**Supplementary Table 1.A**).

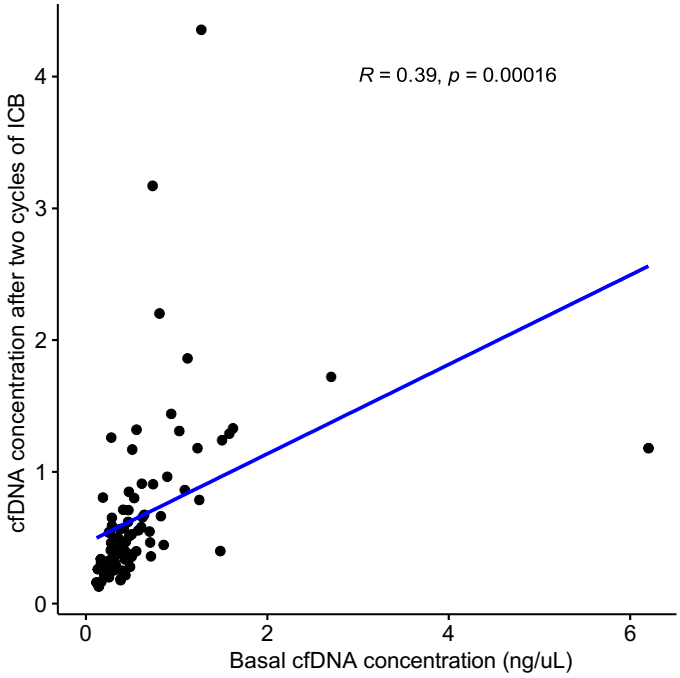

Figure 23. Basal cfDNA concentration correlates with cfDNA concentration at cycle two of ICB. Correlation between the cfDNA concentration before treatment (T1) and after two cycles of ICB therapy (T2).

3.2.2. Basal cfDNA and cfDNA at the second ICB cycle associates with response

The concentration of cfDNA was evaluated as a response predictive biomarker by establishing transversal differences between responders and non-responder at basal and cycle 2 time-points. Since prior to our study the levels of plasma cfDNA and not only ctDNA levels had not been interrogated as predictive biomarkers, the predictive potential of cfDNA was also evaluated for the different categories of responders and non-responders mentioned in section 2.1.2.1. Significant differences in the median concentrations of basal cfDNA (T1) were observed between responder groups for all different response classifications.

Interestingly, in all response evaluations cfDNA yielded a 1,5 higher level of basal cfDNA concentration in patients who progressed at any time of treatment compared with those patients that ultimately achieved the response **(Supplementary Table 1.A).** For early response (based on the first evaluation at month 3 after start of the treatment), cfDNA concentration was higher in non-responder patients (n=29) than in responder patients (n=68) (Wilcoxon Test *p*-value 0.0066). Median basal cfDNA concentration (T1) was 0.57 $ng \cdot uL^{-1}$ in non-responders and 0.39 $ng \cdot uL^{-1}$ **(Figure 24.A)**. A similar scenario was found when response was evaluated at month 6 of treatment. The median basal cfDNA concentration (T1) was 0.57 $ng \cdot uL^{-1}$ in non-responder patients (n=42) and the median basal cfDNA concentration (T1) was 0.39 $ng \cdot uL^{-1}$ in responder patients (n=54) (Wilcoxon Test *p*-value 0.0022) **(Figure 24.B)**. Finally, to assess if basal cfDNA concentration may predict long term response, no-responders (n=60) at the third evaluation after 12 months of ICB had 0.51 $ng \cdot uL^{-1}$ of cfDNA whereas responder patients (n=30) had 0.34 $ng \cdot uL^{-1}$ (Wilcoxon Test *p*-value 0.03) (**Figure 24.C)**. Finally, extreme responders at one year of ICB (n=30) (0.34 $ng \cdot uL^{-1}$) and extreme non responders that were in progression already when first evaluated (n=29) (0.57 $ng \cdot uL^{-1}$) showed differences in terms of cfDNA concentration with a Wilcoxon Test *p*-value of 0.0027 **(Figure 24.D)**.

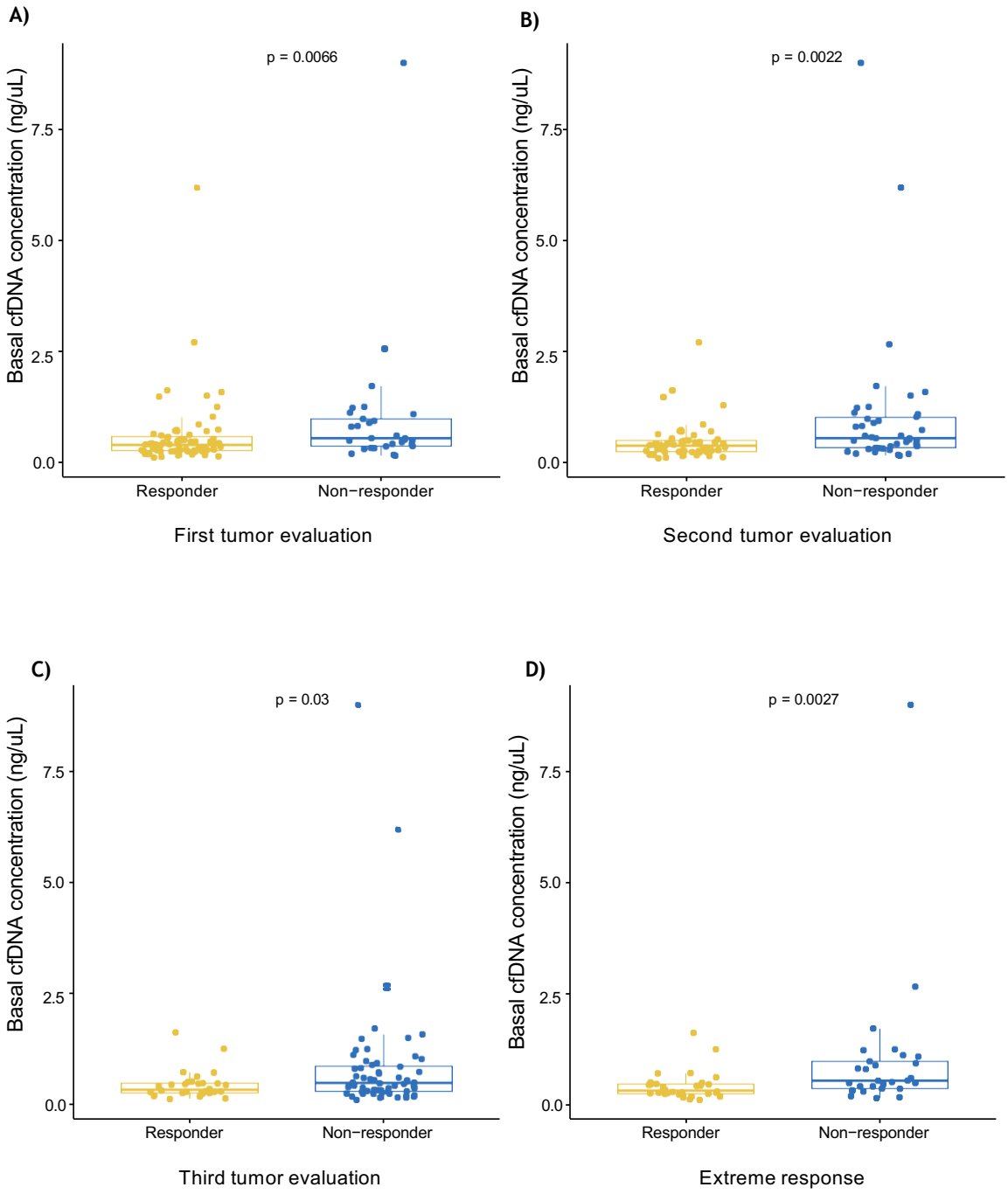

Figure 24: Basal levels of plasmatic cfDNA are significantly higher in non-responders to ICB pre-treatment and during the whole course of the treatment up to the finalization of the follow up (12). A) First tumor evaluation between responders and non-responder patients at three months of treatment. **B)** Response classification based on second tumor evaluation measured at six months of treatment. **C)** Third and final tumor evaluation after one year in ICB treatment. **D)** Also, extreme response was evaluated in those that still responded after twelve months in ICB and those that had progressed at or before three months of treatment.

Interestingly, when it comes to correlation between post-treatment cfDNA concentration and response, differences were only observed at the second cycle of ICB (T2) and the 6-month evaluation **(Supplementary Table 2)**. Again, higher cfDNA concentrations were observed in non-responder patients compared with responders (0.57 ng·uL^{-1} vs 0.40 ng·uL^{-1} (Wilcoxon Test *p*-value 0.026) **(Figure 25).**

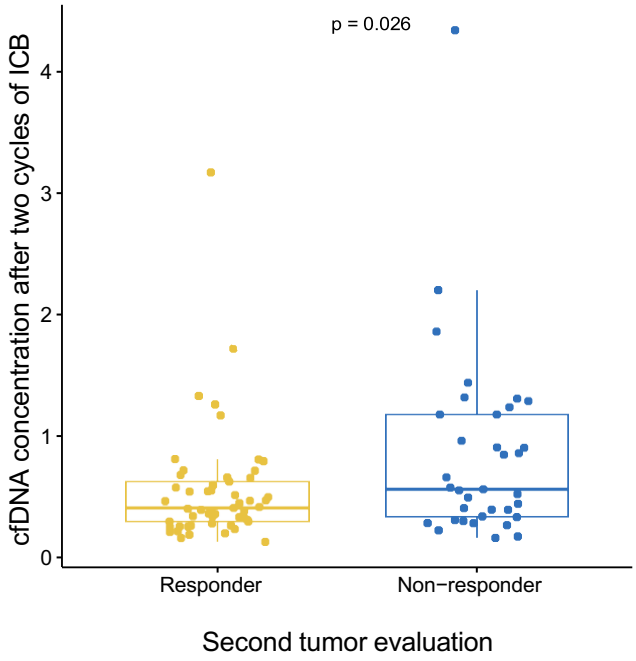

Figure 25: Correlation between cfDNA at the second ICB cycle with tumor response after six months of treatment.

3.2.3. High basal cfDNA concentration as bad prognosis biomarker for overall survival

To investigate the prognosis potential of basal cfDNA concentration on the therapeutic response to ICB treatment, survival studies were performed to

establish a quantitative cut-off value useful to stratify the patients according to the survival risk. The patients were stratified in two groups, high and low concentration based on 0.55 ng·uL^{-1} the optimal cut-off of total plasma cfDNA that best separated the patients according to overall survival. Those patients with basal cfDNA concentrations over 0.55 ng·uL^{-1} showed worse OS (log-rank p-value: 5.7483x10^{-2}) compared with patients with a cfDNA concentration lower than 0.55 ng·uL^{-1}. The median survival for the cohort for patients with a basal cfDNA concentration lower than 0.55 ng·uL^{-1} was of 23.8 months compared to 5.97 months for the patients with a higher cfDNA concentration to investigate the prognosis potential of basal cfDNA concentration on the therapeutic response to ICB treatment, survival studies were performed to establish a quantitative cut-off value useful to stratify the patients according to the survival risk. The patients were stratified in two groups, high and low concentration based on 0.55 ng·uL^{-1}, the optimal cut-off of total plasma cfDNA that best separated the patients according to overall survival. Those patients with basal cfDNA concentrations over 0.55 ng·uL^{-1}showed worse OS (log-rank p-value: 5.7483x10^{-2}) compared with patients with a cfDNA concentration lower than 0.55 ng·uL^{-1}. The median survival for the cohort for patients with a basal cfDNA concentration lower than 0.55 ng·uL^{-1} was of 23.8 months compared to 5.97 months for the patients with a higher cfDNA concentration **(Figure 26).**

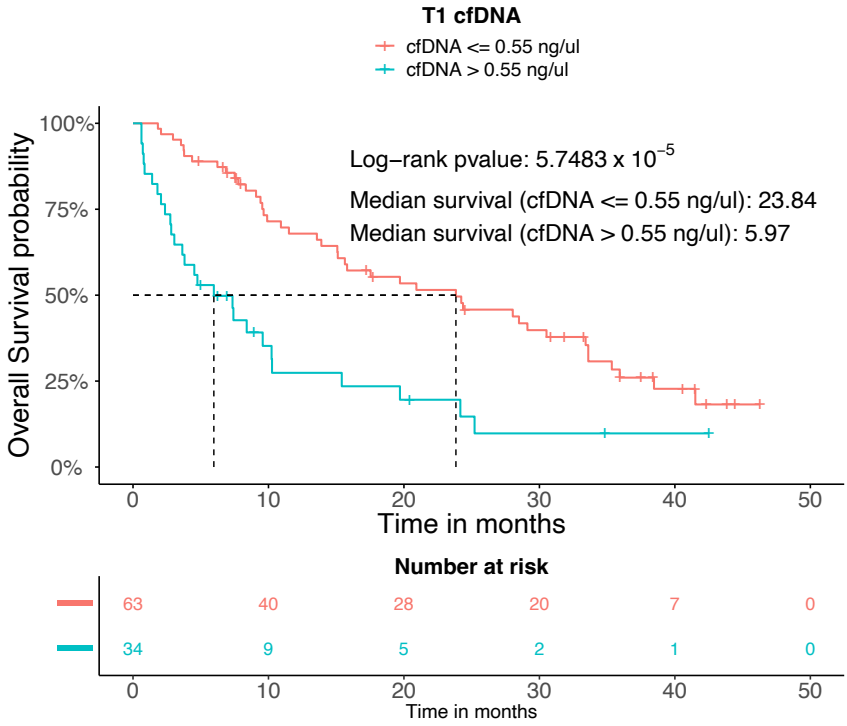

Figure 26: Basal cfDNA concentrations over 0.55 ng·uL^{-1} correlate with bad prognosis. Cut-off estimation was performed using Maxstat package for cfDNA baseline. Thus, Kaplan- Meier overall survival (OS) curves for patients with high versus low cfDNA. High and low grouping refers to the basal cfDNA concentration threshold of 0.55 ng·uL^{-1}. In red, patients with plasma concentration below 0.55 ng/µl, and in blue, patients with plasma cfDNA concentration above 0.55 ng·uL^{-1} Significance for the survival analysis is stated using log-rank test p-values.

3.3. Characterizing circulating epigenetic cfDNA profiles in patients with mNSCLC treated with immune checkpoint blockade.

cfDNA 5mC and 5hmC profiles were generated for 185 samples in 61 mNSCLC patients. There was a total of 61 samples before treatment (T1), 60 samples at cycle two (T2), 33 samples after six months in treatment (T3) and 23 samples after twelve months in treatment (T4). Also 5 samples corresponding to the progression moment (TP) were collected. **Table 6** summarized analysis characteristics performed to this molecular biomarker.

Table 6: Operative characteristics of cfDNA epigenetics markers. This blood biomarker was analyzed in plasma cfDNA before treatment started (T1), after two cycles of ICB (T2), at six months (T3) and at twelve months (T4) of ICB treatment in responder and non-responder patients defined in the 3, 6 and 12 month clinical and imaging evaluations.

Blood biomarker	Treatment time analysis	Response criteria
5mC and 5hmC marks in plasma cell free DNA	Before treatment starts (T1) At second cycle of ICB (T2)	First tumor evaluation (3 months of ICB) Second tumor evaluation (6 months of ICB) Third t tumor evaluation (12 months of ICB) Extreme response

3.3.1. Library pooling compensation optimizes sequencing process.

During the development of this objective, quality control of libraries and hybridization was performed with the aim of optimizing the sequencing process. Firstly, a range of 10 ng to 20 ng of initial fragmented cfDNA was established instead of the 200 ng per protocol. Most final libraries achieved between 7 ng to 20 ng of ligated, glycosylated (T4-BGT+), oxidated (TET2+ only for the 5mC+5hmC track), deaminated and amplified cfDNA **(Figure 27).**

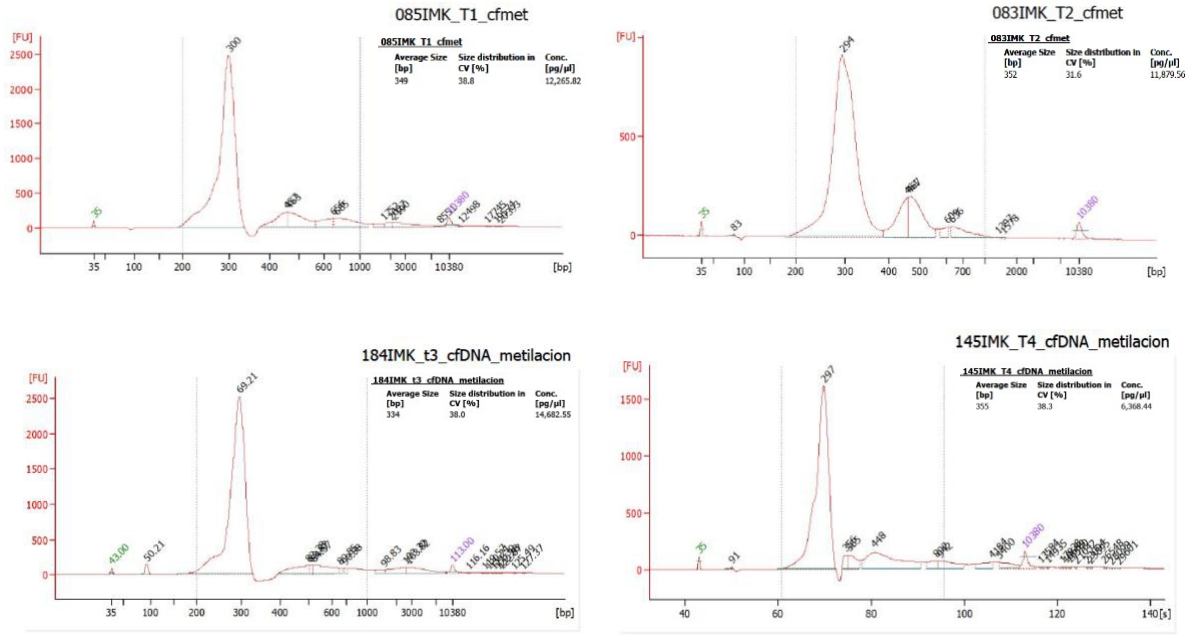

Figure 27: 5hmC and 5mC cfDNA libraries at different time-points. Quality control was performed in all samples before the pooling protocol. Samples showed enrichment in the size range of 200-350 bp after ligation of universal adapters and barcodes. In addition, in each graph, the first and last peaks represent the references (35 bp=lower, 10380 bp= upper). Also, for each sample, average size, size distribution in CV [%] and concentration [pg/uL] was indicated.

However, due to the increased time of glycosylation and deamination processes when 5hmC mark was evaluated, a minimum of initial 20 ng were needed to assure optimal libraries. Thus, a cfDNA concentration step was

implemented in the procedure before the first step of the 5hmC library preparation protocol to handle those amounts in the generally low cfDNA concentration samples. For the 5hmC track, most final libraries also achieved 7 ng to 20 ng of library **(Figure 28)**.

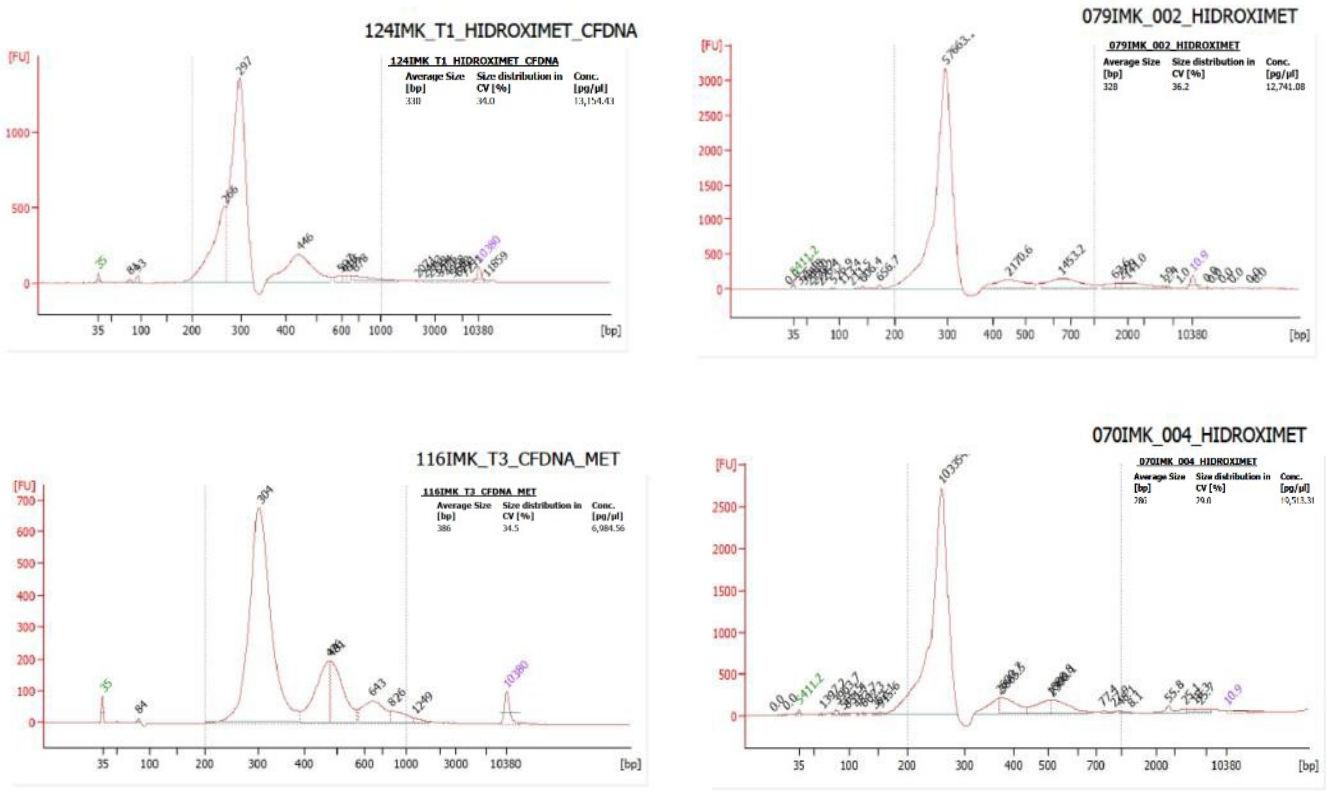

Figure 28: 5hmC cfDNA libraries at different time-points. Quality control was performed in all samples before the pooling protocol. Samples showed enrichment in the size range of 200-350 bp after ligation of universal adapters and barcodes. In addition, in each graph, the first and last peaks represent the references (35 bp=lower, 10380 bp= upper). Also, for each sample, average size, size distribution in CV [%] and concentration [pg/uL] were indicated.

Regarding the hybridization process, the procedure of sample combination into the pool was also improved during the first months of protocol implementation. pM1, pM2, pM3 combined libraries of heterogeneous concentrations, leading to higher standard deviations in the concentration of the

hybridized libraries and to a sequencing decompensation when those high concentration libraries from the pool were preferentially sequenced over the ones with substantially less concentration **(Figure 29)**. pM4, pM5 and pM6 are examples of pools composed of libraries of similar concentrations. Thus, libraries with 4-5 ng/mL were mixed in a four-sample pool, those with 5-8 ng/mL in a six-sample pool and those with higher concentration than 8 ng/mL were mixed in an eight-sample pool. In these balanced pools, we observe less concentration standard deviation **(Table 7).**

Table 7: Pooled epigenetic libraries descriptive statistics. Standard deviation was higher in the non-optimized pools pM1, pM2 and pM3. After observing the sequencing decompensation, pM4, pM5 and pM6 were optimized for three different concentration ranges (BA= bioanalyzer; Std. Deviation= standard deviation).

	BA concentration (ng/mL)					
	pM1	pM2	pM3	pM4	pM5	pM6
Valid	8	8	6	4	6	8
Missing	0	0	0	0	0	0
Mean	5.744	2.316	4.090	4.435	6.888	8.973
Std. Deviation	6.520	3.252	4.991	0.612	0.580	0.902
Minimum	0.263	0.131	0.870	4.060	5.812	7.935
Maximum	16.700	9.540	13.910	5.350	7.350	10.315

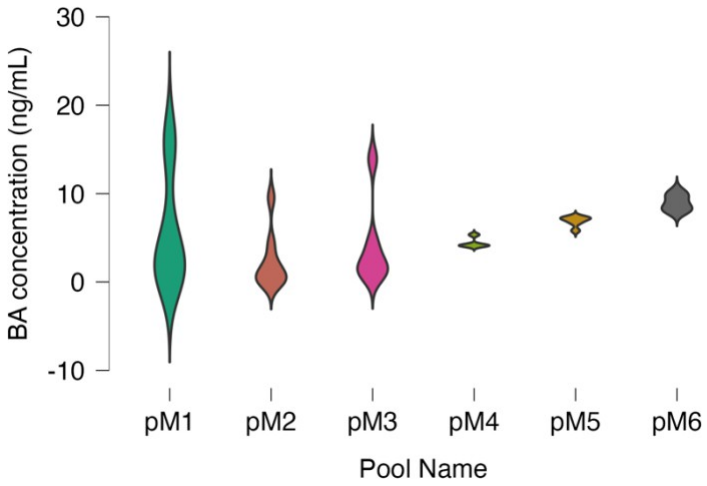

Figure 29: Variability in sample pooled concentration standard deviation. The concentration standard deviation range was higher in the following pools of methylated libraries (pM): pM1, pM2, pM3. After optimization, the methylated libraries pools pM4, pM5 and pM6 had similar concentration ranges. BA concentration: fragment-specific concentration measured by Bioanalyzer.

Sequencing data showed that heterogenous pool samples with lower amount of library concentration achieved less reads than those with higher amounts. Libraries with less concentration had less final raw gigabases in contrast with samples with more amount of concentration **(Figure30).**

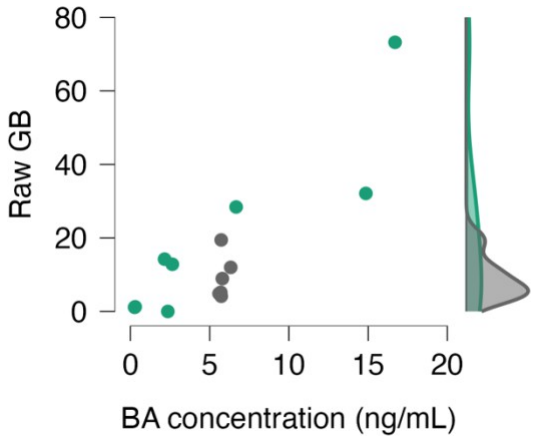

Figure 30: Sequencing data compensation in homogenous pooled samples. Data files after sequencing were similar regarding raw giga bases (GB) when homogenous libraries were pooled. BA: fragment- specific concentration measured by Bioanalyzer.

When it comes to panel coverage, most of the samples achieved more than 50% of panel coverage at different sequencing depths (1X, 10X, 20X and 50X) **(Figure 31.A).** The mean percentage of the panel coverage with 1X of sequencing depth was 72%, 70% with 10X, 68% with 20X and 67% with 50X. Therefore, we used 10X of sequencing/read depth (vertical coverage) and 50% of coverage (horizontal coverage) as minimum filters to select the samples for further analyses. Due to the low amount of plasma cfDNA and taking into consideration the loss during the protocol, amplification cycles were increased from nine to twelve following the manufacturer's recommendations controlling for number of PCR duplicates. Interestingly, except for T1, the percentage of reads on target after deduplication was stable among the different read depths **(Figure 31.B).**

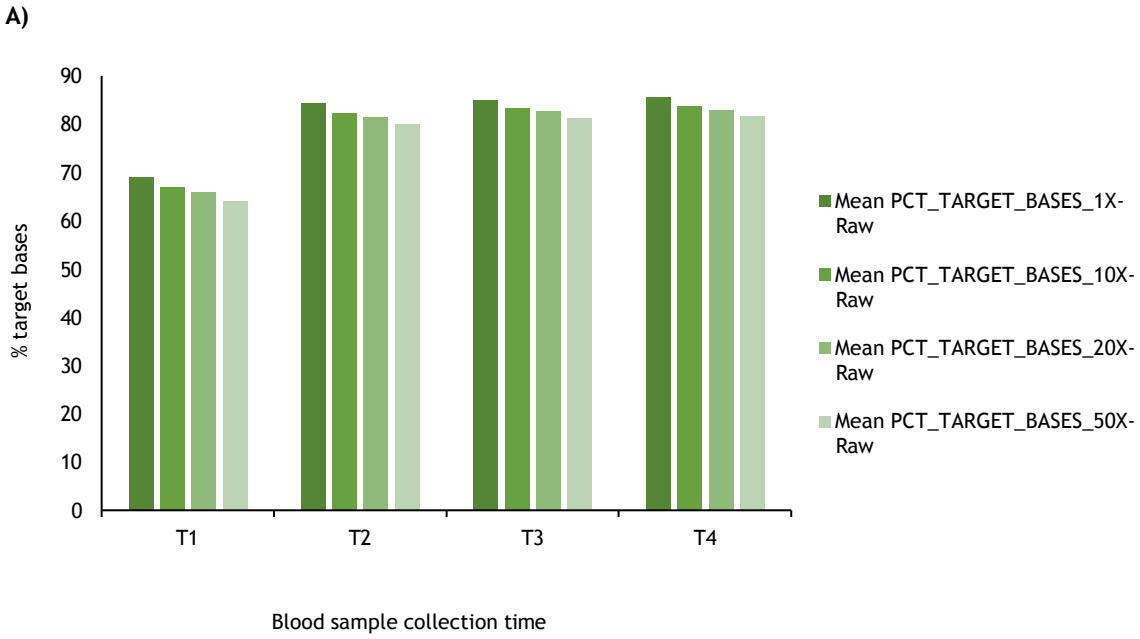

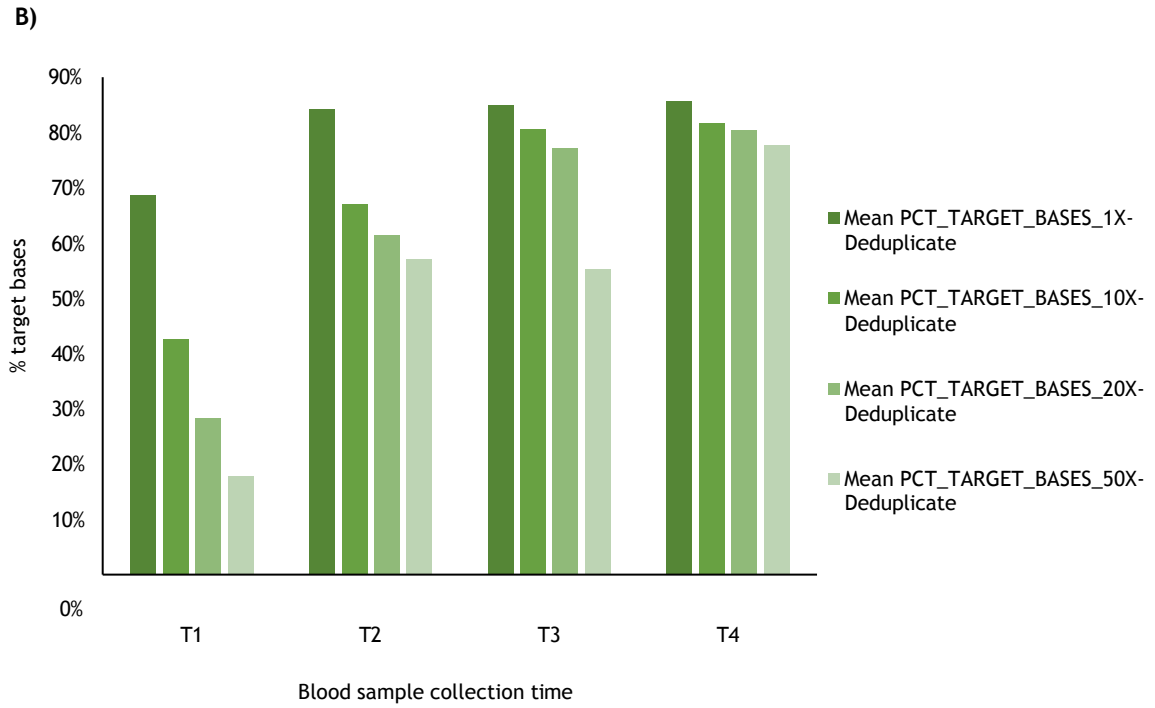

Figure 31: Panel coverage of methylated libraries at different blood time collection. A) Raw percentages of the panel coverage with 1X ,10X, 20X and 50X of sequencing. **B)** Deduplicated percentages of the panel coverage with 1X ,10X, 20X and 50X of sequencing. The longitudinal blood collection workflow was previously described in section 2.1.1. T1 refers to blood samples collected just before treatment starts, T2 at the second cycle, and T3 and T4, six and twelve months, respectively, after the start of the treatment.

3.3.2. Epigenetics patterns in cfDNA are correlated with tumor response.

3.3.2.1. Basal differential cfDNA methylation patterns between responder and non-responder patients.

In this first analysis, from 61 samples collected and processed before treatment (T1), 48 LUAD patients were selected for this analysis. Methylation sequencing batch effect analyses were performed to detect outliers, and, after discarding them, 34 patients were finally eligible for analysis for the 5mC+5hmC track. Of them, 17 were extreme responders (not progressed in the twelve months evaluation) and 17 were non-responder patients at the second tumor evaluation

(six months of ICB). Regarding specific 5mC and 5hmC detection which will be elaborated in Section **3.3.3.**, after outliers filtering, two non-responder patients (at six months if ICB) and six responder patients (at twelve months of ICB) were eligible for this pilot analysis.

3.3.2.1.1. Differentially methylated immune-related genes

To identify profiles of 5hmC and 5mC in cfDNA associated with response, differential methylation analysis was performed in the candidate ICB response genes and regulatory regions. From the different analyses in each of the responder classifications, basal DNA methylation was associated with response only in the medium and long term (at 6 months for non-responders and at 12 months for responders) From this analysis, 48 were differentially methylated (DM) CpG sites (p-value < 0.05). Of them, 30 CpG sites were hypermethylated in responders whereas 18 CpG sites were hypomethylated. These 48 DM CpG sites already stratified the 34 patients according to response **(Figure 32).**

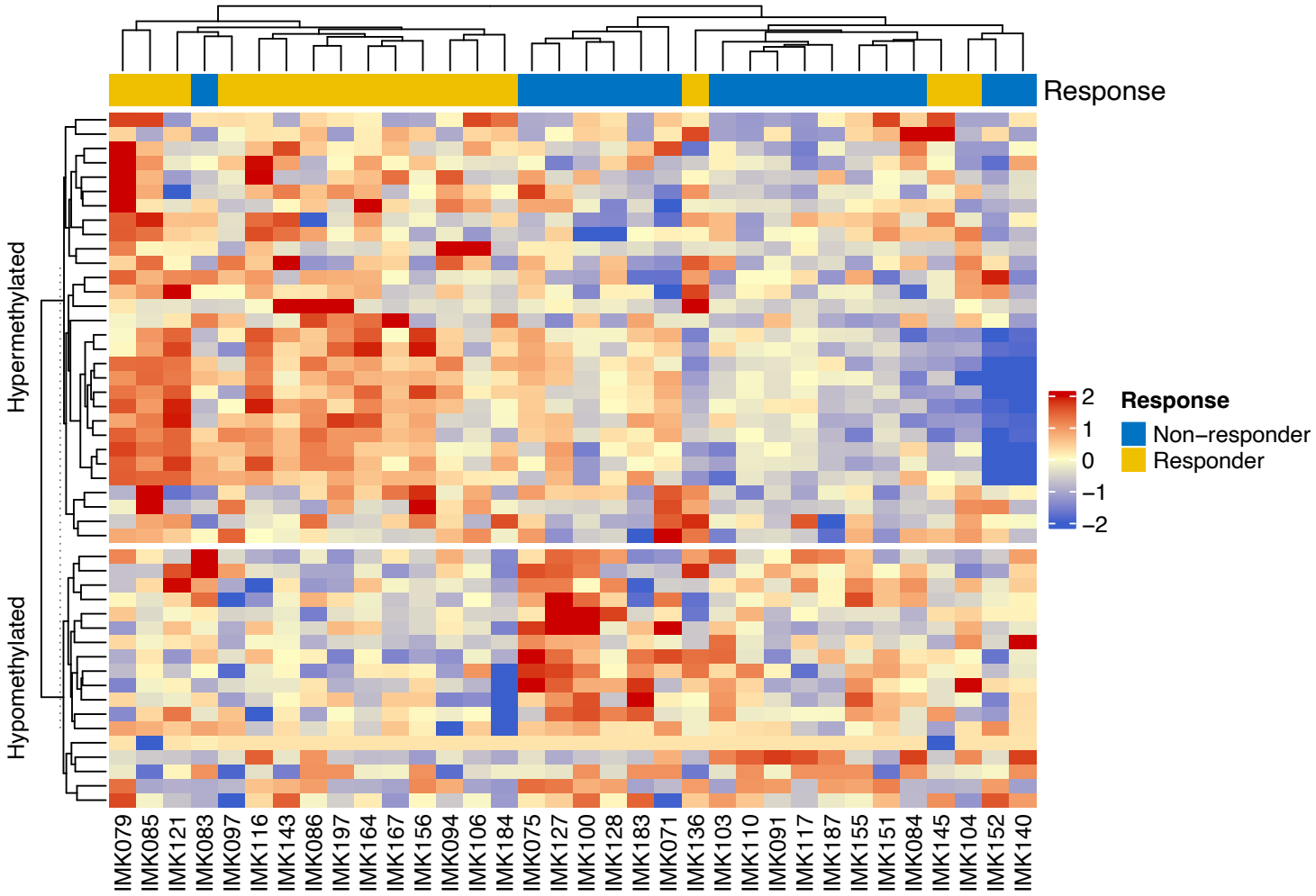

Figure 32: Differently methylated CpG sites stratify responder and non-responder patients before treatment. Heatmap visualization of the 48 differentially methylated CpG sites stratifying between 17 responder patients and 17 non-responder patients. A scale is shown on the right, in which red and blue corresponding to a hyper-and a hypomethylation status, respectively.

Statistical correction for multiparameter correlations decreased the number of significantly associated CpG sites to 3 hypermethylated sites (chromosomal positions chr11:111379323, chr11:111379330 and chr11:111379332) **(Figure 33).** Remarkably, all of them belong to the gene *POU Class 2 Homeobox Associating Factor 1 (POU2AF1)*. This gene is a transcriptional coactivator of the Oct protein of the immune B cells. POU2AF1/Oct are involved in the pre-B1-to-

pre-B2 cell transition, that is essential for the pre-B-cell receptor (pre-BCR) and subsequent BCR signaling at multiple stages of B-cell development. However, other immunological functions are also associated to *POU2AF1*, being highly expressed in those CD4+ T memory cells that have increased survival capability and memory recall potential (Sun et al., 2022). In the context of cancer, *POU2AF1* is reported as the most determinant transcription factor in myeloma multiple. (Chyra et al., 2021). Interestingly, *POU2AF1* has also been found hypermethylated in various types of solid tumors. (Han et al., 2020).

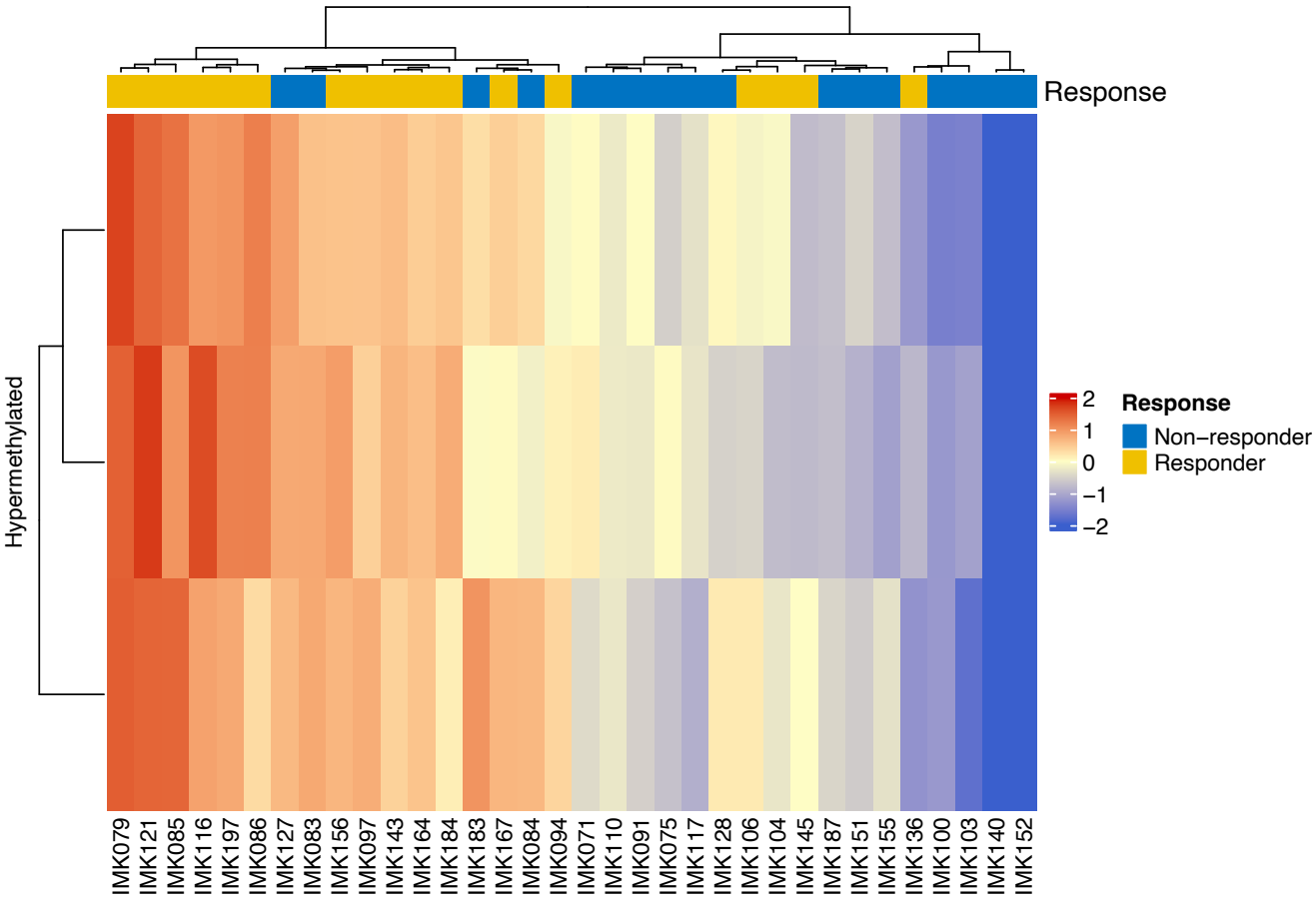

Figure 33: Basal hypermethylation of *POU2AF1* in responder patients. Heatmap visualization of three differentially methylated CpG sites of POU2AF1 stratifying between 17 responder patients and 17 non-responder patients with adjusted p-value of <0.05. A scale is shown on the right, in which red and blue corresponding to a hyper- and a hypomethylation status, respectively.

3.3.2.1.2. Differentially epigenetically enriched genomic regions in basal cfDNA

The differential methylation analysis was also performed for CpGs grouped in potential regulatory regions: CpG Islands (CGI), including and excluding the CGI shores, transcription factors binding sites, and enhancers binding sites. The identified DM regions according to response (DMRs) are described in (**Table 8).**

Table 8: DMRs according to response to ICB.

Analyzed genomic region	DM direction	Chromosomal position	Associated gene	p-value
Core islands and shores	Hypomethylated	chr4:73979811-73984113	Platelet factor 4 (PF4)	< 0.05
	Hypermethylated	chr12:52712128-52716687	Pseudogene keratin 126 (KRT126P)	< 0.05
Core islands, shores and shelves	Hypermethylated	chr12:52710128-52718687	Pseudogene keratin 126 (KRT126P)	< 0.05
Transcription factors binding sites	Hypomethylated	chr11:314360-314920	Interferon Induced Transmembrane Protein 1(IFITM1)	< 0.05
Enhancers binding sites	Hypermethylated	chr11:69012319-69012379	MAS Related GPR Family Member F (MRGPRF)	< 0.05

The individual analysis of the methylation (5mC+5hmC) in CGI cores, shelves and shores did not show any differences between responder and non-responder patients. However, when the analysis of CGI cores and shores was carried out together, 2 regions were found to be differentially methylated in responders

compared with non-responders. One of them was hypomethylated and corresponded to *platelet factor 4 (PF4)*. The other DMR was hypermethylated and located in the pseudogene *keratin 126* (*KRT126P*). Interestingly, this hyper-methylated region was also found with the joint analysis of CGI cores, shores, and shelves (p-value < 0.05). Interestingly, the only Transcription factor binding sites region that is DM in responders is hypomethylated and corresponds to *Interferon Induced Transmembrane Protein 1 gene (IFITM1)*. The encoded protein plays an important role in immunity, is strongly induced by IFN-α and γ and mediates IFN-induced antiproliferative effects (Kim et al., 2020). In addition, correlations between better response to ICB and T cell-induced interferon-γ activity have been reported in some tumors (Grasso et al., 2021). Finally, when Enhancer binding sites were analyzed, a region associated with *MAS Related GPR Family Member F (MRGPRF)* was seen as hypermethylated in responders. In in vivo assays, this gene induces tumor growth and tumorigenesis. Also, over-expression of the MrgprF protein has been shown in skin and lung tissues (Nishimura et al., 2012). Interestingly, *MRGPRF* promoter is hypermethylated in cutaneous melanoma patients with better clinical outcome (Shen et al., 2022).

3.3.2.2. Differential cfDNA methylation patterns between responder and non-responder patients at second cycle of ICB

Samples from a total of 60 patients were collected at the moment of the second ICB cycle (T2) and sequenced for 5mC+5hmC methylation analysis. Of those, 47 patients were classified histologically with LUAD and selected for this analysis. Also, batch-effect controls were performed to exclude technical outliers.

After outliers depletion, 27 patients were finally eligible for analysis with 15 extreme responder patients (still not progressed after twelve months of ICB) and 12 non-responder patients at the second tumor evaluation (six months of ICB).

3.3.2.2.1. Differentially methylated CpG sites

To gain a deeper understanding of the cfDNA methylation profile changes when ICB is administrated, DM CpG sites in cfDNA after two cycles of ICB between responders and non-responder patients were also identified. Notably, in this analysis there were many more (447) DM CpG sites (p-value <0.05), of which109 CpG were hypomethylated and 338 CpG hypermethylated. When multiparameter correction was applied, 6 hypermethylated CpG sites remained significantly DM **(Table 9).**

Table 9: Hypermethylated CpG sites in cfDNA after two cycles of ICB in responder patients

Chromosomal position	Associated gene	p-value (adj.)
chr11:67440347	Coronin 1B (CORO1B)	< 0.05
chr15:58064942	Aldehyde Dehydrogenase 1 Family Member A2 (ALDH1A2)	< 0.05
chr15:58064943	Aldehyde Dehydrogenase 1 Family Member A2 (ALDH1A2)	< 0.05
chr16:46389289	Centromere Protein P (CENPP)	< 0.05
chr16:46389299	Centromere Protein P (CENPP)	< 0.05
chr9:92479080	Asporin (ASPN)	< 0.05

Using the full signature of 447 DM CpGs after 3-4 weeks in ICB treatment, stratification per response group is complete **(Figure 34).**

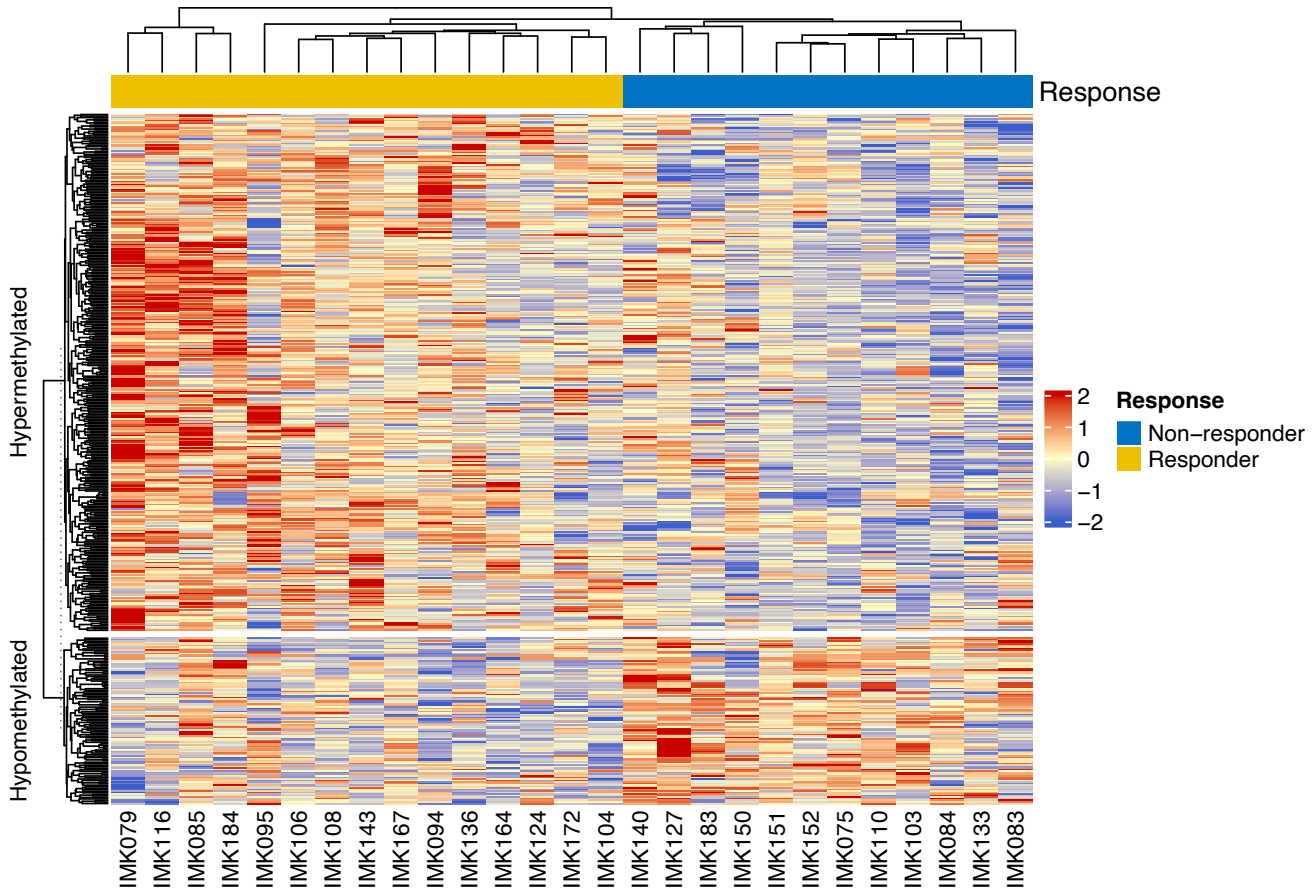

Figure 34: The signature of 447 DM CpG sites in the first weeks after the start of ICB treatment stratifies responders from non-responders. Heatmap visualization of differentially methylated CpG sites. 447 differentially methylated CpG sites stratifying between 15 responders versus 12 non-responder patients with p-value of <0.05. A scale is shown on the right, in which red and blue corresponding to a hyper- and hypomethylation status, respectively.

If only the 6 DM CpGs after adjustment are utilized for the hierarchical separation of responders and non-responders, stratification is suboptimal and the direction of the differential methylation and the biological processes of the genes that contain these CpG sites if homogeneous **(Figure 35).**

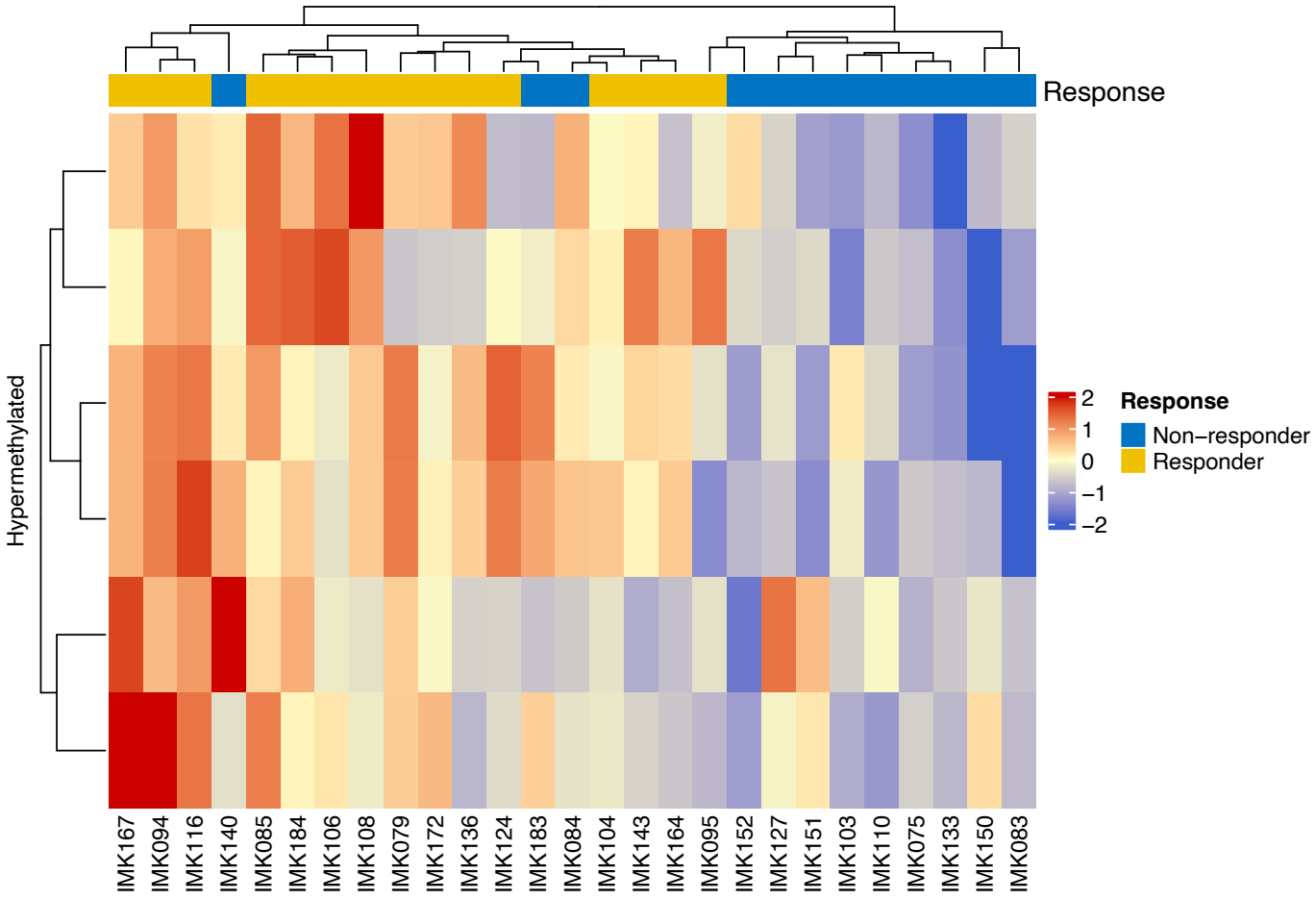

Figure 35: Differently methylated CpG sites in tumor-related genes 3-4 weeks after the start of ICB. Heatmap visualization of differentially methylated CpG sites. Six differentially methylated CpG sites of 15 responder patients and 12 non-responder patients with adjusted p-value of <0.05. A scale is shown on the right, in which red and blue corresponding to a hyper- and hypomethylation status, respectively.

Remarkably, all the genes that contain adjusted DM CpG sites are related to tumorigenesis. Overexpression of *Coronin 1B (CORO1B)*, promotes invasiveness in some tumors. (Allen et al., 2021). *Aldehyde Dehydrogenase 1 Family Member A2 (ALDH1A2)* is involved in metabolism pathways needed for cell proliferation. In some meta-analysis of ALDH1A1 in lung cancer, overexpression in tumor tissues were related to shorter overall survivals. (Dong et al., 2015). *Centromere proteins (CENPs)* have been recently related to malignant tumors and its downregulation to inhibit lung cancer cells proliferation (Shan et al., 2019). Finally, asporin (ASPN),

which is an extracellular matrix (ECM) protein, also promotes cell migration and invasion in some types of cancer (Sasaki et al., 2021).

3.3.2.2.2. Differentially epigenetically enriched genomic regions in basal cfDNA

The differential methylation analysis was also performed to CpGs grouped in potential regulatory regions: CpG Islands (CGI), including and excluding the CGI shores, transcription factors binding sites, and enhancers binding sites. The identified DM regions according to response (DMRs) are described in **Table 10.**

Table 10: Differentially methylated genomic regions in responder patients after two cycles of ICB

Analyzed genomic region	DM direction	Chromosomal position	Associated gene	p-value
Core islands	Hypermethylated	chr2:27442072-27442803	Keratinocyte-associated protein 3 (KRTC3)	< 0.05 (adj.)
Core islands and shores	Hypomethylated	chr6:47475372-47480355	CD2AP Divergent Transcript (CD2AP-DT)	< 0.05
Core islands, shores and shelves	Hypomethylated	chr6:47475372-47480355		< 0.05
Transcription factors binding site	Hypomethylated	chr8:30546840-30547230	StAR Related Lipid Transfer Domain Containing 3 (STARD3)	< 0.05
	Hypermethylated	chr17:39659700-39659890	RNA Binding Protein, MRNA Processing Factor (RBPMS)	< 0.05

Keratinocyte-associated protein 3 (KRTC3) was the only gene containing a significant DMR after multiparameter adjustment **(Figure 36).**

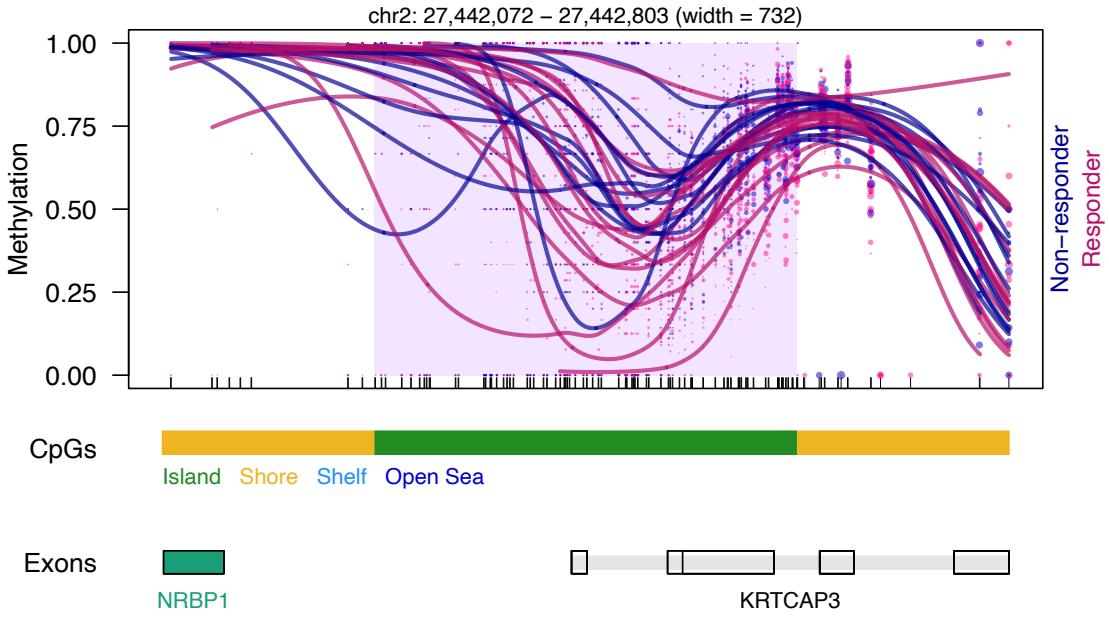

Figure 36: Hypermethylation of keratinocyte-associated protein 3 (KRTC3) in responder patients after ICB. Methylation levels of KRTC3 genomic regions between 15 responder patients and 12 non-responder patients with adjusted p-value of <0.05. Methylation scale is measured between 0-1 based on b-values. Green box indicated methylation location, in this case in core island.

KRTC3 was previously found to be hypermethylated in lung cancer cells Interestingly, hypermethylation of CpG island associated to promoter in this gene was found to be one of the top lung cancer-specific hypermethylated CpG island-associated genes (Kiehl et al., 2017). Contrary, hypomethylation of this gene was found in the other most frequent NSCLC subtype, squamous cell carcinoma (Kwon et al., 2012). Specific methylation patterns in some may be different inside NSCLC histology categories.

The analysis of the CGIs in their different combinations revealed that *CD2AP Divergent Transcript* (*CD2AP-DT*) was hypomethylated in responders. This gene is a long non-coding regulatory RNA that controls *CD2 Associated Protein* (*CD2AP*) transcripts. *CD2AP* is a known stabilizer of the interaction between T cells and antigen-presenting cells (Raju et al., 2018). STARD3 and RBPMS, found to be differentially methylated in transcription factor genomic regions in responders, have also been previously associated with cancer.

3.3.3. Preliminary exploration of the superior informativity of DNA methylation predictors when 5mC and 5hmC are profiled independently.

It was designed a pilot study in which we only included the patients for which the subtracted 5mC and the specific 5hmC tracks were available. After patients' selection following the QC criteria of ≥10x read depth and ≥ 50% reads on target or horizontal coverage, and outliers exclusion, 2 non-responders (6 months evaluation) and six responders (12 months evaluation) were eligible. To compare the mapping of 5hmC+5mC variations versus the mapping of the separate modifications, the ß-values for the three tracks were depicted in a representative gene, *ROR2*. When the composite track of 5mC+5hmC (green colors, named as "cfmeth") was utilized to establish the % of methylation, the differences between non-responders (**Figure 37.A)** and responders (**Figure 37.B**) were not patent. However, in the same panel, the 5hmC track (pink/blue colors, named as "cfhidro"), the 5-hydroxymethylation is very variable among responders and is stable in the non-responders. Likewise, in the inferior panel it is visually evident that responders had a higher CpG methylation variability than the non-responders.

Moreover, the representation of the actual 5mC and 5hmC values showed the impact of the separation of the signals in the actual % of methylation. 5mC values, depicted in pink and named “mC”, are, particularly in responders, not any more homogeneous and higher. In some CpGs, the % of 5mC reached not more than 25% instead **(Figure 37.C and Figure 37.D).** These pilot results highlighted the importance of 5hmC and 5mC separated identification to ensure that DNA methylation differences between responders and non-responders are identified and can be explore as potentially more informative predictors of inducible discrete and local changes in the context of ICB response.

A) Composite track of 5mC+5hmC

No-responders

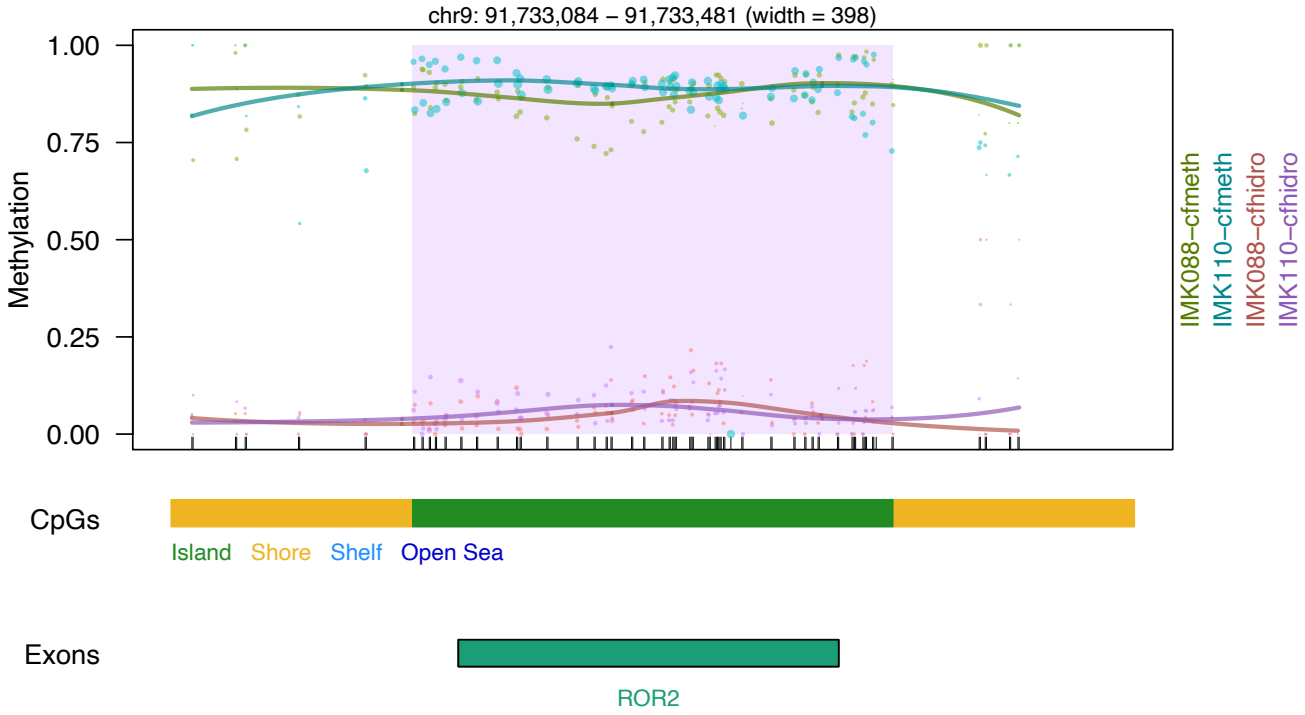

Responders

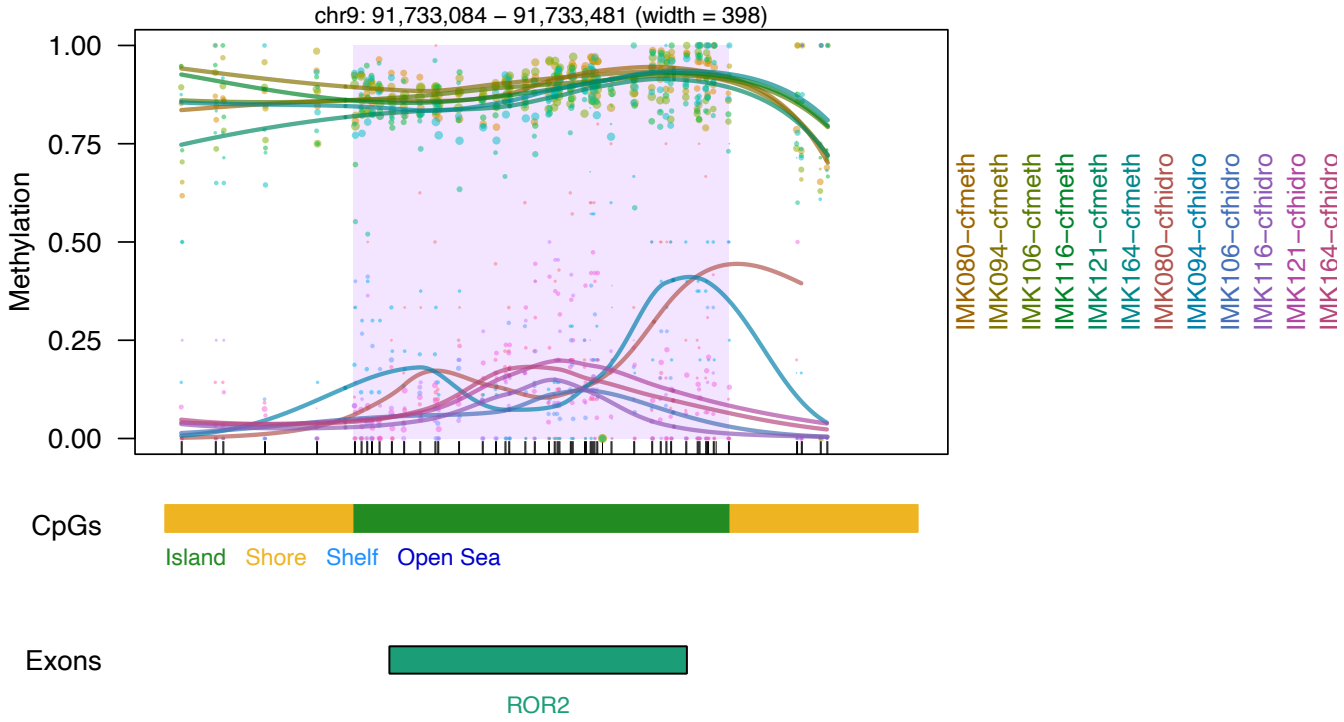

B) Actual 5mC and 5hmC marks

No-responders

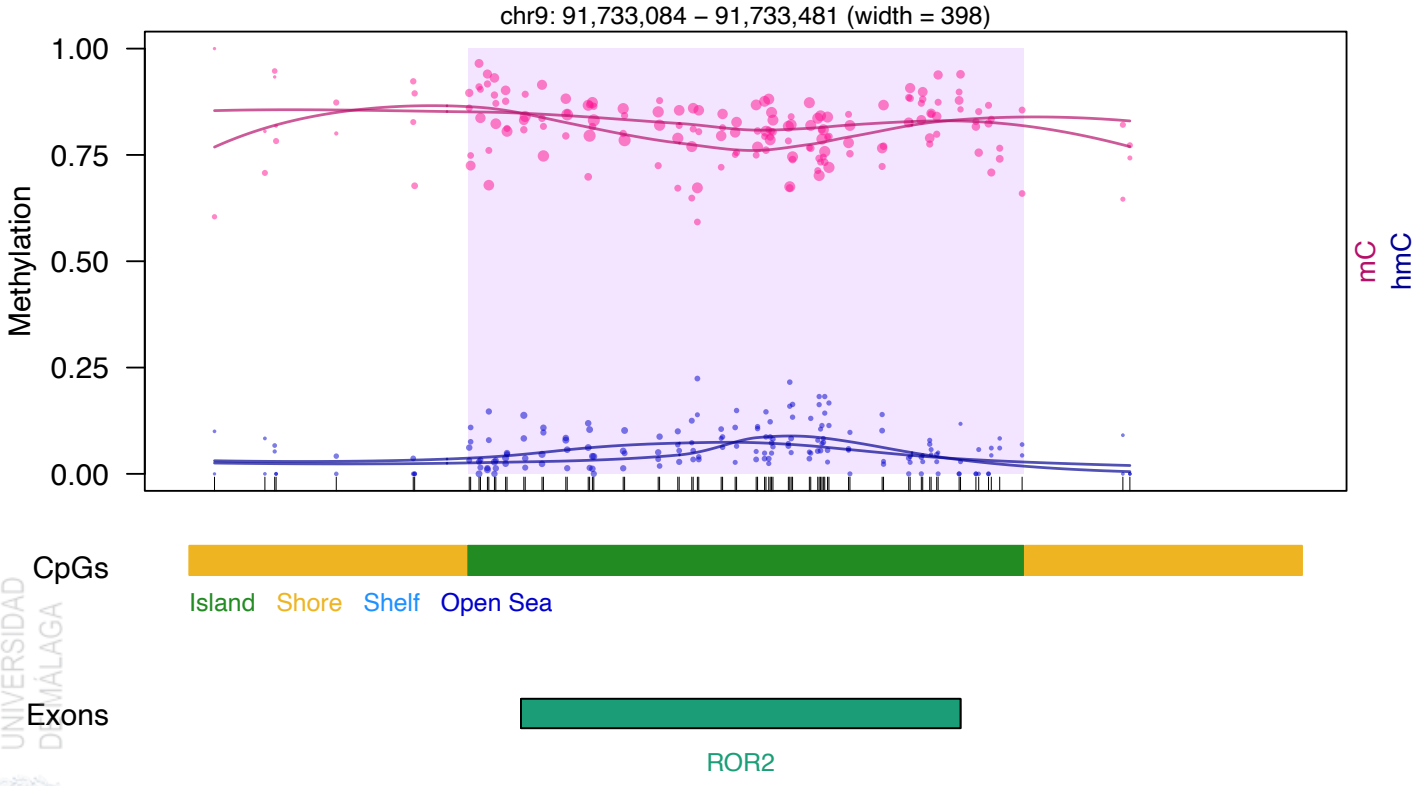

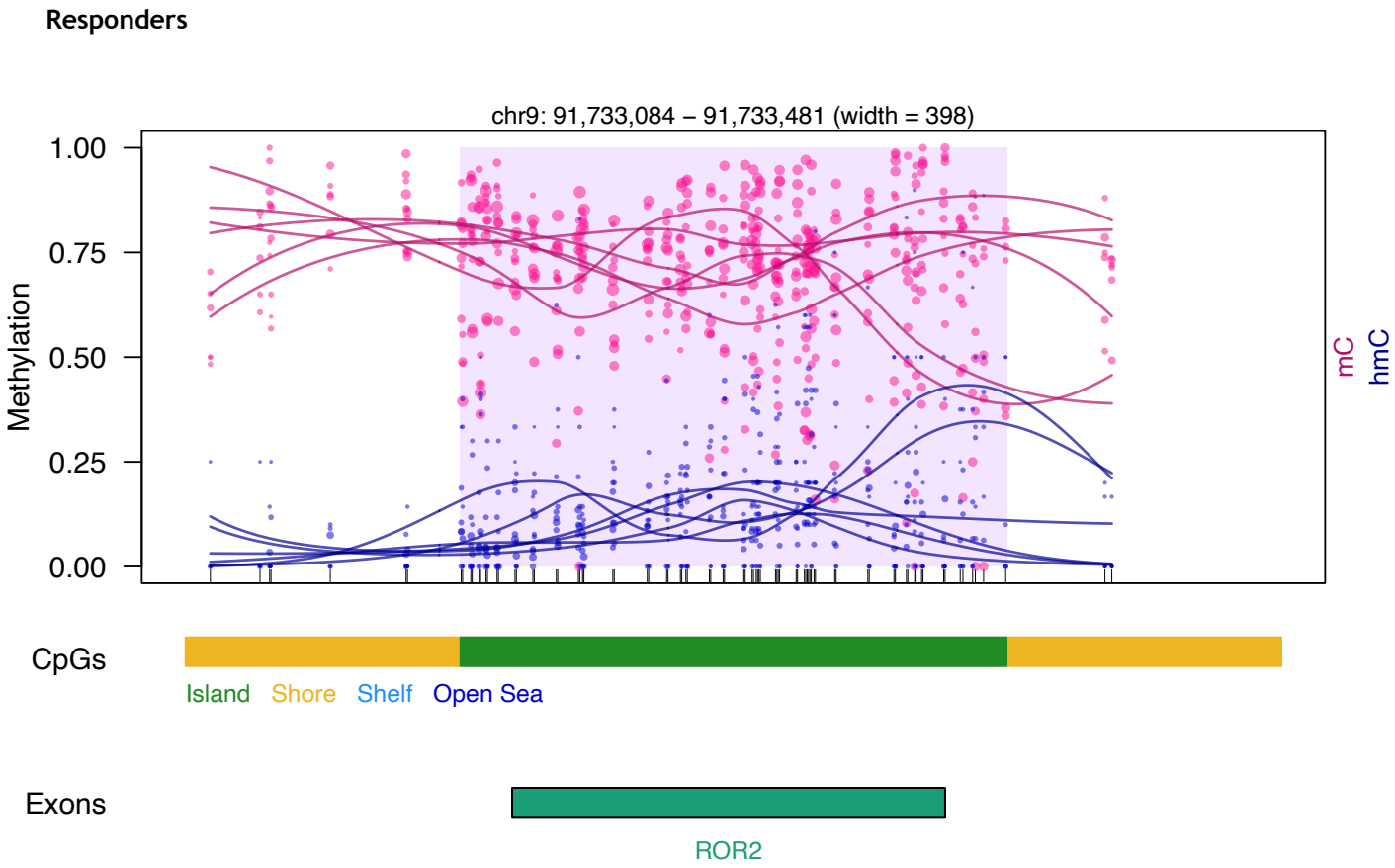

Figure 37. Impact of the separation 5hmC and 5mC signals in actual methylation percentage. **A)** Composite track of 5mC+5hmC (green colors, named as "cfmeth") and 5hmC track (pink/blue colors, named as "cfhidro") was utilized to establish the % of methylation in non-responders and responders **B)** In the inferior panel is represented the actual 5mC (pink colors) and 5hmC (blue colors) in non-responders and responders **.**

3.4. Plasma-derived extracellular vesicles miRNA signature as predictive and prognosis biomarker to Immune Checkpoint Blockade

miRNA were analyzed in 228 plasma-derived EV samples in patients with mNSCLC. There was a total of 79 samples before treatment (T1), 73 samples 3 to 4 weeks after the start of therapy (T2), 38 samples six months (T3) and 22 samples twelve months (T4) after treatment started. Time to progression was also collected in 16 patients. **Table 11** summarizes the analysis characteristics for this molecular biomarker.

Table 11: Characteristics of miRNA from plasma derived EV. The blood biomarker analyzed in this section was the differentially expression of miRNA from plasma derived EV before treatment started (T1), after two cycles of ICB (T2), six months (T3) and twelve months (T4) of ICB in responders and non-responders at three, six and twelve months of tumor evaluation.

Blood biomarker	Treatment time analysis	Response criteria
miRNA from plasma derived EV	Before treatment starts (T1) At second cycle of ICB (T2)	First tumor evaluation (3 months of ICB) Second tumor evaluation (6 months of ICB) Third tumor evaluation (12 months of ICB) Extreme response

3.4.1. Visualization of small extracellular vesicles by nanoparticle tracking analysis and transmission electron microscopy

Different plasma derived EV from mNSCLC and control patients were visualized by NTA, with higher individual points of scattered light corresponding to high concentrations. Regarding tumor samples, there was no significant difference in mean particle concentration (3.76x108 +/- 7.53x107 particles/ml and 2.69x108 +/- 2.50x107 particles/mL) and mean particle size (255.8 +/- 11.7 nm and 229.0 +/- 3.6 nm). When healthy controls were evaluated, less differences in both parameters were found being the median particle concentration (2.96x108 +/- 1.60x107 particles/mL and 3.13x108 +/- 7.48x107 particles/mL). Also, particle size was more similar between both control samples (251.1 +/- 9.1 nm and 246.3+/- 5.7 nm). In all samples, there was a range of two main peaks with the greatest number of particles, at 150 nm and 250 nm corresponding with previously described extracellular vesicles size **(Figure 38)** (Coumans et al., 2017).

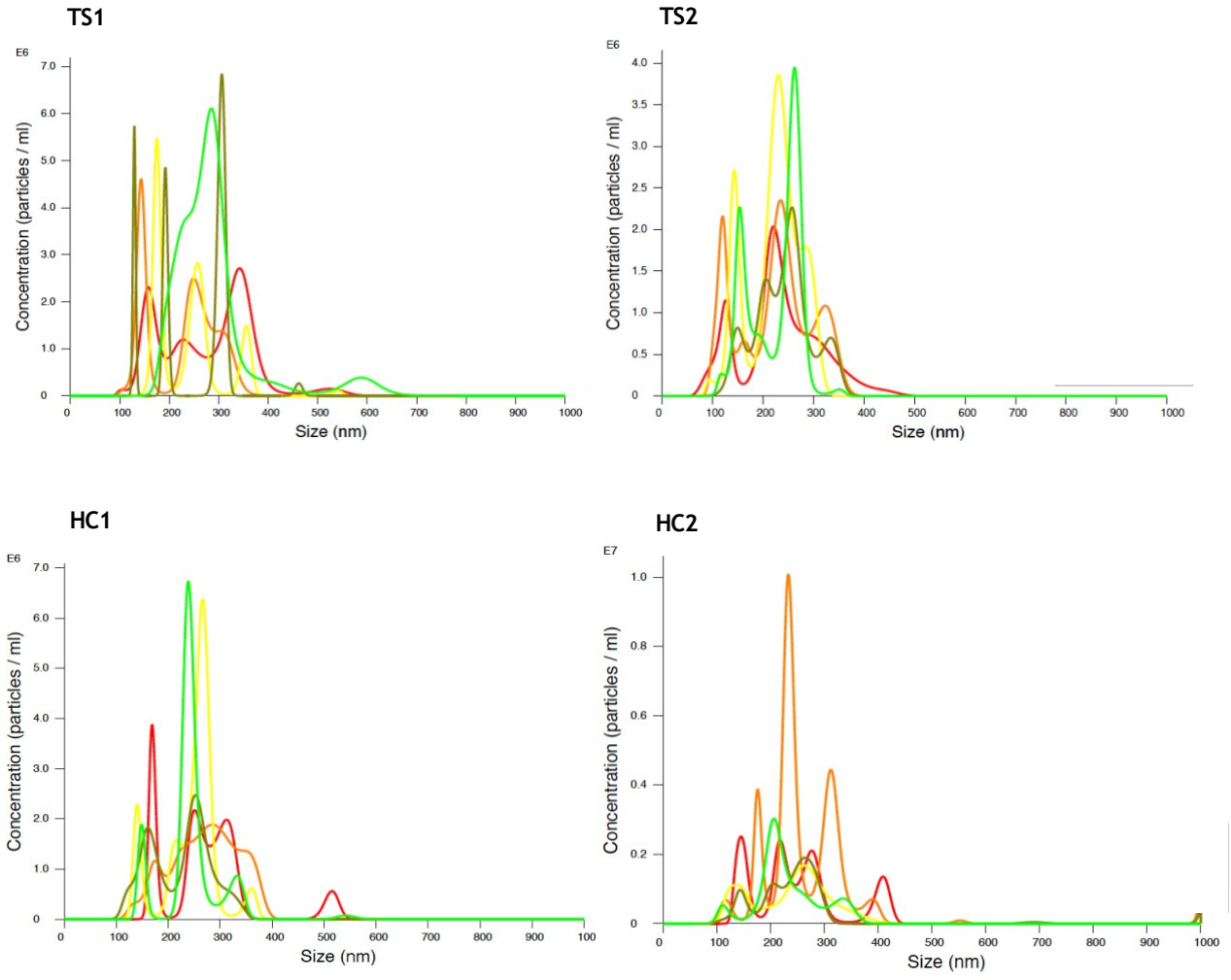

Figure 38. Extracellular vesicles nanoparticle tracking analysis. Representative concentration and size graphs of plasma derived EV as measured by scattered light on the NanoSight 300 nanoparticle tracking analysis (NTA) software. TS1 and TS2=tumor samples one and two. HC1 and HC2=healthy control one and healthy control two.

Transmission electron microscopy **(Figure 39)** also showed particles which were consistent with EV with a mean range of 200 nm. There were no discernible differences between both tumor samples. Regarding control samples, there was one sample with lower mean size, 100 nm compared with other control and tumor samples. However, this difference did not exceed the normal mean size of EV (Coumans et al., 2017b).

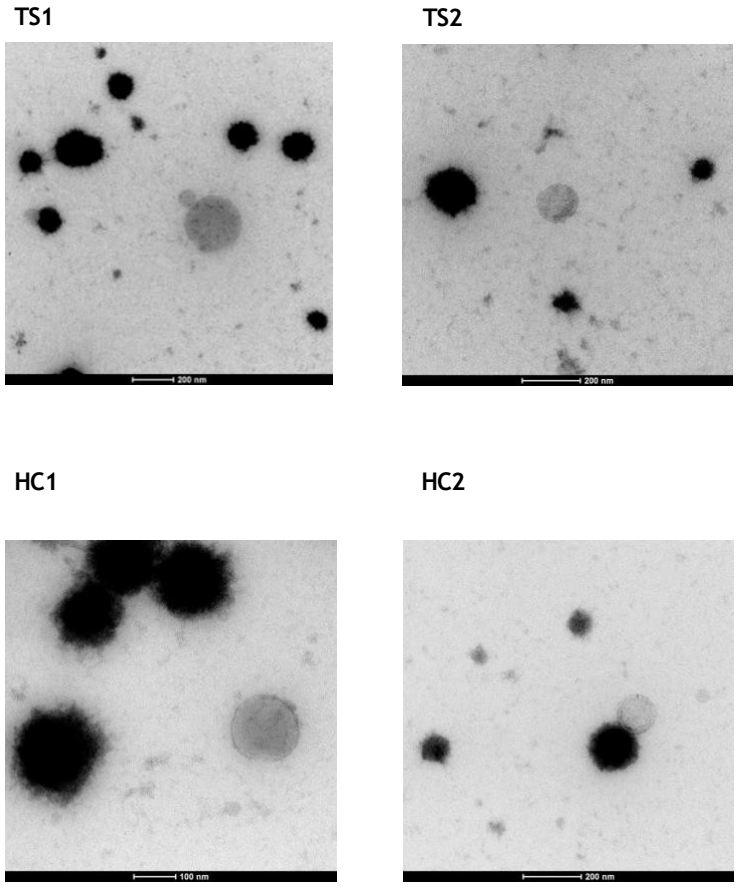

Figure 39. Images of isolated EV taken by transmission electron microcopy (TEM). Representative images from tumor samples (TS1 and TS2) and healthy controls (HC1 and HC2). Particles displayed lipid bilayer membranes and had a mean size of 200 nm (Scale bar = 200 nm and 100 nm).

3.4.2. miRNA signature from plasma derived EV associate with response to ICB and survival in mNSCLC

Investigation of candidate miRNA was performed by smallRNA sequencing. First, an important analysis required for EV biomarker studies was determined whether smallRNA profiles were similar along treatment administration and response criteria.

3.4.2.1. Small RNA fragments enriched in plasma-derived EV.

To ensure that the input of total RNA was sufficient quality for small-RNA sequencing, quality checks were performed in all samples across total RNA from plasma-derived EV isolation. Bioanalyzer profiles were evaluated for each sample, before small-RNA library preparation. In **Figure 40** there are some total RNA Bioanalyzer profiles. Graphs show two quality parameters for RNA sequencing: RNA integrity number equivalent (RINe) widely used to assess RNA integrity and DV200, which evaluates the percentage of fragments of >200 nucleotides. Almost all samples, time collection independent, had a low average RINe between 1.5-2.5. In addition, in almost all samples just 30% of RNA fragments were higher than 200 nucleotides, being most of the fragment size between 25 and 200 nucleotides. Tape Station counterparts showed the same quality control results. Regarding total RNA concentration isolated, there was a variable range of ng, between 100 ng to 500 ng in some samples. However, there was not any correlation between higher total RNA concentrations and sample time collection.

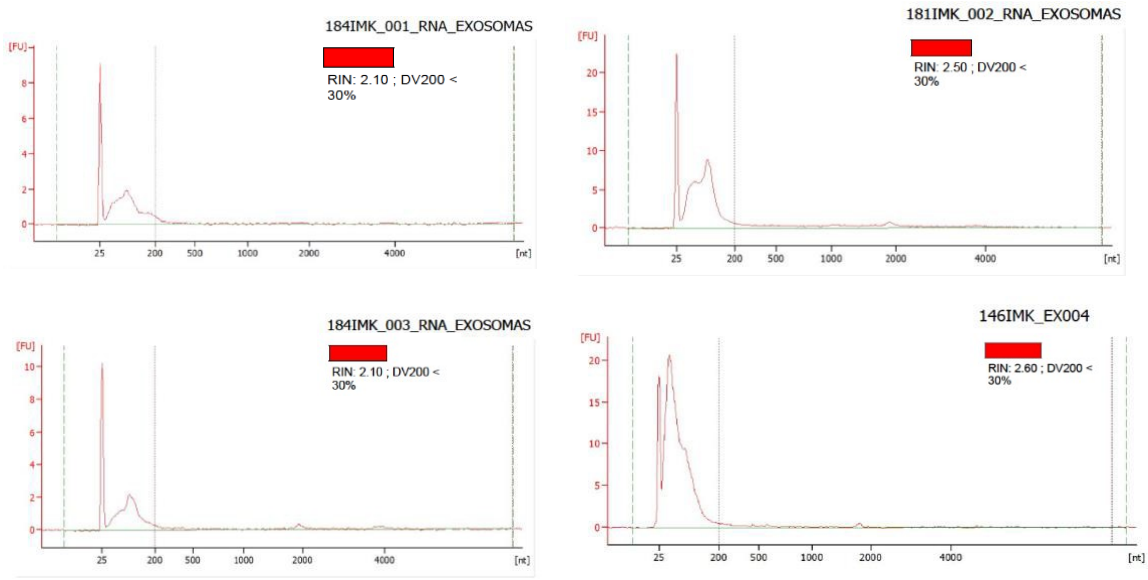

Figure 40: Plasma derived EV total RNA was enriched in small RNA fragments. Quality control was performed in all samples before small-RNA libraries preparation by our laboratory. Samples showed enrichment in fractions in the size range of small-RNA. In addition, in each graph, the first and last peaks represent the references (25 bp=lower, 1500 bp= upper). Also, RINe and DVV200 were indicated.

3.4.2.2. Similar small-RNA profiles before and during ICB treatment

At this point, EV small RNA analysis shown in **Figure 41** revealed the presence of the same diversity of small non-coding RNA species in all the plasma samples before and during ICB treatment. These subsets included piRNA, rRNA, scaRNA, lncRNA, snoRNA, snRNA, miscRNA, circRNA, and Y-RNA. This latter one was the smallRNA type with a higher percentage in all blood samples before and after ICB. If focused on miRNA, the percentage of these EV small-RNA inside EV were smaller than other subsets of small-RNA. Also, there was found that the percentage of miRNA before treatment started (T1) was lower compared with samples collected after different treatment times (T2, T3, T4). These findings

supported the notion that small-RNA subset distribution in EV is stable in both before and after treatment. On the other side, the lower percentage of miRNA before treatment compared with the amount in samples during treatment administration, may indicate that ICB could stimulate transcriptomics changes in mNSCLC patients in response to immunotherapy.

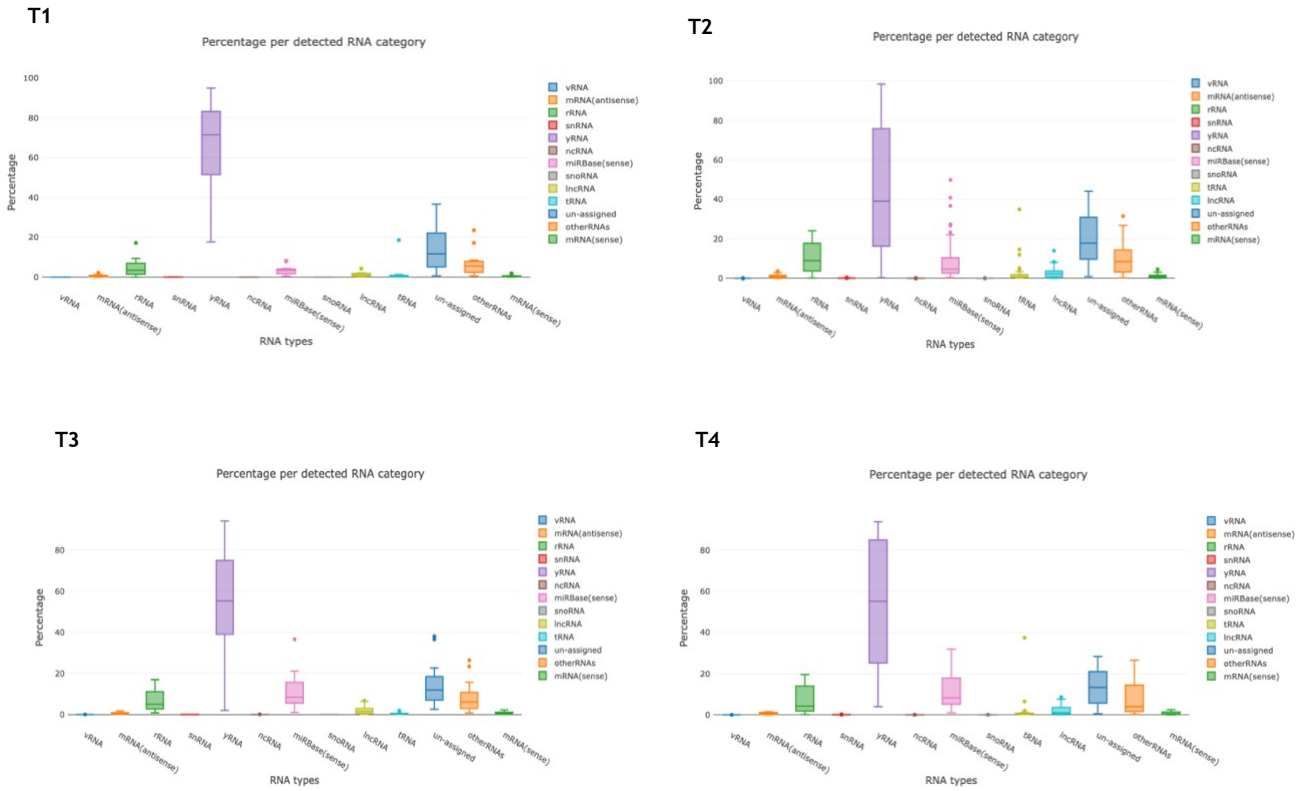

Figure 41: Similar small-RNA subset profiles in mNSCLC patients before and after ICB treatment at different times. Small-RNA classes were homogeneous in plasma-derived EV from all samples. Regarding miRNA showed a lower percentage in samples collected before ICB started. (Graphs were obtained from RNAtoolBox software).

In order to provide more information about genome mapping an overall number of genome mapped reads and assigned reads were obtained. When the percentage of miRNA mapping was evaluated, miRNA mapping corresponded to

less than 20% of all genome and assigned reads in all plasma samples. A total of 2652 miRNA were mapped **(Figure 42).**

T1

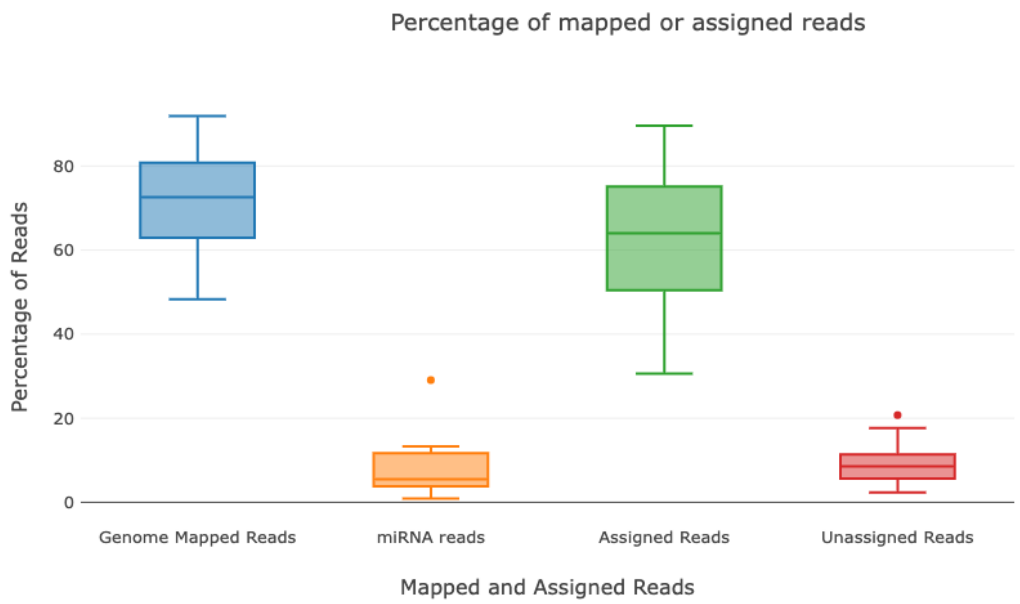

T2

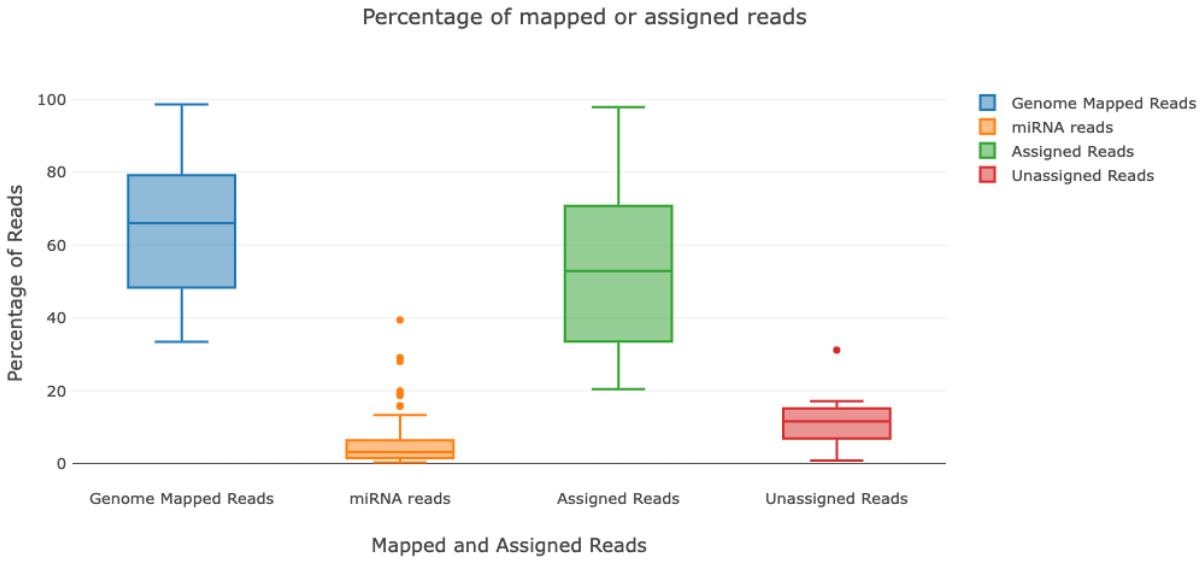

T3

T4

Figure 42. Total sequencing reads did not differ between blood samples before and after ICB treatment. The percentages of genome mapped reads with assigned reads and corresponding miRNA assigned mapped reads. (Graphs were obtained from RNAtoolBox software).

3.4.2.3. Predictive and prognostic value of differentially expressed miRNA derived from plasmatic EV between responder and non-responder mNSCLC patients treated with ICB.

3.4.2.3.1. Clustering long responder patients based on basal miRNA signature.

Different miRNA expression profiles were evaluated to characterize the response mechanisms to ICB in mNSCLC. Thus, differential expression analysis was performed between different response criteria previously described in Section **2.1.1.2.** Differentially expressed profiles of miRNA were identified between 30 extreme responders (at 12 months of ICB) and 24 non-responder patients (at 3 months of ICB) in EV before treatment started. A total of 18 miRNA differentially expressed with 8 miRNA upregulated and 10 downregulated in responder patients **(Table 12).**

Table 12. Differentially expressed miRNA between responder patients at twelve months of ICB and non-responder patients at three months of ICB before treatment started. Table shows miRNA annotation, logarithm of the fold change between both responders group and the adjusted p-value for each miRNA. Positive fold change means up regulation in responders whereas negative fold change means downregulation in responder patients.

DE miRNA	Fold Change	p-value (adj.)
hsa-miR-1-3p	-2,838	0,004
hsa-miR-34c-5p	-2,272	0,005
hsa-miR-1246	-2,146	0,011
hsa-miR-134-5p	-2,135	0,002
hsa-miR-199b-5p	-1,996	0,006
hsa-miR-574-3p	-1,794	0,004
hsa-miR-145-5p	-1,751	0,030
hsa-miR-375-3p	-1,730	0,033
hsa-miR-200a-3p	-1,666	0,014
hsa-miR-143-3p	-1,662	0,002
hsa-miR-96-5p	1,554	0,030
hsa-miR-3913-5p	1,634	0,041
hsa-miR-144-5p	1,718	0,011
hsa-miR-144-3p	1,725	0,008
hsa-miR-4732-5p	1,920	0,032
hsa-miR-15b-3p	1,923	0,011
hsa-miR-451a	2,206	0,002
hsa-miR-1224-5p	2,648	0,006

With the aim to visualize previously described DE miRNA in both groups, a heatmap was represented. Interestingly heat map reveals a clustering trend of up and downregulated DE miRNA in the vast majority of responder patients **(Figure 43).** Thus, additionally, study correlations between clinicopathological variables and clustered responder subjects were performed. This analysis showed that there was no statistical significance between clustered patients and clinical characteristics **(Supplementary Table 3)**. These results may indicate that clustering of responder patients could be result of these upregulated and downregulated miRNA signature before.

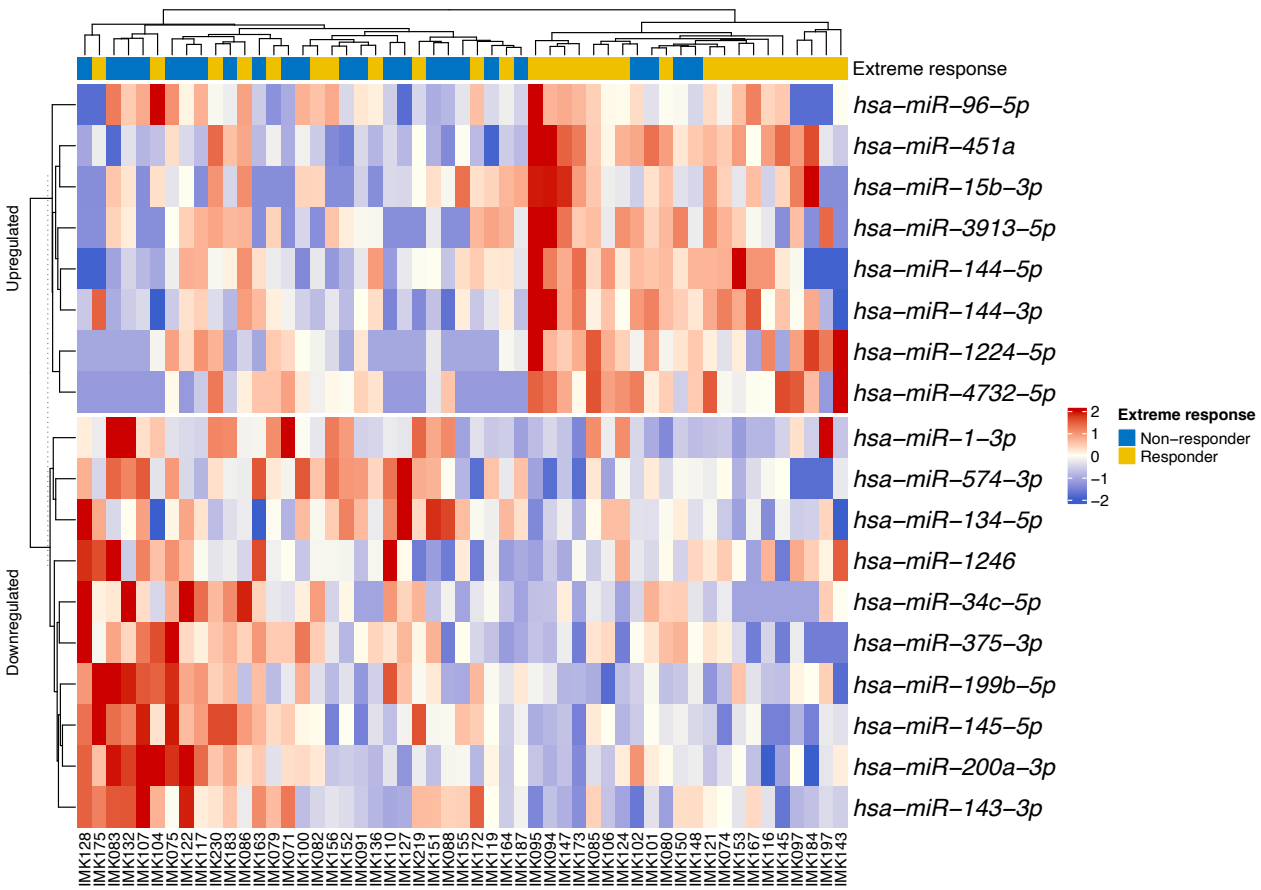

Figure 43: Clustering of responder patients based on miRNA expression. Heatmap of DE miRNA between 30 responder and 24 non-responder patients before treatment (T1). A scale is shown on the right, in which red and blue correspond to a higher and a lower expression status, respectively.

Tumor suppressor and oncogene are both roles associated to the most DE miRNA found in this analysis. Downregulated miRNA in the responder patients such as hsa-miR-1-3p, hsa-miR-134-5p or hsa-miR-375-3p were found to act as tumor suppressor in cancer and related to lung cancer progression and survival (Wang et al., 2019) (Cheng et al., 2017) (Pan et al., 2017). On the other hand, hsa-miR-451a or hsa-miR-1224-5p both upregulated in responder patients, usually serve as a tumor suppressor in many cancers including NSCLC. This analysis may indicate different miRNA roles associated to NSCLC and response to ICB (Ma et al., 2022) (Soofiyani et al., 2021).

3.4.2.3.2. Differential expression miRNA tumor suppressor signature after two cycles of ICB correlate with tumor response.

To study if ICB stimulated different miRNA expression pattern, differences between both groups of responder patients were also assessed after two cycles of ICB. In this analysis, only 9 miRNA were found to be differentially expressed. Interestingly, when analyzed all DE miRNA, only hsa-miR-375-3p (Log2(FC)= -3,261) and hsa-miR-134-5p (Log2(FC)= -1,892) kept downregulated in responder mNSCLC patients before and after treatment. Responder patients showed some other tumor suppressor upregulated found to be differentially expressed in further analysis **(Table 13).**

Table 13. miRNA differentially expressed between responder patients at twelve months of ICB and non-responder patients at three months of ICB after two cycles of ICB. Table shows miRNA annotation, logarithm of the fold change between both responders group and the adjusted p value for each miRNA. Positive fold change means up regulation in responders whereas negative fold change means downregulation in responder patients.

DE miRNA	Fold Change	p-value (adj.)
hsa-miR-375-3p	-3,261	0,006
hsa-miR-3138	-3,022	0,000
hsa-miR-4433b-3p	-2,116	0,035
hsa-miR-134-5p	-1,892	0,008
hsa-miR-548o-3p	-1,821	0,008
hsa-miR-200b-3p	1,746	0,028
hsa-miR-19b-3p	2,279	0,008
hsa-miR-3613-5p	2,503	0,009
hsa-miR-205-5p	4,237	0,0002

3.4.2.3.3. Plasma-derived extracellular vesicles miRNA predicts survival in mNSCLC

The miRNA patterns associated to plasma derived EV were different when analyzed basal samples and samples after two cycles of ICB between responder and non-responder patients. Thus, the prognostic value of both DE miRNA patterns was assessed. In both cases, a risk score was developed based on plasma-derived EV miRNA differentially expressed before and after the second cycle of ICB. Basal DE miRNA signature revealed that mNSCLC patients in the high-risk score had shorter overall survival (median OS 8,42 months vs 24,16 months p<0.001) **(Figure 44.A)**. Regarding DE miRNA signature after two cycles of ICB, patients in the high-risk score had shorter overall survival (median OS 10.22 months vs 28.49 months, p<0.001) **(Figure 44.B)**.

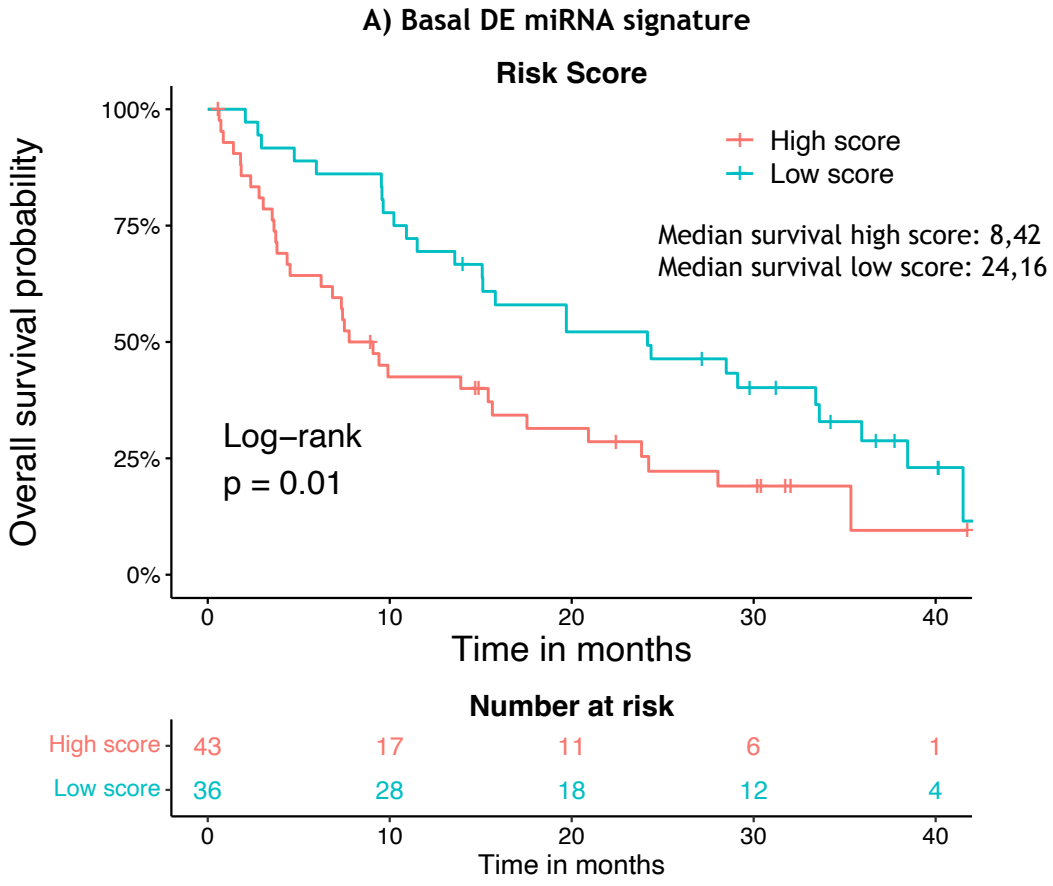

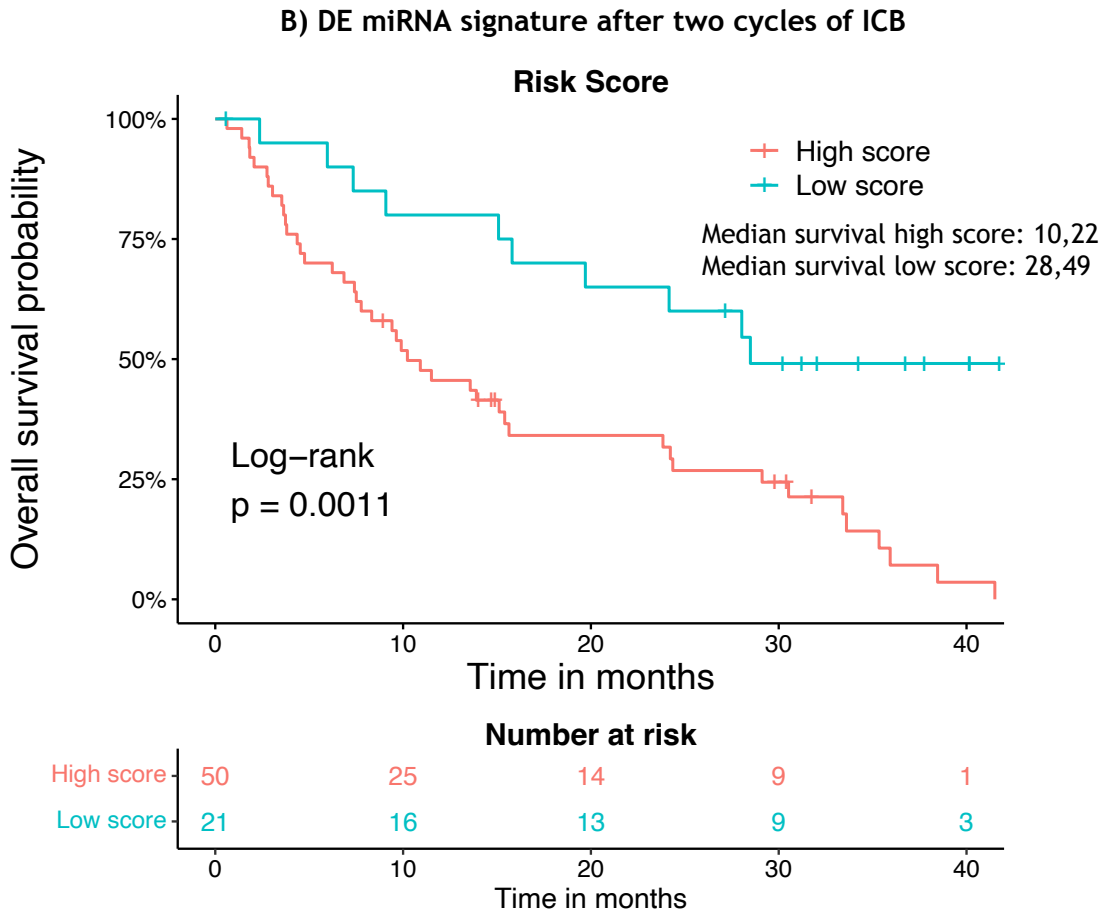

Figure 44. Differential expression miRNA signature predicted overall survival in mNSCLC patients. Kaplan-Meier overall survival (OS) curves for patients with high-risk score versus low-risk score based on A) basal DE miRNA when compared responder and non-responder patients (p-value < 0.01), and B) DE miRNA after two cycles of ICB when compared responder and non-responder patients (p-value <0.0011). Significance for the survival analysis was calculated with the log-rank test.

3.4.2.3.4. Longitudinal analysis of differential expression miRNA during ICB treatment between responder and non-responder patients.

Longitudinal analysis was performed in extreme responder and non-responder mNSCLC patients. To evaluate miRNA expression dynamics in each responder patient group before and during ICB treatment. Only statistically significant differences were observed when compared plasma derived EV miRNA

expression from blood samples before treatment (T1) and after two cycles of ICB (T2) in both groups. By comparing extreme non-responders uniquely between T1 and T2, a total of 24 downregulated and just 1 upregulated miRNA were found differentially expressed after second cycle of ICB **(Table 14.A).** However, taking into consideration responder patients, only a total of 16 DE miRNA were observed, with 9 downregulated and 7 upregulated after the second cycle of ICB **(Table 14.B).** Overall, non-responder patients had more expression changes associated with miRNA derived from circulating EV when they were administrated with ICB.

Table 14. miRNA differentially expressed analysis in each responder group before and after ICB. A) DE miRNA in the non-responder group and **B)** DE miRNA in the responders group.

A) Non-responder patients.

DE miRNA	Fold Change	p-value
hsa-miR-1-3p	-4,054	0,00007
hsa-miR-1298-5p	-2,962	0,001
hsa-miR-658	-2,353	0,012
hsa-miR-10395-5p	-2,314	0,004
hsa-miR-130b-5p	-2,314	0,010
hsa-miR-185-5p	-2,306	0,011
hsa-miR-10395-3p	-2,221	0,004
hsa-miR-125a-3p	-2,162	0,001
hsa-miR-134-5p	-1,929	0,016
hsa-miR-328-3p	-1,912	0,026
hsa-miR-10527-5p	-1,842	0,016
hsa-miR-320d	-1,820	0,020
hsa-miR-708-3p	-1,798	0,010

hsa-miR-378c	-1,778	0,014
hsa-miR-378d	-1,744	0,031
hsa-miR-199b-5p	-1,719	0,046
hsa-miR-92a-1-5p	-1,706	0,023
hsa-miR-320a-3p	-1,683	0,012
hsa-miR-2110	-1,638	0,040
hsa-miR-1291	-1,623	0,034
hsa-miR-10b-3p	-1,595	0,031
hsa-miR-193a-5p	-1,576	0,024
hsa-miR-3614-5p	-1,542	0,046
hsa-miR-505-5p	-1,520	0,040
hsa-miR-6724-5p	2,146	0,023

B) Responder patients

DE miRNA	Fold Change	p-value
hsa-miR-215-5p	-2,682	0,0004
hsa-miR-363-5p	-2,028	0,001
hsa-miR-4732-5p	-1,942	0,017
hsa-miR-130b-5p	-1,763	0,031
hsa-miR-5010-5p	-1,684	0,017
hsa-miR-320a-3p	-1,533	0,007
hsa-miR-1224-5p	-1,524	0,040
hsa-miR-324-5p	-1,515	0,044
hsa-miR-615-3p	-1,514	0,031
hsa-miR-200b-3p	1,584	0,031
hsa-miR-203a-3p	1,669	0,042
hsa-miR-200a-3p	1,810	0,013
hsa-miR-199b-5p	2,088	0,002
hsa-miR-205-5p	2,513	0,001
hsa-miR-302a-5p	2,947	0,002
hsa-miR-206	3,045	0,003

3.4.2.3.5. Tumor suppressor miRNA expression is associated with extreme response to ICB in mNSCLC patients.

All differentially expressed miRNA were found to be involved in tumor progression, proliferation, and apoptosis. Thus, to evaluate DE miRNA derived from plasmatic EV characteristics pattern of each group, some DE miRNA were analyzed individually in responder patients and then in non-responder patients.

Firstly, comparison in extreme non-responder patients before (T1) and after ICB (T2) showed hsa-miR-1-3p being the most downregulated miRNA (Log2(FC)= -4.05) **(Table 14.A).** This miRNA, which was observed related to lung cancer progression, was also up regulated in most of non-responder patients compared with responders when compared basal samples **(Figure 43)** (Wang et al., 201). As it is shown in **Figure 45**, hsa-miR-1-3p was also more upregulated in most of the non-responders at basal levels compared with samples after two cycles of ICB **(Figure 45.A).** In addition, when evaluate the dynamics of this miRNA along ICB treatment in non-responder patients, expression of hsa-miR-1-3p kept more downregulated in blood samples collected also at six months of ICB compared with basal expression levels **(Figure 45.B).** As hsa-miR-1-3p plays an important role as tumor suppressor in NSCLC, all these results may indicate that downregulation during treatment of this miRNA could be involved in tumor progression and early resistance to ICB treatment.

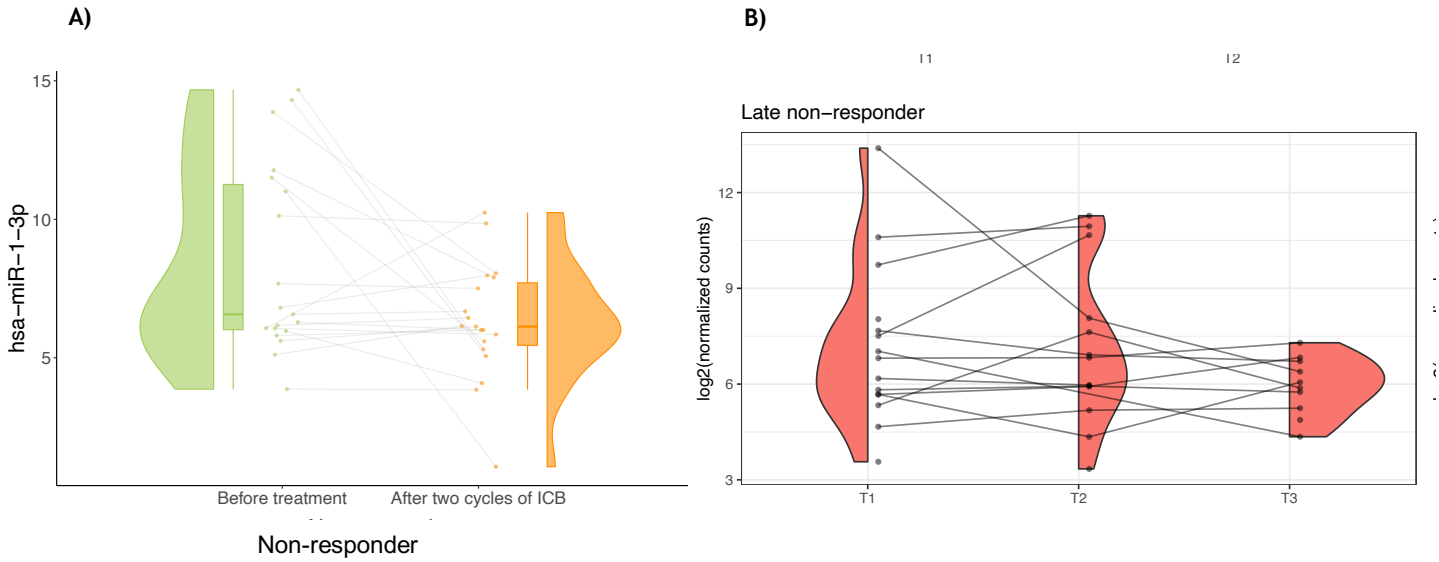

Figure 45: Hsa-miR-1-3p downregulated after ICB in non-responder patients after ICB. Changes in expression of candidate DE miRNA, showed downregulation of hsa-miR-1-3p after **A)** two cycles of ICB and **B)** six months of ICB.

Notably there were more interesting miRNA candidates in this analysis. Tumor suppressor hsa-miR-1298-5p has been reported as downregulated in mNSCLC patients and associated to poor overall survival (Du et al., 2019). These studies correlated with our results as hsa-miR-1298-5p showed lower expression after two cycles of ICB when compared with basal levels (Log2(FC)= -2,96) **(Figure 46.A).** Other miRNA with most downregulation expression was hsa-miR-658 (Log2(FC)= -2,35) **(Figure 46.B).** Downregulated expression levels in EV of hsa-miR-658 in NSCLC patients compared to healthy donors were shown (Z. Zhang et al., 2020). Also, this miRNA has been observed to be involved in chemo-resistant mechanism across exosomes secreted by resistant lung cancer cells (Azuma et al., 2020). Our results may indicate that downregulation of hsa-miR-658 derived from plasmatic EV could be involved in resistance to ICB in mNSCLC.

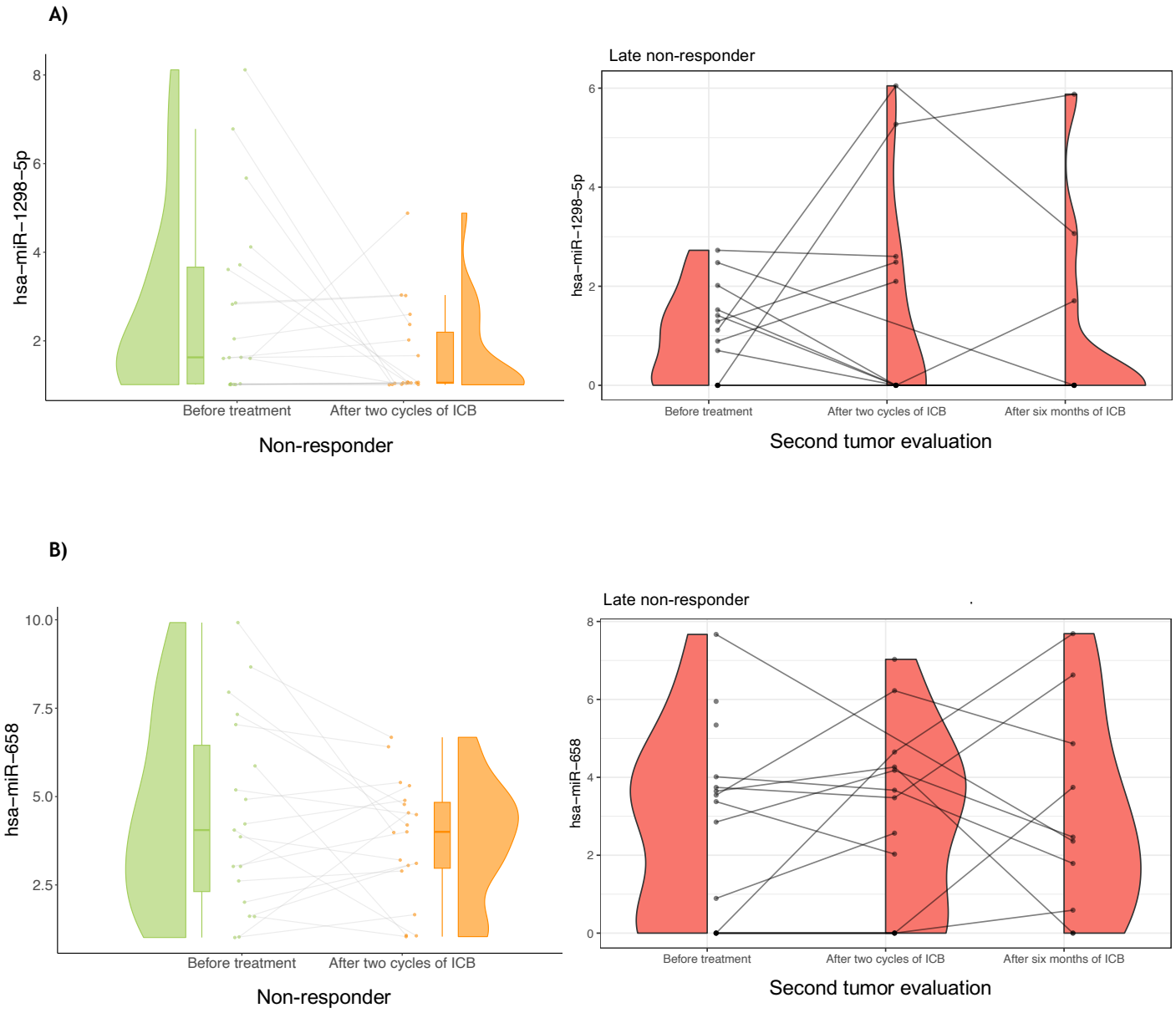

Figure 46: Downregulation of some tumor suppressor miRNA after ICB in non-responder patients at three months of tumor evaluation. Changes in expression of candidate DE miRNA, showed downregulation of **A)** hsa-miR-1298-5p and **B)** hsa-miR-658 after two cycles and six months of ICB.

Interestingly, in this analysis hsa-miR-6724-5p, which has been also found to be involved in tumor progression (Bonab et al., 2022b) was the only upregulated miRNA in T2 samples (Log2(FC)= 2,146). Also, patients who did not respond at six

months of ICB (T3) had similar upregulated expression levels when compared with samples after two cycles of ICB. Thus, hsa-miR-6724-5p may interfere in the absence of response to treatment in some mNSCLC patients once ICB has started **(Figure 47).**

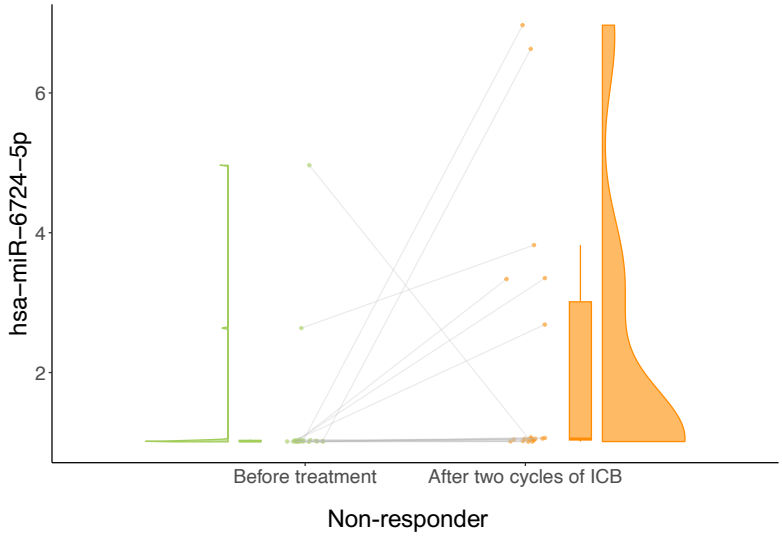

Figure 47: Upregulation of hsa-miR-6724-5p in non-responder patients after ICB. Hsa-miR-6724-5p was the only upregulated miRNA after two cycles of treatment (T2).

In responder patients DE miRNA analysis before and after treatment (T2), there were a group of tumor suppressor miRNA that were trending upregulated. On the one hand, hsa-miR-206 (Log2(FC)= 3,045) and hsa-miR-302a-5p (Log2(FC)= 2,947) showed higher expression values after the second cycle of treatment (T2) compared to samples before treatment (T1). In fact, it was checked the expression levels of both miRNA in blood samples of long-term responder patients, and as expected, they kept their expression high **(Figure 48.A and Figure 48.B).** Both miRNA were associated with apoptosis induction and tumor proliferation suppression in NSCLC (M. Liao & Peng, 2020) (Cheng et al., 2019). These results in responder patients may also indicate that ICB induces expression of some tumor suppressor miRNA.

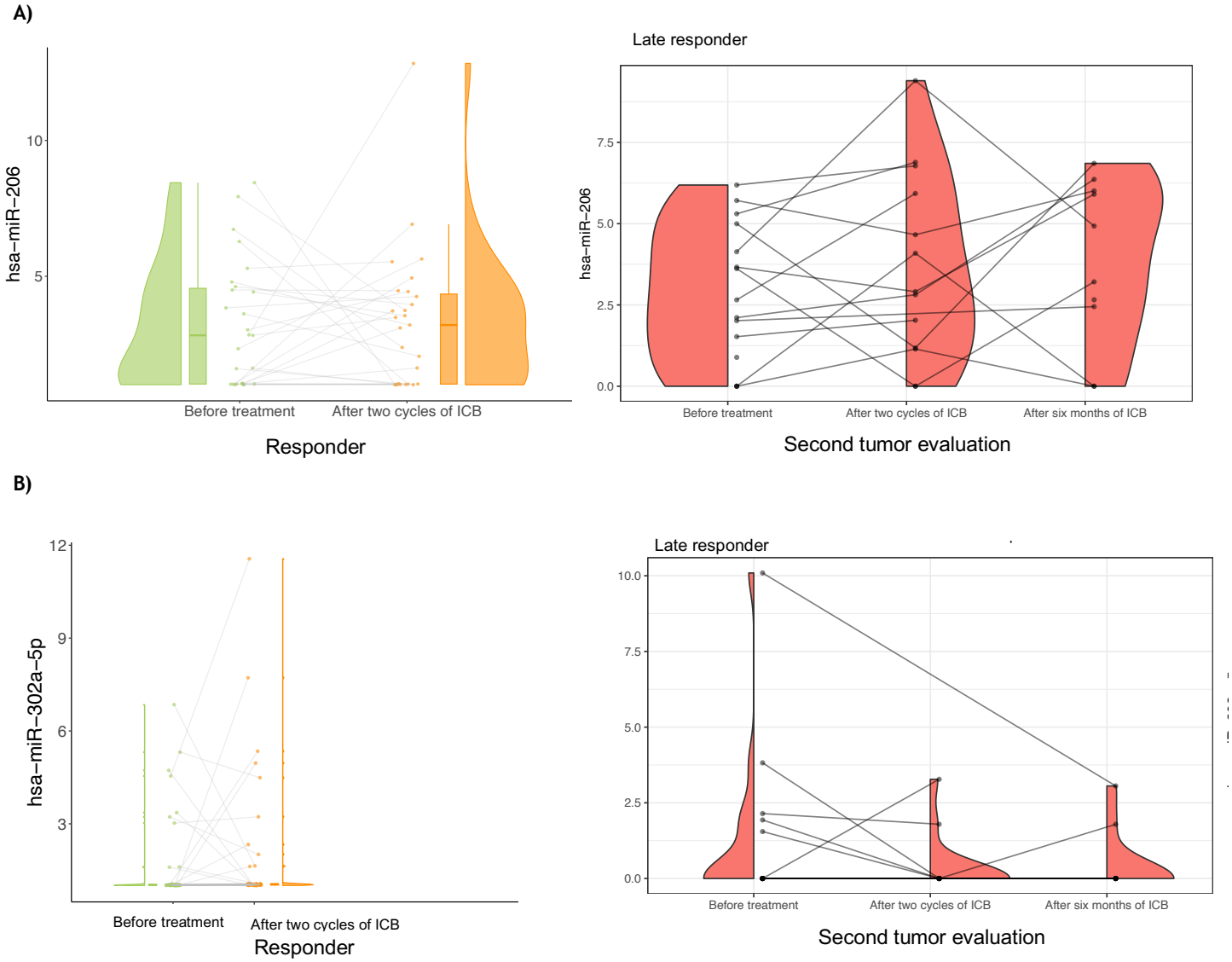

Figure 48: Upregulation of hsa-miR-206 and hsa-miR-302-5p induced by two cycles of ICB in patients in patients with response duration to ICB. Expression levels of **A)** hsa-miR-206 and **B)** has-miR-302-5p were higher after two cycles of ICB (T2) when compared with basal levels (T1) and after six months of ICB (T3).

Regarding hsa-miR-200b-3p (Log2(FC)= 1,584) and hsa-miR-205-5p (Log2(FC)= 2,513) increased their expression after ICB treatment. Both miRNA were also upregulated when compared with non-responder patients after two cycles of IBC. In addition, expression levels of both miRNA demonstrated to be similar in plasma derived EV when samples after six months of treatment (T3) and

samples after twelve months of treatment (T4) were also analyzed (**Figure 49.A and Figure 49.B).** Both miRNA, which were increased before ICB started in this group of patients compared with non-responders, act as tumor suppressor in cancer (Jo et al., 2022b) (Ferrari & Gandellini, 2020).

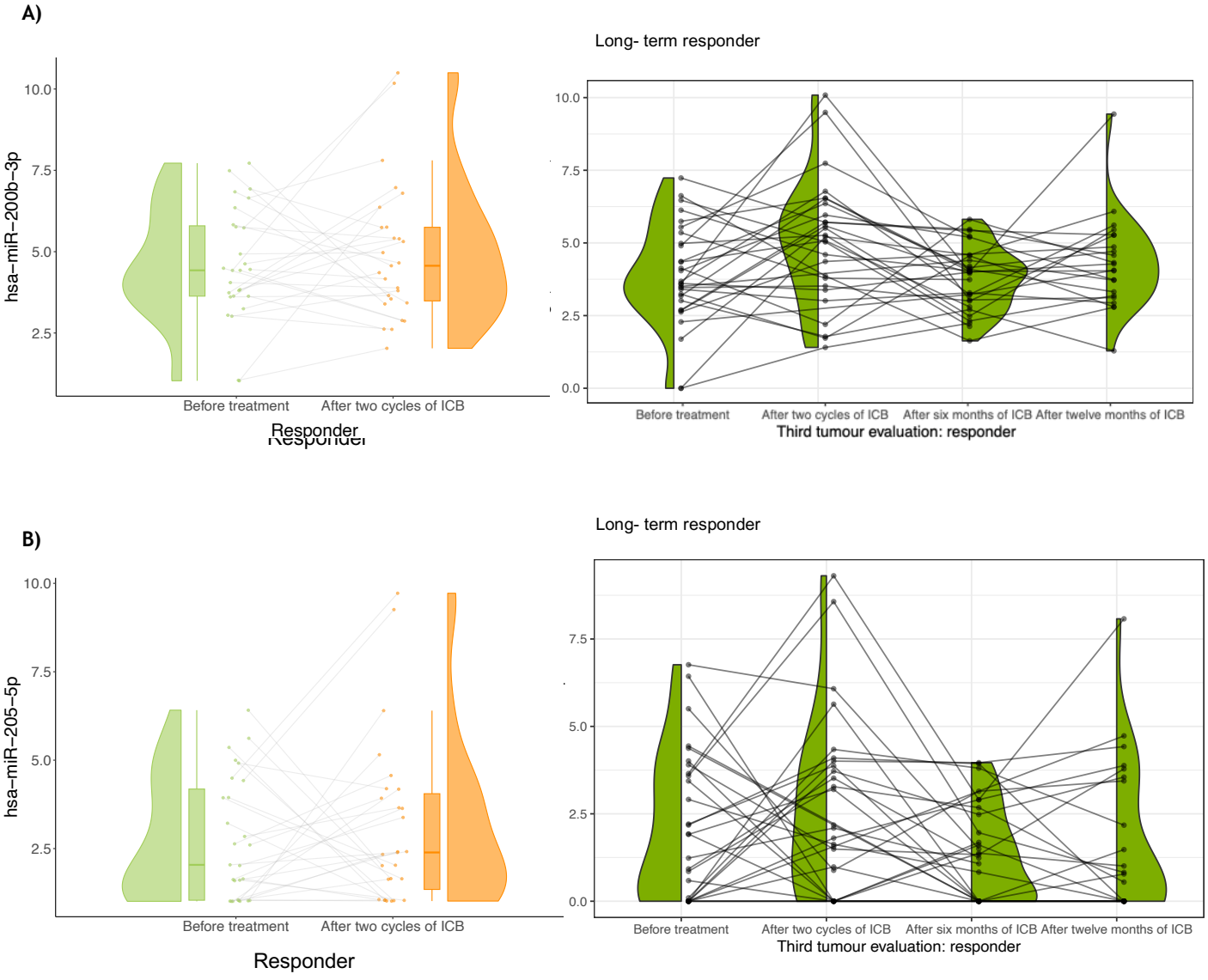

Figure 49: Tumor suppressor miRNA expressed before and during ICB treatment in patients with long term response. Hsa-miR-200b-3p **(A)** and has-miR-205-5p **(B)** were upregulated before and after two cycles of ICB. Also, they were found to be upregulated after six (T3) and twelve months of ICB (T4).

All previously described results showed that there may be a specific population of miRNA that was distinctively expressed in responder and non-responder patients. As a result, DE miRNA in both responder groups may constitute a specific panel of suppressor tumor miRNA that have potential as response biomarkers to ICB in mNSCLC.

3.4.2.3.6. Differentially expressed miRNA as part of immune system pathway signaling in mNSCLC patients.

To determine the functional relevance of the miRNA that have been identified in both response patient groups, differentially expressed miRNA were analyzed through biological pathways software Ingenuity Pathway Analysis and miRNA Enrichment and Annotation. All biological pathways were based on experimental evidence, with statistically significant associations shown.

i) miRNA-Targeted mRNAs network mainly involved in immunological pathways.

To identify potential biological mechanisms influenced by the dysregulation of miRNA expression before ICB, an analysis using the microRNA target filter tool in IPA was conducted in different DE miRNA set conditions **(Table 15)**. The applied significance filter showed a number of miRNA targeting mRNA involved in different signaling pathways such as “non-small cell lung cancer”, “cellular and humoral immune response” and specifically “PD-1 signaling”. Considering all the groups of DE miRNA in each analysis, it was observed that in general the paired miRNA/mRNA molecules were more abundant in the “cellular and humoral

immune response" pathway than in the "non-small cell lung cancer" and "PD-1 signaling" pathways (**Table 15**).

Table 15: mRNA-miRNA network involved in NSCLC and immune signaling pathways. It was summarized for all analysis the number of total miRNA and their targeted mRNA with the number of these molecules involved in different pathways.

Comparison analysis	Total miRNA/mRNA	NSCLC signaling miRNA/mRNA	Cellular immune response miRNA/mRNA	Humoral immune response miRNA/mRNA	PD-1 cancer immunotherapy miRNA/mRNAs
DE miRNA (T1) responders vs non-responders	16/248	6/13	11/115	10/37	6/8
DE miRNA (T2) responders vs non-responders	6/41	1/1	3/10	3/5	2/2
DE miRNA responders (T1) vs responders (T2)	9/76	2/3	6/29	6/14	4/6
DE miRNA non-responders (T1) vs non-responders (T2)	19/540	8/15	11/169	11/82	9/9

In the basal DE miRNA from responder and non-responder a total of 248 mRNAs interaction based on 16 of the 18 DE miRNA were revealed. Additionally, the differential expression IPA Core analysis of the dysregulated miRNA revealed the miRNA and mRNA targeted implied in cancer and immune pathways. As it has been previously reported, almost 99% of EV are generated from hematopoietic cells while less than 1% are derived from tissues (Alberro et al., 2021). Thus, it was expected that most of the plasma derived EV DE miRNA and their targeted

mRNA molecules were involved in immunological signal pathways. Consistent with this, there were more miRNA and mRNA targeted molecules involved in the pathways related to the immune system. If we focus on NSCLC signaling, a network of 6 miRNA and 13 mRNA was observed.

When comparing responder with non-responder patients to ICB before treatment (T1) and after treatment (T2) less interaction between miRNA and their targeted mRNA was observed in all the significant pathways. Only 41 mRNA based on 6 of the 9 DE miRNA were found. Regarding NSCLC signaling, after the second cycle of ICB there was only 1 miR-mRNA interaction, and only 10 mRNA interactions based on 3 miRNA when selecting immune response pathways. The analysis of DE miRNA in responder patients comparing pre and post-treatment samples (second cycle) yielded only 9 DE miRNA from a total of 15 miRNA with 76 targeted mRNA. However, in non-responders, there were 19 DE miRNA from 25 of total DE miRNA that interacted with 540 mRNA. This higher number of miRNA-mRNA interactions in responders was consistent in all significant pathways (**Table 15**). In addition, this dysregulation was also observed when this analysis was performed in both conditions. In responder patients, 41 canonical pathways were related to cancer while 73 were related to cancer in non-responders.

ii) miRNA/mRNA genetic networks involved in immune and lung cancer specific pathways.

Specific genes and molecules were part of the miRNA/mRNA network when the core expression analysis function included in IPA was carried out. Different miRNA-mRNA relationships appeared when we analyzed the DE miRNA in responder patients before (T1) and after the second cycle of ICB (T2). Interestingly, some up-regulated miRNA after the second cycle of ICB, such us hsa-miR-205-5p or hsa-miR-200B-3P, may inhibit genes like *Pdcd4, PTEN, STAT5B, TGFB2,* and *YAP1*, that in turninhibit both cell death and immune signaling pathways **(Figure 50).**

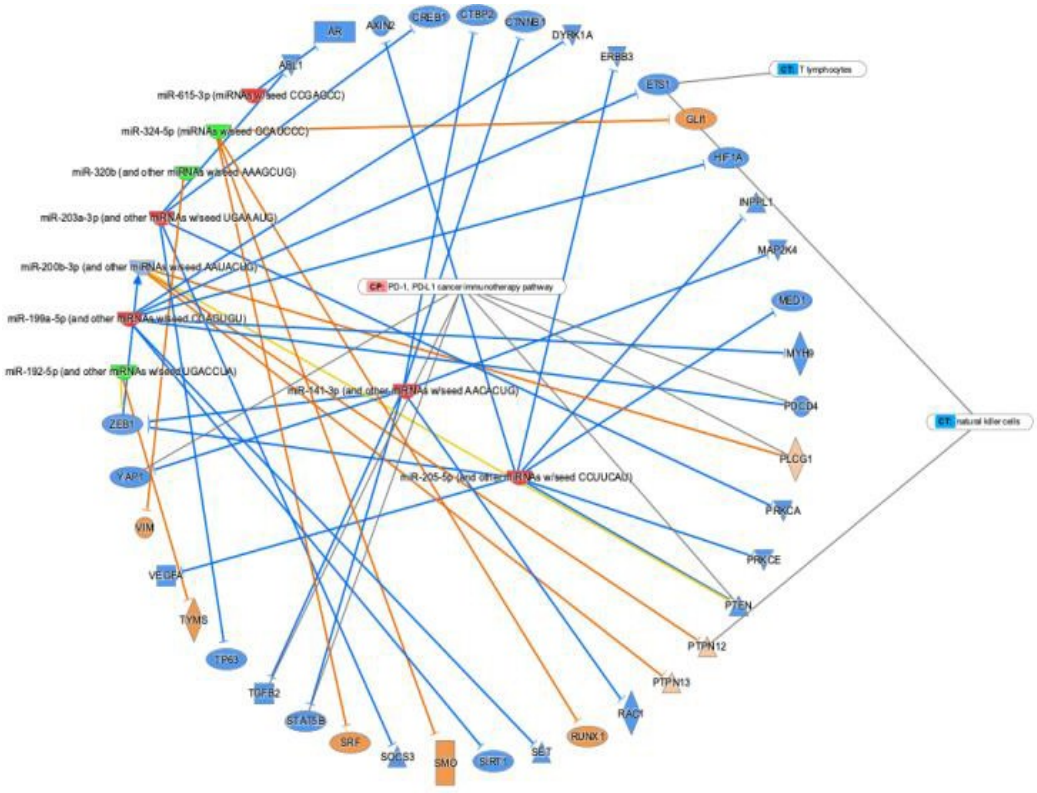

Figure 50: Ingenuity Pathway Analysis of the top up and downregulated miRNA and their target genes in responder patients before ICB and after the second cycle of treatment. The solid arrows indicate direct interactions, and the dotted arrows indicate indirect interaction between the differentially expressed miRNA and their predicted targets. The intensity of the respective colors indicates the fold expression (more intense orange indicates more upregulation and more intense blue indicates more downregulation).

To identify differences between conditions and their relationship with NSCLC, several comparison analyses were performed between DE miRNA from T1 in responder and non-responder patients and DE miRNA atT2 in responder and non-responder patients. Several relevant miRNA were detected in the "non-small cell lung cancer" signaling pathway. For example, hsa-miR-1-3p and hsa-miR-375- 3p, that are downregulated in non-responder patients, control cell proliferation through interaction with cyclins and cyclins dependent kinases **(Figure 51).**

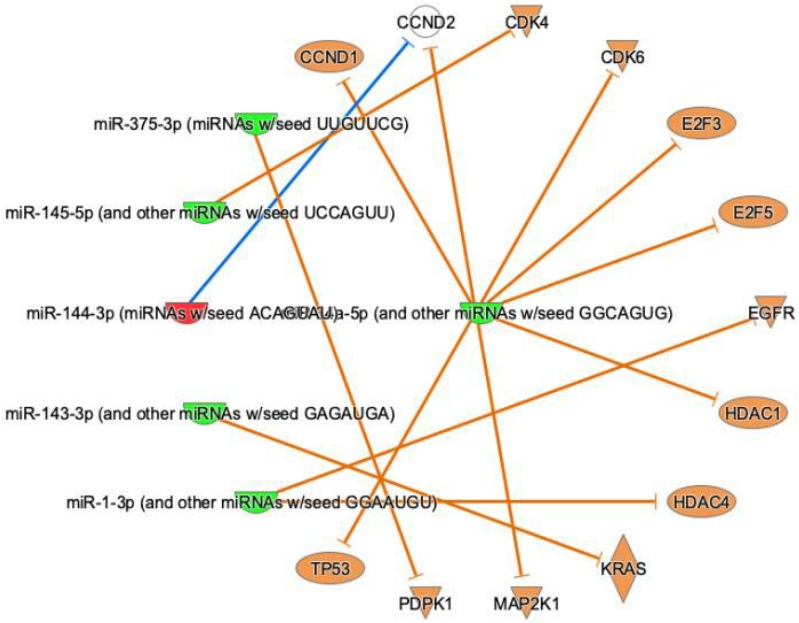

Figure 51: Downregulation of tumor suppressor miRNA activate cell proliferation via cyclins and cyclins dependent kinases in non-responder patients. IPA comparison analysis of the two different comparisons for DE miRNA before and after second cycle of treatment between responder and non-responder patients in NSCLC pathway. The intensity of the respective colors indicates the fold expression (more intense orange indicates more upregulation and more intense blue indicates more downregulation).

iii) Functional enrichment analysis revealed a basal miRNA signature associated to CD56+ immune cells.

a functional enrichment analysis of DE miRNA between responder and non-responder patients at T1 and T2. Using the over-Representation Analysis (ORA) algorithm, most of DE miRNA before the first cycle of ICB (T1) and after de second cycle of ICB (T2) were overrepresented in lung cancer, such as "lung squamous cell carcinoma" and "microvesicles" pathways. When enrichment analysis ((G)SEA) algorithm was applied to DE miRNA before treatment, a signature of miRNA enriched in CD56+ immune cells was identified (**Figure 52)**. Interestingly, CD56+ NK cells have been recently correlated with good response to ICB in lung cancer (Ruiz et al., 2023).

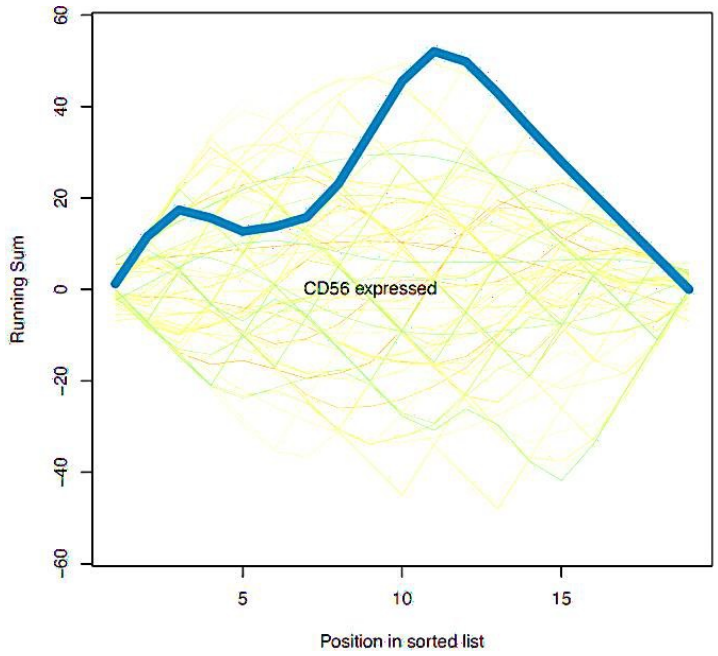

Figure 52: Basal signature of plasma derived EV miRNA enriched in CD56+ immune cells. Functional enrichment analysis of DE miRNA before treatment in responder and non-responder patients using Gene set enrichment analysis (GSEA) algorithm at miRNA Enrichment Analysis and Annotation tool (miEAA).

3.5. Circulating immune cells characterization

Total counts of specific circulating immune cell blood populations and their dynamics from pre-treatment to post-ICB treatment were assessed. Flow cytometry data and biochemistry tests were collected at different ICB times in 273 blood samples: 97 samples before treatment (T1), 88 samples three to four weeks after the start of therapy (T2), 54 samples six months (T3) and 34 samples twelve months (T4) after treatment started. **Table 16** summarized analysis characteristics performed to these molecular biomarkers.

Table 16: Circulating immune cells characterization. The blood biomarker analyzed in this aim was differences of circulating immune cell levels before treatment started (T1) and after two cycles of ICB (T2) in responder and non- responder patients at three, six and twelve months of tumor evaluation.

Blood biomarker	Treatment time analysis	Response criteria
Blood-derived circulating immune cells	Before treatment starts (T1)	First tumor evaluation (3 months of ICB)
	At second cycle of ICB (T2)	Second tumor evaluation (6 months of ICB)
	After six and twelve months of ICB (T3 and T4)	Third tumor evaluation (12 months of ICB)
		Extreme response

3.5.1. Basal circulating immune cell blood profiles and association with response

Quantification of the main immune cells lineages in peripheral blood was plotted separately for responders and non-responders to determinate whether basal circulating immune cells could be used as indicators of responses, regarding previously described response criteria Section **2.1.1.2. (Supplementary Table 4).** Only statistical differences were observed in pre-treatment monocyte cell number being increased in those who progressed after two cycles of ICB (early no responder patients) (Wilcoxon Test p-value 0.029) **(Figure 53).**

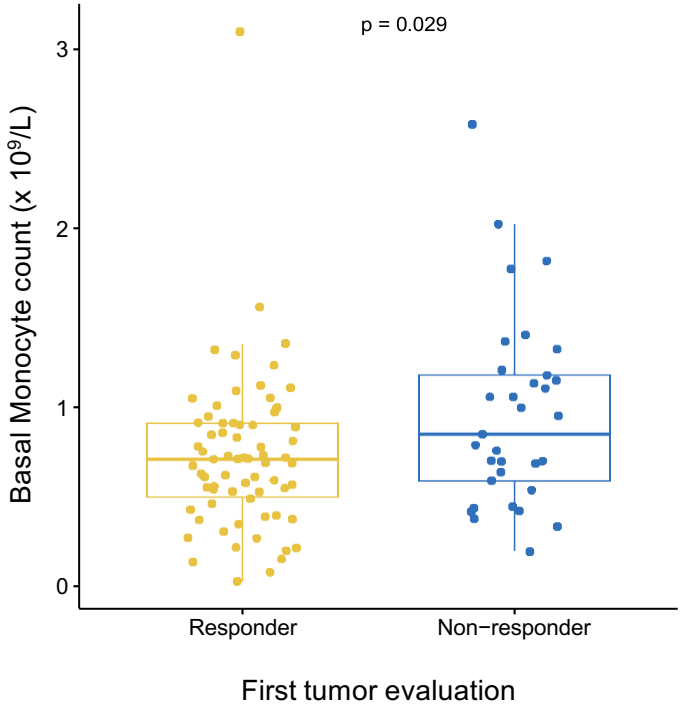

Figure 53: Basal monocytes cells increased in early non-responder mNSCLC patients. Non-responder patients at three months of treatment had higher levels of monocytes compared with early responder patients at three months of ICB.

3.5.2. Dynamic changes of circulating immune cell blood populations and association with response during ICB treatment

As ICB treatment is correlated with circulating immune cells changes, analysis of these subsets was performed during ICB treatment and correlated with response criteria. At this point, administration of treatment had different effects in circulating immune cells in those patients who respond and not to ICB treatment.

After the second cycle of ICB (T2) the number CD3+ T cells and specially number of helper lymphocytes CD3+CD4+ T cells, were increased in those patients who responded early to ICB after second cycle of treatment (early responders) (Wilcoxon Test p-value 0.021), and in patients who responded after six months of ICB (Wilcoxon Test p-value 0.017). Interestingly, this T cell subset is also higher when responder patients were evaluated after twelve months of ICB (extreme response) (Wilcoxon Test p-value 0.032) **(Figure 54A and Figure 54.B).**

Blood from responder at one year of treatment have also increased these CD3+CD4+ T cells (Wilcoxon Test p-value 0.041) **(Figure 54.C).** Previous studies have correlated CD4+ T cells lymphopenia with poor survival in lung cancers (Eberst et al., 2022). Thus, it may indicate that abundance of CD4+ T cells could be induced by ICB and lead to better response to this treatment.

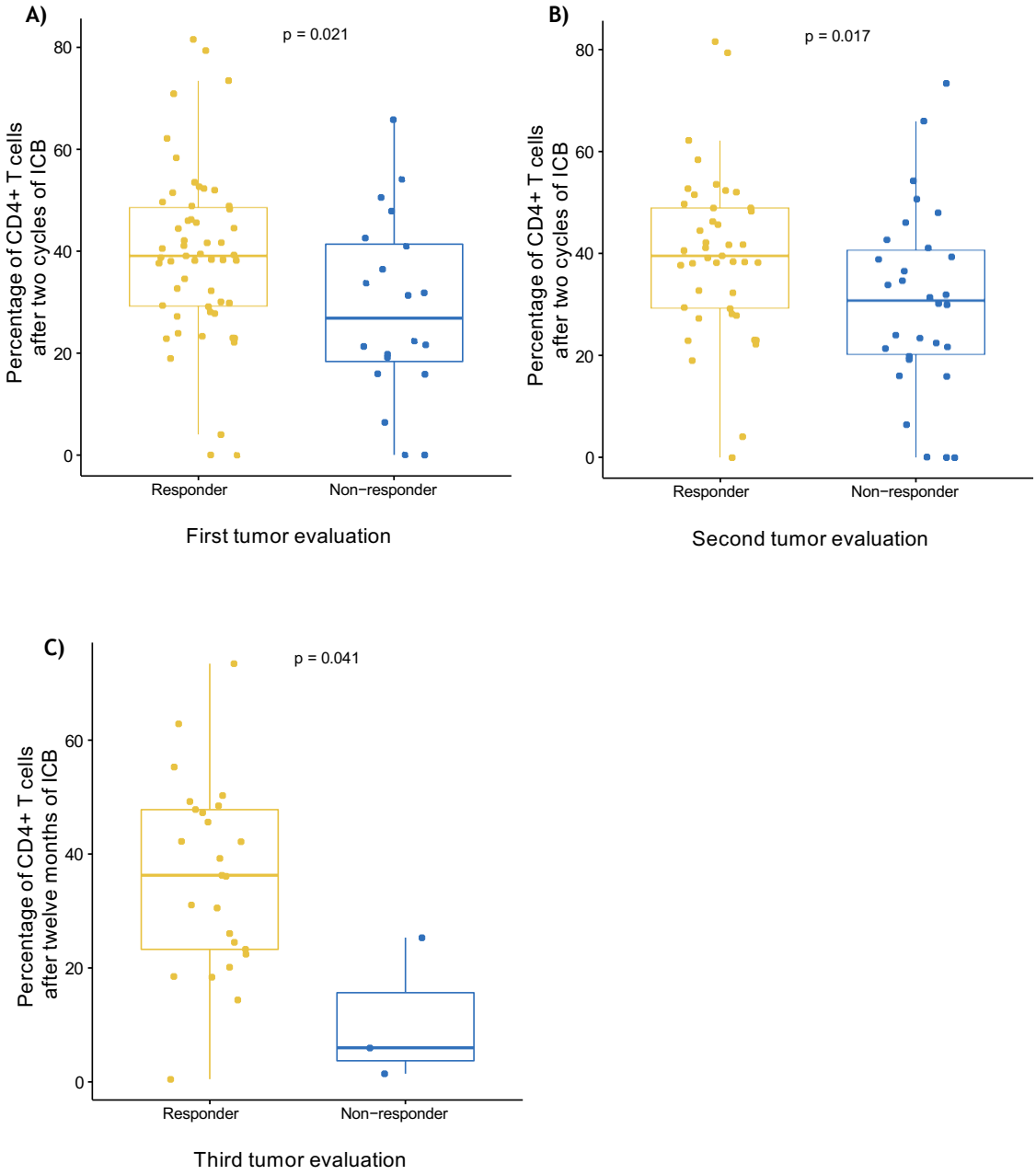

Figure 54. Increased levels of circulating CD4+ T cells in mNSCLC patients responding to ICB. Helper T cells (CD3+CD4+) were found to be at higher levels in responder mNSCLC blood samples at second cycle of ICB treatment (T2) when **A)** early response, **B)** response at six months and **C)** response at one year of treatment was evaluated. Also, long-term responders kept higher levels of helper T cells (CD3+CD4+).

As is well known, CD8+ cytotoxic T lymphocytes (CTLs) and exhausted CD8+ T (CD3+CD8+ CD274+) T cells play a significant role in antitumor immunotherapy. Another goal of this immune cell characterization was to study how ICB treatment may affected exhausted CD8+ PD-L1+ (CD3+CD8+ CD274+) T cells and how this is correlated with ICB response. Remarkably, these specific cells show statistical significance between responder and non-responder patients after two cycles of ICB when tumoral response were evaluated after six months of ICB, (Wilcoxon Test p-value 0.029). Interestingly, exhausted phenotype decreased in responder patients when blood samples after six months of ICB were evaluated compared with non-responder patients (Wilcoxon Test p-value 0.008). It may indicate that during exhaustion, CD8+ T cells lose several functions which include the ability to recognize and attack tumoral cells (Wherry, 2011). **(Figure 55).**

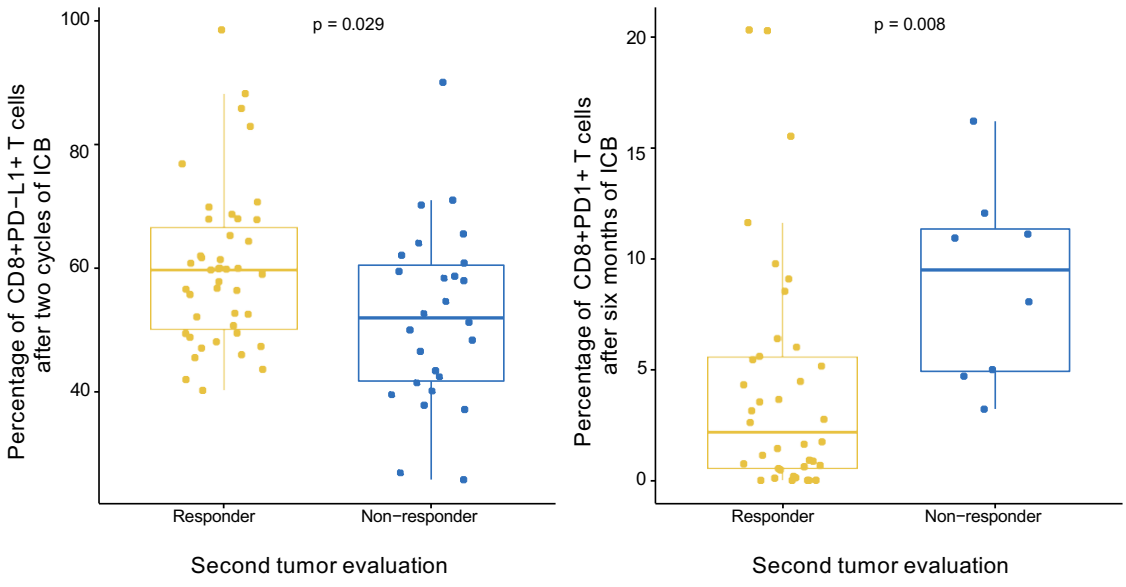

Figure 55. Increased levels of circulating exhausted CD8+PD-L1+ T cells in responder mNSCLC patients during ICB treatment. A) Exhausted CD8+PDL1+ T (CD3+CD8+274+) levels after two cycles of ICB may correlate with response**. B)** However, percentage of this phenotype at six months of treatment decreased in responder patients but kept high in non-responders.

Other leukocytes cells were increased in non-responder patients, also at different response evaluations. Number of neutrophiles were increased in those patients who progressed at different ICB treatment evaluation, first tumor evaluation and second tumor evaluation (Wilcoxon Test p-value 0.0046 and Wilcoxon Test p-value 0.04, respectively) **(Figure 56.A and Figure 56.B).** Neutrophiles still kept higher in blood samples (T3) in non-responder patients at second tumor evaluation (six month of treatment) compare with those patients who respond at one year of ICB (Wilcoxon Test p-value 0.016) and at third tumor evaluation (Wilcoxon Test p-value 0.009) **(Figure 56.C and Figure 56.D).**

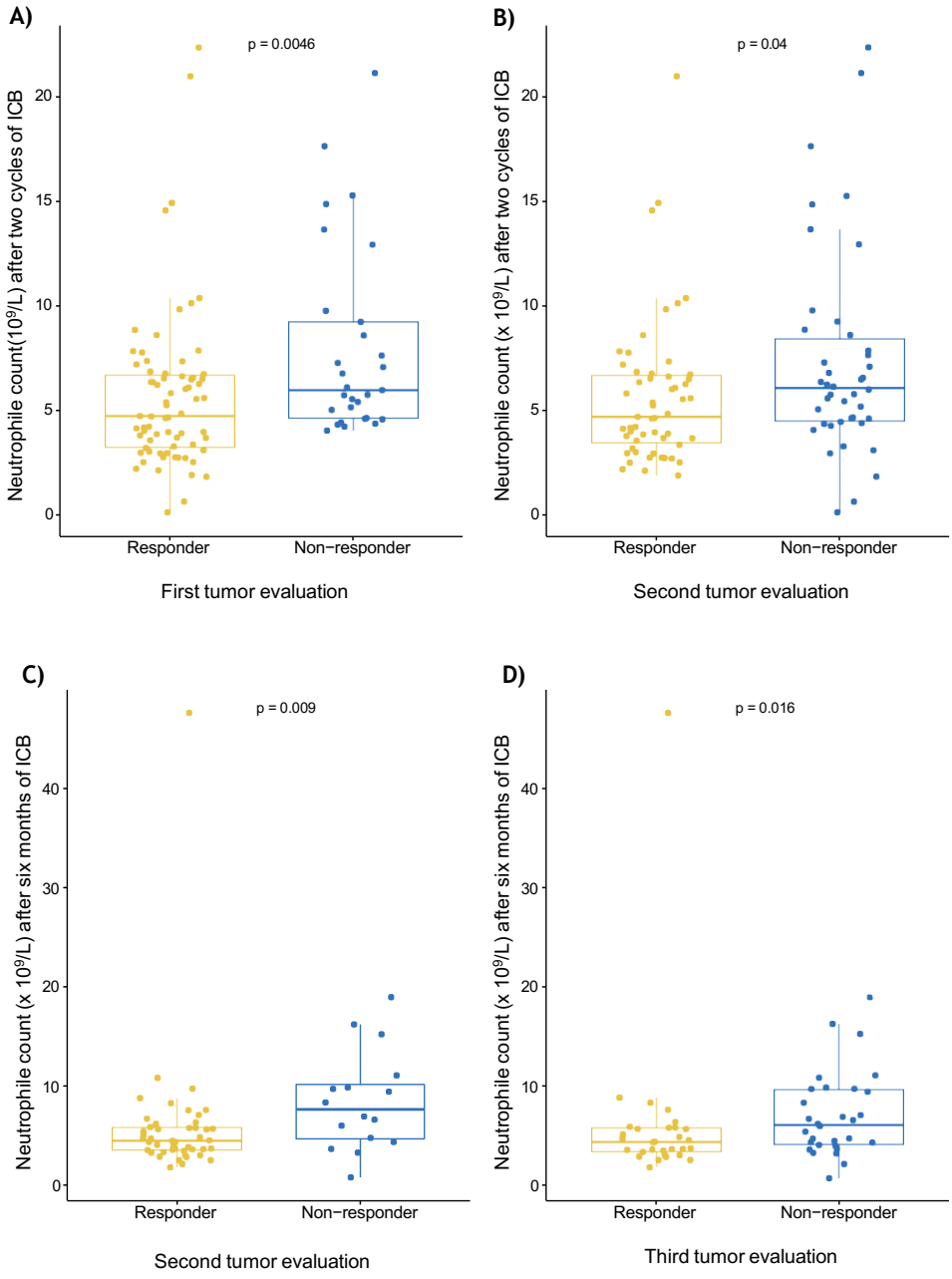

Figure 56. Post-treatment elevated number of neutrophiles in mNSCLC non-responder patients. Pre-treatment neutrophile count was higher in non-responders in different clinical evaluations. **A)** First tumor evaluation; **B)** Second tumor evaluation. Counts of neutrophiles after 6 months of ICB were also higher in non-responders for both the response at C) six and D) twelve months.

Numerous studies have correlated neutrophile-to-lymphocyte (NLR) to response to ICB. An elevated number of neutrophils as quantified by NLR was correlated with shortened survival in NSCLC (Ren et al., 2019). As neutrophiles and lymphocytes in our mNSCLC cohort showed changes between responder and non-responder patients along disease evolution, which may correlate with clinical responses, the relative NLR ratios were further analyzed. As expected, the NLR ratios between pre-treatment (T1) and first two cycles of ICB (T2) were statistically significant when response at six months were assessed (Wilcoxon Test p-value 0.057) (Wilcoxon Test p-value 0.049) **(Figure 57.A and Figure 57.B**). Neutrophiles kept at higher levels in blood samples after six months of ICB. So, to see the evolution of the NLR ratio during ICB treatment, it was calculated the NLR ratio between pre- treatment and six months of ICB (T3). Responder patients still have lower NLR ratio levels compared with those non-responder patients at six months of treatment (**Figure 57.C.)**

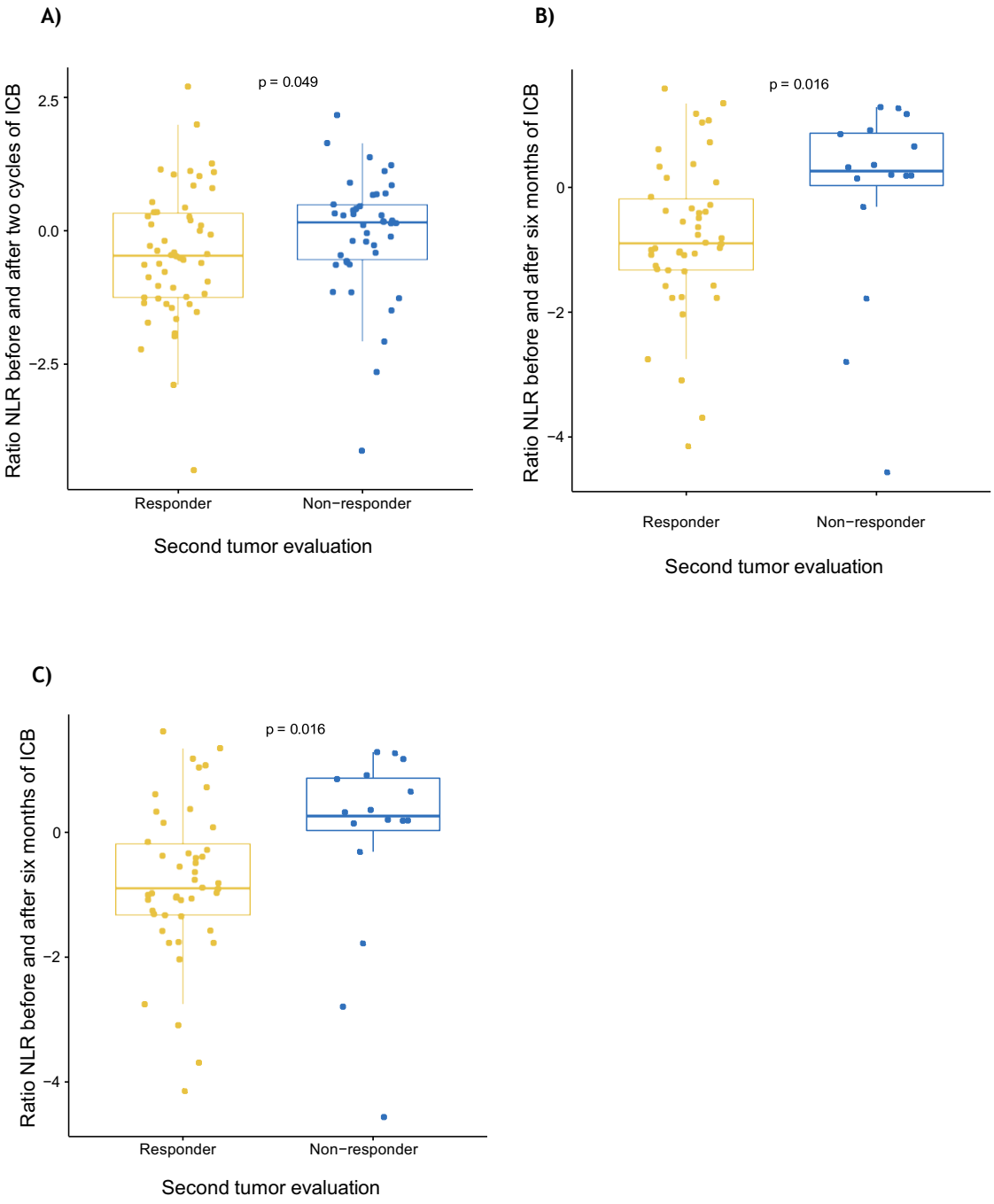

Figure 57. Higher NLR ratios during ICB in mNSCLC non-responder patients. Neutrophil-to-lymphocyte (NLR) ratios were estimated between pre-treatment (T1) and two cycles after ICB blood-sample (T2) and correlate with **A)** early response, **B)** response at six. **C)** NLR ratio between pre-treatment (T1) and treatment at six months (T3) were also higher when correlated with response at six months

Exploratory analyses of other circulating immune cells during ICB treatment revealed an increased amount of eosinophiles cells associated to response to ICB. Surprisingly, these cells did not correlate with response at the beginning of ICB. However, this tendency started when blood from patients who have been at least six months and twelve months with ICB was analyzed (T3, T4). Samples collected at six months of ICB correlated with the second tumor evaluation (Wilcoxon Test p-value 0.0051) and third tumor evaluation (Wilcoxon Test p-value 0.0022). Also, samples collected at one year of ICB also correlated with third tumor evaluation (Wilcoxon Test p-value 0.045) (**Figure 58).** Many studies have focused on the role of eosinophils in tumors like NSCLC. It is largely known how eosinophils infiltrate tumors and in most cases are associated with an improved prognosis (Davis & Rothenberg, 2014). Thus, our results may indicate a key role of these circulating immune cells in patients who responded to ICB after six months of treatment.

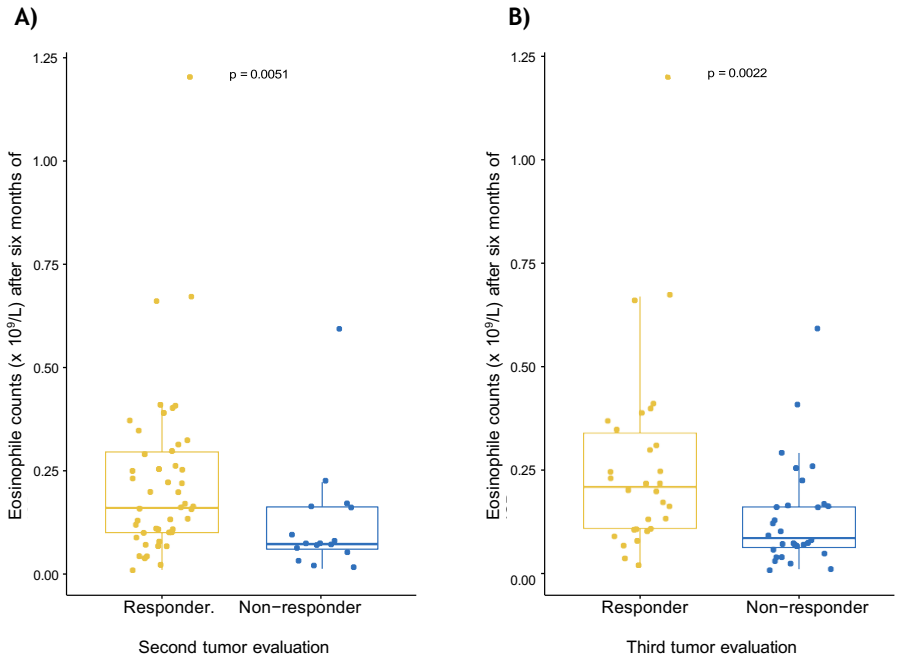

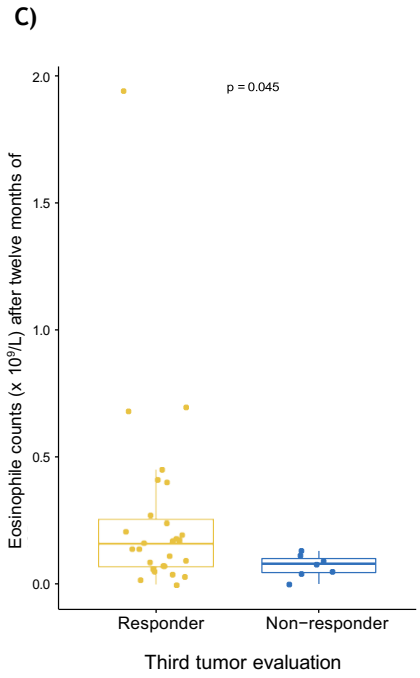

Figure 58. Abundance of eosinophils in mNSCLC patients with long lasting ICB response. A) More than two cycles of ICB during six months have shown to increase the number of eosinophils in responder patients at second tumor evaluation (response 6 months) and **B)** in long-term responders (response one year). **C)** Also, this abundance was observed in blood after one year of ICB in long-responder patients.

3.5.3. Prognostic value of circulating immune cells

The survival analysis revealed that levels of basal monocytes or CD3+PDL1+ T cells (CD3+CD274+CD279-) profiles had not significant correlations with overall survival (OS). However, after 3-4 weeks in treatment (T2) some circulating immune cells significantly correlated with survival. Specifically, Kaplan-Meier survival analysis revealed a significantly better survival of patients with high CD3+CD4+ T cells levels (median 24.33 vs 8.33 months, log-rank p-value (log-rank p-value: $2.024x10^{-3}$) **(Figure 59.A).** On the contrary, high levels of neutrophiles after second cycle of ICB were associated to shorter OS (median 10.92 vs 29.11

months, log-rank test p-value 2.8569x10^{-2}) **(Figure 59.B).** High eosinophils counts after second cycle of ICB were associated to longer OS (median 10.92 vs 29.11 months, log-rank test p-value 5.0281x10^{-2})

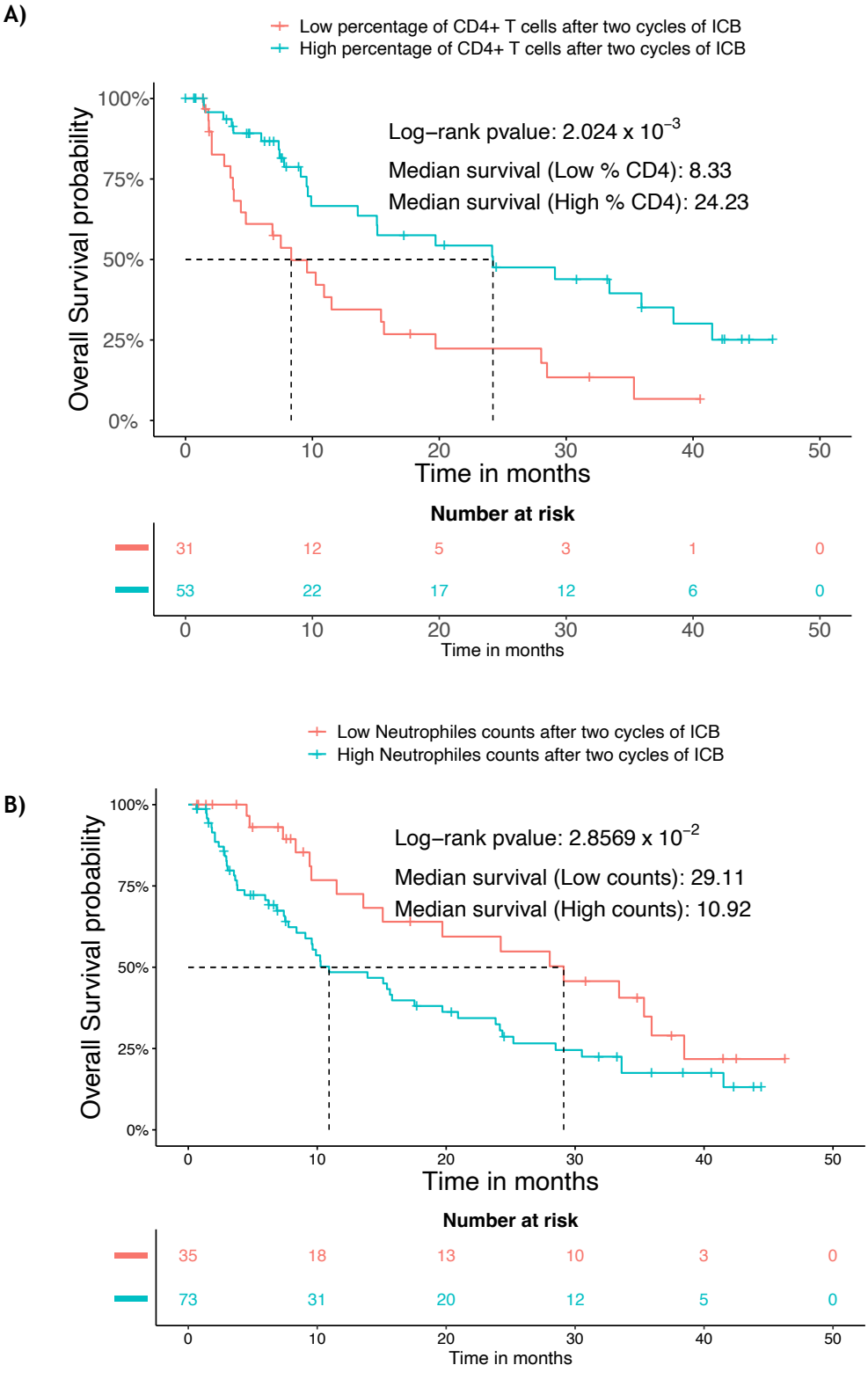

C)

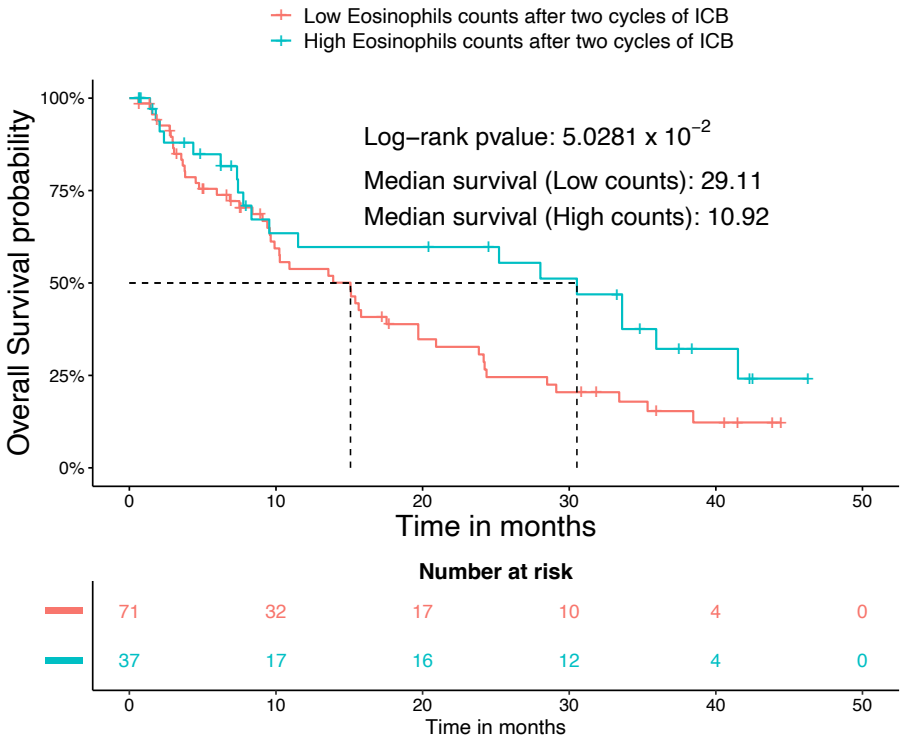

Figure 59. Overall survival curve for basal circulating immune cells. A) Kaplan-Meier overall survival plot of high and low levels of post-treatment helper CD3+CD4+ T cells. **B)** Kaplan-Meier overall survival plot for basal neutrophils cells high and low levels. **C)** Kaplan-Meier overall survival plot for eosinophils cells high and low levels after two cycles of ICB. Significance for the survival analysis in a and b was calculated with the log-rank test.

3.6. Prognostic multivariant models based on previously described biomarkers.

Until this section, univariate analyses identified correlations between cfDNA concentration and clinical outcome. In this last section, multivariate Cox-regression analyses were performed to identify which clinical variable may independently influence overall survival. Thus, cfDNA and variables which are already well known to be prognostic and predictive biomarkers such as age at treatment, Eastern ECOG score, Lactate dehydrogenase (LDH), and PDL status were included **(Table 17).**

Table 17: Multivariant prognosis model. The previously described biomarker based on cfDNA concentration was integrated to develop the multivariant prognosis model to predict survival in mNSCLC patients that are candidates to ICB.

Blood biomarker	Variables used	Cohort patient
Multivariate Model	cfDNA (T1) Clinical variables currently validated: ECOG, age, LDH, PDL1	mNSCLC

The univariate results showed that cfDNA concentrations over 0.55 ng/µL were also associated with worse outcomes and were independent predictors for OS with a hazard ratio of 3.09 CI (1.6–5.9) and p value < 0.001 **(Figure 60.A).** Additionally univariate analyses in clinical characteristics showed that these

factors did not have independent prognostic value on shortened survival **(Figure 60.B).**

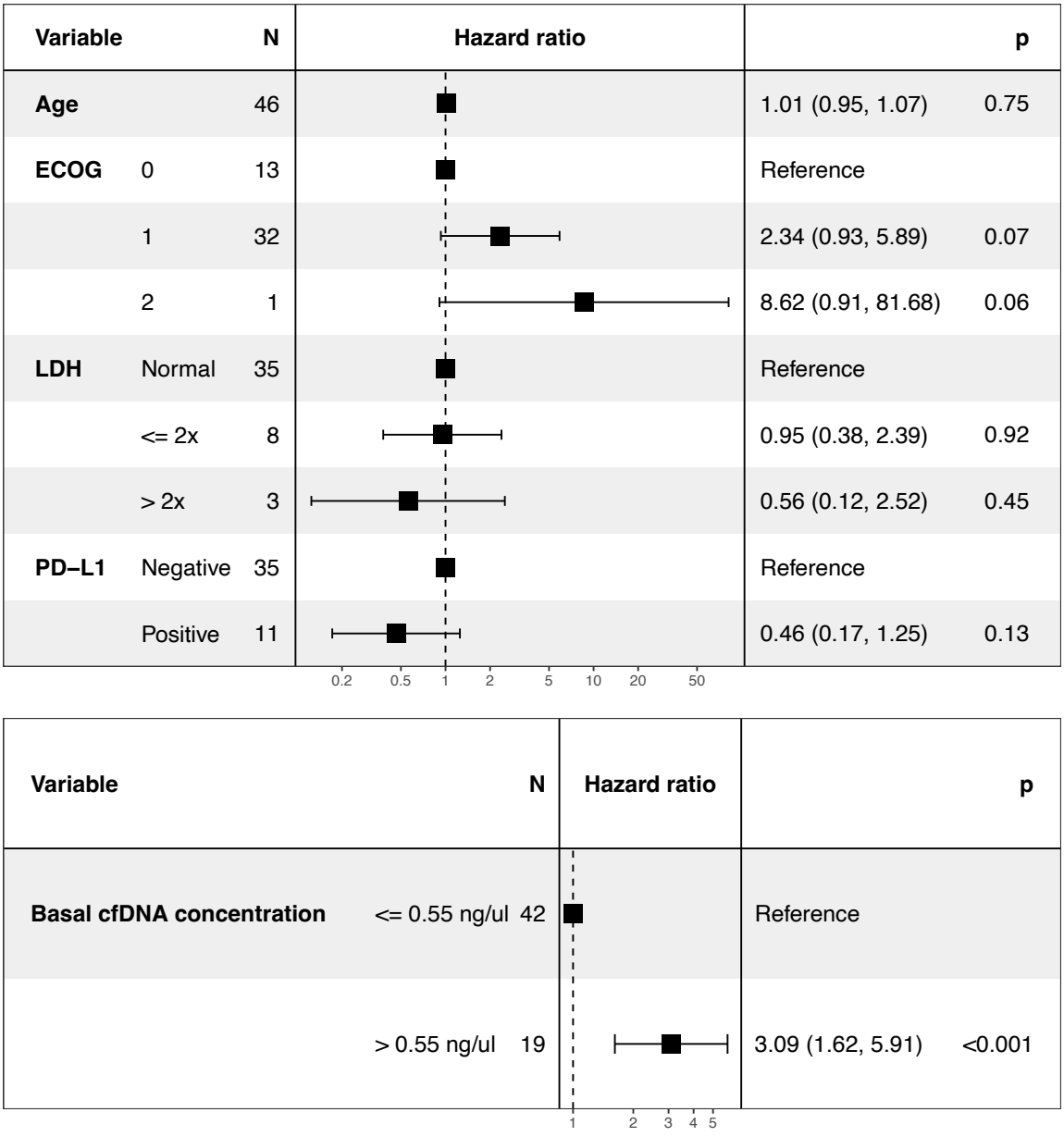

Figure 60. Univariate analyses of clinical variables. A) Univariate analysis of clinical variables selected like age, ECOG, LDH, PDL-1. **B)** Univariate analysis of basal cfDNA concentration cut off.

As shown in **Supplementary Table 1**, the basal cfDNA concentration correlated with higher LDH levels. Thus, basal cfDNA has also been speculated to be surrogate biomarker of these clinical variables. To evaluate this behavior,

multivariate analyses were performed using all variables together. The results showed that cfDNA was an independent predictor for OS with a hazard ratio of 2,51 CI (0,97-,45) and p value 0,06 **(Figure 61).**

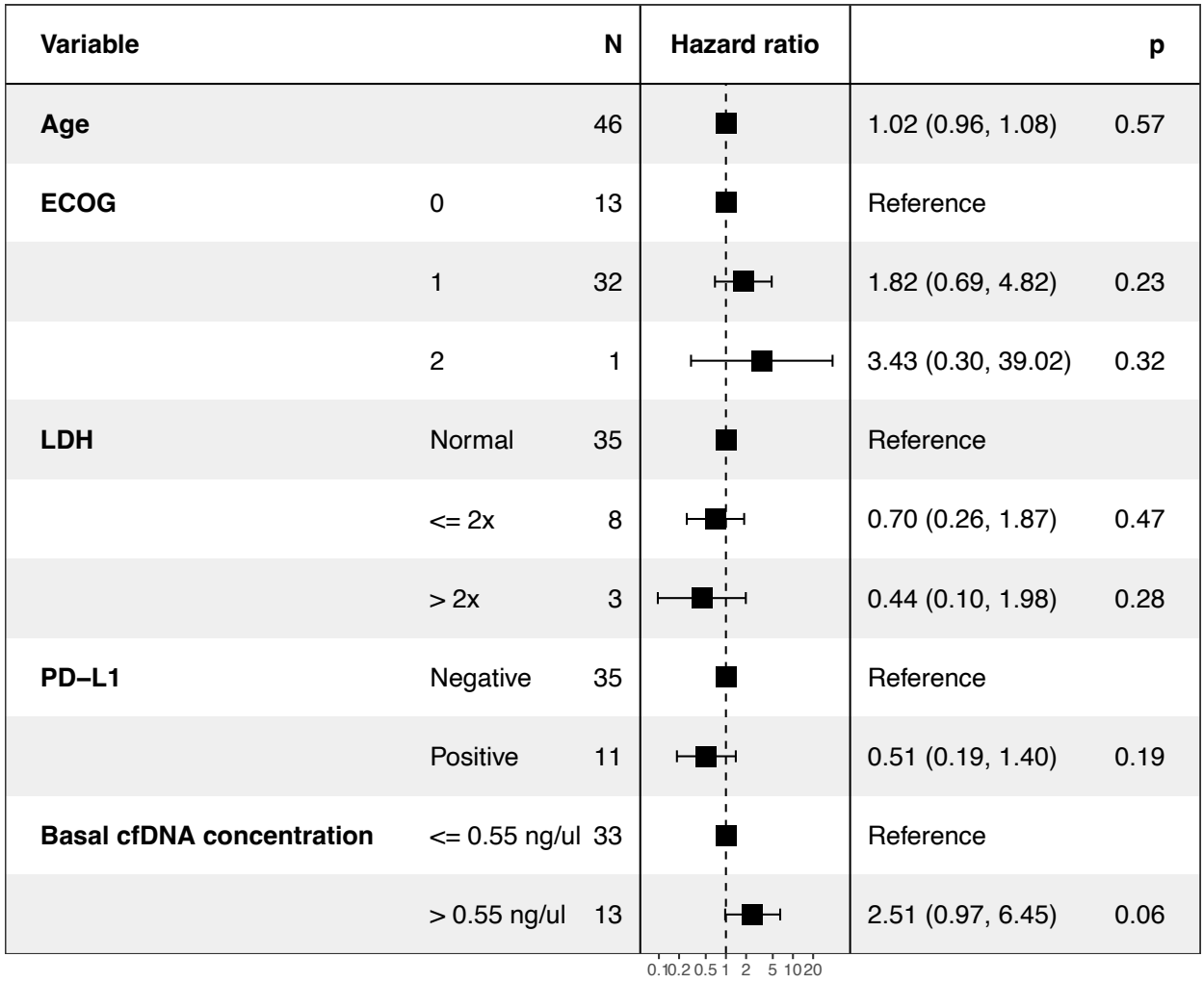

Figure 61. Multivariate analyses of clinical variables. Variables selected were age, ECOG, LDH, PDL-1 and basal cfDNA concentration cut off.

Finally, the potential prognosis potential of cfDNA concentration was compared with the established model based on the established clinical variables with the AUC estimator proposed by (Uno et al., 2007). The summary AUC output of our cfDNA model was 0.71, whereas the clinical model had an AUC of 0.55.

Moreover, the combination of the cfDNA concentration and age at treatment, ECOG, LDH, and PDL1 status, outperforms the individual model by reaching a summary AUC of 0.74 **(Figure 62).**

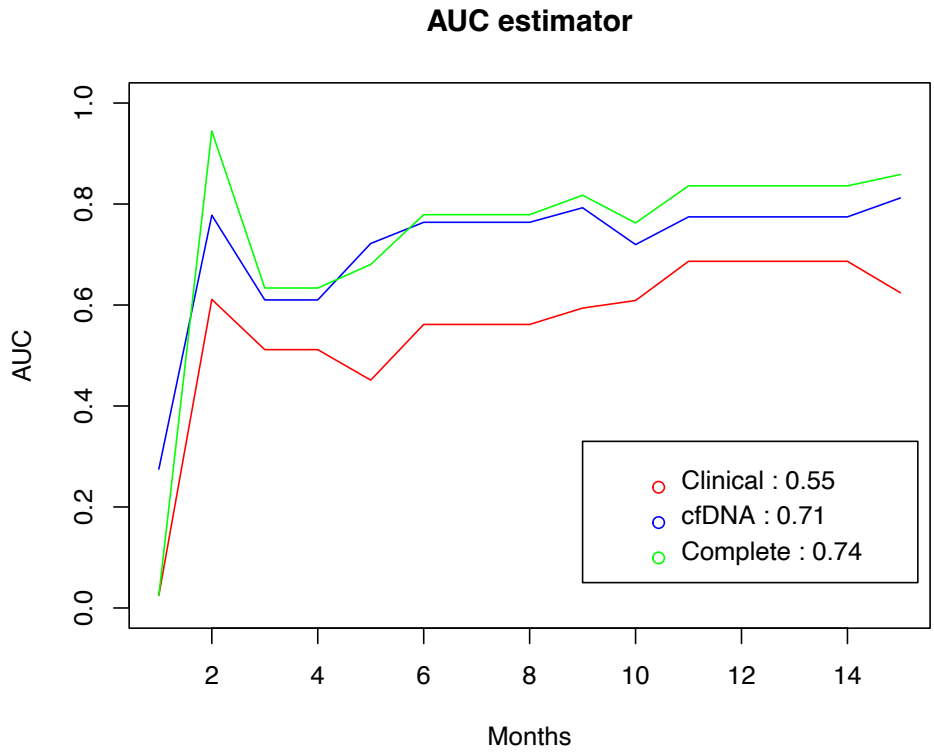

Figure 62. Prognostic models of basal cfDNA concentration. Comparison of the prognostic potential of the cfDNA prognostic models using the AUC estimator.

CHAPTER IV: DISCUSSION

Identifying and understanding biomarkers is essential for personalized cancer treatment, as they help tailor therapies to the specific characteristics of each patient's tumor, and in the context of immunotherapy, each patient´s immune system at the moment of treatment. Cancer diagnosis, prognosis, and treatment agglutinizes an important number of biomarkers, 30% of reported biomarkers (McKean et al., 2020). Biomarkers may facilitate cancer early detection and help in diagnosis accuracy or in tumor subtyping. Many biomarkers can be profiled using minimally invasive procedures, such as blood tests or urine samples, and provide real-time information on the molecular characteristics of a patient's cancer (Cyll et al., 2017). They provide prognostic information, helping to predict the likely course of the disease and can also have predictive value regarding the response to a particular treatment. This personalized approach to treatment selection helps to optimize therapeutic strategies, leading to more effective and targeted therapies. All these advantages make them a promising tool in our field of work, cancer immunotherapy (Safonov et al., 2016). Although in general they have substantially improved the detection and management of cancer, many tumors still have high mortality rates. One approach to fight this involves addressing the current limitations of cancer biomarkers. They have to do with suboptimal sensitivity and specificity, inherent heterogeneity and evolution, interference with other patient conditions or tissue-specificity. Also, process development-related limitations like high costs and the need of rigorous validation and standardization before approved and widespread use in clinical practice. (Sarhadi & Armengol, 2022).

Immunotherapy, and especially immune checkpoint blockade (ICB), is one of the leading treatments for solid tumors, including lung cancer. Patients eligible for ICB increased from 1.54% in 2011 to 43.63% in 2018, and total responders departed from less than 0.14% to reach a rate of 12.46%. Some of these responders have achieved durable response evidenced by a plateau of the treatment "tails" in Kaplan-Meier survival curves (Haslam & Prasad, 2019). Moreover, ICB-treated patients present less aggressive adverse effects than those described by classical therapies like chemotherapy or radiotherapy. (Morad et al., 2021). ICB based monoclonal-antibodies can block inhibitory signals in the immune system, particularly those mediated by molecules like PD-1, PD-L1, and CTLA-4. As tumor can evade the immune system's surveillance and elimination mechanisms by expressing these inhibitory immune signals, the blockade mediated by ICB unleashes the immune system, allowing it to mount a more robust and effective attack against cancer cells (Topalian, 2017). Promising results from a small first-in-human trial of the anti–PD-1, PD-L1 and CTLA-4 led to drug approval of anti-CTLA-4 Ipilimumab (2011) or anti PD-1 Nivolumab or Pembrolizumab (2014) for many solid tumors like melanomas, kidney cancers or lung cancers. Although immune checkpoint blockade (ICB) has shown significant success in treating various cancers, there are some limitations and challenges associated with this approach. First, the response rates vary widely among different cancer types and patients. Treatment effectiveness decrease in those tumors that do not express ICB target checkpoint proteins (PD-1, PD-L1, and CTLA-4) (Postow et al., 2015). Second, patients with rapidly acquired primary resistance and other patients may initially respond to ICB but may later develop resistance or secondary resistance. The mechanisms of resistance are complex and can involve genetic alterations,

changes in the tumor microenvironment, and other factors (Johnson et al., 2018). Another crucial challenge is the presence of toxicity and immune-related adverse events (irAEs) mainly in the gastrointestinal tract, endocrine glands, skin, and liver (Postow et al., 2018). Also, the complexity of the tumor microenvironment, the tumor heterogeneity, and the complex and intricate process of metastasis should be mentioned (El-Sayes et al., 2021).

All these factors affect the existence of well-defined and validated predictive biomarkers for ICB response. For these reasons biomarkers may play a crucial role in guiding the use of immunotherapy for cancer treatment. Identifying specific biomarkers might help to determine which patients are more likely to respond to immunotherapy, allowing for a more personalized and effective approach. ICB-related-biomarker identification has become even more needed in some prevalent and aggressive tumors like metastatic non-small cell lung cancer (NSCLC). Patients with > 50% programmed death-ligand-1 (PD-L1) positivity of the tumor by immunohistochemistry are likely to response better to ICB, being now standard of care for most patients with non–small-cell lung cancer (NSCLC) (Ellis et al., 2017). This tumor, which survival rate still does not exceed 5 years in Europe, is currently the leading death cause with 18% of the total mortality associated with neoplastic processes (Sung et al., 2021).

The main problem of NSLCL remains in late diagnosis in patients with higher risk of developing this tumor. Despite great efforts to settle annual screening initiatives based on low-dose helical computed tomography (LDH-CT) for patients aged 55 to 80 with a history of smoking 30 or more pack-years, early diagnosis

remained very low (Jemal & Fedewa, 201) (De Koning et al., 2020). So, although early diagnosis is to be essential to decrease NSCLC prevalence, unfortunately most of the patients are still diagnosed at advance stages. (Duma et al., 2019). In these patients' therapy is mainly used to improve survival and quality of life with the aim of reducing symptoms. Patients with non-targetable mutations are eligible for ICB which may be administrated in combination with chemotherapy (Hendriks et al., 2023). Understanding metastatic NSCLC pathology mechanisms and identifying response biomarkers is crucial for selecting patients who are more likely to benefit from ICB and for optimizing treatment strategies in NSCLC patients.

Thus, in this thesis the aim was to use novel approaches and a very selected patient cohort for identifying new promising ICB response and biomarkers in liquid biopsy with prognostic and/or predictive value in mNSCLC patients. One promising non-invasive response to ICB biomarker is plasma-derived cfDNA. cfDNA originates from many sources and is released to the blood through diverse cell death mechanisms including necrosis, secretion apoptosis and via NETosis (Kustanovich et al., 2019) (Moss et al., 2018). However, the global use of cfDNA concentration as response biomarker to ICB is far less explored because specificity is presumed to be low. Higher cfDNA amounts is an established marker of many biological processes including cancer. In fact, cancer patients have greater plasma derived cfDNA concentrations compared with those of healthy controls (Spector et al., 2023).

Presumably, the presence, quantity, and quality of cfDNA could potentially serve as indicators of disease aggressiveness and the potential responsiveness of tumors, especially in the context of immune checkpoint blockade (ICB) treatment where tumor cell death mechanisms may differ from those induced by other cancer treatments. The differences in cfDNA amounts between responder and non-responder patients with mNSCLC treated with ICB and their value as response biomarkers were not completely clear. Interestingly, our results in a cohort of 97 mNSCLC patients showed that non-responder patients at different tumor response evaluations (after two months, six and twelve months of ICB) had higher basal plasma-derived cfDNA than those responder patients in different tumor response evaluations. In addition, cfDNA was independent of most clinical and molecular patient cohort characteristics. Remarkably, there was an association with smoking status. However, when examining the clinical significance of this association by studying correlations with the number of cigarette packages, no further relationship was established. In keeping with our results, there is no knowledge that can guarantee increasing levels of cfDNA from smoke exposure. Remarkably, the other clinical variable found to be associated with higher amount of cfDNA was the presence of bone metastases. Some studies have also demonstrated that NSCLC patients with bone metastases had higher cfDNA amounts with poor survival rates. (Ye et al., 201) (Chai et al., 2021).

When lung tumoral metastases settle in bones, this may be directly associated with increased bone marrow activity, cell proliferation and thus cfDNA release. Regarding this, it was recently demonstrated that the majority amount of cfDNA is mainly contributed by white blood cells, predominantly by

neutrophils, being circulating tumoral DNA (ctDNA) less than 1% of total cfDNA (Mattox et al., 2023). This finding, together with our results may indicate that cfDNA acts as a predictive response biomarker to ICB with higher amount in those patients who do not respond to treatment and had greater number of bone metastases.

On the other hand, the prognostic role of ctDNA and survival has been deeply studied. Pre-treatment ctDNA and dynamic changes in response to treatment are prognostic biomarkers in some cancer patients treated with ICB (Al-Showbaki et al., 2023). The prognosis value of cfDNA it has been demonstrated in this study with a cfDNA concentration > 0.55 ng/µl at the start of ICB that predicts worse overall survival. The simplicity and replicability potential in any laboratory with ctDNA protocols tackle most of the ctDNA implementation difficulties. These results imply a departing point for the exploration of cfDNA concentration as an agnostic biomarker that could be used for tracking progression and therefore increasing the negative predictive value (Dang and Park 2022). In addition, such a cost-effective and affordable approach confronts disparity and is feasible retrospective validation and for prospective validation in Clinical Trials.

Most research focuses on cfDNA genomics alteration detected also in tumor tissues. However, epigenetics changes in cfDNA have been demonstrated to be a useful tool to study transcriptional programs and cellular states in a variety of tissues and conditions apart from cancer (Baca et al., 2023). Of the two most stable cytosine modifications, 5mC and 5hmC, DNA methylation marks have been extensively studied to understand gene silencing and transcriptional

consequences. However, 5hmC is far less explored, with some initial studies reporting its association with tumorigenesis or transcriptomic reprogramming, being the latter a positive instead of silencing impact on transcription (Fujikura et al., 2021). Ten-eleven-translocation proteins (TET1, TET2, and TET3) convert 5-methylcytosine (5mC) to 5-hydroxymethylcytosine (5hmC) being an active DNA demethylation mark enriched mostly in active genomic loci. (Shao et al., 2022). Precise mapping of genome-wide 5hmC and 5mC distributions revealed real epigenetic alteration in CpG sites across genomic regions including transcriptional regulatory sequences (Z. Wang et al., 2020).

In our study, both marks were interrogated in a cancer-related designed panel based on previous results (Onieva, Xiao, et al., 2022). The 5mC+5hmc protocol and 5hmC variations were optimized in this Thesis for low working cfDNA concentrations (10 ng to 20 ng) instead of the recommended 200 ng. Our results showed that early after ICB administration, the number of differentially methylated (DM) CpG sites and genomic regions in relation to response increased, compared with number of DM CpGs and DMRs in basal cfDNA. Moreover, this DM CpG sites after ICB stratified better the patients based on tumor response to ICB. Although most of DM sites and regions were associated with non-adjusted p-values, the genes bearing them were very relevant for characterizing the resistance mechanisms that might be stabilized or triggered by ICB *(POU2AF1,* involved in pre-BCR and subsequent BCR signaling, was hypermethylated in responder patients (Zhao et al., 2007). Considering that this transcriptional co-activator is key for establishing the response of B-cells to antigens and for germinal centers formation (Chyra et al., 2021), and has been reported as differentially overexpressed in the

melanoma patients of our cohort treated with (Onieva et al., 2022b) it is counter-intuitive that silencing by increased methylation would contribute to response to ICB. However, it must be considered that in this section, the traditional composite mark of 5mC+5hmC was profiled, and hypermethylation could be either hyper5mC or hyper5hmC.

Other immune pathway-related genes with DM genomics regions before treatment have also been associated with tumor pathogenesis in some cancers (Pucci et al., 2016) (Kim et al., 2020) (Shen et al., 2022). In contrast, when DM genomics regions after 3-4 weeks of ICB (T2), most of the related genes were directly involved in cancer or acted as tumor suppressors (Allen et al., 2021) (Shan et al., 2019) (Sasaki et al., 2021).

As could be suggested from the *POU2AF1* results, profiling the individual 5mC and 5hmC is relevant for those genes that can be populated with 5hmC. We have previously characterized the abundancy of 5hmC in genes that are important for development and terminal organ differentiation (Ivanov et al., 2013). Moreover, 5hmC marks discrete and very specific regions that are responsive to xenobiotics (Single base resolution analysis of 5-hydroxymethylcytosine in 188 human genes: implications for hepatic gene expression (Ivanov et al. 2016). In line with this, the protocol optimized in this thesis unmasked interindividual variations in responders that were undetected with the 5mC+5hmC profiling. Added to the fact that the differences according to response were more prominent early after the start of the treatment than before treatment, one could hypothesize that specific 5hmC also determines the induced reprogramming after exposure to ICB

and is necessary to identify signatures that optimally stratify the patients in the context of medium and long-term response.

Extracellular vesicles (EV) are potentially valuable biomarkers for non-invasive molecular diagnostics, prognosis and treatment follow up, due to their substantial nucleic acid and protein composition. They mediate intracellular communication, being the third most important type of cell-to-cell signaling (Kalluri & LeBleu, 2020). Relevant studies that have demonstrated a strong correlation between tumor-derived EV miRNA and immunosuppressive tumor microenvironment, facilitating a reduction in tumor immunogenicity in several tumor types (Whiteside, 2017) (Y. Yang et al., 2018). In terms of liquid biopsy feasibility, the use of plasma derived EV miRNA only requires a patient blood sample and has other advantages in terms of clinical settings, due to the protection of the EV cargo exerted by the lipid bilayer. DE analysis of plasma derived EV miRNA have shown a different gene expression signatures of tumor suppressor miRNA in responder and non-responders. They include up to 8 miRNA which have been previously described as tumor suppressors in lung tissues and NSCLC, hsa-miR-144-5p, hsa-miR-1224-5p or hsa-miR-451-a among them. (Pu et al., 2021) (Ma et al., 2022) (Bai & Wu, 2019).

Notably, it did not observe any potential statistical bias based on clinical variables, suggesting that the expression of these miRNA might influence the response to ICB treatment. By comparing DE miRNA before and after the second cycle of ICB treatment it could be observed that hsa-miR-375-3p and hsa-miR-134-5p were the only miRNA that remain downregulated in responder patients. Both miRNA could potentially act as suppressors of tumor growth via modulation of

apoptosis and cellular proliferation in NSCLC patients. (Cheng et al., 2017) (Pan et al., 2017).

There is evidence of the relevance of hsa-miR-375 as a tumor inhibitor, inhibiting proliferation and metastasis while promoting apoptosis of SCC subtype tumors (Gan et al., 2023). In our responder patients, this miRNA was downregulated both basally and after ICB. Since the greatest percentage of our cohort patients had LUAD subtype, these results may indicate there may be an association between NSCLC subtype and miRNA expression patterns. After the second cycle of ICB, upregulated miRNA in responder patients also act as tumor suppressors in NSCLC (Jo et al., 2022)

Consistently, non-responder patients had a signature of several miRNA that were downregulated after ICB treatment and were also tumor suppressors. Has-miR-1-3p was extensively evaluated as a tumor suppressor in the tumorigenesis processes in the literature. More recently, miRNA-1-3p has been reported as down-regulated in NSCLC tissue and plasma samples (Wang et al., 2019) (Sheervalilou et al., 2019). Similar results were found when other downregulated miRNA were analyzed. Tumor tissue low expression of hsa-miR-1298-5p was also related to a worse outcome in in patients with NSCLC (Du et al., 2019). In addition, plasma-derived EV hsa-miR-1298 was demonstrated to be a potential diagnostic biomarker for other cancer types (Matboli et al., 2020).

hsa-miR-6724-5p only showed an expression increase after the second cycle of treatment. Overexpression of this miRNA is involved in tumor progression in

different neoplasms (Bonab et al., 2022) (Usuba et al., 2018). Conversely, responder patients had upregulated some tumor suppressor miRNA like hsa-miR-206 and has-miR-302a-5p when comparing EV miRNA before and after the second cycle of treatment. Over-expression of hsa-miR-206 may induce apoptosis and tumor inhibition acting as tumor suppressor. (Zhang, Y et al., 2015) Consistently, reduction of hsa-miR-206 in NSCLC tissues and cells lines correlated with poor survival rates (Liao & Peng, 2020). Moreover, in vivo hepatocellular carcinoma models have identified miRNA-206 as responsible for cytotoxic T lymphocytes (CTL) cell recruitment and expansion. (Liu et al., 2021). This CTL recruitment role of hsa-miR-206 suggests that treatment based on ICB may induce the expression of this miRNA. This hypothesis supports our analysis when we compare plasma-derived EV levels of hsa-miR-206 before and after the second cycle of immunotherapy in responder patients. Additionally, hsa-miR-302a-5p has also been observed to suppress NSCLC proliferation and metastasis being the inhibition of integrin α6 (ITGA6) mRNA one of its main mechanisms (Cheng et al., 2019).

Remarkably, a comprehensive analysis performed by (Xu & Guo, 2021) demonstrated the relationships between ITGA6 expression levels and common immune checkpoints including CD274 (PD-L1). These results showed a significant correlation between ITGA6 and CD274. Thus, blockade of PD-L1 signaling after the second cycle of ICB may induce hsa-miR302a-5P over-expression with a down-regulation of ITGA6 levels in the responder patients enrolled in this study.

To explore and confirm the predictive value of these plasma derived EV DE miRNA in NSCLC, a risk score based on all DE miRNA before and after the

treatment in all patients enrolled in this study has been developed. Among patients with low-risk score, ICB therapy was more likely to be beneficial, demonstrating that responder and non-responder patients have different immune tumor microenvironments. Therefore, we propose that the risk score may function as a sensitive measure for anticipating the response of NSCLC patients to ICI therapy. Regarding functional enrichment analysis of DE miRNA, in different conditions we showed that most has-miRNA were highly related to immune cell signaling pathways and expressed in cancerous tissues, especially in lung tissue and microvesicles. Interestingly, enrichment analysis of DE miRNA before treatment between responder and non-responder patients showed a signature of some upregulated miRNA and downregulated miRNA which mainly related to CD56+ natural killer cells. This correlates with previous studies where lower proportions of $CD56^{bright}$ CD16- PDL-1+ NK cells, with regulatory capacities, were associated with a higher OS in lung cancer patients receiving immunotherapy. (Ruiz et al., 2023). In this context future prospective NK cell phenotyping studies will be performed to focus on this area of exploration to validate the role of these cells to predict response in NSCLC patients under ICB. From a clinical point of view, it is highly interesting to identify responders and non-responder patients by employing a liquid biopsy set of biomarkers panel. Plasma-derived EV miRNA-based response biomarkers may be a reasonable tool to predict response to immune checkpoint inhibitors in different tumors, like NSCLC. Furthermore, an early adaptation to therapy as suggested by this smallRNA expression dynamics, might impact the progression-free or overall survival of patients.

Characterization of circulating immune cells obtained non-invasively from blood, was also carried out. In recent years, several studies suggest that different immune cell populations might be useful biomarkers to predict immunotherapy efficacy. In this sense, the objective of our study was to provide a detailed analysis of different circulating immune cell subsets before and after ICB treatment in our mNSCLC cohort.

An elevated peripheral monocyte count is negatively prognostic in some tumors, being a higher pre-therapy absolute monocyte counts a bad prognostic biomarker in lung cancer (Parikh et al., 2018), (Wen et al., 2019) (Wen et al., 2015). In line with these studies, in this study an association between peripheral monocyte count before treatment and response to ICB was found when tumor response was evaluated at three months of ICB. Correlations with overall survival or progression free survivals could not be established.

However, when blood samples after treatment were characterized and correlated with response, there were found some statistically significant circulating immune cells between responders and non-responders and with prognostic value. CD4+ T cells, largely known as anti-tumor immune cells able to direct immune responses against tumors, were increased during ICB treatment in responder patients (Eberst et al., 2022) Interestingly, differences in CD4+ T cells between both groups were kept until one year of treatment and, in all cases, correlated with tumor response at different time evaluations. Our results also coincided with previous studies where CD4+ T cells lymphopenia correlated with poor survival in lung cancer (Tay et al., 2020). Cytotoxic anti-tumor activity is

mediated by CD8+T cells. In some situations, CD8+ T cells may express PD-L1 (CD279) and regulate or inhibit CD8+ T cells function (Y. Zheng et al., 2022). The mechanisms of anti–PD-1/PD-L1 ICB consists of reversing the exhaustion of CD8+PD-L1++ T cells and thus, patients with CD8+PD-L1+ T cells exhausted phenotype are likely to respond better to treatment as it was showed in our results. Tumor-associated neutrophils (TANs) were recently highlighted to contribute to the resistance of some tumors to ICB (Feng et al., 2023). Prognostic value of circulating neutrophils confirmed that greater circulating number of neutrophils in comparison to lymphocytes correlated with shortened survival in NSCLC (Ren et al., 2019).

Also, in our cohort neutrophils as well as NLR are found to be higher in non-responder patients during ICB treatment at different tumor response evaluation. Both molecular biomarkers were demonstrated to predict response to ICB in mNSCLC. Surprisingly, eosinophils, allergens and infections related immune cells increased in responder patients when six months of ICB was administrated and this increasing circulating number correlated with both groups of responders. By expressing MHC class II and co-stimulatory molecules (CD40, CD80/86, CTLA-4) they may regulate T-cell proliferation (Davis & Rothenberg, 2014). However, antitumoral activity of tumor-associated tissue eosinophilia (TATE) differs between tumors. In some of them, as also our results showed, the abundance of eosinophils improved overall survival independently of other standard prognostic factors.

Integration of all predictive and prognostic biomarkers in the context of ICB treatment, allow to reach specificities way over previous monogenic markers as well as better patient stratification with more efficient personalized therapeutic approaches. Thus, in this thesis, a pilot prognostic multivariate model integrated with current clinical variables and basal cfDNA cut off was performed. The results showed that cfDNA non-arbitrary threshold improved the survival prediction algorithms over the models built on bad prognosis clinical variables such as age, ECOG, LDH and PDL1, which is particularly relevant given the high resistance associated with ICB.

All biomarkers proposed in this thesis may be collected by non-invasive methods, what is better clinically accepted by patients compared with other invasive ones such as tumor tissues biopsy. Also, all of them have demonstrated to allow the constant monitoring of disease progression avoiding current imaging techniques, computed tomography (CT) or magnetic resonance imaging (MRI), which are useful but with imply high economic and highly specialized labor costs that limit routine clinical use.

CHAPTER V: GENERAL CONCLUSIONS

1. Non-responder mNSCLC patients exhibit higher basal cfDNA levels, with associations observed with smoking status and the presence of bone metastases.
2. cfDNA concentration exceeding 0.55 ng/µl at the start of ICB predicts worse overall survival, indicating prognostic potential.
3. cfDNA concentration could be a cost-effective and replicable biomarker for tracking progression and guiding treatment strategies.
4. Precise mapping of the 5hmC and 5mC distributions in a panel of candidate genes related to ICB response reveals epigenetic alterations in CpG sites across genomic regions, including transcription regulatory sequences.
5. The protocol for mapping composite and individual 5mC and 5hmC allows down scalation of the minimal input cfDNA amount from 200 ng to 10-20 ng.
6. The number of differentially methylated (DM) CpG sites and genomic regions increases from 48 to 447 CpGs from basal to early post-ICB treatment, indicating that these epigenetic modifications are marking early reprogramming processes induced by the treatment.
7. DM CpG sites after ICB better stratifies the patients according to clinical response.
8. Genes associated with DM sites, such as POU2AF1, are relevant for characterizing resistance mechanisms to ICB and are enriched in immune related pathways, evidencing that epigenetics plays a role in these mechanisms.

9. Individual profiling of 5mC and 5hmC unmasks patients´ interindividual variations specific to the response group that would be discarded if the composite signal was profiled as happens in traditional bisulfite sequencing.
10. Differential expression (DE) analysis of plasma-derived EV miRNA reveals distinct gene expression signatures in responder and non-responder patients, including tumor suppressor miRNA relevant to lung tissues and NSCLC.
11. Basal DE analysis of plasma-derived EV miRNA can stratify mNSCLC patients according to response to ICB.
12. After 3-4 weeks in ICB treatment, tumor suppressor miRNA are re- programmed in the patients, being upregulated in responders (e.g. hsa-miR- 206, hsa-miR-302a-5p) and downregulated in non-responders (e.g. hsa-miR-1- 3p, hsa-miR-1298-5p).
13. Expression profiles of specific EV-associated smallRNA (e.g. hsa-miR-375) mark NSCLC histological subtype and are stable after treatment.
14. Risk scores based on basal or at second cycle differentially expressed EV- miRNA predict overall survival in mNSCLC patients treated with ICB.
15. Functional enrichment of pre-treatment DE EV-miRNA highlights their numerical relevance to immune cell signaling pathways, especially those associated with CD56+ natural killer cells supporting their potential role in predicting ICB therapy response.
16. The blood immune cells profiling confirms the predictive and/or prognosis potential of known biomarkers and reveals new associations that can serve for establishing long-standing and accessible predictors:
    a. Elevated basal counts of peripheral monocytes are negatively associated with response to ICB in mNSCLC.

b. CD4+ T cells are increased during ICB treatment in responders over several clinical evaluations, maintaining differences with non-responders until one year of treatment.
c. After two cycles, CD8+PD-L1+ T cells exhausted phenotype is associated with a better response to anti–PD-1/PD-L1 ICB.
d. Neutrophiles and Neutrophile-to-Lymphocyte Ratio (NLR) are higher in non-responders during ICB treatment compared with responders.
e. Eosinophils increase in responder patients after six months of ICB, correlating with clinical response.

17. The pilot prognostic multivariate model that incorporates clinical variables and the cfDNA cut off, improves survival prediction algorithms compared to models based on traditional prognostic clinical variables (age, ECOG, LDH, and PDL1).
18. All proposed biomarkers in the study are non-invasively collected and enable basal prediction as well as constant monitoring of disease progression. Some of them are easily implemented in clinical practice in terms of financial, equipment and technical specialization costs.

General conclusion:

The basal state and dynamics of liquid biopsy biomarkers of various natures predicts response and/or prognosis that can be assembled in superior risk scores and prognostic models. DNA and RNA epigenetic status and post-treatment aberrations offer new insights into the regulatory mechanisms governing ICB response and resistance.

REFERENCES

Akalin A, Kormaksson M, Li S, Garrett-Bakelman FE, Figueroa ME, Melnick A, Mason CE (2012). "methylKit: a comprehensive R package for the analysis of genome-wide DNA methylation profiles." *Genome Biology*, 13(10). https://doi.org/10.18129/B9.bioc.methylKit.

Al-Showbaki, L., Wilson, B. E., Tamimi, F., Molto, C., Mittal, A., Cescon, D. W., & Amir, E. (2023). Changes in circulating tumor DNA and outcomes in solid tumors treated with immune checkpoint inhibitors: a systematic review. *Journal for ImmunoTherapy of Cancer*, *11*(2), e005854. https://doi.org/10.1136/jitc-2022-005854.

Alberro, A., Iparraguirre, L., Fernandes, A., & Otaegui, D. (2021). Extracellular vesicles in blood: sources, effects, and applications. *International Journal of Molecular Sciences*, *22*(15), 8163. https://doi.org/10.3390/ijms22158163.

Allen, J. L., Walk, E. L., Rhodes, K. L., Markwell, S. M., Papenberg, B. W., Wu, H. G., Garcia, M., Bear, J. E., & Weed, S. A. (2021). Abstract 2882: Coronin 1B Overexpression promotes invasion of HPV- HNSCC. *Cancer Research*, *81*(13_Supplement), 2882. https://doi.org/10.1158/1538-7445.am2021-2882.

Alix-Panabières, C., & Pantel, K. (2014). Challenges in circulating tumour cell research. *Nature Reviews Cancer*, *14*(9), 623–631. https://doi.org/10.1038/nrc3820.

Alix-Panabières, C., & Pantel, K. (2016). Clinical Applications of Circulating Tumor Cells and Circulating Tumor DNA as Liquid Biopsy. *Cancer Discovery*, *6*(5), 479–491. https://doi.org/10.1158/2159-8290.CD-15-1483.

Anagnostou, V., Smith, K. N., Forde, P. M., Niknafs, N., Bhattacharya, R., White, J., Zhang, T., Adleff, V., Phallen, J., Wali, N., Hruban, C., Guthrie, V. B., Rodgers, K., Naidoo, J., Kang, H., Sharfman, W., Georgiades, C., Verde, F., Illei, P., … Velculescu, V. E. (2017). Evolution of Neoantigen Landscape during Immune Checkpoint Blockade in Non-Small Cell Lung Cancer. *Cancer Discovery*, *7*(3), 264–276. https://doi.org/10.1158/2159-8290.CD-16-0828.

Antonia, S., Villegas, A., Daniel, D. B., Vicente, D., Murakami, S., Hui, R., Yokoi, T., Chiappori, A., Lee, K. H., De Wit, M., Cho, B. C., Bourhaba, M., Quantin, X., Tokito, T., Mekhail, T., Planchard, D., Kim, Y., Karapetis, C. S., Hiret, S., . . . Özgüroğlu, M. (2017). Durvalumab after chemoradiotherapy in stage III Non–Small-Cell lung cancer. *The New England Journal of Medicine*, *377*(20), 1919-1929. https://doi.org/10.1056/nejmoa1709937.

Arbour, K. C., & Riely, G. J. (2019). Systemic therapy for locally advanced and metastatic Non–Small cell lung cancer. *JAMA*, *322*(8), 764. https://doi.org/10.1001/jama.2019.11058.

Ascierto, M. L., Kmieciak, M., Idowu, M. O., Manjili, R., Zhao, Y., Grimes, M., Dumur, C., Wang, E., Ramakrishnan, V., Wang, X.-Y., Bear, H. D., Marincola, F. M., & Manjili, M. H. (2012). A signature of immune function genes associated with recurrence-free survival in breast cancer patients. *Breast Cancer Research and Treatment*, *131*(3), 871–880. https://doi.org/10.1007/s10549-011-1470-x.

Baca, S. C., Seo, J., Davidsohn, M. P., Fortunato, B., Semaan, K., Sotudian, S., Lakshminarayanan, G., Dióssy, M., Qiu, X., Zarif, T. E., Savignano, H., Canniff, J. P., Madueke, I., Saliby, R. M., Zhang, Z., Li, R., Jiang, Y., Taing, L., Awad, M. M., . . . Freedman, M. L. (2023). Liquid biopsy epigenomic profiling for cancer subtyping. *Nature Medicine*, *29*(11), 2737-2741. https://doi.org/10.1038/s41591-023-02605-z.

Bai, H., & Wu, S. (2019). <P>MIR-451: A novel biomarker and potential therapeutic target for cancer</P> *OncoTargets and Therapy*, *Volume 12*, 11069-11082. https://doi.org/10.2147/ott.s230963.

Bai, L., Li, W., Zheng, W., Xu, D., Chen, N., & Cui, J. (2020). Promising targets based on pattern recognition receptors for cancer immunotherapy. *Pharmacological Research*, *159*, 105017. https://doi.org/10.1016/j.phrs.2020.105017.

Bai, R., Lv, Z., Xu, D., & Cui, J. (2020). Predictive biomarkers for cancer immunotherapy with immune checkpoint inhibitors. *Biomarker Research*, *8*(1), 34. https://doi.org/10.1186/s40364-020-00209-0.

Barrueto, L., Caminero, F., Cash, L., Makris, C., Lamichhane, P., & Deshmukh, R. R.

(2020). Resistance to Checkpoint Inhibition in Cancer Immunotherapy. *Translational Oncology*, *13*(3), 100738. https://doi.org/10.1016/j.tranon.2019.12.010.

Bebelman, M. P., Smit, M. J., Pegtel, D. M., & Baglio, S. R. (2018). Biogenesis and function of extracellular vesicles in cancer. *Pharmacology & Therapeutics*, *188*, 1–11. https://doi.org/10.1016/j.pharmthera.2018.02.013.

Bindea, G., Mlecnik, B., Angell, H. K., & Galon, J. (2014). The immune landscape of human tumors: Implications for cancer immunotherapy. *OncoImmunology*, *3*(2), e27456. https://doi.org/10.4161/onci.27456.

Blumenthal, G. M., & Pazdur, R. (2017). Approvals in 2016: The march of the checkpoint inhibitors. *Nature Reviews Clinical Oncology*, *14*(3), 131–132. https://doi.org/10.1038/nrclinonc.2017.15.

Bonab, R. A., Asfa, S., Kontou, P. I., Karakülah, G., & Pavlopoulou, A. (2022). Identification of neoplasm-specific signatures of mIRNA interactions by employing a systems biology approach. *PeerJ*, *10*, e14149. https://doi.org/10.7717/peerj.14149.

Boon, T., Cerottini, J.-C., Van den Eynde, B., van der Bruggen, P., & Van Pel, A. (1994). Tumor Antigens Recognized by T Lymphocytes. *Annual Review of Immunology*, *12*(1), 337–365. https://doi.org/10.1146/annurev.iy.12.040194.002005

Brueckl, W. M., Ficker, J. H., & Zeitler, G. (2020). Clinically relevant prognostic and predictive markers for immune-checkpoint-inhibitor (ICI) therapy in non-small cell lung cancer (NSCLC). *BMC Cancer*, *20*(1), 1185. https://doi.org/10.1186/s12885-020-07690-8.

Buchbinder, E. I., & Desai, A. (2016). CTLA-4 and PD-1 Pathways: Similarities, Differences, and Implications of Their Inhibition. *American Journal of Clinical Oncology*, *39*(1), 98–106. https://doi.org/10.1097/COC.0000000000000239.

Cai, Z., Poulos, R. C., Liu, J., & Zhong, Q. (2022). Machine learning for multi-omics data integration in cancer. *iScience*, *25*(2), 103798. https://doi.org/10.1016/j.isci.2022.103798.

Califf, R. M. (2018). Biomarker definitions and their applications. *Experimental Biology*

and Medicine, *243*(3), 213–221. https://doi.org/10.1177/1535370217750088.

Carbone, D. P., Reck, M., Paz-Ares, L., Creelan, B. C., Horn, L., Steins, M., Felip, E., Van Den Heuvel, M. M., Ciuleanu, T., Badin, F., Ready, N., Hiltermann, T. J. N., Nair, S., Juergens, R. A., Peters, S., Minenza, E., Wrangle, J., Abreu, D. R., Borghaei, H., . . . Socinski, M. A. (2017). First-Line nivolumab in stage IV or recurrent Non–Small-Cell lung cancer. *The New England Journal of Medicine*, *376*(25), 2415-2426. https://doi.org/10.1056/nejmoa1613493.

Chai, X., Yinwang, E., Wang, Z., Wang, Z., Xue, Y., Li, B., Zhou, H., Zhang, W., Wang, S., Zhang, Y., Li, H., Mou, H., Sun, L., Qu, H., Wang, F., Zhang, Z., Chen, T., & Ye, Z. (2021). Predictive and prognostic biomarkers for lung cancer bone metastasis and their therapeutic value. *Frontiers in Oncology*, *11*. https://doi.org/10.3389/fonc.2021.692788.

Chalmers, Z. R., Connelly, C. F., Fabrizio, D., Gay, L., Ali, S. M., Ennis, R., Schrock, A., Campbell, B., Shlien, A., Chmielecki, J., Huang, F., He, Y., Sun, J., Tabori, U., Kennedy, M., Lieber, D. S., Roels, S., White, J., Otto, G. A., … Frampton, G. M. (2017). Analysis of 100,000 human cancer genomes reveals the landscape of tumor mutational burden. *Genome Medicine*, *9*(1), 34. https://doi.org/10.1186/s13073-017-0424-2.

Champiat, S., Dercle, L., Ammari, S., Massard, C., Hollebecque, A., Postel-Vinay, S., Chaput, N., Eggermont, A., Marabelle, A., Soria, J.-C., & Ferté, C. (2017). Hyperprogressive Disease Is a New Pattern of Progression in Cancer Patients Treated by Anti-PD-1/PD-L1. *Clinical Cancer Research*, *23*(8), 1920–1928. https://doi.org/10.1158/1078-0432.CCR-16-1741.

Chen, D. S., & Mellman, I. (2013). Oncology Meets Immunology: The Cancer-Immunity Cycle. *Immunity*, *39*(1), 1–10. https://doi.org/10.1016/j.immuni.2013.07.012.

Chen, D. S., & Mellman, I. (2017). Elements of cancer immunity and the cancer–immune set point. *Nature*, *541*(7637), 321–330. https://doi.org/10.1038/nature21349.

Chen, N., Fang, W., Zhang, L., Peng, P., Wang, J., Zhan, J., Hong, S., Huang, J., Liu, L., Jin, S., Zhou, T., Chen, Y., Zhang, H., & Zhang, L. (2017). KRAS mutation-induced upregulation of PD-L1 mediates immune escape in human lung adenocarcinoma. *Cancer*

Immunology, Immunotherapy, *66*(9), 1175-1187. https://doi.org/10.1007/s00262-017-2005-z.

Chen, S., Zhou, Y., Chen, Y., & Gu, J. (2018). FASTP: an ultra-fast all-in-one FASTQ preprocessor. Bioinformatics, 34(17), i884-i890. https://doi.org/10.1093/bioinformatics/bty560.

Chen, W., Zhuang, X., Qi, R., & Qiao, T. (2019). MiR-302a-5p suppresses cell proliferation and invasion in non-small cell lung carcinoma by targeting ITGA6. *American journal of translational research*, *11*(7), 4348–4357.

Cheng, L., Zhan, B., Luo, P., & Wang, B. (2017). MIRNA-375 regulates the cell survival and apoptosis of human non-small cell carcinoma by targeting HER2. *Molecular Medicine Reports*, *15*(3), 1387-1392. https://doi.org/10.3892/mmr.2017.6112.

Chevallier, M., Borgeaud, M., Addeo, A., & Friedlaender, A. (2021). Oncogenic driver mutations in non-small cell lung cancer: past, present and future. *World journal of clinical oncology*, *12*(4), 217-237. https://doi.org/10.5306/wjco.v12.i4.217.

Chyra, Z., Samur, M. K., Aktaş-Samur, A., Yao, Y., Derebail, S., Perini, T., Xu, Y., Morelli, E., Adamia, S., Park, W. D., Lin, C. Y., Shirasaki, R., Shammas, M. A., Mitsiades, C. S., Hájek, R., Fulciniti, M., & Munshi, N. C. (2021). B cell transcriptional coactivator POU2AF1 (BOB-1) is an early transcription factor modulating the protein synthesis and ribosomal biogenesis in multiple myeloma: with therapeutic implication. *Blood*, *138*(Supplement 1), 2670. https://doi.org/10.1182/blood-2021-152121.

Clark SB, Alsubait S. Non–Small Cell Lung Cancer. 2023 Sep 4. In: StatPearls [Internet]. Treasure Island (FL): StatPearls Publishing; 2023 Jan–. PMID: 32965978.

Coumans, F., Brisson, A., Buzás, E. I., Dignat-George, F., Drees, E. E., El-Andaloussi, S., Emanueli, C., Gąsecka, A., Hendrix, A., Hill, A. F., Lacroix, R., Lee, Y., Van Leeuwen, T. G., Mackman, N., Mäger, I., Nolan, J. P., Van Der Pol, E., Pegtel, D. M., Sahoo, S., . . . Nieuwland, R. (2017). Methodological guidelines to study extracellular vesicles. *Circulation Research*, *120*(10), 1632-1648. https://doi.org/10.1161/circresaha.117.309417.

Cyll, K., Ersvær, E., Vlatkovic, L., Pradhan, M., Kildal, W., Kjær, M. A., Kleppe, A., Hveem, T. S., Carlsen, B., Gill, S., Löffeler, S., Haug, E. S., Wæhre, H., Sooriakumaran, P., & Danielsen, H. E. (2017). Tumour heterogeneity poses a significant challenge to cancer biomarker research. *British Journal of Cancer*, *117*(3), 367-375. https://doi.org/10.1038/bjc.2017.171.

Davis, A. A., & Patel, V. G. (2019). The role of PD-L1 expression as a predictive biomarker: An analysis of all US Food and Drug Administration (FDA) approvals of immune checkpoint inhibitors. *Journal for ImmunoTherapy of Cancer*, *7*(1), 278. https://doi.org/10.1186/s40425-019-0768-9.

Davis, B. P., & Rothenberg, M. E. (2014). Eosinophils and cancer. *Cancer immunology research*, *2*(1), 1-8. https://doi.org/10.1158/2326-6066.cir-13-0196

De Koning, H. J., Van Der Aalst, C. M., De Jong, P. A., Scholten, E. T., Nackaerts, K., Heuvelmans, M. A., Lammers, J. J., Weenink, C., Yousaf-Khan, U., Horeweg, N., Van 't Westeinde, S., Prokop, M., Mali, W. P., Hoesein, F. A. A. M., Van Ooijen, P. M. A., Aerts, J., Bakker, M. A. D., Thunnissen, E., Verschakelen, J., Oudkerk, M. (2020). Reduced Lung-Cancer mortality with volume CT screening in a randomized trial. *The New England Journal of Medicine, 382(6)*, 503-513. https://doi.org/10.1056/nejmoa1911793

Delyon, J., Mateus, C., Lefeuvre, D., Lanoy, E., Zitvogel, L., Chaput, N., Roy, S., Eggermont, A. M. M., Routier, E., & Robert, C. (2013). Experience in daily practice with ipilimumab for the treatment of patients with metastatic melanoma: An early increase in lymphocyte and eosinophil counts is associated with improved survival. *Annals of Oncology*, *24*(6), 1697–1703. https://doi.org/10.1093/annonc/mdt027

Devarakonda, S., Rotolo, F., Tsao, M.-S., Lanc, I., Brambilla, E., Masood, A., Olaussen, K. A., Fulton, R., Sakashita, S., McLeer-Florin, A., Ding, K., Le Teuff, G., Shepherd, F. A., Pignon, J.-P., Graziano, S. L., Kratzke, R., Soria, J.-C., Seymour, L., Govindan, R., & Michiels, S. (2018). Tumor Mutation Burden as a Biomarker in Resected Non–Small-Cell Lung Cancer. *Journal of Clinical Oncology*, *36*(30), 2995–3006. https://doi.org/10.1200/JCO.2018.78.1963.

Dong, W., Peng, J., Gao, H., Zhang, T., Tan, Y., & Hu, Y. (2015). ALDH1 Expression and the Prognosis of Lung Cancer: A Systematic Review and Meta-Analysis. *Heart, Lung and Circulation*, *24*(8), 780-788. https://doi.org/10.1016/j.hlc.2015.03.021

Doyle, L., & Wang, M. (2019). Overview of Extracellular Vesicles, Their Origin, Composition, Purpose, and Methods for Exosome Isolation and Analysis. *Cells*, *8*(7), 727. https://doi.org/10.3390/cells8070727

Du, Z., Wu, J., Wang, J., Yan, L., Zhang, S., Shang, Z., & Zuo, W. (2019). MicroRNA-1298 is downregulated in non-small cell lung cancer and suppresses tumor progression in tumor cells. *Diagnostic Pathology*, *14*(1). https://doi.org/10.1186/s13000-019-0911-4

Duan, F., Duitama, J., Al Seesi, S., Ayres, C. M., Corcelli, S. A., Pawashe, A. P., Blanchard, T., McMahon, D., Sidney, J., Sette, A., Baker, B. M., Mandoiu, I. I., & Srivastava, P. K. (2014). Genomic and bioinformatic profiling of mutational neoepitopes reveals new rules to predict anticancer immunogenicity. *Journal of Experimental Medicine*, *211*(11), 2231–2248. https://doi.org/10.1084/jem.20141308

Dubin, K., Callahan, M. K., Ren, B., Khanin, R., Viale, A., Ling, L., No, D., Gobourne, A., Littmann, E., Huttenhower, C., Pamer, E. G., & Wolchok, J. D. (2016). Intestinal microbiome analyses identify melanoma patients at risk for checkpoint-blockade-induced colitis. *Nature Communications*, *7*(1), 10391. https://doi.org/10.1038/ncomms10391

Duma, N., Santana-Dávila, R., & Molina, J. R. (2019). Non–Small cell lung cancer: Epidemiology, screening, diagnosis, and treatment. *Mayo Clinic Proceedings, 94(8),* 1623-1640. https://doi.org/10.1016/j.mayocp.2019.01.013.

Eberst, G., Vernerey, D., Laheurte, C., Meurisse, A., Kaulek, V., Cuche, L., Jacoulet, P., Almotlak, H., Lahourcade, J., Gainet-Brun, M., Fabre, E., Pimpec-Barthes, F. L., Adotévi, O., & Westeel, V. (2022). Prognostic value of CD4+ T lymphopenia in non-small cell lung cancer. *BMC Cancer*, *22*(1). https://doi.org/10.1186/s12885-022-09628-8

El-Sayes, N., Vito, A., & Mossman, K. (2021). Tumor heterogeneity: a great barrier in the age of cancer immunotherapy. *Cancers*, *13*(4), 806. https://doi.org/10.3390/cancers13040806.

Ellis, P., Vella, E. T., & Ung, Y. C. (2017). Immune checkpoint inhibitors for Patients with Advanced Non–Small-Cell Lung Cancer: a systematic review. *Clinical Lung Cancer*, *18*(5), 444-459.e1. https://doi.org/10.1016/j.cllc.2017.02.001.

Erbe, R., Wang, Z., Wu, S., Xiu, J., Zaidi, N., La, J., Tuck, D., Fillmore, N., Giraldo, N. A., Topper, M., Baylin, S., Lippman, M., Isaacs, C., Basho, R., Serebriiskii, I., Lenz, H.-J., Astsaturov, I., Marshall, J., Taverna, J., … Fertig, E. J. (2021). Evaluating the impact of age on immune checkpoint therapy biomarkers. *Cell Reports*, *36*(8), 109599. https://doi.org/10.1016/j.celrep.2021.109599

Fallarino, F., Fields, P. E., & Gajewski, T. F. (1998). B7-1 Engagement of Cytotoxic T Lymphocyte Antigen 4 Inhibits T Cell Activation in the Absence of CD28. *The Journal of Experimental Medicine*, *188*(1), 205–210. https://doi.org/10.1084/jem.188.1.205.

Farsad, M. (2020). FDG PET/CT in the staging of lung cancer. *Current Radiopharmaceuticals*, *13*(3), 195-203. https://doi.org/10.2174/1874471013666191223153755.

Fassan, M. (2018). Molecular Diagnostics in Pathology: Time for a Next-Generation Pathologist? *Archives of Pathology & Laboratory Medicine*, *142*(3), 313–320. https://doi.org/10.5858/arpa.2017-0269-RA

FDA-NIH Biomarker Working Group. (2016). *BEST (Biomarkers, EndpointS, and other Tools) Resource*. Food and Drug Administration (US). http://www.ncbi.nlm.nih.gov/books/NBK326791/

Feng, H., Shuda, M., Chang, Y., & Moore, P. S. (2008). Clonal Integration of a Polyomavirus in Human Merkel Cell Carcinoma. *Science*, *319*(5866), 1096–1100. https://doi.org/10.1126/science.1152586

Fehlmann, T., Kern, F., Laham, O., Backes, C., Solomon, J., Hirsch, P., Volz, C., Müller, R., & Keller, A. (2021). MIRMaster 2.0: Multi-species Non-coding RNA sequencing Analyses at Scale. *Nucleic Acids Research*, *49*(W1), W397-W408. https://doi.org/10.1093/nar/gkab268.

Felip, E., Altorki, N. K., Zhou, C., Vallières, E., Martinez-Martí, A., Rittmeyer, A., Chella, A., Reck, M., Goloborodko, O., Huang, M., Belleli, R., McNally, V., Srivastava, M. K.,

Bennett, E., Gitlitz, B., & Wakelee, H. (2023). Overall survival with adjuvant atezolizumab after chemotherapy in resected stage II-IIIA non-small-cell lung cancer (IMPOWER010): a randomised, multicentre, open-label, phase III trial. *Annals of Oncology*, *34*(10), 907-919. https://doi.org/10.1016/j.annonc.2023.07.001.

Feng, M., Wang, F., Liu, X., Hao, T., Zhang, N., Deng, M., Pan, Y., & Kong, R. (2023). Neutrophils as key regulators of tumor immunity that restrict immune checkpoint blockade in liver cancer. *Cancer biology and medicine*, 1-17. https://doi.org/10.20892/j.issn.2095-3941.2023.0019.

Ferrari, E., & Gandellini, P. (2020). Unveiling the ups and downs of MIR-205 in physiology and Cancer: transcriptional and post-transcriptional mechanisms. *Cell Death and Disease*, *11*(11). https://doi.org/10.1038/s41419-020-03192-4.

Fessler, J., Matson, V., & Gajewski, T. F. (2019). Exploring the emerging role of the microbiome in cancer immunotherapy. *Journal for ImmunoTherapy of Cancer*, *7*(1), 108. https://doi.org/10.1186/s40425-019-0574-4.

Fujikura, K., Alruwaii, Z., Haffner, M. C., Trujillo, M. A., Roberts, N. J., Hong, S. M., Macgregor-Das, A. M., Goggins, M., Roy, S., Meeker, A. K., Ding, D., Wright, M. J., He, J., Hruban, R. H., & Wood, L. D. (2021). Downregulation of 5-hydroxymethylcytosine is an early event in pancreatic tumorigenesis. *The Journal of Pathology, 254(3)*, 279-288. https://doi.org/10.1002/path.5682.

Fumet, J.-D., Truntzer, C., Yarchoan, M., & Ghiringhelli, F. (2020). Tumour mutational burden as a biomarker for immunotherapy: Current data and emerging concepts. *European Journal of Cancer*, *131*, 40–50. https://doi.org/10.1016/j.ejca.2020.02.038.

Gabrielson, E. (2006). Worldwide trends in lung cancer pathology. *Respirology*, *11*(5), 533-538. https://doi.org/10.1111/j.1440-1843.2006.00909.x.

Gainor, J. F., Rizvi, H., Jimenez Aguilar, E., Mooradian, M., Lydon, C. A., Anderson, D., Tenet, M., Sauter, J. L., Mino-Kenudson, M., Shaw, A. T., Awad, M. M., & Hellmann, M. D. (2018). Response and durability of anti-PD-(L)1 therapy in never- or light-smokers with non-small cell lung cancer (NSCLC) and high PD-L1 expression. *Journal of Clinical Oncology*, *36*(15_suppl), 9011–9011.

https://doi.org/10.1200/JCO.2018.36.15_suppl.9011.

Galluzzi, L., Buqué, A., Kepp, O., & Zitvogel, L. (2015). Immunological effects of conventional chemotherapy and targeted anticancer agents. *Cancer Cell*, *28*(6), 690- 714. https://doi.org/10.1016/j.ccell.2015.10.012

Galon, J., Angell, H. K., Bedognetti, D., & Marincola, F. M. (2013). The Continuum of Cancer Immunosurveillance: Prognostic, Predictive, and Mechanistic Signatures. *Immunity*, *39*(1), 11–26. https://doi.org/10.1016/j.immuni.2013.07.008.

Galuppini, F., Dal Pozzo, C. A., Deckert, J., Loupakis, F., Fassan, M., & Baffa, R. (2019). Tumor mutation burden: From comprehensive mutational screening to the clinic. *Cancer Cell International*, *19*(1), 209. https://doi.org/10.1186/s12935-019-0929-4.

Gan, J., Yu, Z., Liu, S., Mu, G., Zhao, J., Jiang, W., Li, J., Li, Q., Wu, Y., Wang, X., Che, D., Li, X., Huang, X., & Meng, Q. (2023). MicroRNA-375 restrains the progression of lung squamous cell carcinoma by modulating the ERK pathway via UBE3A-mediated DUSP1 degradation. *Cell Death Discovery*, *9*(1). https://doi.org/10.1038/s41420-023-01499-7.

Gandara, D. R., Paul, S. M., Kowanetz, M., Schleifman, E., Zou, W., Li, Y., Rittmeyer, A., Fehrenbacher, L., Otto, G., Malboeuf, C., Lieber, D. S., Lipson, D., Silterra, J., Amler, L., Riehl, T., Cummings, C. A., Hegde, P. S., Sandler, A., Ballinger, M., … Shames, D. S. (2018). Blood-based tumor mutational burden as a predictor of clinical benefit in non-small-cell lung cancer patients treated with atezolizumab. *Nature Medicine*, *24*(9), 1441–1448. https://doi.org/10.1038/s41591-018-0134-3.

Gandhi, L., Rodríguez-Abreu, D., Gadgeel, S. M., Esteban, E., Felip, E., De Angelis, F., Dómine, M., Clingan, P. R., Hochmair, M., Powell, S., Cheng, S. Y., Bischoff, H., Peled, N., Grossi, F., Jennens, R., Reck, M., Hui, R., Garon, E. B., Boyer, M., . . . Garassino, M. C. (2018). Pembrolizumab plus chemotherapy in metastatic Non–Small-Cell lung cancer. *The New England Journal of Medicine*, *378*(22), 2078-2092. https://doi.org/10.1056/nejmoa1801005.

Garon, E. B., Rizvi, N. A., Hui, R., Leighl, N., Balmanoukian, A. S., Eder, J. P., Patnaik, A., Aggarwal, C., Gubens, M., Horn, L., Carcereny, E., Ahn, M.-J., Felip, E., Lee, J.-S., Hellmann, M. D., Hamid, O., Goldman, J. W., Soria, J.-C., Dolled-Filhart, M., … Gandhi,

L. (2015). Pembrolizumab for the Treatment of Non–Small-Cell Lung Cancer. *New England Journal of Medicine*, *372*(21), 2018–2028. https://doi.org/10.1056/NEJMoa1501824.

Ghorani, E., Rosenthal, R., McGranahan, N., Reading, J. L., Lynch, M., Peggs, K. S., Swanton, C., & Quezada, S. A. (2018). Differential binding affinity of mutated peptides for MHC class I is a predictor of survival in advanced lung cancer and melanoma. *Annals of Oncology*, *29*(1), 271–279. https://doi.org/10.1093/annonc/mdx687.

Gómez-Martín, C., Scheepbouwer, C., García-Moreno, A., Carmona-Sáez, P., Fromm, B., Keller, A., & Hackenberg, M. (2022). SRNABench and SRNAToolbox 2022 Update: Accurate MIRNA and SNCRNA profiling for model and non-model organisms. *Nucleic Acids Research*, *50*(W1), W710-W717. https://doi.org/10.1093/nar/gkac363.

Grasso, C. S., Tsoi, J., Onyshchenko, M., Abril-Rodríguez, G., Ross-Macdonald, P., Wind-Rotolo, M., Champhekar, A. S., Medina, E., Torrejon, D. Y., Shin, D. S., Tran, P., Kim, Y. J., Puig-Saus, C., Campbell, K. M., Vega-Crespo, A., Quist, M. J., Martignier, C., Luke, J. J., Wolchok, J. D., . . . Ribas, A. (2021). Conserved interferon-Γ signaling drives clinical response to immune checkpoint blockade therapy in melanoma. *Cancer Cell*, *39*(1), 122. https://doi.org/10.1016/j.ccell.2020.11.015.

Han, B., Yang, X., Zhang, P., Zhang, Y., Tu, Y., He, Z., Li, Y., Yuan, J., Dong, Y., Hosseini, D. K., Zhou, T., & Sun, H. (2020). DNA methylation biomarkers for nasopharyngeal carcinoma. *PLOS ONE*, *15*(4), e0230524. https://doi.org/10.1371/journal.pone.0230524.

Han, Y., Liu, D., & Li, L. (2020). PD-1/PD-L1 pathway: Current researches in cancer. *American Journal of Cancer Research*, *10*(3), 727–742.
He, X., & Xu, C. (2020). Immune checkpoint signaling and cancer immunotherapy. *Cell Research*, *30*(8), 660–669. https://doi.org/10.1038/s41422-020-0343-4.

Haslam, A., & Prasad, V. (2019). Estimation of the percentage of US patients with cancer who are eligible for and respond to checkpoint inhibitor immunotherapy drugs. *JAMA network open*, *2*(5), e192535. https://doi.org/10.1001/jamanetworkopen.2019.2535.

Hellmann, M. D., Nathanson, T., Rizvi, H., Creelan, B. C., Sanchez-Vega, F., Ahuja, A., Ni, A., Novik, J. B., Mangarin, L. M. B., Abu-Akeel, M., Liu, C., Sauter, J. L., Rekhtman, N., Chang, E., Callahan, M. K., Chaft, J. E., Voss, M. H., Tenet, M., Li, X.-M., … Wolchok,

J. D. (2018). Genomic Features of Response to Combination Immunotherapy in Patients with Advanced Non-Small-Cell Lung Cancer. *Cancer Cell*, *33*(5), 843-852.e4. https://doi.org/10.1016/j.ccell.2018.03.018.

Hendriks, L., Kerr, K. M., Menis, J., Mok, T., Nestle, U., Passaro, A., Peters, S., Planchard, D., Smit, E. F., Solomon, B. J., Veronesi, G., & Reck, M. (2023). Oncogene-Addicted Metastatic Non-small-cell Lung Cancer: ESMO Clinical Practice Guideline for Diagnosis, Treatment and Follow-up. *Annals of Oncology*, *34*(4), 339-357. https://doi.org/10.1016/j.annonc.2022.12.009.

Henry, N. L., & Hayes, D. F. (2012). Cancer biomarkers. *Molecular Oncology*, *6*(2), 140–146. https://doi.org/10.1016/j.molonc.2012.01.010.

Herbst, R. S., Morgensztern, D., & Boshoff, C. (2018). The Biology and management of non-small cell lung cancer. *Nature*, *553*(7689), 446-454. https://doi.org/10.1038/nature25183.

Herbst, R. S., Soria, J.-C., Kowanetz, M., Fine, G. D., Hamid, O., Gordon, M. S., Sosman, J. A., McDermott, D. F., Powderly, J. D., Gettinger, S. N., Kohrt, H. E. K., Horn, L., Lawrence, D. P., Rost, S., Leabman, M., Xiao, Y., Mokatrin, A., Koeppen, H., Hegde, P. S., … Hodi, F. S. (2014). Predictive correlates of response to the anti-PD-L1 antibody MPDL3280A in cancer patients. *Nature*, *515*(7528), 563–567. https://doi.org/10.1038/nature14011.

High TMB Predicts Immunotherapy Benefit. (2018). *Cancer Discovery*, *8*(6), 668–668. https://doi.org/10.1158/2159-8290.CD-NB2018-048.

Hirsch, F. R., Scagliotti, G. V., Mulshine, J. L., Kwon, R., Curran, W. J., Wu, Y.-L., &Paz-Ares, L. (2017). Lung cancer: Current therapies and new targeted treatments. *The Lancet*, *389*(10066), 299–311. https://doi.org/10.1016/S0140-6736(16)30958-8.

Hubbard, R., Venn, A., Lewis, S., & Britton, J. (2000). Lung cancer and cryptogenic fibrosing alveolitis. *American Journal of Respiratory and Critical Care Medicine*, *161*(1), 5-8. https://doi.org/10.1164/ajrccm.161.1.9906062.

Isaacs, J. D., Wing, M. G., Greenwood, J. D., Hazleman, B. L., Hale, G., & Waldmann, H.

(2003). A therapeutic human IgG4 monoclonal antibody that depletes target cells in humans. *Clinical and Experimental Immunology*, *106*(3), 427–433. https://doi.org/10.1046/j.1365-2249.1996.d01-876.x.

Ivanov, M., Kals, M., Kacevska, M., Barragán, I., Kasuga, K., Rane, A., Metspalu, A., Milani, L., & Ingelman-Sundberg, M. (2013). Ontogeny, distribution and potential roles of 5-hydroxymethylcytosine in human liver function. *GenomeBiology.com (London. Print)*, *14*(8), R83. https://doi.org/10.1186/gb-2013-14-8-r83.

Ivanov, M., Kals, M., Lauschke, V. M., Barragán, I., Ewels, P., Käller, M., Axelsson, T., Lehtiö, J., Milani, L., & Ingelman-Sundberg, M. (2016). Single base resolution analysis of 5-hydroxymethylcytosine in 188 human genes: Implications for hepatic gene expression. *Nucleic Acids Research*, *44*(14), 6756-6769. https://doi.org/10.1093/nar/gkw316

Jänne, P. A., Riely, G. J., Gadgeel, S. M., Heist, R. S., Ou, S. I., Pacheco, J. M., Johnson, M. L., Sabari, J. K., Leventakos, K., Yau, E., Bazhenova, L., Negrão, M. V., Pennell, N. A., Zhang, J., Anderes, K., Der-Torossian, H., Kheoh, T., Velastegui, K., Yan, X., . . . Spira, A. I. (2022). Adagrasib in Non–Small-Cell lung cancer harboring a KRASG12C mutation. *The New England Journal of Medicine*, *387*(2), 120-131. https://doi.org/10.1056/nejmoa2204619.

Jemal, A., & Fedewa, S. A. (2017). Lung cancer screening with Low-Dose Computed Tomography in the United States—2010 to 2015. *JAMA Oncology, 3(9),* 1278. https://doi.org/10.1001/jamaoncol.2016.6416.

Jiang, M., Jia, K., Wang, L., Li, W., Chen, B., Liu, Y., Wang, H., Zhao, S., He, Y., & Zhou, C. (2021). Alterations of DNA damage response pathway: Biomarker and therapeutic strategy for cancer immunotherapy. *Acta Pharmaceutica Sinica B*, *11*(10), 2983–2994. https://doi.org/10.1016/j.apsb.2021.01.003.

Jo, H., Shim, K., & Jeoung, D. (2022). Potential of the MIR-200 family as a target for developing Anti-Cancer therapeutics. *International Journal of Molecular Sciences*, *23*(11), 5881. https://doi.org/10.3390/ijms23115881.

Johnson, D. B., Chandra, S., & Sosman, J. A. (2018). Immune Checkpoint inhibitor toxicity in 2018. *JAMA*, *320*(16), 1702. https://doi.org/10.1001/jama.2018.13995.

Kalluri, R. (2016). The biology and function of exosomes in cancer. *Journal of Clinical Investigation*, *126*(4), 1208–1215. https://doi.org/10.1172/JCI81135.

Kalluri, R., & LeBleu, V. S. (2020). The biology , function , and biomedical applications of exosomes. *Science*, *367*(6478), eaau6977. https://doi.org/10.1126/science.aau6977.

Kazandjian, D., Gong, Y., Keegan, P., Pazdur, R., & Blumenthal, G. M. (2019). Prognostic Value of the Lung Immune Prognostic Index for Patients Treated for Metastatic Non-Small Cell Lung Cancer. *JAMA Oncology*, *5*(10), 1481. https://doi.org/10.1001/jamaoncol.2019.1747.

Kern, F., Fehlmann, T., Solomon, J., Schwed, L., Grammes, N., Backes, C., Van Keuren-Jensen, K., Craig, D. W., Meese, E., & Keller, A. (2020). MIEAA 2.0: Integrating multi-species microRNA enrichment analysis and workflow management systems. *Nucleic Acids Research*, *48*(W1), W521-W528. https://doi.org/10.1093/nar/gkaa309.

Kiehl, S., Zimmermann, T., Savai, R., Pullamsetti, S. S., Seeger, W., Bartkuhn, M., & Dammann, R. (2017). Epigenetic silencing of downstream genes mediated by tandem orientation in lung cancer. *Scientific Reports*, *7*(1). https://doi.org/10.1038/s41598-017-04248-w.

Kim, S. H., Choi, H. I., Choi, M. R., An, G. Y., Binas, B., Jung, K. H., & Chai, Y. G. (2020). Epigenetic regulation of IFITM1 expression in lipopolysaccharide-stimulated human mesenchymal stromal cells. *Stem Cell Research & Therapy*, *11*(1). https://doi.org/10.1186/s13287-019-1531-3.

Kirk, G. D., Merlo, C. A., O'Driscoll, P., Mehta, S. H., Galai, N., Vlahov, D., Samet, J. M., & Engels, E. A. (2007). HIV infection is associated with an increased risk for lung cancer, independent of smoking. *Clinical Infectious Diseases*, *45*(1), 103-110. https://doi.org/10.1086/518606.

Krueger, F., & Andrews, S. (2011). Bismark: a flexible aligner and methylation caller for Bisulfite-Seq applications. *Bioinformatics*, *27*(11), 1571-1572. https://doi.org/10.1093/bioinformatics/btr167.

Kubli, S. P., Berger, T., Araujo, D. V., Siu, L. L., & Mak, T. W. (2021). Beyond immune checkpoint blockade: Emerging immunological strategies. *Nature Reviews Drug Discovery*, *20*(12), 899–919. https://doi.org/10.1038/s41573-021-00155-y.

Kustanovich, A., Schwartz, R., Peretz, T., & Grinshpun, A. (2019). Life and death of circulating cell-free DNA. *Cancer Biology & Therapy*, *20*(8), 1057-1067. https://doi.org/10.1080/15384047.2019.1598759.

Kwon, Y. H., Lee, S. J., Koh, J. S., Kim, S., Lee, H. W., Kang, M. G., Bae, J. B., Kim, Y., & Park, J. H. (2012). Genome-Wide analysis of DNA methylation and the gene expression change in lung cancer. *Journal of Thoracic Oncology*, *7*(1), 20-33. https://doi.org/10.1097/jto.0b013e3182307f62.

Langer, C. J., Gadgeel, S. M., Borghaei, H., Papadimitrakopoulou, V. A., Patnaik, A., Powell, S., Gentzler, R. D., Martins, R., Stevenson, J. P., Jalal, S. I., Panwalkar, A., Yang, J. C., Gubens, M. A., Sequist, L. V., Awad, M. M., Fiore, J., Ge, Y., Raftopoulos, H., & Gandhi, L. (2016). Carboplatin and pemetrexed with or without pembrolizumab for advanced, non-squamous non-small-cell lung cancer: a randomised, phase 2 cohort of the open-label KEYNOTE-021 study. *Lancet Oncology*, *17*(11), 1497-1508. https://doi.org/10.1016/s1470-2045(16)30498-3.

Langmead, B., Trapnell, C., Pop, M., & Salzberg, S. L. (2009). Ultrafast and memory-efficient alignment of short DNA sequences to the human genome. *GenomeBiology.com (London. Print)*, *10*(3), R25. https://doi.org/10.1186/gb-2009-10 3-r25.

Lee, J. H., Long, G. V., Boyd, S., Lo, S., Menzies, A. M., Tembe, V., Guminski, A., Jakrot, V., Scolyer, R. A., Mann, G. J., Kefford, R. F., Carlino, M. S., & Rizos, H. (2017). Circulating tumour DNA predicts response to anti-PD1 antibodies in metastatic melanoma. *Annals of Oncology*, *28*(5), 1130–1136. https://doi.org/10.1093/annonc/mdx026.

Lei, Y., Li, X., Huang, Q., Zheng, X., & Liu, M. (2021). Progress and Challenges of Predictive Biomarkers for Immune Checkpoint Blockade. *Frontiers in Oncology*, *11*,

617335. https://doi.org/10.3389/fonc.2021.617335.

Li, C., Li, C., Zhi, C., Liang, W., Wang, X., Chen, X., Lv, T., Shen, Q., Song, Y., Lin, D., & Liu, H. (2019). Clinical significance of PD-L1 expression in serum-derived exosomes in NSCLC patients. *Journal of Translational Medicine*, *17*(1), 355. https://doi.org/10.1186/s12967-019-2101-2.

Li, J., Hui, Z., Sun, L., Xu, W., & Wang, X. (2019). Prognostic value of site-specific metastases in lung cancer: a population based study. *Journal of Cancer, 10(14),* 3079-3086. https://doi.org/10.7150/jca.30463.

Li, X., Song, W., Shao, C., Shi, Y., & Han, W. (2019). Emerging predictors of the response to the blockade of immune checkpoints in cancer therapy. *Cellular & Molecular Immunology*, *16*(1), 28–39. https://doi.org/10.1038/s41423-018-0086-z.

Liakou, C. I., Kamat, A., Tang, D. N., Chen, H., Sun, J., Troncoso, P., Logothetis, C., & Sharma, P. (2008). CTLA-4 blockade increases IFNγ-producing CD4 $^{+}$ ICOS ^{hi} cells to shift the ratio of effector to regulatory T cells in cancer patients. *Proceedings of the National Academy of Sciences*, *105*(39), 14987–14992. https://doi.org/10.1073/pnas.0806075105.

Liao, M., & Peng, L. (2020). MIR-206 may suppress non-small lung cancer metastasis by targeting CORO1C. *Cellular & Molecular Biology Letters*, *25*(1). https://doi.org/10.1186/s11658-020-00216-x.

Liao, Y., Smyth, G. K., & Shi, W. (2013). FeatureCounts: an efficient general purpose program for assigning sequence reads to genomic features. *Bioinformatics*, *30*(7), 923-930. https://doi.org/10.1093/bioinformatics/btt656.

Lindeman, N. I., Cagle, P. T., Aisner, D. L., Arcila, M. E., Beasley, M. B., Bernicker, E. H., Colasacco, C., Đačić, S., Hirsch, F. R., Kerr, K. M., Kwiatkowski, D. J., Ladanyi, M., Nowak, J. A., Sholl, L. M., Temple-Smolkin, R., Solomon, B., Souter, L., Thunnissen, E., Tsao, M., . . . Yatabe, Y. (2018). Updated Molecular Testing Guideline for the Selection of Lung Cancer Patients for Treatment With Targeted Tyrosine Kinase Inhibitors: Guideline From the College of American Pathologists, the International Association for the Study of Lung Cancer, and the Association for Molecular Pathology. *Archives of*

Pathology & Laboratory Medicine, *142*(3), 321-346. https://doi.org/10.5858/arpa.2017-0388-cp.

Liu, N., Wang, X., Steer, C. J., & Song, G. (2021). MicroRNA-206 promotes the recruitment of CD8+ T cells by driving M1 polarisation of Kupffer cells. *Gut*, gutjnl- 324170. https://doi.org/10.1136/gutjnl-2021-324170.

Liu, Q.-W., He, Y., & Xu, W. W. (2022). Molecular functions and therapeutic applications of exosomal noncoding RNAs in cancer. *Experimental & Molecular Medicine*, *54*(3), 216–225. https://doi.org/10.1038/s12276-022-00744-w.

Love, M. I., Huber, W., & Anders, S. (2014). Moderated estimation of fold change and dispersion for RNA-SEQ data with DESEQ2. *Genome Biology*, *15*(12). https://doi.org/10.1186/s13059-014-0550-8.

Lung Cancer with a High Tumor Mutational Burden. (2018). *New England Journal of Medicine*, *379*(11), 1093–1094. https://doi.org/10.1056/NEJMc1808566.

Ma, M., Li, J., Zhang, Z., Sun, J., Liu, Z., Zeng, Z., Ouyang, S., & Kang, W. (2022). The role and mechanism of microRNA-1224 in human cancer. *Frontiers in Oncology*, *12*. https://doi.org/10.3389/fonc.2022.858892.

Manfredi, F., Cianciotti, B. C., Potenza, A., Tassi, E., Noviello, M., Biondi, A., Ciceri, F., Bonini, C., & Ruggiero, E. (2020). TCR Redirected T Cells for Cancer Treatment: Achievements, Hurdles, and Goals. *Frontiers in Immunology*, *11*, 1689. https://doi.org/10.3389/fimmu.2020.01689.

Manz, K., Fenchel, K., Eilers, A., Morgan, J., Wittling, K., & Dempke, W. (2019). Efficacy and Safety of Approved First-Line tyrosine kinase inhibitor treatments in metastatic renal cell carcinoma: A Network Meta-Analysis. *Advances in Therapy*, 37(2), 730- 744. https://doi.org/10.1007/s12325-019-01167-2.

Marabelle, A., Le, D. T., Ascierto, P. A., Di Giacomo, A. M., De Jesus-Acosta, A., Delord, J.-P., Geva, R., Gottfried, M., Penel, N., Hansen, A. R., Piha-Paul, S. A., Doi, T., Gao, B., Chung, H. C., Lopez-Martin, J., Bang, Y.-J., Frommer, R. S., Shah, M., Ghori, R., … Diaz Jr, L. A. (2020). Efficacy of Pembrolizumab in Patients With Noncolorectal High

Microsatellite Instability/Mismatch Repair–Deficient Cancer: Results From the Phase II KEYNOTE-158 Study. *Journal of Clinical Oncology*, *38*(1), 1–10. https://doi.org/10.1200/JCO.19.02105.

Margaret Sullivan Pepe, Ruth Etzioni, Ziding Feng, John D. Potter, Mary Lou Thompson, Mark Thornquist, Marcy Winget, Yutaka Yasui. (2001). Biomarkers and surrogate endpoints: Preferred definitions and conceptual framework. *Clinical Pharmacology & Therapeutics*, *69*(3), 89–95. https://doi.org/10.1067/mcp.2001.113989.

Matboli, M., Labib, M. E., Nasser, H. A., El-Tawdi, A. H. F., Habib, E. K., & Ali-Labib, R. (2020). Exosomal MIR-1298 and LNCRNA-RP11-583F2.2 expression in hepatocellular carcinoma. *Current Genomics*, *21*(1), 46-55. https://doi.org/10.2174/1389202920666191210111849.

Mathivanan, S., Ji, H., & Simpson, R. J. (2010). Exosomes: Extracellular organelles important in intercellular communication. *Journal of Proteomics*, *73*(10), 1907–1920. https://doi.org/10.1016/j.jprot.2010.06.006.

Mattox, A. K., Douville, C., Wang, Y., Popoli, M., Ptak, J., Silliman, N., Dobbyn, L., Schaefer, J., Lu, S., Pearlman, A. H., Cohen, J. D., Tie, J., Gibbs, P., Lahouel, K., Bettegowda, C., Hruban, R. H., Tomasetti, C., Jiang, P., Chan, K. C. A., … Vogelstein, B. (2023). The Origin of Highly Elevated Cell-Free DNA in Healthy Individuals and Patients with Pancreatic, Colorectal, Lung, or Ovarian Cancer. *Cancer Discovery*, *13*(10), 2166–2179. https://doi.org/10.1158/2159-8290.CD-21-1252.

McGranahan, N., Furness, A. J. S., Rosenthal, R., Ramskov, S., Lyngaa, R., Saini, S. K., Jamal-Hanjani, M., Wilson, G. A., Birkbak, N. J., Hiley, C. T., Watkins, T. B. K., Shafi, S., Murugaesu, N., Mitter, R., Akarca, A. U., Linares, J., Marafioti, T., Henry, J. Y., Van Allen, E. M., … Swanton, C. (2016). Clonal neoantigens elicit T cell immunoreactivity and sensitivity to immune checkpoint blockade. *Science*, *351*(6280), 1463–1469. https://doi.org/10.1126/science.aaf1490.

McKean, W. B., Moser, J., Rimm, D. L., & Hu-Lieskovan, S. (2020). Biomarkers in precision Cancer immunotherapy: promise and challenges. *American Society of Clinical Oncology educational book*, *40*, e275-e291. https://doi.org/10.1200/edbk_280571.

McShane, L. M., Altman, D. G., Sauerbrei, W., Taube, S. E., Gion, M., & Clark, G. M. (2005). REporting Recommendations for Tumour MARKer Prognostic Studies (REMARK). *European Journal of Cancer*, *41*(12), 1690-1696. https://doi.org/10.1016/j.ejca.2005.03.032.

Miao, D., Margolis, C. A., Gao, W., Voss, M. H., Li, W., Martini, D. J., Norton, C., Bossé, D., Wankowicz, S. M., Cullen, D., Horak, C., Wind-Rotolo, M., Tracy, A., Giannakis, M., Hodi, F. S., Drake, C. G., Ball, M. W., Allaf, M. E., Snyder, A., … Van Allen, E. M. (2018). Genomic correlates of response to immune checkpoint therapies in clear cell renal cell carcinoma. *Science*, *359*(6377), 801–806. https://doi.org/10.1126/science.aan5951.

Misra, B. B., Langefeld, C., Olivier, M., & Cox, L. A. (2019). Integrated omics: Tools, advances and future approaches. *Journal of Molecular Endocrinology*, *62*(1), R21–R45. https://doi.org/10.1530/JME-18-0055.

Mlecnik, B., Tosolini, M., Kirilovsky, A., Berger, A., Bindea, G., Meatchi, T., Bruneval, P., Trajanoski, Z., Fridman, W.-H., Pagès, F., & Galon, J. (2011). Histopathologic-Based Prognostic Factors of Colorectal Cancers Are Associated With the State of the Local Immune Reaction. *Journal of Clinical Oncology*, *29*(6), 610–618. https://doi.org/10.1200/JCO.2010.30.5425.

Molina, J. R., Yang, P., Cassivi, S. D., Schild, S. E., & Adjei, A. A. (2008). Non-Small cell lung cancer: Epidemiology, risk factors, treatment, and survivorship. *Mayo Clinic Proceedings*, *83*(5), 584-594. https://doi.org/10.4065/83.5.584.

Morad, G., Helmink, B. A., Sharma, P., & Wargo, J. A. (2021). Hallmarks of response, resistance, and toxicity to immune checkpoint blockade. *Cell*, *184*(21), 5309- 5337. https://doi.org/10.1016/j.cell.2021.09.020.

Moss, J., Magenheim, J., Neiman, D., Zemmour, H., Loyfer, N., Korach, A., Samet, Y., Maoz, M., Druid, H., Arner, P., Fu, K. Y., Kiss, E., Spalding, K. L., Landesberg, G., Zick, A., Grinshpun, A., Shapiro, A. M. J., Grompe, M., Wittenberg, A. D., . . . Dor, Y. (2018). Comprehensive human cell-type methylation atlas reveals origins of circulating cell-free DNA in health and disease. *Nature Communications*, *9*(1). https://doi.org/10.1038/s41467-018-07466-6.

Motz, G. T., & Coukos, G. (2013). Deciphering and Reversing Tumor Immune Suppression. *Immunity*, *39*(1), 61–73. https://doi.org/10.1016/j.immuni.2013.07.005

Mullard, A. (2013). New checkpoint inhibitors ride the immunotherapy tsunami. *Nature Reviews Drug Discovery*, *12*(7), 489–492. https://doi.org/10.1038/nrd4066.

Nakamura, Y. (2019). Biomarkers for Immune Checkpoint Inhibitor-Mediated Tumour Response and Adverse Events. *Frontiers in Medicine*, 6. https://doi.org/10.3389/fmed.2019.00119.

Nalejska, E., Mączyńska, E., & Lewandowska, M. A. (2014). Prognostic and Predictive Biomarkers: Tools in Personalized Oncology. *Molecular Diagnosis & Therapy*, *18*(3), 273–284. https://doi.org/10.1007/s40291-013-0077-9.

National Cancer Institute. Common Terminology Criteria for Adverse Events (CTCAE). (2021). https://ctep.cancer.gov/protocoldevelopment/electronic_applications/ctc.htm

National Center for Chronic Disease Prevention and Health Promotion (US) Office on Smoking and Health. The Health Consequences of Smoking—50 Years of Progress: A Report of the Surgeon General. Atlanta (GA): Centers for Disease Control and Prevention (US); 2014. PMID: 24455788.

Nicholson, A. G., Tsao, M. S., Beasley, M. B., Borczuk, A. C., Brambilla, É., Cooper, W. A., Đačić, S., Jain, D., Kerr, K. M., Lantuéjoul, S., Noguchi, M., Papotti, M., Rekhtman, N., Scagliotti, G. V., Van Schil, P., Sholl, L. M., Yatabe, Y., Yoshida, A., & Travis, W. D. (2022). The 2021 WHO Classification of Lung Tumors: Impact of advances since 2015. *Journal of Thoracic Oncology, 17(3),* 362-387. https://doi.org/10.1016/j.jtho.2021.11.003.

Nishimura, S., Uno, M., Kaneta, Y., Fukuchi, K., Nishigohri, H., Hasegawa, J., Komori, H., Takeda, S., Enomoto, K., Nara, F., & Agatsuma, T. (2012). MRGD, a MAS-related G-protein coupled receptor, promotes tumorigenisis and is highly expressed in lung cancer. *PLOS ONE*, *7*(6), e38618. https://doi.org/10.1371/journal.pone.0038618

Okonechnikov, K., Conesa, A., & García-Alcalde, F. (2015). QUALIMAP 2: Advanced multi-sample quality control for high-throughput sequencing data. *Bioinformatics*, *32*(2), 292-294. https://doi.org/10.1093/bioinformatics/btv566.

Olivier, M., Asmis, R., Hawkins, G. A., Howard, T. D., & Cox, L. A. (2019). The Need for Multi-Omics Biomarker Signatures in Precision Medicine. *International Journal of Molecular Sciences*, *20*(19), 4781. https://doi.org/10.3390/ijms20194781.

Onieva, J. L., Cháves, P., Oliver, J., Garrido-Barros, M., Zafra, J. M. L., Sojo, B., Sánchez, A., Álvarez, M., Jiménez, P. L., Alba, E., Berciano, M., Rueda, A., Cobo-Dols, M., Pérez-Ruiz, E., & Barragán, I. (2022). Abstract 1910: FlowTOTAL: A Comprehensive Bioinformatics Workflow for Flow Cytometry Automatic Analysis. *Cancer Research*, *82*(12_Supplement), 1910. https://doi.org/10.1158/1538-7445.am2022-1910.

Onieva, J. L., Xiao, Q., Berciano-Guerrero, M., Laborda-Illanes, A., De Andrea, C., Guerrero, P. C., Piñeiro, P., Garrido-Aranda, A., Gallego, E., Sojo, B., Gálvez, L., Chica-Parrado, R., Cuadra, J. D. P., Pérez-Ruiz, E., Farngren, A., Lozano, M. J., Álvarez, M., Jiménez, P. A., Sánchez-Muñoz, A., . . . Barragán, I. (2022). High IGKC-Expressing intratumoral plasma cells predict response to immune checkpoint blockade. *International Journal of Molecular Sciences*, *23*(16), 9124. https://doi.org/10.3390/ijms23169124.

Pan, J., Zhang, F., Sun, C., Li, S., Li, G., Gong, F., Tao, B., He, J., Hua, R., Hu, W., Zhu, Y., Wang, X., He, Q., & Li, D. (2017). MIR-134: a human cancer suppressor? Molecular Therapy - Nucleic Acids, 6, 140-149. https://doi.org/10.1016/j.omtn.2016.11.003.

Pardoll, D. M. (2012). The blockade of immune checkpoints in cancer immunotherapy. *Nature Reviews Cancer*, *12*(4), 252–264. https://doi.org/10.1038/nrc3239.

Parikh, K., Kumar, A., Ahmed, J., Anwar, A., Puccio, C., Chun, H. G., Fanucchi, M., & Lim, S. H. (2018). Peripheral monocytes and neutrophils predict response to immune checkpoint inhibitors in patients with metastatic non-small cell lung cancer. *Cancer Immunology, Immunotherapy*, *67*(9), 1365-1370. https://doi.org/10.1007/s00262-018-2192-2.

Paz-Ares, L., Doebele, R. C., Farago, A. F., Liu, S., Chawla, S. P., Tosi, D., Blakely, C. M., Krauss, J. C., Sigal, D., Bazhenova, L., John, T., Besse, B., Wolf, J., Seto, T., Chow-Maneval, E., Ye, C., Simmons, B., & Demetri, G. D. (2019). Entrectinib in NTRK Fusion-positive Non-small cell lung Cancer (NSCLC): Integrated Analysis of Patients (PTS) enrolled

in STARTRK-2, STARTRK-1 and ALKA-372-001. *Annals of Oncology*, *30*, ii48- ii49. https://doi.org/10.1093/annonc/mdz063.011.

Paz-Ares, L., Luft, A., Vicente, D., Tafreshi, A., Gümüş, M., Mazières, J., Hermes, B., Şenler, F. Ç., Csõszi, T., Fülöp, A., Rodríguez-Cid, J. R., Wilson, J., Sugawara, S., Kato, T., Lee, K. H., Cheng, Y., Novello, S., Halmos, B., Li, X., . . Investigators, K. (2018). Pembrolizumab plus chemotherapy for squamous Non–Small-Cell lung cancer. *The New England Journal of Medicine*, *379*(21), 2040-2051. https://doi.org/10.1056/nejmoa1810865.

Pio, R., Ajona, D., Ortiz-Espinosa, S., Mantovani, A., & Lambris, J. D. (2019). Complementing the Cancer-Immunity Cycle. *Frontiers in Immunology*, *10*, 774. https://doi.org/10.3389/fimmu.2019.00774.

Possick, J. D. (2017). Pulmonary Toxicities from Checkpoint Immunotherapy for Malignancy. *Clinics in Chest Medicine*, *38*(2), 223–232. https://doi.org/10.1016/j.ccm.2016.12.012.

Postow, M. A., Callahan, M. K., & Wolchok, J. D. (2015). Immune Checkpoint Blockade in Cancer Therapy. *Journal of Clinical Oncology*, *33*(17), 1974–1982. https://doi.org/10.1200/JCO.2014.59.4358.

Pritchard, A. L., Burel, J. G., Neller, M. A., Hayward, N. K., Lopez, J. A., Fatho, M., Lennerz, V., Wölfel, T., & Schmidt, C. W. (2015). Exome Sequencing to Predict Neoantigens in Melanoma. *Cancer Immunology Research*, *3*(9), 992–998. https://doi.org/10.1158/2326-6066.CIR-15-0088.

Provencio, M., Nadal, E., González-Larriba, J., Martinez-Martí, A., Bernabé, R., Bosch-Barrera, J., Casal-Rubio, J., Calvo, V., Insa, A., Ponce, S., Reguart, N., De Castro, J., Mosquera, J., Cobo-Dols, M., Aguilar, A., Vivanco, G. L., Camps, C., López-Castro, R., Morán, T., Romero, A. (2023). Perioperative nivolumab and chemotherapy in stage III Non–Small-Cell lung cancer. *The New England Journal of Medicine*, *389*(6), 504-513. https://doi.org/10.1056/nejmoa2215530.

Pu, R., Pu, M., Huang, H., & Cui, Y. (2021). MicroRNA 144 inhibits cell migration and invasion and regulates inflammatory cytokine secretion through targeting toll like

receptor 2 in non-small cell lung cancer. *Archives of Medical Science*, *17*(4), 1028-1037. https://doi.org/10.5114/aoms.2020.93084.

Pucci, F., Rickelt, S., Newton, A., Garris, C., Nunes, E. A., Evavold, C. L., Pfirschke, C., Engblom, C., Mino-Kenudson, M., Hynes, R. O., Weissleder, R., & Pittet, M. J. (2016). PF4 promotes platelet production and lung cancer growth. *Cell Reports*, *17*(7), 1764- 1772. https://doi.org/10.1016/j.celrep.2016.10.031.

Pulla, M. P., Serna-Blasco, R., Nadal, E., Insa, A., García-Campelo, Rubio, J. C., Dómine, M., Majem, M., Abreu, D. R., Martinez-Martí, A., De Castro, J., Cobo, M., Vivanco, G. L., Del Barco, E., Bernabé, R., Viñolas, N., Aranda, I. B., Viteri, S., Pereira, E., . . . Romero, A. (2022). Overall survival and biomarker analysis of neoadjuvant nivolumab plus chemotherapy in operable Stage IIIA Non–Small-Cell lung cancer (NADIM Phase II trial). *Journal of Clinical Oncology*, *40*(25), 2924-2933. https://doi.org/10.1200/jco.21.02660.

Qin, S., Xu, L., Yi, M., Yu, S., Wu, K., & Luo, S. (2019). Novel immune checkpoint targets: Moving beyond PD-1 and CTLA-4. *Molecular Cancer*, *18*(1), 155. https://doi.org/10.1186/s12943-019-1091-2.

Quezada, H., Guzmán-Ortiz, A. L., Díaz-Sánchez, H., Valle-Rios, R., & Aguirre-Hernández, J. (2017). Omics-based biomarkers: Current status and potential use in the clinic. *Boletín Médico Del Hospital Infantil de México (English Edition)*, *74*(3), 219–226. https://doi.org/10.1016/j.bmhime.2017.11.030.

Raju, S., Kometani, K., Kurosaki, T., Shaw, A. S., & Egawa, T. (2018). The adaptor molecule CD2AP in CD4 T cells modulates differentiation of follicular helper T cells during chronic LCMV infection. *PLOS Pathogens*, *14*(5), e1007053. https://doi.org/10.1371/journal.ppat.1007053.

Ramos-Casals, M., Brahmer, J. R., Callahan, M. K., Flores-Chávez, A., Keegan, N., Khamashta, M. A., Lambotte, O., Mariette, X., Prat, A., & Suárez-Almazor, M. E. (2020). Immune-related adverse events of checkpoint inhibitors. *Nature Reviews Disease Primers*, *6*(1), 38. https://doi.org/10.1038/s41572-020-0160-6.

Reck, M., Popat, S., Reinmuth, N., De Ruysscher, D., Kerr, K. M., & Peters, S. (2014). Metastatic Non-small-cell lung Cancer (NSCLC): ESMO Clinical Practice Guidelines for diagnosis, treatment and follow-up. *Annals of Oncology*, *25*, iii27- iii39. https://doi.org/10.1093/annonc/mdu199.

Reck, M., Rodríguez-Abreu, D., Robinson, A., Hui, R., Csõszi, T., Fülöp, A., Gottfried, M., Peled, N., Tafreshi, A., Cuffe, S., O'Brien, M., Rao, S., Hotta, K., Leiby, M. A., Lubiniecki, G. M., Shentu, Y., Rangwala, R., & Brahmer, J. R. (2016). Pembrolizumab versus chemotherapy for PD-L1–Positive Non–Small-Cell lung cancer. *The New England Journal of Medicine*, *375*(19), 1823-1833. https://doi.org/10.1056/nejmoa1606774.

Ren, F., Zhao, T., Liu, B., & Pan, L. (2019). <P>Neutrophil–lymphocyte ratio (NLR) predicted prognosis for advanced non-small-cell lung cancer (NSCLC) patients who received immune Checkpoint blockade (ICB)</P> *OncoTargets and Therapy*, *Volume 12*, 4235-4244. https://doi.org/10.2147/ott.s199176.

Ricciuti, B., Mira, A., Andrini, E., Scaparone, P., Michelina, S. V., Pecci, F., Cantini, L., De Giglio, A., Lamberti, G., Ambrogio, C., & Metro, G. (2022). How to manage KRAS G12C-mutated advanced non-small-cell lung cancer. *Drugs Context* ., *11*, 1-11. https://doi.org/10.7573/dic.2022-7-4.

Rizvi, H., Sanchez-Vega, F., La, K., Chatila, W., Jonsson, P., Halpenny, D., Plodkowski, A., Long, N., Sauter, J. L., Rekhtman, N., Hollmann, T., Schalper, K. A., Gainor, J. F., Shen, R., Ni, A., Arbour, K. C., Merghoub, T., Wolchok, J., Snyder, A., … Hellmann, M. D. (2018). Molecular Determinants of Response to Anti–Programmed Cell Death (PD)-1 and Anti–Programmed Death-Ligand 1 (PD-L1) Blockade in Patients With Non–Small-Cell Lung Cancer Profiled With Targeted Next-Generation Sequencing. *Journal of Clinical Oncology*, *36*(7), 633–641. https://doi.org/10.1200/JCO.2017.75.3384.

Rizvi, N. A., Cho, B. C., Reinmuth, N., Lee, K., Ahn, M., Luft, A., Van Den Heuvel, M., Cobo, M., Smolin, A., Vicente, D., Moiseyenko, V., Antonia, S., Moulec, S. L., Robinet, G., Natale, R. B., Nakagawa, K., Zhao, L., Stockman, P. K., Chand, V. K., & Peters, S. (2018). Durvalumab with or without tremelimumab vs platinum-based chemotherapy as first-line treatment for metastatic non-small cell lung cancer: MYSTIC. *Annals of Oncology*, *29*, x40-x41. https://doi.org/10.1093/annonc/mdy511.005.

Rosenberg, J. E., Hoffman-Censits, J., Powles, T., van der Heijden, M. S., Balar, A. V., Necchi, A., Dawson, N., O'Donnell, P. H., Balmanoukian, A., Loriot, Y., Srinivas, S., Retz, M. M., Grivas, P., Joseph, R. W., Galsky, M. D., Fleming, M. T., Petrylak, D. P., Perez-Gracia, J. L., Burris, H. A., … Dreicer, R. (2016). Atezolizumab in patients with locally advanced and metastatic urothelial carcinoma who have progressed following treatment with platinum-based chemotherapy: A single-arm, multicentre, phase 2 trial. *The Lancet*, *387*(10031), 1909–1920. https://doi.org/10.1016/S0140-6736(16)00561-4.

Ross, J. S., Goldberg, M. E., Albacker, L. A., Gay, L. M., Agarwala, V., Elvin, J. A., Vergilio, J.-A., Suh, J., Ramkissoon, S., Severson, E., Daniel, S., Ali, S. M., Schrock, A. B., Frampton, G. M., Fabrizio, D., Miller, V. A., Singal, G., Abernethy, A., & Stephens, P. J. (2017). Immune checkpoint inhibitor (ICPI) efficacy and resistance detected by comprehensive genomic profiling (CGP) in non-small cell lung cancer (NSCLC). *Annals of Oncology*, *28*, v404. https://doi.org/10.1093/annonc/mdx376.004.

Rossi, G., & Ignatiadis, M. (2019). Promises and Pitfalls of Using Liquid Biopsy for Precision Medicine. *Cancer Research*, *79*(11), 2798–2804. https://doi.org/10.1158/0008-5472.CAN-18-3402.

Ruiz, M. G., Ramírez-Labrada, A., Lastra, R. P., Martínez-Lostao, L., Paño-Pardo, J. R., Sesma, A., Zapata-García, M., Moratiel, A., Quílez, E., Torres-Ramón, I., Yubero, A., Domingo, M. P., Esteban, P., Gálvez, E. M., Pardo, J., & Isla, D. (2023). A subset of PD-1-Expressing CD56Bright NK cells identifies patients with good response to immune checkpoint inhibitors in lung cancer. *Cancers*, *15*(2), 329. https://doi.org/10.3390/cancers15020329.

Sade-Feldman, M., Yizhak, K., Bjorgaard, S. L., Ray, J. P., De Boer, C. G., Jenkins, R. W., Lieb, D. J., Chen, J. H., Frederick, D. T., Barzily-Rokni, M., Freeman, S. S., Reuben, A., Hoover, P. J., Villani, A.-C., Ivanova, E., Portell, A., Lizotte, P. H., Aref, A. R., Eliane, J.-P., … Hacohen, N. (2018). Defining T Cell States Associated with Response to Checkpoint Immunotherapy in Melanoma. *Cell*, *175*(4), 998-1013.e20. https://doi.org/10.1016/j.cell.2018.10.038.

Safonov, A., Wang, S. Y., Gross, C. P., Agarwal, D., Bianchini, G., Pusztai, L., & Hatzis, C. (2016). Assessing Cost-utility of predictive biomarkers in Oncology: A streamlined

approach. *Breast Cancer Research and Treatment*, *155*(2), 223-234. https://doi.org/10.1007/s10549-016-3677-3.

Samatov, T. R., Tonevitsky, A. G., & Schumacher, U. (2013). Epithelial-mesenchymal transition: Focus on metastatic cascade, alternative splicing, non-coding RNAs and modulating compounds. *Molecular Cancer*, *12*(1), 107. https://doi.org/10.1186/1476-4598-12-107.

Sarhadi, V., & Armengol, G. (2022). Molecular biomarkers in cancer. *Biomolecules*, *12*(8), 1021. https://doi.org/10.3390/biom12081021.

Sasaki, Y., Takagane, K., Konno, T., Itoh, G., Kuriyama, S., Yanagihara, K., Yashiro, M., Yamada, S., Murakami, S., & Tanaka, M. (2021). Expression of asporin reprograms cancer cells to acquire resistance to oxidative stress. *Cancer Science*, *112*(3), 1251-1261. https://doi.org/10.1111/cas.14794.

Schumacher, T. N., Scheper, W., & Kvistborg, P. (2019). Cancer Neoantigens. *Annual Review of Immunology*, *37*(1), 173–200. https://doi.org/10.1146/annurev-immunol-042617-053402.

Schumacher, T. N., & Schreiber, R. D. (2015). Neoantigens in cancer immunotherapy. *Science*, *348*(6230), 69–74. https://doi.org/10.1126/science.aaa4971.

Schwartz, L. H., Litière, S., De Vries, E. G., Ford, R., Gwyther, S. J., Mandrekar, S. J., Shankar, L., Bogaerts, J., Chen, A., Dancey, J., Hayes, W., Hodi, F. S., Hoekstra, O. S., Huang, E. P., Lin, N. U., Liu, Y., Therasse, P., Wolchok, J. D., & Seymour, L. (2016). RECIST 1.1—Update and clarification: from the RECIST Committee. *European Journal of Cancer*, *62*, 132-137. https://doi.org/10.1016/j.ejca.2016.03.081.

Seidel, D., Zander, T., Heukamp, L. C., Peifer, M., Bos, M., Fernández-Cuesta, L., Leenders, F., Lü, X., Ansén, S., Gardizi, M., Nguyen, C., Berg, J., Russell, P. A., Wainer, Z., Schildhaus, H., Rogers, T., Solomon, B., Pao, W., Carter, S. L., Lang, U. (2013). A Genomics-Based Classification of human lung tumors. *Science Translational Medicine*, *5*(209). https://doi.org/10.1126/scitranslmed.3006802.

Seymour, L., Bogaerts, J., Perrone, A., Ford, R., Schwartz, L. H., Mandrekar, S. J., Lin, N. U., Litière, S., Dancey, J., Chen, A., Hodi, F. S., Therasse, P., Hoekstra, O. S., Shankar, L., Wolchok, J. D., Ballinger, M., Caramella, C., & De Vries, E. G. (2017). IRECIST: Guidelines for Response Criteria for Use in Trials Testing Immunotherapeutics. *Lancet Oncology*, *18*(3), e143-e152. https://doi.org/10.1016/s1470-2045(17)30074-8.

Shan, L., Zhao, M., Lu, Y., Ning, H., Yang, S., Song, Y., Chai, W., & Shi, X. (2019). CENPE promotes lung adenocarcinoma proliferation and is directly regulated by FOXM1. *International Journal of Oncology*. https://doi.org/10.3892/ijo.2019.4805.

Sharma, P., & Allison, J. P. (2015). The future of immune checkpoint therapy. *Science*, *348*(6230), 56–61. https://doi.org/10.1126/science.aaa8172.

Sharma, S. (2009). Tumor markers in clinical practice: General principles and guidelines. *Indian Journal of Medical and Paediatric Oncology*, *30*(01), 1–8. https://doi.org/10.4103/0971-5851.56328.

Shao, J., Wang, S., West-Szymanski, D. C., Karpus, J., Shah, S., Ganguly, S., Smith, J., Zu, Y., He, C., & Li, Z. (2022). Cell-free DNA 5-hydroxymethylcytosine is an emerging marker of acute myeloid leukemia. *Scientific Reports*, *12*(1). https://doi.org/10.1038/s41598-022-16685-3.

Sheervalilou, R., Lotfi, H., Shirvaliloo, M., Sharifi, A., Nazemiyeh, M., & Zarghami, N. (2019). Circulating MIR-10B, MIR-1 and MIR-30A expression profiles in lung cancer: possible correlation with clinico-pathologic characteristics and lung cancer detection. *PubMed*, *8*(2), 118-129. https://doi.org/10.22088/ijmcm.bums.8.2.118.

Shen, Q., Han, Y., Wu, K., He, Y., Jiang, X., Liu, P., Xia, C., Xiong, Q., Li, R., Chen, Q., Zhang, Y., Zhao, S., Yang, C., & Chen, Y. (2022). MRGPRF acts as a tumor suppressor in cutaneous melanoma by restraining PI3K/AkT signaling. *Signal Transduction and Targeted Therapy*, *7*(1). https://doi.org/10.1038/s41392-022-00945-9.

Shim, J., Brindle, L., Simon, M., & George, S. (2013). A Systematic Review of Symptomatic Diagnosis of lung Cancer. *Family Practice*, *31*(2), 137 148. https://doi.org/10.1093/fampra/cmt076.

Siegel, R. L., Miller, K. D., Fuchs, H. E., & Jemal, A. (2022). Cancer statistics, 2022. *CA: A Cancer Journal for Clinicians*, *72*(1), 7–33. https://doi.org/10.3322/caac.21708.

Simon, R., Paik, S., & Hayes, D. F. (2009). Use of archived specimens in evaluation of prognostic and predictive biomarkers. *JNCI: Journal of the National Cancer Institute*, *101*(21), 1446-1452. https://doi.org/10.1093/jnci/djp335.

Sivan, A., Corrales, L., Hubert, N., Williams, J. B., Aquino-Michaels, K., Earley, Z. M., Benyamin, F. W., Man Lei, Y., Jabri, B., Alegre, M.-L., Chang, E. B., & Gajewski, T. F. (2015). Commensal *Bifidobacterium* promotes antitumor immunity and facilitates anti–PD-L1 efficacy. *Science*, *350*(6264), 1084–1089. https://doi.org/10.1126/science.aac4255.

Skoulidis, F., Li, B. T., Dy, G. K., Price, T., Falchook, G. S., Wolf, J., Italiano, A., Schüler, M., Borghaei, H., Barlési, F., Kato, T., Curioni-Fontecedro, A., Sacher, A. G., Spira, A. I., Ramalingam, S. S., Takahashi, T., Besse, B., Anderson, A., Ang, A., . . . Govindan, R. (2021). Sotorasib for lung cancers with KRAS P.G12C mutation. *The New England Journal of Medicine*, *384*(25), 2371-2381. https://doi.org/10.1056/nejmoa2103695.

Snyder, A., Makarov, V., Merghoub, T., Yuan, J., Zaretsky, J. M., Desrichard, A., Walsh, L. A., Postow, M. A., Wong, P., Ho, T. S., Hollmann, T. J., Bruggeman, C., Kannan, K., Li, Y., Elipenahli, C., Liu, C., Harbison, C. T., Wang, L., Ribas, A., … Chan, T. A. (2014). Genetic Basis for Clinical Response to CTLA-4 Blockade in Melanoma. *New England Journal of Medicine*, *371*(23), 2189–2199. https://doi.org/10.1056/NEJMoa1406498.

Soofiyani, S. R., Hosseini, K., Soleimanian, A., Abkhooei, L., Hoseini, A. M., Tarhriz, V., & Ghasemnejad, T. (2021). An overview on the role of MIR-451 in lung cancer: diagnosis, therapy, and prognosis. *MicroRNA*, *10*(3), 181-190. https://doi.org/10.2174/2211536610666210910130828.

Spector, B. L., Harrell, L., Sante, D., Wyckoff, G. J., & Willig, L. K. (2023). The methylome and cell-free DNA: current applications in medicine and pediatric disease. *Pediatric Research*, *94*(1), 89-95. https://doi.org/10.1038/s41390-022-02448-3.

Srivastava, S., & Kramer, B. S. (2000). Early Detection Cancer Research Network. *Laboratory Investigation*, *80*(8), 1147–1148. https://doi.org/10.1038/labinvest.3780122.

Srivastava, S., & Wagner, P. D. (2020). The Early Detection Research Network: A National Infrastructure to Support the Discovery, Development, and Validation of Cancer Biomarkers. *Cancer Epidemiology, Biomarkers & Prevention*, *29*(12), 2401–2410. https://doi.org/10.1158/1055-9965.EPI-20-0237.

Steuer, C. E., & Ramalingam, S. S. (2018). Tumor Mutation Burden: Leading Immunotherapy to the Era of Precision Medicine? *Journal of Clinical Oncology*, *36*(7), 631–632. https://doi.org/10.1200/JCO.2017.76.8770.

Steuer, C. E., Jegede, O., Dahlberg, S. E., Wakelee, H. A., Keller, S. M., Tester, W. J., Gandara, D. R., Graziano, S. L., Adjei, A. A., Butts, C., Ramalingam, S. S., & Schiller, J. H. (2021). Smoking behavior in patients with Early-Stage NSCLC: A report from ECOG-ACRIN 1505 trial. *Journal of Thoracic Oncology*, *16*(6), 960-967. https://doi.org/10.1016/j.jtho.2020.12.017.

Sullivan, M. J. L., Thorn, B., Haythornthwaite, J. A., Keefe, F., Martin, M., Bradley, L. A., & Lefebvre, J. C. (2001). Theoretical Perspectives on the Relation Between Catastrophizing and Pain: *The Clinical Journal of Pain*, *17*(1), 52–64. https://doi.org/10.1097/00002508-200103000-00008.

Sun, W., Kim, H. J., Perovanović, J., Hughes, E. P., Du, J., Ibarra, A., Hale, J. S., Williams, M. A., & Tantin, D. (2022). OCA-B/POU2AF1 is sufficient to promote CD4+T cell memory and prospectively identifies memory precursors. *bioRxiv (Cold Spring Harbor Laboratory)*. https://doi.org/10.1101/2022.09.21.508912.

Sung, H., Ferlay, J., Siegel, R. L., Laversanne, M., Soerjomataram, I., Jemal, A., & Bray, F. (2021b). Global Cancer Statistics 2020: GLOBOCAN Estimates of Incidence and Mortality Worldwide for 36 Cancers in 185 Countries. *CA: A Cancer Journal for Clinicians*, *71*(3), 209–249. https://doi.org/10.3322/caac.21660.

Takeda, M., Takahama, T., Sakai, K., Shimizu, S., Watanabe, S., Kawakami, H., Tanaka, K., Sato, C., Hayashi, H., Nonagase, Y., Yonesaka, K., Takegawa, N., Okuno, T., Yoshida, T., Fumita, S., Suzuki, S., Haratani, K., Saigoh, K., Ito, A., … Nishio, K. (2021). Clinical Application of the FoundationOne CDx Assay to Therapeutic Decision-Making for Patients with Advanced Solid Tumors. *The Oncologist*, *26*(4), e588–e596.

https://doi.org/10.1002/onco.13639.

Tam, W. L., & Weinberg, R. A. (2013). The epigenetics of epithelial-mesenchymal plasticity in cancer. *Nature Medicine*, *19*(11), 1438–1449. https://doi.org/10.1038/nm.3336.

Tay, R. E., Richardson, E. K., & Toh, H. C. (2020). Revisiting the role of CD4+ T cells in cancer immunotherapy—new insights into old paradigms. *Cancer Gene Therapy*, *28*(1-2), 5-17. https://doi.org/10.1038/s41417-020-0183-x.

Thai, A., Solomon, B., Sequist, L. V., Gainor, J. F., & Heist, R. S. (2021). Lung cancer. *The Lancet*, *398*(10299), 535-554. https://doi.org/10.1016/s0140-6736(21)00312-3.

The National Lung Screening Trial Research Team. Reduced Lung-Cancer mortality with Low-Dose Computed Tomographic Screening. (2011). *The New England Journal of Medicine, 365(5*), 395-409. https://doi.org/10.1056/nejmoa1102873.

Tietze, J. K., Angelova, D., Heppt, M. V., Reinholz, M., Murphy, W. J., Spannagl, M., Ruzicka, T., & Berking, C. (2017). The proportion of circulating CD45RO + CD8 + memory T cells is correlated with clinical response in melanoma patients treated with ipilimumab. *European Journal of Cancer*, *75*, 268–279. https://doi.org/10.1016/j.ejca.2016.12.031.

Topalian, S. L. (2017). Targeting immune checkpoints in cancer therapy. *JAMA*, *318*(17), 1647. https://doi.org/10.1001/jama.2017.14155.

Topalian, S. L., Taube, J. M., & Pardoll, D. M. (2020). Neoadjuvant checkpoint blockade for cancer immunotherapy. *Science*, *367*(6477), eaax0182. https://doi.org/10.1126/science.aax0182.

Tredan, O., Galmarini, C. M., Patel, K., & Tannock, I. F. (2007). Drug Resistance and the Solid Tumor Microenvironment. *JNCI Journal of the National Cancer Institute*, *99*(19), 1441–1454. https://doi.org/10.1093/jnci/djm135.

Tsuboi, M., Herbst, R. S., John, T., Kato, T., Majem, M., Grohé, C., Wang, J., Goldman, J. W., Lü, S., Su, W. C., De Marinis, F., Shepherd, F. A., Lee, K. H., Le, N. D.,

Dechaphunkul, A., Kowalski, D. M., Poole, L., Bolanos, A., Rukazenkov, Y., & Wu, Y. (2023). Overall survival with osimertinib in resected EGFR-Mutated NSCLC. *The New England Journal of Medicine*, *389*(2), 137-147. https://doi.org/10.1056/nejmoa2304594.

Tumeh, P. C., Harview, C. L., Yearley, J. H., Shintaku, I. P., Taylor, E. J. M., Robert, L., Chmielowski, B., Spasic, M., Henry, G., Ciobanu, V., West, A. N., Carmona, M., Kivork, C., Seja, E., Cherry, G., Gutierrez, A. J., Grogan, T. R., Mateus, C., Tomasic, G., … Ribas, A. (2014). PD-1 blockade induces responses by inhibiting adaptive immune resistance. *Nature*, *515*(7528), 568–571. https://doi.org/10.1038/nature13954.

Uno, H., Cai, T., Tian, L., & Wei, L. J. (2007). Evaluating prediction Rules Fort-Year survivors with censored regression models. *Journal of the American Statistical Association*, *102*(478), 527-537. https://doi.org/10.1198/016214507000000149.

Usuba, W., Urabe, F., Yamamoto, Y., Matsuzaki, J., Sasaki, H., Ichikawa, M., Takizawa, S., Aoki, Y., Niida, S., Kato, K., Egawa, S., Chikaraishi, T., Fujimoto, H., & Ochiya, T. (2018). Circulating mIRNA panels for specific and early detection in bladder cancer. *Cancer Science*, *110*(1), 408-419. https://doi.org/10.1111/cas.13856.

Vasioukhin, V., Anker, P., Maurice, P., Lyautey, J., Lederrey, C., & Stroun, M. (1994). Point mutations of the N- *ras* gene in the blood plasma DNA of patients with myelodysplastic syndrome or acute myelogenous leukaemia. *British Journal of Haematology*, *86*(4), 774–779. https://doi.org/10.1111/j.1365-2141.1994.tb04828.x.

Vestergaard, L. K., De Oliveira, D. N. P., Poulsen, T. S., Høgdall, C., & Høgdall, E. (2021). OncomineTM Comprehensive Assay V3 vs. OncomineTM Comprehensive Assay Plus. *Cancers*, *13*(20), 5230. https://doi.org/10.3390/cancers13205230.

Walk, E. E., Yohe, S. L., Beckman, A., Schade, A., Zutter, M. M., Pfeifer, J., Berry, A. B., & on behalf of the College of American Pathologists Personalized Health Care Committee. (2020). The Cancer Immunotherapy Biomarker Testing Landscape. *Archives of Pathology & Laboratory Medicine*, *144*(6), 706–724. https://doi.org/10.5858/arpa.2018-0584-CP.

Wang, F., Zhao, Q., Wang, Y.-N., Jin, Y., He, M.-M., Liu, Z.-X., & Xu, R.-H. (2019). Evaluation of *POLE* and *POLD1* Mutations as Biomarkers for Immunotherapy Outcomes Across Multiple Cancer Types. *JAMA Oncology*, *5*(10), 1504.

https://doi.org/10.1001/jamaoncol.2019.2963.

.

Wang, Y., Luo, X., Liu, Y., Han, G., & Sun, D. (2019). Long noncoding RNA RMRP promotes proliferation and invasion via targeting MIR-1-3P in non–small-cell lung cancer. *Journal of Cellular Biochemistry*, *120*(9), 15170-15181. https://doi.org/10.1002/jcb.28779.

Wang, Z., Aguilar, E. G., Luna, J. I., Dunai, C., Khuat, L. T., Le, C. T., Mirsoian, A., Minnar, C. M., Stoffel, K. M., Sturgill, I. R., Grossenbacher, S. K., Withers, S. S., Rebhun, R. B., Hartigan-O'Connor, D. J., Méndez-Lagares, G., Tarantal, A. F., Isseroff, R. R., Griffith, T. S., Schalper, K. A., … Monjazeb, A. M. (2019). Paradoxical effects of obesity on T cell function during tumor progression and PD-1 checkpoint blockade. *Nature Medicine*, *25*(1), 141–151. https://doi.org/10.1038/s41591-018-0221-5.

Wang, Z., Du, M., Yuan, Q., Guo, Y., Hutchinson, J. N., Li, S., Zheng, Y., Wang, J., Mucci, L. A., Lin, X., Hou, L., & Christiani, D. C. (2020). Epigenomic analysis of 5-hydroxymethylcytosine (5HMC) reveals novel DNA methylation markers for lung cancers. *Neoplasia*, *22*(3), 154-161. https://doi.org/10.1016/j.neo.2020.01.001.

Wang, Z., Duan, J., Cai, S., Han, M., Dong, H., Zhao, J., Zhu, B., Wang, S., Zhuo, M., Sun, J., Wang, Q., Bai, H., Han, J., Tian, Y., Lu, J., Xu, T., Zhao, X., Wang, G., Cao, X., … Wang, J. (2019). Assessment of Blood Tumor Mutational Burden as a Potential Biomarker for Immunotherapy in Patients With Non–Small Cell Lung Cancer With Use of a Next-Generation Sequencing Cancer Gene Panel. *JAMA Oncology*, *5*(5), 696. https://doi.org/10.1001/jamaoncol.2018.7098.

Weiss, G. J., Beck, J., Braun, D. P., Bornemann-Kolatzki, K., Barilla, H., Cubello, R., Quan, W., Sangal, A., Khemka, V., Waypa, J., Mitchell, W. M., Urnovitz, H., & Schütz, E. (2017). Tumor Cell–Free DNA Copy Number Instability Predicts Therapeutic Response to Immunotherapy. *Clinical Cancer Research*, *23*(17), 5074–5081. https://doi.org/10.1158/1078-0432.CCR-17-0231.

Wen, J., Ye, F., Huang, X., Li, S., Yang, L., Xiao, X., & Xie, X. (2015). Prognostic significance of preoperative circulating monocyte count in patients with breast cancer. *Medicine*, *94*(49), e2266. https://doi.org/10.1097/md.0000000000002266.

Wen, S., Chen, N., Jin, P., Wei, L., Qian, F., Yin, S., He, X., Qiu, M., & Hu, Y. (2019). Peripheral monocyte counts Predict the clinical outcome for patients with colorectal Cancer: A systematic review and meta-analysis. *European Journal of Gastroenterology & Hepatology*, *31*(11), 1313-1321. https://doi.org/10.1097/meg.0000000000001553.

Wherry, E. J. (2011). T cell exhaustion. *Nature Immunology*, *12*(6), 492-499. https://doi.org/10.1038/ni.2035.

Whiteside, T. L. (2017). The effect of tumor-derived exosomes on immune regulation and cancer immunotherapy. *Future Oncology*, *13*(28), 2583-2592. https://doi.org/10.2217/fon-2017-0343.

Wilhelm-Benartzi, C. S., Mt-Isa, S., Fiorentino, F., Brown, R., & Ashby, D. (2017). Challenges and methodology in the incorporation of biomarkers in cancer clinical trials. *Critical Reviews in Oncology/Hematology*, *110*, 49–61. https://doi.org/10.1016/j.critrevonc.2016.12.008.

Wolf, Y., Bartok, O., Patkar, S., Eli, G. B., Cohen, S., Litchfield, K., Levy, R., Jiménez-Sánchez, A., Trabish, S., Lee, J. S., Karathia, H., Barnea, E., Day, C.-P., Cinnamon, E., Stein, I., Solomon, A., Bitton, L., Pérez-Guijarro, E., Dubovik, T., … Samuels, Y. (2019). UVB-Induced Tumor Heterogeneity Diminishes Immune Response in Melanoma. *Cell*, *179*(1), 219-235.e21. https://doi.org/10.1016/j.cell.2019.08.032.

Wu, K., Yi, M., Qin, S., Chu, Q., Zheng, X., & Wu, K. (2019). The efficacy and safety of combination of PD-1 and CTLA-4 inhibitors: A meta-analysis. *Experimental Hematology & Oncology*, *8*(1), 26. https://doi.org/10.1186/s40164-019-0150-0.

Wu, Y., Ju, Q., Jia, K., Yu, J., Shi, H., Wu, H., & Jiang, M. (2018). Correlation between sex and efficacy of immune checkpoint inhibitors (PD -1 and CTLA -4 inhibitors). *International Journal of Cancer*, *143*(1), 45–51. https://doi.org/10.1002/ijc.31301.

Xiao, Q., Nobre, A., Piñeiro, P., Berciano-Guerrero, M.-Á., Alba, E., Cobo, M., Lauschke, V., & Barragán, I. (2020). Genetic and Epigenetic Biomarkers of Immune Checkpoint Blockade Response. *Journal of Clinical Medicine*, *9*(1), 286. https://doi.org/10.3390/jcm9010286.

Xu, J., & Guo, Y. (2021). A comprehensive analysis of different gene classes in pancreatic cancer: SIGLEC15 may be a promising immunotherapeutic target. *Investigational New Drugs*, *40*(1), 58-67. https://doi.org/10.1007/s10637-021-01176-5

Yabroff, K. R., Wu, X.-C., Negoita, S., Stevens, J., Coyle, L., Zhao, J., Mumphrey, B. J., Jemal, A., & Ward, K. C. (2022). Association of the COVID-19 Pandemic With Patterns of Statewide Cancer Services. *JNCI: Journal of the National Cancer Institute*, *114*(6), 907–909. https://doi.org/10.1093/jnci/djab122.

Yadav, S. P. (2007). The wholeness in suffix -omics, -omes, and the word om. *Journal of Biomolecular Techniques: JBT*, *18*(5), 277.

Yang, C. J., Kumar, A., Klapper, J. A., Hartwig, M. G., Tong, B. C., Harpole, D. H., Berry, M. F., & D'Amico, T. A. (2019). A National analysis of Long-term survival following thoracoscopic versus open lobectomy for Stage I non-small-cell lung cancer. *Annals of Surgery*, *269*(1), 163-171. https://doi.org/10.1097/sla.0000000000002342.

Yang, Y., Li, C. W., Chan, L., Wei, Y., Hsu, J. M., Xia, W., Ho, J., Hou, J., Hsu, J. L., Sun, L., & Hung, M. (2018). Exosomal PD-L1 harbors active defense function to suppress T cell killing of breast cancer cells and promote tumor growth. *Cell Research*, *28*(8), 862-864. https://doi.org/10.1038/s41422-018-0060-4.

Ye, Y., Luo, Z., & Shi, D. (2019). Use of cell free DNA as a prognostic biomarker in non-small cell lung cancer patients with bone metastasis. *The International Journal of Biological Markers*, *34*(4), 381-388. https://doi.org/10.1177/1724600819854452.

Yi, M., Dong, B., Chu, Q., & Wu, K. (2019). Immune pressures drive the promoter hypermethylation of neoantigen genes. *Experimental Hematology & Oncology*, *8*(1), 32, s40164-019-0156–0157. https://doi.org/10.1186/s40164-019-0156-7.

Yi, M., Jiao, D., Xu, H., Liu, Q., Zhao, W., Han, X., & Wu, K. (2018). Biomarkers for predicting efficacy of PD-1/PD-L1 inhibitors. *Molecular Cancer*, *17*(1), 129. https://doi.org/10.1186/s12943-018-0864-3.

Yi, M., Qin, S., Zhao, W., Yu, S., Chu, Q., & Wu, K. (2018). The role of neoantigen in immune checkpoint blockade therapy. *Experimental Hematology & Oncology*, *7*(1), 28. https://doi.org/10.1186/s40164-018-0120-y.

Yu, Y., Yang, Y., Li, H., & Fan, Y. (2023). Targeting HER2 alterations in non-small cell lung cancer: therapeutic breakthrough and challenges. *Cancer Treatment Reviews*, *114*, 102520. https://doi.org/10.1016/j.ctrv.2023.102520

Yugi, K., Kubota, H., Hatano, A., & Kuroda, S. (2016). Trans-Omics: How To Reconstruct Biochemical Networks Across Multiple 'Omic' Layers. *Trends in Biotechnology*, *34*(4), 276–290. https://doi.org/10.1016/j.tibtech.2015.12.013

Zhang, K., Hong, X., Song, Z., Xu, Y., Li, C., Wang, G., Zhang, Y., Zhao, X., Zhao, Z., Zhao, J., Huang, M., Huang, D., Qi, C., Gao, C., Cai, S., Gu, F., Hu, Y., Xu, C., Wang, W., … Liu, L. (2020). Identification of Deleterious *NOTCH* Mutation as Novel Predictor to Efficacious Immunotherapy in NSCLC. *Clinical Cancer Research*, *26*(14), 3649–3661. https://doi.org/10.1158/1078-0432.CCR-19-3976.

Zdanov, S., Mandapathil, M., Eid, R. A., Adamson-Fadeyi, S., Wilson, W., Qian, J., Carnie, A., Tarasova, N. I., Mkrtichyan, M., Berzofsky, J. A., Whiteside, T. L., & Khleif, S. N. (2016). Mutant KRAS conversion of conventional T cells into regulatory T cells. *Cancer immunology research*, *4*(4), 354-365. https://doi.org/10.1158/2326-6066.cir-15-0241.

Zhang, Y. J., Xu, F., Zhang, Y. J., Li, H. B., Han, J. C., & Li, L. (2015). miR-206 inhibits non small cell lung cancer cell proliferation and invasion by targeting SOX9. *International journal of clinical and experimental medicine*, *8*(6), 9107–9113. PMID: 26309565.

Zhang, Y., Park, C., Bennett, C., Thornton, M., & Kim, D. (2021). Rapid and accurate alignment of nucleotide conversion sequencing reads with HISAT-3N. *Genome Research*, *31*(7), 1290-1295. https://doi.org/10.1101/gr.275193.120.

Zhao, C., Inoue, J., Imoto, I., Otsuki, T., Iida, S., Ueda, R., & Inazawa, J. (2007). POU2AF1, an amplification target at 11Q23, promotes growth of multiple myeloma cells by directly regulating expression of a B-cell maturation factor, TNFRSF17. *Oncogene*, *27*(1), 63-75. https://doi.org/10.1038/sj.onc.1210637.

Zheng, Y., Liang, H., Chen, Z., Li, Y., Zhou, B., Hu, R., Chen, S., Xiao, H., Ma, Y., Xie, G., Yang, J., Li, Y., & Shen, L. (2022). PD-L1+CD8+ T cells enrichment in lung cancer exerted regulatory function and tumor-promoting tolerance. *iScience*, *25*(2), 103785. https://doi.org/10.1016/j.isci.2022.103785.

Zheng, H., & Takano, Y. (2011). NNK-Induced Lung Tumors: A Review of Animal model. *Journal of Oncology*, *2011*, 1-8. https://doi.org/10.1155/2011/635379.

Zhou, G. (2019). Tobacco, air pollution, environmental carcinogenesis, and thoughts on conquering strategies of lung cancer. *Cancer biology and medicine*, *16*(4), 700- 713. https://doi.org/10.20892/j.issn.2095-3941.2019.0180

SUPPLEMENTARY DATA

Supplementary Table 1.A: Correlation between cfDNA concentrations before ICB and categorical clinical characteristics.

Clinical variables	p-value (adj.)
Sex	0,096
Diagnosis subtype	0,446
ICI treatment	0,144
Previous treatment lines	0,514
Lung metastases	0,487
Lymph node metastases	0,451
Skin metastases	0,307
Brain metastases	0,162
Bone metastases	0,0031
Liver metastases	0,224
ECOG	0,072
PDL1	0,649
LDH	0,0107
Maximum toxicity grade	0,229
Response at three months of ICB	0,00656
Response at six months of ICB	0,00218
Response at one year of ICB	0,0297
Extreme response	0,00268

Supplementary Table 1.B: Correlation between cfDNA concentrations before ICB and numerical clinical characteristics.

Clinical variables	p-value	Correlation
Number of metastases	0,068	0,19
Lymphocytes	0,1	-0,17
Basophils	0,7	-0,04
Eosinophils	0,57	-0,058
Leukocytes	0,19	0,13
Neutrophiles	0,12	0,16
Monocytes	0,44	0,08
CD19 + B cells	0,88	0,018
CD3+ T cells	0,2	-0,15
CD3+ CD8+ T cells	0,88	-0,019
CD3+ PD1+ T cells	0,094	0,2
CD3+PDL1+ T cells	0,068	0,22
CD4+ T cells	0,69	0,047
CD4+ Regulatory T cells	0,73	-0,04
CD8+PD1+ T cells	0,091	0,2
CD8+PDL1+ T cells	0,15	-0,17
Natural Killers	0,46	0,084
PDL1.cell	0,63	-0,051
Regulatory T cells	0,67	-0,05
Platelets	0,48	0,073
Recist (mm)	0,33	0,1
Hemoglobin	0,032	-0,22
cfDNA (T2)	0,00016	0,39
cfDNA (T3)	0,75	0,044
cfDNA (T4)	0,16	0,25

Supplementary Table 2. Correlation between cfDNA concentrations at different ICB treatment cycles and response criteria.

	Clinical variables	p-value
cfDNA after two cycles of ICB (T2)	Response at three months of ICB	0,0564
	Response at six months of ICB	0,0261
	Response at one year of ICB	0,32
	Extreme response	0,0455
cfDNA after six months of ICB (T3)	Response at three months of ICB	N/A
	Response at six months of ICB	0,519
	Response at one year of ICB	0,48
	Extreme response	N/A
cfDNA after twelve months of ICB (T4)	Response at three months of ICB	N/A
	Response at six months of ICB	N/A
	Response at one year of ICB	0,122
	Extreme response	N/A

Supplementary Table 3: Correlation between clustered responder patients based on basal DE miRNA and clinical characteristics.

Clinical characteristics	p value
Age	0,582
Sexº	0,312
Diagnosis subtype	0,709
Stage at diagnosis	0,148
ICB treatment	0,866
Previous treatment lines	0,661
Lung metastases	0,88
Lymph node metastases	0,789
Skin metastases	0,312
Brain metastases	0,511
Bone metastases	0,643
Liver metastases	0,661
ECOG	0,656
PDL1	0,745
LDH	0,079

APPENDIX

Most relevant ICB prognostic and response biomarkers. Most relevant reported response and prognosis biomarkers related to T-cell reinvigoration ICB in different types of tumors focusing on the predictive power and the screening procedure.

Biomarker		Type	Target of the test	Assay/Predictive value
Tumor mutational burden (TMB)		Genetic	Tumor	WES targeted next generation sequencing. High TMB associated with clinical benefit
Tumor neoantigen load		Genetic/ Epigenetics	Tumor	WES. In come tumors with low neoantigen intratumor heterogeneity (ITH) and high clonal neoantigen load the OS is significantly better.
DNA damage response pathways (MMR/MSI)		Genetic	Tumor	Targeted next generation sequencing. High genetic variation of MMR/MSI associated with clinical benefit
Specific mutated gene pathways	IFNG 1/2	Genetic	Tumor	WES. JAK1/2 mutation indicates bad response and resistance to ICB
	JAK1, JAK2			WES. JAK1/2 mutation indicates bad response and resistance to ICB

	PBRM1			WES. PBRM1 loss of function indicates bad response
	B2M			WES. B2M mutation indicates bad response
	PBAF			WES. PBAF loss of function indicates more efficient ICB
	NOTCH	Genetic/ Transcriptional		WES and RNAseq. NOTCH deletion as favorable predictor of IICB
	EGFR	Genetic		WES. EGFR amplification indicates bad response
	MDM2/MDM4			WES. MDM2/MDM4 amplification indicates bad response
	KRAS/TP53			WES. TP53/KRAS mutation indicates good response
	STK11/LKB1			WES. Major driver of primary resistance to PD-1 blockade in KRAS-mutant lung adenocarcinomas. Mutant STK11/LKB1 is associated with worse PFS and OS
	Foundation One			FoundationOne by WES to provide genetic information about tumors.

PDL-1	Histopathological	Immune/tumor	IHC. In advanced NSCLC patients treated with Nivolumab, PD-L1 expression predicts OS, PFS. In PD-L1 negative metastatic NSCLC, ICB efficacy is equivalent to chemotherapy.
Immunoscore	Histopathological	TME	CD3 and CD8 or CD8 and CD45RO by IHC. Multivariate analysis in colorectal tumors shows a significant correlation of Immunoscore with disease specific survival, disease free survival and OS.
TME gene expression profiling	Transcriptional	TME	RNAseq of some genes such as perforin 1, granzyme B, Th1 cytokines, MHC-II, NKG7, ICO1, IGK, GBP1, STAT1, IGLL5, OCLN and IFN-γ-induced immune gene
TILs	Histopathological /Transcriptional	TME	scRNA-seq. CD4+ and CD8+ T cells, FOXP3+ T cells, CD20+ B cells, CD134+ and CD137+ cells, NKp46+ cells and

			CD39+CD8+ are positively associated with OS after ICB treatment.
Amount/clonality of TCR repertoire	Genetic/Transcriptional	TME	WES and sequencing. High clonality of TCR repertoire significantly correlated with clinical response to ICB.
Circulating CD45RO+/CD8+ T cells	Cellular	Immune	Flow cytometry. High value indicates better response
Circulating CD69+MIP1B+ NK cells			Flow cytometry. High value indicates bad response
CD14+CD16-HLA-Drhi monocytes cells			Flow cytometry. High value indicates bad response
Neutrophils/lymphocytes ratio			Flow cytometry. High value indicates poor prognosis
Total eosinophils			Flow cytometry. High value indicates better response
Absolute lymphocyte count (ALC)			Flow cytometry. High value indicates better response
LDH	Secreted	Serum	LDH ELISA. Elevated value indicates bad response
CTCs	Cellular	Tumor	Flow cytometry. High value indicates bad

			response and progression disease
ctDNA	Genetic	Tumor	ctDNA level by next generation sequencing. High value of ctDNA drop indicates good response
Exosomes	Transcriptomic	Tumor	miRNAseq. Role not clear although high value indicates could indicate progression disease
Cytokines CXCL11	Secreted	Serum	CXCL11 level examined by bead-based multiplexed immunoassay. High value indicates bad response
Cytokines CXCL9, CXCL10	Secreted	Plasma	ELISA. Levels after anti-PD1 + anti-CTLA4 treatment are higher in responders vs non-responders
TNF-alpha	Secreted	Plasma	ELISA. TNF-aplha as biomarkers of poor prognosis
IL-6	Secreted	Plasma	ELISA. IL-6 a as biomarkers of poor prognosis
C-reactive protein (CRP)	Secreted	Serum	CRP by Immunofiltration. High value indicates good response
IL-8	Secreted	Plasma	ELISA. High levels are associated with poor prognosis